

UNIVERSIDADE FEDERAL DO RIO GRANDE DO SUL
PROGRAMA DE PÓS-GRADUAÇÃO EM FÍSICA
DOCTORAL THESIS

**Time evolution of weakly turbulent processes in the presence
of collisional interactions in astrophysical plasmas***

(Evolução temporal de processos fracamente turbulentos na presença de efeitos
colisionais em plasmas astrofísicos)

Sabrina Tigik Ferrão

Doctoral Thesis prepared under the supervision
of Professor Luiz Fernando Ziebell, presented to
the Physics Graduation Program of the Instituto
de Física at UFRGS, in partial fulfillment of the
requirements for obtaining the title of Doctor in
Sciences.

Porto Alegre
December 2, 2019

*Project financed by the Conselho Nacional de Desenvolvimento Científico e Tecnológico (CNPq) and
the Coordenação de Aperfeiçoamento Pessoal de Nível Superior (CAPES).

Acknowledgments

First of all, I acknowledge the dedication of my supervisor, Luiz Fernando Ziebell, whose guidance, encouragement, and patience (tons of) made this work possible. Further, I would like to state my sincere appreciation for the trusting he always demonstrated to have in my capabilities for developing high-quality research and for his availability to discuss my work, giving me insightful advice.

In the academic scope, I would like to thank Peter Yoon for the years of productive collaboration and for receiving me with great hospitality during my stay at the University of Maryland. I also want to express my earnest appreciation to Dr. Adolfo Viñas, who dedicated a part of his time to teach me PIC simulation and discuss the subtleties of the kinetic theory of plasmas during my time in the University of Maryland. As special mentions, I would like to thank Jeferson Arenzon, Renato Pakter, and Rudi Gaelzer for their willingness to help me with my postdoc applications when I randomly appeared at their offices.

From the Graduate Program in Physics, I am grateful to Liane Thier Ruschel for the kind and efficient assistance in dealing with bureaucratic procedures and the most diverse document requests. I also thank Mari Nunes for her patience and goodwill in dealing with everyday trouble of grad students.

On the personal side, I thank Felipe for his comprehension, patience, support and encouragement during my undergrad and graduate years. I am also grateful to Gabriel for his love and refined sense of humor that cheers me up even in the saddest days.

Agradeço especialmente à minha mãe, Diná, por ter me criado para ser uma mulher livre e a não aceitar qualquer papel na sociedade que não seja o que eu considere o melhor para mim. *Mãe, essa tese é dedicada a ti. Sem teu exemplo, eu não estaria onde estou. Obrigada por tudo!*

From my friends and colleagues from UFRGS, I am grateful to Nicole for the companionship that ranges from hard-working weekends to life celebrations. *Nicole, grad school would be terribly boring without you.* I also thank Amanda for showing me how to be prepared for life, Demétrius for the cheerful annoyance, and Vinícius for the light talks and for sharing his delicious bread. A special thanks to Thales, my example of plasma physicist, and to Fernanda, whose intelligence and dedication will always be my inspiration. Special mentions to colleagues that were part of this journey and deserved to be remembered: Alexandre, Gustavo, João and Larissa.

From Maryland, I am especially grateful to Jacek for the infinite talks, solid companionship and (mutual) support. *Jacek, you made my time in CP much better. Dziękuję bardzo!*

“You’re in a bad shape! Apparently, you have developed a soul.”
— Yevgeny Zamyatin, We

Abstract

The weak turbulence theory has been an important theoretical tool for the study of nonlinear kinetic instabilities in plasmas. For a long time, this theory treated exclusively of the study of oscillatory processes and its influence in the plasma dynamics. The long-lasting timescale of nonlinear processes, however, suggests that collisional processes might have some effect in the late plasma dynamics, acting alongside nonlinear collective effects. In a recent work [P. H. Yoon et al., Phys. Rev. E 93:033203 (2016)], collisional effects and collective processes were systematically incorporated, starting from first principles, in the weak turbulence theory equations, considering electrostatic oscillations. The outcome of this innovative approach was a formal mathematical expression for the collisional damping rate for Langmuir and ion-sound waves, and the discovery of a new fundamental process of emission of electrostatic fluctuations, in the ion-sound and Langmuir frequency range, caused by binary interactions of particles, named *electrostatic bremsstrahlung*. In the present study we introduce the first numerical analysis of these two new equations and discuss the relevance of these numerical results in the solar physics scope. The first work to be discussed concerns the collisional damping equation, and in it we compare the results of numerical integration of the rigorous expression with the damping rate calculated with the widely applied *Spitzer formula*. We show that the Spitzer approximation highly over-estimates the intensity of collisional attenuation of plasma waves. The lack of relevance of the collisional damping rate gets further demonstrated when we compare it with the collisionless (Landau) damping rate. In the second work to be discussed, we analyze the so-far ignored electrostatic bremsstrahlung effect. We show that the presence of electrostatic bremsstrahlung emission modifies the Langmuir spectrum, which in turn alters the shape of the initial electron velocity distribution, assumed to be Maxwellian. After a long time-evolution period (numerical integration), the system seems to arrive to a new quasi-steady state, in which the shape of the electron velocity distribution resembles the shape of a core-halo distribution function, i.e., composed by a Maxwellian core and a suprathermal tail. The outcomes of both analyses are unprecedented; the prospects and possibilities for further studies on this subject are promising. In the end, we also present an extra result, indirectly related to the main subject of this doctoral project, regarding the analysis of the complete set of electromagnetic weak turbulence equations, in the presence of a core-halo velocity distribution function.

Resumo

A teoria de turbulência fraca tem sido uma importante ferramenta teórica para o estudo de instabilidades cinéticas não lineares em plasmas. Por um longo tempo, esta teoria tratou exclusivamente do estudo de processos oscilatórios e de sua influência na dinâmica do plasma. Entretanto, a escala de tempo de longa duração dos processos não lineares sugere que processos colisionais podem ter algum efeito na dinâmica do plasma, atuando em conjunto com os efeitos dos processos coletivos não-lineares. Em um trabalho recente [P. H. Yoon et al., Phys. Rev. E 93:033203 (2016)], efeitos colisionais e processos coletivos foram sistematicamente incorporados, partindo de primeiros princípios, nas equações da teoria de turbulência fraca, considerando oscilações eletrostáticas. O resultado dessa abordagem inovadora foi uma expressão matemática formal para a taxa de amortecimento colisional para ondas de Langmuir e íon-acústicas, e a descoberta de um novo processo fundamental de emissão de flutuações eletrostáticas, na faixa de frequência das ondas de Langmuir e das ondas íon-acústicas, causado por interações binárias entre partículas do plasma, nomeado como *bremssstrahlung eletrostático*. Neste estudo, introduzimos as primeiras análises numéricas relativas a essas duas novas equações e discutimos a relevância desses resultados numéricos no contexto da física solar. O primeiro trabalho a ser discutido se refere à nova equação para o amortecimento colisional, e nele comparamos o resultado da integração numérica dessa expressão, com a largamente usada *fórmula de Spitzer*. Com isso conseguimos mostrar que a aproximação de Spitzer superestima em muito a intensidade da atenuação colisional das ondas de plasma. Além disso, a falta de relevância da taxa de amortecimento colisional fica demonstrada quando a comparamos com a taxa de amortecimento não colisional (de Landau). No segundo trabalho, analizamos o até então ignorado efeito de *bremssstrahlung eletrostático*. Mostramos que a presença da emissão de *bremssstrahlung eletrostático* modifica o espectro das ondas de Langmuir que, por sua vez, altera a forma da função de distribuição inicial dos elétrons, suposta Maxwelliana. Após um longo tempo de evolução temporal (integração numérica), o sistema parece chegar a um novo estado quase-estacionário, no qual a forma da função de distribuição de velocidades dos elétrons lembra a forma de uma função de distribuição núcleo-halo, ou seja, composta por um núcleo Maxwelliano e uma cauda supratérmica. Os resultados de ambas análises são sem precedentes; as perspectivas e as possibilidades para novos estudos neste assunto são promissoras. No final é também apresentado um resultado extra, indiretamente relacionado ao assunto principal desse projeto de trabalho de doutorado, relativo à análise do conjunto completo de equações eletromagnéticas da teoria de turbulência fraca, na presença de uma função de distribuição de velocidades núcleo-halo.

Contents

1	Introduction	1
1.1	Applications to astrophysical plasmas	4
1.1.1	Solar and space physics	4
1.1.2	The Sun and the near-Earth environment	6
1.1.3	The solar corona	6
1.2	Thesis organization	9
2	Kinetic theory of plasmas	10
2.1	The Vlasov-Maxwell system of equations	12
2.2	Low amplitude electrostatic oscillations	13
3	Weak turbulence theory	14
3.1	Nonlinear kinetic equations	14
3.1.1	Wave kinetic equation for linear eigenmodes	18
3.2	Weak turbulence equations for Langmuir and ion-sound waves	20
4	Weak turbulence for collisional plasmas	23
4.1	Inclusion of noneigenmodes	24
4.1.1	Absence of noneigenmode contribution to quasilinear wave kinetic equation	25
4.1.2	Noneigenmode contribution to particle kinetic equation	26
4.2	Noneigenmode contribution to nonlinear wave kinetic equation	29
4.2.1	Generalized wave kinetic equation for L and S waves	34
5	Weakly turbulent processes in the presence of collisional interactions	36
5.1	Collisional damping rates for plasma waves	37
5.2	Generation of suprathermal electrons by collective processes in collisional plasmas	43
5.2.1	Dimensionless equations	43
6	Final remarks	51
A	Improved approximation for the second order susceptibility	53
A.1	Original approximation	53

A.2 Alternative approach	55
B Asymptotic equilibrium	60
C Extra publication	64
D Two-dimensional time evolution of beam-plasma instability in the presence of binary collisions	78

List of Figures

1.1	Main boundaries of the heliosphere and the location of both Voyager missions.	5
1.2	NASA's present and future heliophysics system observatory. The number between parenthesis under the probe's name is the total number of spacecrafts that compose the mission.	6
1.3	ESA's past, present, and future science missions for studying the solar system.	7
1.4	Solar corona captured during the total solar eclipse of 2017 (top panel) and 2019 (lower panel). The reddish contour at some regions is the chromosphere, and the reddish arcs are solar prominences, chromospheric plasma structures that penetrate the coronal region. Credit: Nicolas Lefaudeux, accessed at 15/08/2019.	8
B.1	Asymptotic spectrum of Langmuir waves for several values of κ index and Maxwellian distribution. (a) With electrostatic bremsstrahlung emission and collisional damping. (b) Without bremsstrahlung emission and collisional damping.	63

Chapter 1

Introduction

In the context of plasma kinetic theory, processes involving waves and kinetic instabilities, the so-called *collective processes*, are almost exclusively associated with situations in which the effects of collisional dissipation can be neglected, what happens when the studied phenomenon evolves in a much shorter time-scale than the collisional relaxation time of the plasma in question [1]. In such cases, the plasma dynamics may be described by the Vlasov-Maxwell system, a complex set of coupled equations whose solution invariably will depend on some degree of approximation. In the presence of small amplitude oscillations in a fully ionized plasma, we can make use of perturbation theory in order to solve such complicated system [2]. From this method, one may obtain simpler approximations like the linear theory and the quasilinear formalism, and also more complex formulations, like the weak turbulence theory, which takes into account low-order nonlinearities on the plasma dynamics.

With the lowest order of this chain of perturbative approximations, the linear theory, it is possible to obtain the dispersion relations, which are mathematical expressions that not only help us on identifying the different oscillatory modes that may be excited in plasmas, but also wholly characterize these oscillations. Valuable information like how these waves propagate and the frequencies that will resonate with the plasma particles, resulting in damping or amplification of these oscillations [3–5], are given by the dispersion relations. This information, however, is static. There is no way to know, based solely on the linear formulation, any further development of the system, how these waves will evolve in time from a given initial state, for instance. Thus, to clarify if these oscillations will grow until their amplitudes become too large to be treated by a perturbative method, or if they will rapidly increase and saturate, or if they will be completely damped, or if they will decrease a little and then saturate, a certain degree of nonlinearity must be taken into account. That is the purpose of the quasilinear approximation.

In the quasilinear theory, low-order nonlinear terms are kept in the equation for the time evolution of the velocity distribution function. The velocity distribution will then evolve in time

through a process of diffusion in velocity space, in which the diffusion coefficient depends on the spectral energy density of the waves. The dispersion relation is formally given by the same expression obtained under the linear theory, except that now it depends on a time-dependent velocity distribution function, which must vary in a much slower time-scale than the period of the plasma oscillations. Under such condition, the gradual changing on the velocity space shape slowly modifies the shape of the wave spectrum, whose new form will alter the velocity distribution function and so on, until a new quasi-stationary equilibrium state is attained [5]. However, depending on the phenomenon being described, this saturation state reached under the quasilinear approximation might keep on evolving if higher order nonlinearities are taken into account [6]. This kind of nonlinear analysis is given by the *weak turbulence theory*, which is the next step in this chain of perturbative approximations.

Mostly developed in the period between the late 1950s and early 1970s [6–14], the weak turbulence theory has become a valuable theoretical tool for the analysis of nonlinear phenomena in plasmas since then, being applied in several studies until nowadays [15–21]. Its complex formulation is constituted by a set of coupled kinetic equations, which describe the time evolution of the velocity distribution functions of the plasma particles and the time evolution of the spectral intensities of the plasma wave modes. The development of the weak turbulence theory was resumed in a relatively recent series of papers, where the author, starting from first principles, has extended the original formalism in order to include new effects. In the initial work, it was considered only the propagation of electrostatic oscillations, taking into account the effects of both wave-wave and wave-particle interactions [22]. Later, the formalism was expanded, and discrete particle effects, related to spontaneous emission and spontaneous scattering processes, were included [23]. In a further extension, the effects of the propagation of electromagnetic waves were incorporated into the revised formulation [24, 25].

The equations of this revised version of the weak turbulence theory have been the subject of extensive studies involving nonlinear analysis and two-dimensional numerical integration applied to the time evolution of the Langmuir turbulence [26–30] in a fully ionized and unmagnetized plasma, and in other studies that also include the emission of electromagnetic waves [31–33]. Some studies using a one-dimensional approach have also been made [34–36]. The Langmuir turbulence is a by-product of the instability generated when an energetic electron beam interacts with a background plasma. The electron beam alters the electron velocity distribution triggering the so-called *bump-in-tail instability*. Besides being recurrently used in textbooks as an illustrative example of the quasilinear diffusion process [4–6], the bump-in-tail instability also has an essential role in the study of type II and type III radio bursts [37–43]. In this context, the relevance of a more accurate description of nonlinear kinetic instabilities in plasmas, represented here by the beam-plasma interaction, becomes clear.

The next step towards a more complete description of weakly-turbulent processes in

plasmas is the inclusion of collisional effects in the formalism. So far, the effects of binary collisions have been neglected under the time-scale argument, mentioned in the first paragraph. This assumption can be considered quite precise for the evolution of the bump-in-tail instability under the quasilinear approximation. In such regimen, the plasma quickly saturates in a quasi-equilibrium state and the time evolution entirely ceases. However, when nonlinear processes are considered in the dynamics, one cannot be sure if this argument still holds. Basically, for the system to evolve inside the weak turbulence theory limitations, the incident beam must be tenuous, and the oscillations must have low amplitude (after all, the turbulence ought to be weak). Under such conditions, the time evolution of the system occurs in a time interval that is way longer than the oscillation period of the plasma waves being studied. In fact, there are studies that show that nonlinear effects keep acting in the system in a time-scale that goes far beyond the saturation time of the quasilinear instability, to the extent that an asymptotic analysis of the new quasi-equilibrium state of the turbulent process becomes relevant [29–32, 44].

The hypothesis about the probable relevance of binary collisions in the nonlinear dynamics of the beam-plasma interaction was numerically tested in [45] (see Appendix D). In this work, a linearized form of the Landau collision integral was added to the particle kinetic equation, and the weak turbulence theory's complete set of self-consistent, electrostatic equations was numerically integrated in two-dimensions. It was shown that collisions indeed do affect the plasma dynamics in a time-scale that is very close to the time-scale of action of nonlinear effects. Beyond the purely theoretical conjecture, combining collective processes and collisional effects have some important applications in solar physics. In the solar hard X-ray emission analysis, for instance, the models used for interpreting the spectra measured by the Reuven Ramaty High Energy Solar Spectroscopic Imager (RHESSI)¹ that employ quasilinear/nonlinear wave instabilities with some kind of collisional dissipation (collisional damping for the waves, binary collisions for the particles) are usually empirically adapted merely by adding an *ad hoc* expression into the particles and wave kinetic equations to fit the observed data [46–51]. However, there is no rigorous theory to compare and support such models. Moreover, though the formalism in [45] makes use of the full Landau collision integral in the particle kinetic equation, it does not take into account collisional damping effects in the wave equation, which is widely used in these empirical models. The point is: until that moment, there was not a proper theoretical tool to deal with the combination of collective processes and collisional interaction.

In a recent paper [52], it was presented the first rigorous theory that, starting from first principles, incorporates collisional effects into the already well established weak turbulence formalism. The authors used the same standard weak turbulence perturbative method but, instead of keeping only the collective eigenmodes in the linear and nonlinear wave-particle interactions, they also kept the effects of the non-collective fluctuations emitted by thermal particles. The outcome is a complete nonlinear description, from first principles, of the propagation of

¹For more information about the mission see: <https://hesperia.gsfc.nasa.gov/rhessi3/>.

electrostatic oscillations in the presence of both wave and particle collisional dissipation and a new equation describing a hitherto unknown process. This new effect depicts the emission of electrostatic radiation, in the eigenmode frequency range, caused by particle scattering. Since this is a form of braking radiation, the authors named it as *electrostatic bremsstrahlung*.

1.1 Applications to astrophysical plasmas

Astrophysical plasmas are observed in a vast range of densities, temperatures, magnetic fields, ionization degree, and scale lengths [53]. Starting in the outer layers of Earth's atmosphere, passing through the solar wind in the interplanetary space, to the stellar interiors and atmospheres, accretion disks and molecular clouds, it is estimated that something around $99 \sim 99.9\%$ of the observable matter in the universe is in the plasma state. Under cosmic conditions, even the weakly ionized gas of the neutral hydrogen regions around galaxies or in the atmosphere of cold stars have a strong reaction to electromagnetic fields, exhibiting the characteristic collective behavior of plasmas and, therefore, are also considered plasmas [53–55].

As soon as the pervasiveness of the plasma state in space came as a fact, plasma physics began to be recognized as an essential component in the multidisciplinary framework of astrophysics [56–60]. At the same time, the analysis and interpretation of observational data started to have increasing relevance in the progress of theoretical, computational, and experimental plasma physics research [52, 61–64]. In this context of mutual collaboration, the solar and interplanetary plasma research has a pivotal contribution. The accessibility to direct, in situ measurements, highly resolved remote sensing and high-resolution spectroscopy, turned the solar system into a space plasma laboratory. Processes like magnetic reconnection, particle acceleration, shocks, and turbulence can be closely observed by space probes, and the understanding acquired may be extended or adapted to address similar phenomena observed in remote astrophysical environments [65].

The theory developed during this graduate research analyses the combined action of nonlinear kinetic instabilities and collisional processes in the context of solar physics. To contextualize our work within the solar plasma research, in Subsections 1.1.1, 1.1.2 and 1.1.3 we present a brief review of the current research in solar and space physics and the phenomena related to this work. The corresponding paper is pointed in a footnote.

1.1.1 Solar and space physics

The domain of solar and space physics is the *heliosphere*, a cavity in the interstellar medium, created by the constant supersonic flow of solar plasma that permeates the interplanetary space. This region encloses the solar system and extends for approximately 140AU^2 in the

²An AU (astronomical unit) is defined as the mean distance between the Sun and Earth, $1\text{AU} \approx 150 \times 10^6\text{km}$.

surrounding galactic space. Its outer limit is the *heliopause*, an interface zone where the outgoing pressure of the solar plasma balances the incoming pressure from the interstellar medium. This comet-shaped plasma bubble [66], also has an inner boundary, the *termination shock*, which delimits the sphere of absolute influence of the solar plasma. Beyond the termination shock, at roughly 100AU from the Sun, extending out to the heliopause, lies the *heliosheath*. In this region, the solar wind particles start being subjected to increasing external pressure, transitioning to a subsonic, turbulent flow that blends and interacts directly with the matter in the local interstellar medium [67]. In Figure 1.1, we have a depiction of the regions and boundaries described above, and the current location of both Voyager missions, that are already outside the heliosphere, in the interstellar space.

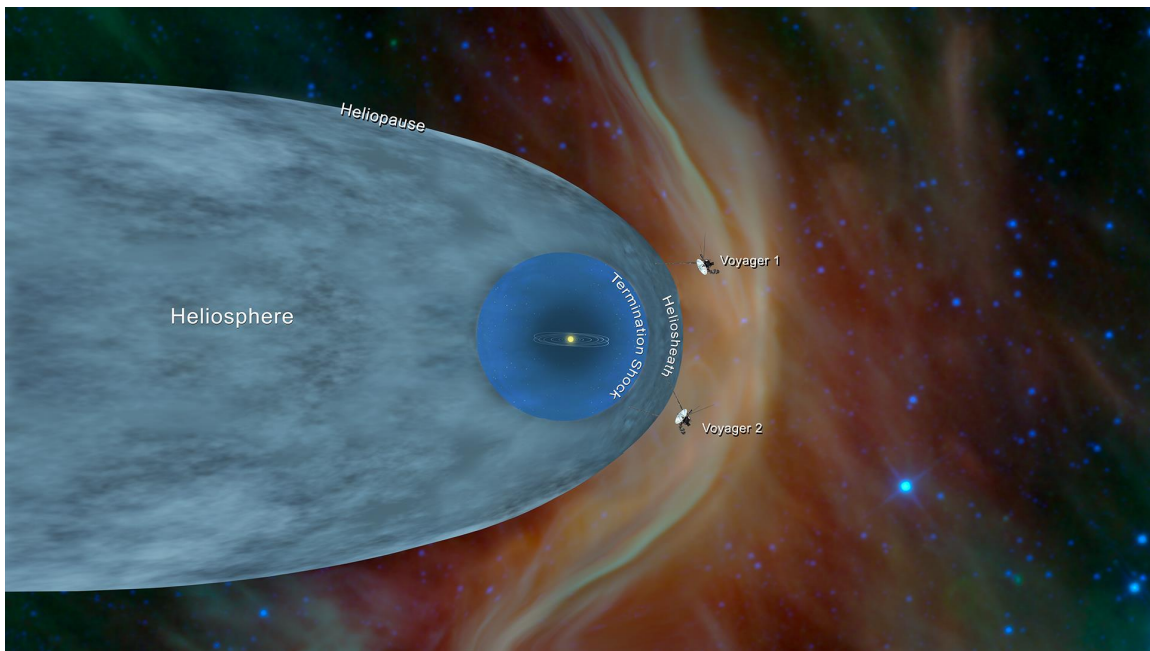


Figure 1.1: Main boundaries of the heliosphere and the location of both Voyager missions.

Credit: [NASA/JPL-Caltech](#), accessed at 08/08/2019.

The ultimate goal of heliophysics can be summarized as the search for a better understanding of the solar dynamics and how it affects the Earth, other planetary bodies, and the interstellar medium. The heliosphere is a coupled system, where different interacting elements that might look unrelated at first sight are connected by underlying plasma processes [67]. A great example of this interconnection is the relation between the appearing of sunspots and the occurrence of non-recurrent geomagnetic storms, which are the most intense space weather disturbances. Evidence of such relationship started to appear at the end of the 19th century. However, the correct hypothesis supporting this correlation (coronal mass ejections associated with solar flares), which depended on advances in plasma physics theory, came along only in 1929 [68, 69].

1.1.2 The Sun and the near-Earth environment

A better comprehension of the Sun and the dynamic space around our planet goes beyond the pure scientific curiosity. This accessible space physics laboratory can indeed lead to discoveries that can be applied and extended to remote cosmic systems. However, the primary reason behind the international effort (see Figures 1.2 and 1.3) on understanding the complex physics of the Sun and interplanetary space is to unlock means of predicting the occurrence and intensity of solar activity, and anticipate how the near-Earth environment will be affected. Reliable forecasting of the space weather is essential for protecting electronic equipment, radio communications, GPS signal and humans in space from the effects of the interaction between the dense, magnetized plasma of coronal mass ejections with the geomagnetic field, and also from the energetic radiation emitted by solar flares³. Extreme coronal mass ejections can also cause stronger geomagnetic disturbances that may affect terrestrial infrastructure such as electric power grids [67].

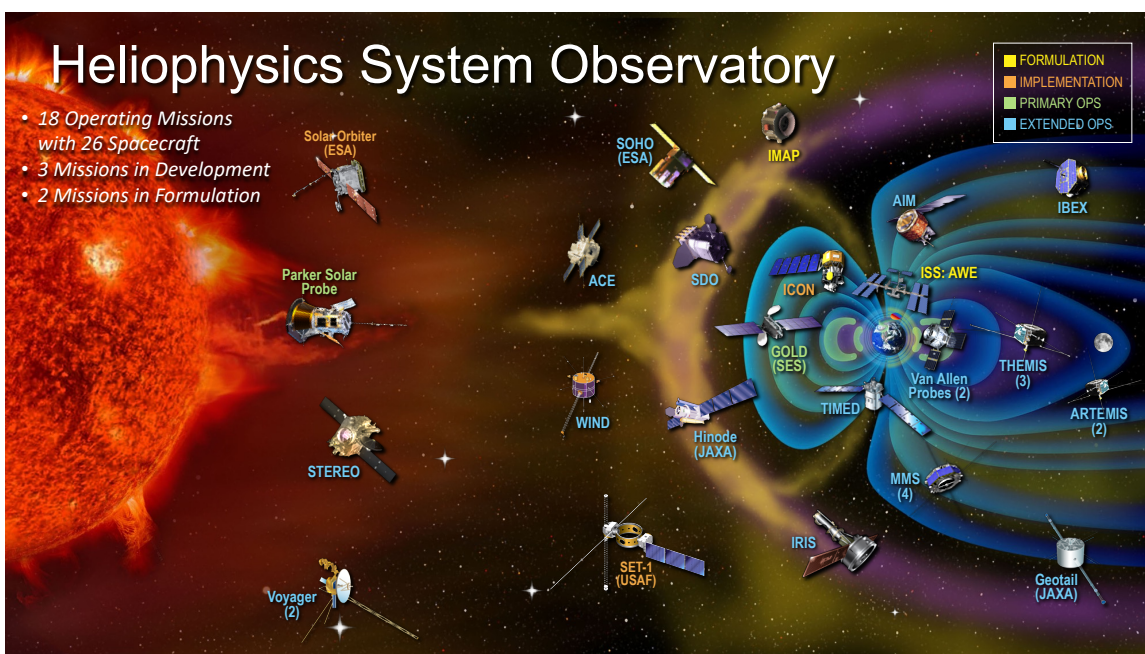


Figure 1.2: NASA's present and future heliophysics system observatory. The number between parenthesis under the probe's name is the total number of spacecrafts that compose the mission.

Credit: [NASA](#), accessed at 10/08/2019.

1.1.3 The solar corona

The source of the tenuous magnetized plasma permeating the heliosphere, and also the origin of solar particles and radiation that may cause disruptive space weather around Earth, is the outermost layer of the Sun: the solar corona [70, 71]. The solar corona can be

³The emission of hard X-rays and type III radio bursts, both generated during solar flares, are addressed in [45] (see Appendix D).

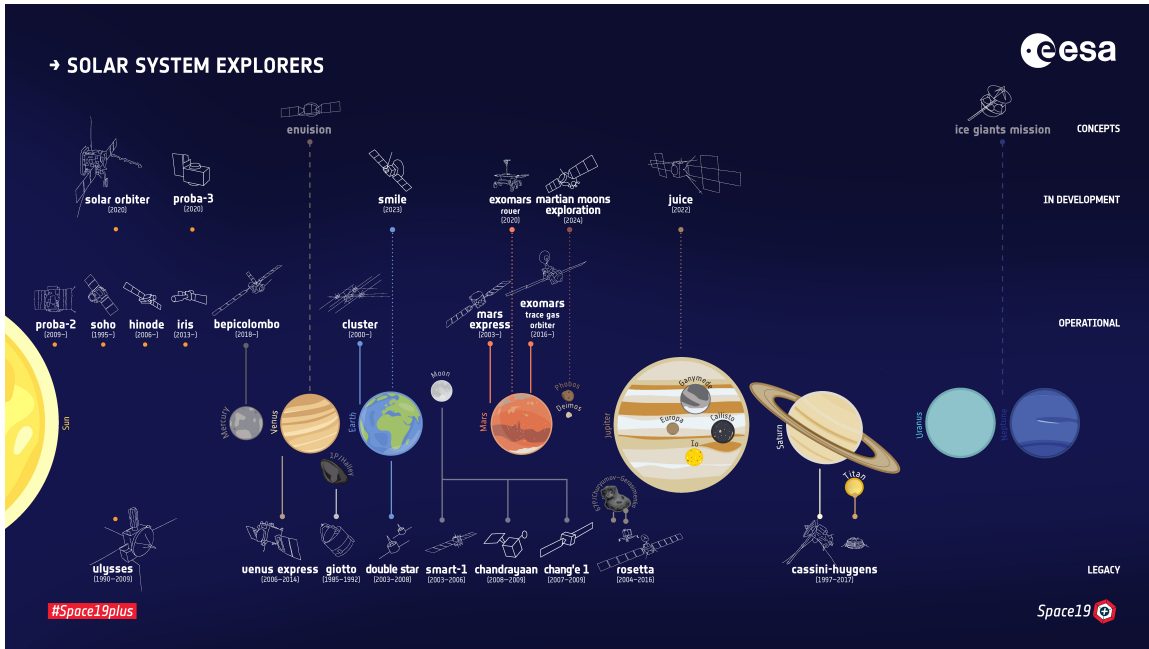


Figure 1.3: ESA's past, present, and future science missions for studying the solar system.

Credit: [ESA](#), accessed at 10/08/2019.

easily recognized as the bright halo that appears around the hidden Sun during solar eclipses. [Figure 1.4](#) shows two beautiful photographs of the corona, taken in two different solar eclipses, August 21 2017 and July 2 2019. In both pictures, one can see the moon covering the bright photosphere, allowing us to have a glimpse of the thin, but ultra-hot coronal plasma.

Counter-intuitively, the solar corona is, at the same time, the most tenuous and the hottest outer layer of the Sun. At the top of the chromosphere, where the temperature might reach 20,000 K, in a relatively narrow interface, the *solar transition region*, the plasma temperature rises abruptly to $\sim 10^6$ K [72]. It has been almost eighty years since the extreme coronal temperature came as the only reasonable explanation for the origin of the spectral lines observed in the solar corona [73], in a classical case of an answer that brings a more troublesome question. Since then, several mechanisms have been proposed [74–77], not only to comprehend the heating of the solar corona, but also the acceleration of the solar wind. Another unsolved problem that is directly connected to the inverted temperature profile of the solar corona and particle acceleration in the Sun, is regarding where and how the non-Maxwellian velocity distribution functions with suprathermal tails, observed in the solar wind, are formed⁴.

⁴The generation of suprathermal electrons in the lower corona and its consequences to the coronal heating problem are tackled in [78] (see [section 5.2](#)).

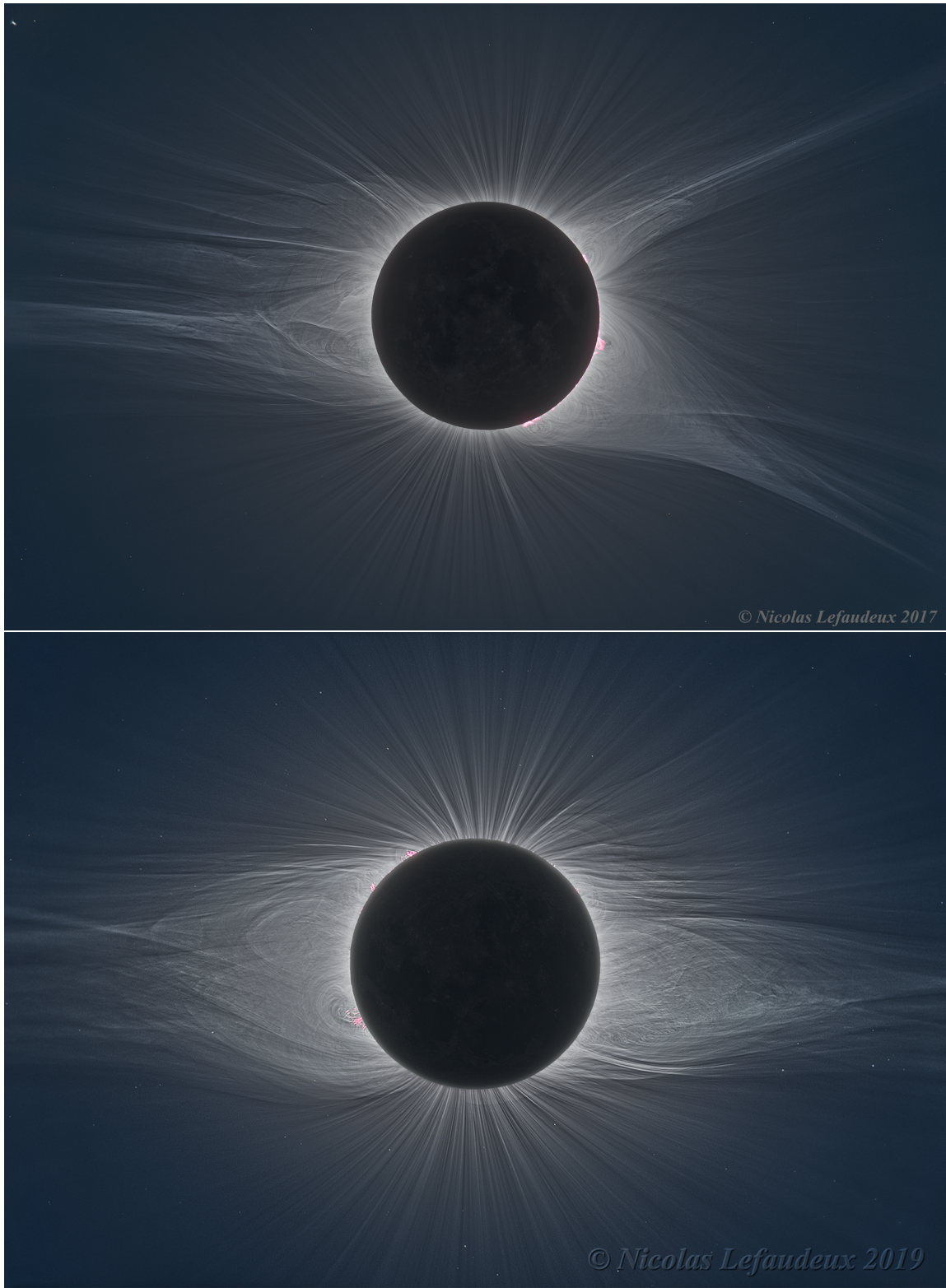


Figure 1.4: Solar corona captured during the total solar eclipse of 2017 (top panel) and 2019 (lower panel). The reddish contour at some regions is the chromosphere, and the reddish arcs are solar prominences, chromospheric plasma structures that penetrate the coronal region. Credit: [Nicolas Lefaudeux](#), accessed at 15/08/2019.

1.2 Thesis organization

Considering the context presented above, the working proposal of this PhD Thesis is to put forward the first numerical analysis of the new weak turbulence theory for collisional plasmas [52] and explore its applications in the solar physics scope. In Chapter 2, we make a brief review of the basic plasma kinetic theory for electrostatic oscillations. Chapter 3 revises the procedure for obtaining the weak turbulence equations for Langmuir and ion-sound waves and the quasilinear equation for the particle dynamics.

The main subject of this thesis is discussed in Chapter 4. In Section 4.1 we show the methodology used in the formulation of this new generalization and the outcome of its inclusion in the quasilinear wave equation, and in the particle kinetic equation. Section 4.2 describes the inclusion of the noneigenmode fluctuations in the nonlinear wave equations and the resulting terms, which are the main concern of the present analysis. In Chapter 5, we contextualize the present work regarding the theory discussed in the previous chapter and present the results obtained in appended papers. Chapter 6, summarizes the results and discuss some remarking conclusions obtained in this analysis. At the end of this chapter, we also elaborate on the perspectives for this new generalized formalism and its relevance for the next generation of solar physics research.

In the end, we have four appendices. Appendix A depicts an improved approximation for the second order susceptibility of the electrostatic bremsstrahlung for Langmuir waves. In Appendix B we discuss the similarities of the asymptotic equilibrium state of the Langmuir waves spectrum, considering a combination of an inverse power-law kappa distribution and a Maxwellian distribution, in the presence and the absence of the electrostatic bremsstrahlung effect. The discussion in Appendix B is related to the article appended in Appendix C, which is parallel research and is only slightly connected to the main subject of this work. Appendix D shows the paper that summarizes the results of my Master's dissertation, which may be considered the starting point of this doctoral research.

Chapter 2

Kinetic theory of plasmas

Plasmas are ionized gases that exhibit collective behavior. Composed of positive and negative charges and neutral particles, a plasma is said to be *neutral* when the quantity of particles with opposite charges is the same [79], and *nonneutral* when it is constituted - or have a significant excess - of one kind of charge [80]. For the present work, we assume a fully ionized hydrogen plasma, which is overall neutral and does not contain any neutral particle. In such a case, half the total number of particles is given by protons and the other half by electrons.

Electrons and ions are sources of electric and magnetic fields. Due to the long-range nature of these fields, particles can interact simultaneously, at distance, with several other particles in the system. The effective range of these interactions is determined by the *Debye length*

$$\lambda_{De} = \sqrt{\frac{k_B T_e}{4\pi n e^2}}, \quad (2.1)$$

where T_e is the electron temperature¹, k_B the Boltzmann constant, n the plasma density and e the electron charge. This means that a specific charge will interact effectively only with other charges that are inside of a virtual sphere with radius given by λ_{De} , being almost completely shielded from the influence of particles outside the *Debye sphere*. The self-consistent interaction between charged particles and electric and magnetic fields, creates fluctuations in the local neutrality of the plasma, giving rise to the series of oscillations and complex wave phenomena that characterize the plasma's collective behavior [4]. Describing the precise state of a plasma, in a given time, requires the knowledge of the $6N$ phase-space coordinates of each particle, and also the microscopic amplitudes of the electric and magnetic fields at each point in space [79]. Such exact representation is clearly a non-practical approach for a many-body system like the plasma. However, this microscopic formulation can be approximated to a macroscopic description by taking the average of the microscopic quantities and making suitable assumptions to truncate

¹Due to the high mobility, electrons are the main responsible for maintaining the Debye shielding. There are specific situations where this is not true [4], but they are outside of the scope of the current study.

the correlation functions at an appropriate point [79]. This will lead to the plasma kinetic equations, which is the first of a hierarchy of approximations that also includes the multi-fluid and magnetohydrodynamic theories. The application of each one of these formulations will depend on the context and the scale of the phenomena being described [4]. In this work we are interested in small-scale processes that depend on velocity-space properties, requiring a kinetic description of the plasma.

Based on the concepts and methods of statistical mechanics, together with the Maxwell equations, the kinetic theory is the most fundamental description of the plasma dynamics, providing a formal, self-consistent evolution of plasma processes. As in the case of neutral gases, the kinetic formalism of plasmas takes into account the variations of the velocity distribution function $f(\mathbf{r}, \mathbf{v}, t)$ in the phase-space, for each particle species. Statistically, this means that the product between the distribution function and the volume element in the hexa-dimensional phase-space $f_\alpha(\mathbf{r}, \mathbf{v}, t)d^3rd^3v$ represents the probability of finding a particle of species α in a volume element d^3r around \mathbf{r} and in a velocity volume element d^3v around \mathbf{v} , at the instant t [79].

Like in the case of non-ionized gases, the statistical description of the plasma dynamics is given by the Boltzmann equation

$$\frac{\partial f_\alpha(\mathbf{r}, \mathbf{v}, t)}{\partial t} + \mathbf{v} \cdot \nabla_{\mathbf{r}} f_\alpha(\mathbf{r}, \mathbf{v}, t) + \frac{\mathbf{F}}{m_\alpha} \cdot \nabla_{\mathbf{v}} f_\alpha(\mathbf{r}, \mathbf{v}, t) = \left(\frac{\partial f_\alpha(\mathbf{r}, \mathbf{v}, t)}{\partial t} \right)_{\text{coll}}. \quad (2.2)$$

Above, on the left-hand side, the differential vector operators $\nabla_{\mathbf{r}}$ and $\nabla_{\mathbf{v}}$ represent, respectively, the gradients in (x, y, z) space and (v_x, v_y, v_z) velocity coordinates. The quantity \mathbf{F} is the acting force in the system, and m_α is the mass of the particles of kind α , which, in a fully ionized plasma, can assume two values: electrons $\alpha = e$ and ions $\alpha = i$. The right-hand side depicts the temporal variation of the velocity distribution function due to collisions between the system's particles.

Collisional interactions are the central point of the present thesis. However, the formalism presented in Chapter 4, departs from the weak turbulence equations, which are the kinetic description of nonlinear, low-amplitude instabilities in a collisionless plasma. The contributions of the correlations between *source* fluctuations, which account for collisional interactions (see. [79, 81]), are then retrieved with the inclusion of noneigenmode contributions in the wave and particle kinetic equations². Therefore, at this point, it will be assumed that collisions can be neglected.

²For instance, in Section 4.1, it will be shown that including the noneigenmode fluctuations in the weak turbulence's formal particle kinetic equation leads to an expression that accounts for the collisional interactions that appear on the right-hand side of equation (2.2).

2.1 The Vlasov-Maxwell system of equations

In the absence of collisions, the plasma dynamics is given by the Vlasov-Maxwell system, which is composed of the Vlasov movement equation

$$\frac{\partial f_\alpha(\mathbf{r}, \mathbf{v}, t)}{\partial t} + \mathbf{v} \cdot \nabla_{\mathbf{r}} f_\alpha(\mathbf{r}, \mathbf{v}, t) + \frac{\mathbf{F}}{m_\alpha} \cdot \nabla_{\mathbf{v}} f_\alpha(\mathbf{r}, \mathbf{v}, t) = 0. \quad (2.3)$$

In the general case, the acting force in Eqs. (2.2) and (2.3) is given by the Lorentz force added by an external force, which, at kinetic scales, is also of electromagnetic nature. Therefore, in *cgs* units³, \mathbf{F} has the following form

$$\mathbf{F} = \sum_{\alpha} q_{\alpha} \left[\mathbf{E}(\mathbf{r}, t) + \frac{1}{c} \mathbf{v} \times \mathbf{B}(\mathbf{r}, t) \right] + \mathbf{F}_{\text{ext}}, \quad (2.4)$$

where q_{α} is the charge of the particles of kind α , and c is the speed of light. The quantities $\mathbf{E}(\mathbf{r}, t)$ and $\mathbf{B}(\mathbf{r}, t)$ are, respectively, the electric and magnetic fields, which are described by the Maxwell equations

$$\nabla \cdot \mathbf{E} = 4\pi\rho \quad (2.5)$$

$$\nabla \cdot \mathbf{B} = 0 \quad (2.6)$$

$$\nabla \times \mathbf{E} = -\frac{1}{c} \frac{\partial \mathbf{B}}{\partial t} \quad (2.7)$$

$$\nabla \times \mathbf{B} = \frac{4\pi}{c} \mathbf{J} + \frac{1}{c} \frac{\partial \mathbf{E}}{\partial t}. \quad (2.8)$$

In a statistical description, the charge density ρ and the current density \mathbf{J} depend on the velocity distribution function

$$\rho(\mathbf{r}, t) = \sum_{\alpha} q_{\alpha} \int_v f_{\alpha}(\mathbf{r}, \mathbf{v}, t) d^3 v \quad (2.9)$$

$$\mathbf{J}(\mathbf{r}, t) = \sum_{\alpha} q_{\alpha} \int_v \mathbf{v} f_{\alpha}(\mathbf{r}, \mathbf{v}, t) d^3 v. \quad (2.10)$$

Together, the expressions (2.3), (2.5), (2.6), (2.7), (2.8), (2.9) and (2.10) form a closed self-consistent set of coupled nonlinear equations, which is responsible for the description of a myriad of oscillatory processes that may occur in plasmas and how they affect (and are affected by) the velocity distribution function, in the absence of collisions. The solution of such complicated system will invariably depend on some degree of approximation.

Considering the extensive variety of nonlinear processes that might occur in a plasma, the appropriate way to deal with these equations will depend on intrinsic characteristics of the

³The use of cgs units will be consistent through all this work.

plasma and the nature of the phenomenon under consideration. For low amplitude oscillations in a fully ionized plasma, one may employ perturbation theory in order to solve the Vlasov equation [2].

2.2 Low amplitude electrostatic oscillations

We are interested in the presence of high-frequency electrostatic waves propagating in a homogeneous, fully ionized and unmagnetized plasma, which is initially in equilibrium. Under such conditions, we may consider $\mathbf{B} = \mathbf{0}$. Thus, the Vlasov equation takes the following form

$$\frac{\partial f_\alpha}{\partial t} + \mathbf{v} \cdot \nabla f_\alpha + \frac{q_\alpha}{m_\alpha} \mathbf{E} \cdot \nabla_{\mathbf{v}} f_\alpha = 0, \quad (2.11)$$

where the electric field is given by

$$\nabla \cdot \mathbf{E} = 4\pi \sum_\alpha q_\alpha \int_v f_\alpha(\mathbf{r}, \mathbf{v}, t) d^3 v. \quad (2.12)$$

Assuming low amplitude oscillations, we may approximate these equations by introducing a small first order perturbation into the initial velocity distribution function and, assuming $\mathbf{E}_0 = 0$, we introduce a small first order electric field :

$$f_\alpha(\mathbf{r}, \mathbf{v}, t) = f_{\alpha 0}(\mathbf{v}) + f_{\alpha 1}(\mathbf{r}, \mathbf{v}, t), \quad (2.13)$$

$$\mathbf{E}(\mathbf{r}, t) = \mathbf{E}_1(\mathbf{r}, t). \quad (2.14)$$

Until this point, the linear, quasilinear and nonlinear formulations are identical. For a further evaluation we must decide if substitute Eqs. (2.13) and (2.14) in Eq. (2.11) as they are and then eliminate all nonlinear terms in the Vlasov equation. Or if we take the average of Eqs. (2.13) and (2.14) and use the averaged quantities to keep some degree of nonlinearity in the movement equation. The subsequent deduction for each case was carefully detailed and discussed in Chapters 2 and 3 of Ref. [81]. Therefore, in order to maintain the focus on the objectives of the present work, we reproduce in the next chapter only a brief review of the deduction of the weak turbulence theory equations.

Chapter 3

Weak turbulence theory

The weak turbulence theory is what we may call a “borderline approach” because, despite the fact that it deals with some more intense instabilities, we must assure that these fluctuations are still inside the weak turbulence limit, i.e., that the turbulence is weak enough to be treated by a perturbative method. Such boundary is defined by a comparison between the averaged kinetic energy of the particles per volume unity $\mathcal{E}_{kin} = \bar{n}m < v^2 > /2$, and the energy density \mathcal{E}_f , which is associated with the fluctuations of the perturbative electric field. Thus, by “weak turbulence” we mean

$$\mathcal{E}_f \ll \mathcal{E}_{kin}, \quad (3.1)$$

that is, the energy density of the fluctuations must be much smaller than the kinetic energy density of the particles. This condition is related to the slow wave-growing assumption [11], which is central for the further development of nonlinear kinetic equations, as will be discussed further.

The following discussion is a reduced version of the comprehensive demonstration presented in Section 3.2 of Ref. [81]. We also use the same notation and logic sequence. Any deviation from [81] will be explained in a footnote.

3.1 Nonlinear kinetic equations

Let us consider the propagation of electrostatic oscillations in a homogeneous, unmagnetized and fully ionized plasma. Thus, in the absence of collisions, the movement equation is given by the electrostatic Vlasov equation

$$\frac{\partial f_a(\mathbf{r}, \mathbf{v}, t)}{\partial t} + \mathbf{v} \cdot \nabla f_a(\mathbf{r}, \mathbf{v}, t) + \frac{e_a}{m_a} \mathbf{E}(\mathbf{r}, t) \cdot \frac{\partial f_a(\mathbf{r}, \mathbf{v}, t)}{\partial \mathbf{v}} = 0, \quad (3.2)$$

where the electric field is given by

$$\nabla \cdot \mathbf{E}(\mathbf{r}, t) = 4\pi\hat{n} \sum_a e_a \int d^3v f_a(\mathbf{r}, \mathbf{v}, t). \quad (3.3)$$

In the above equations, f_a is the velocity distribution function, where the subscript “ a ” is the kind of particle: $a = i$ for ions and $a = e$ for electrons. For an overall neutral plasma, the average number density of the ions and the electrons is the same, $\hat{n} = \hat{n}_e = \hat{n}_i$.

Proceeding under the perturbative approach, we assume small fluctuations and write the velocity distribution function and the electric field as a sum of an equilibrium zero-order term and a small first-order fluctuation

$$\begin{aligned} f_a(\mathbf{r}, \mathbf{v}, t) &= F_a(\mathbf{v}) + \delta f_a(\mathbf{r}, \mathbf{v}, t) \\ \mathbf{E}(\mathbf{r}, t) &= \delta \mathbf{E}(\mathbf{r}, t), \end{aligned} \quad (3.4)$$

where the zero-order electric field is assumed to be zero and F_a is the equilibrium velocity distribution function.

Substituting (3.4) in (3.2) we obtain

$$\frac{\partial F_a}{\partial t} + \frac{e_a}{m_a} \delta \mathbf{E} \cdot \frac{\partial F_a}{\partial \mathbf{v}} + \frac{\partial \delta f_a}{\partial t} + \mathbf{v} \cdot \nabla \delta f_a + \frac{e_a}{m_a} \delta \mathbf{E} \cdot \frac{\partial \delta f_a}{\partial \mathbf{v}} = 0. \quad (3.5)$$

Taking the average¹ of Eq. (3.5), we obtain a kinetic equation for the time evolution of the equilibrium velocity distribution function

$$\frac{\partial F_a}{\partial t} = -\frac{e_a}{m_a} \left\langle \delta \mathbf{E} \cdot \frac{\partial \delta f_a}{\partial \mathbf{v}} \right\rangle. \quad (3.6)$$

Subtracting (3.6) from (3.5) we obtain an equation for the fluctuations

$$\frac{\partial \delta f_a}{\partial t} + \mathbf{v} \cdot \nabla \delta f_a + \frac{e_a}{m_a} \delta \mathbf{E} \cdot \frac{\partial F_a}{\partial \mathbf{v}} + \frac{e_a}{m_a} \left[\delta \mathbf{E} \cdot \frac{\partial \delta f_a}{\partial \mathbf{v}} - \left\langle \delta \mathbf{E} \cdot \frac{\partial \delta f_a}{\partial \mathbf{v}} \right\rangle \right] = 0. \quad (3.7)$$

It is interesting to mention that at this stage, Eqs. (3.6) and (3.7) are precisely the same as those leading to the quasilinear approximation. Thus, at this point, one must choose if the quasilinear approach is enough, or if a nonlinear formulation is necessary. In the first case all terms proportional to $\delta \mathbf{E} \delta f_a$ are neglected in the equation for the fluctuations². We shall keep these terms and proceed with the nonlinear approach.

Now, we assume the that fluctuations may be decomposed in terms of the Fourier-Laplace

¹For more details see subsection 3.1.1 of Ref. [81].

²See subsection 3.1.2 of [81].

transformation over the fast time-scale of the fluctuations, while amplitudes of the spectra vary in a slow time-scale

$$\begin{aligned}\delta f_a(\mathbf{r}, \mathbf{v}, t) &= \int d^3k \int_L d\omega \delta f_{\mathbf{k}, \omega}^a(\mathbf{v}, t) e^{i(\mathbf{k} \cdot \mathbf{r} - \omega t)}, \\ \delta f_{\mathbf{k}, \omega}^a(\mathbf{v}, t) &= \frac{1}{(2\pi)^4} \int d^3r \int_0^\infty dt \delta f_a(\mathbf{r}, \mathbf{v}, t) e^{-i(\mathbf{k} \cdot \mathbf{r} - \omega t)}, \\ \delta \mathbf{E}(\mathbf{r}, t) &= \int d^3k \int_L d\omega \delta \mathbf{E}_{\mathbf{k}, \omega}(t) e^{i(\mathbf{k} \cdot \mathbf{r} - \omega t)}, \\ \delta \mathbf{E}_{\mathbf{k}, \omega}(t) &= \frac{1}{(2\pi)^4} \int d^3r \int_0^\infty dt \delta \mathbf{E}(\mathbf{r}, t) e^{-i(\mathbf{k} \cdot \mathbf{r} - \omega t)},\end{aligned}\tag{3.8}$$

where the integration path is taken along L , stretching from $\omega = -\infty + i\sigma$ to $\omega = \infty + i\sigma$, in which $\sigma > 0$ and $\sigma \rightarrow 0$. We should emphasize that we assume slow and adiabatic time-dependence for the spectral amplitudes $\delta f_{\mathbf{k}, \omega}^a(\mathbf{v}, t)$ and $\delta \mathbf{E}(t)_{\mathbf{k}, \omega}$ in the above transformation.

The Fourier-Laplace transformation of nonlinear terms, where we have the product of two functions, is given by the convolution of these functions

$$\begin{aligned}\frac{1}{(2\pi)^4} \int d^3r \int dt \delta f_a(\mathbf{r}, \mathbf{v}, t) \delta \mathbf{E}(\mathbf{r}, t) e^{-i(\mathbf{k} \cdot \mathbf{r} - \omega t)} &= \int d^3k' \int d\omega' \delta f_{\mathbf{k}', \omega'}^a \delta \mathbf{E}_{\mathbf{k}-\mathbf{k}', \omega-\omega'} \\ &= \int d^3k' \int d\omega' \delta f_{\mathbf{k}-\mathbf{k}', \omega-\omega'}^a \delta \mathbf{E}_{\mathbf{k}', \omega'}.\end{aligned}\tag{3.9}$$

Applying these transformations to the Vlasov-Maxwell system, we obtain a set of hierarchical equations composed by the formal particle kinetic equation [22]

$$\frac{\partial F_a}{\partial t} = -\frac{e_a}{m_a} \frac{\partial}{\partial \mathbf{v}} \cdot \int d^3k \int d\omega \int d^3k' \int d\omega' \langle \delta \mathbf{E}_{\mathbf{k}', \omega'} \delta f_{\mathbf{k}, \omega}^a \rangle e^{i(\mathbf{k} + \mathbf{k}') \cdot \mathbf{r} - i(\omega + \omega')t};\tag{3.10}$$

the equation of the fluctuating distribution evolution

$$\begin{aligned}\left(\omega - \mathbf{k} \cdot \mathbf{v} + i \frac{\partial}{\partial t} \right) \delta f_{\mathbf{k}, \omega}^a &= -i \frac{e_a}{m_a} \delta \mathbf{E}_{\mathbf{k}, \omega} \cdot \frac{\partial F_a}{\partial \mathbf{v}} - i \frac{e_a}{m_a} \frac{\partial}{\partial \mathbf{v}} \cdot \int d^3k' \int d\omega' \\ &\times [\delta \mathbf{E}_{\mathbf{k}', \omega'} \delta f_{\mathbf{k}-\mathbf{k}', \omega-\omega'}^a - \langle \delta \mathbf{E}_{\mathbf{k}', \omega'} \delta f_{\mathbf{k}-\mathbf{k}', \omega-\omega'}^a \rangle];\end{aligned}\tag{3.11}$$

and the differential form of the Gauss law for the electric field fluctuations

$$\mathbf{k} \cdot \delta \mathbf{E}_{\mathbf{k}, \omega} = -4\pi \hat{n} i \sum_a e_a \int d^3v \delta f_{\mathbf{k}, \omega}^a.\tag{3.12}$$

The bracketed terms in Eqs. (3.10) and (3.11) represent the ensemble averages over the phases of the perturbation. One may notice that the above set of equations is not closed, since the solution for $\delta f_{\mathbf{k}, \omega}^a$ requires knowing the two-body correlation $\langle \delta f_{\mathbf{k}, \omega}^a \delta f_{\mathbf{k}', \omega'}^a \rangle$, which depends on the tertiary correlation $\langle \delta f_{\mathbf{k}, \omega}^a \delta f_{\mathbf{k}', \omega'}^a \delta f_{\mathbf{k}'', \omega''}^a \rangle$, and so on.

On the left-hand side of Eq. (3.10) we have retained the slow adiabatic derivative $i(\partial/\partial t)$. To deal with that we employ two-step approximation [22] and redefine the angular frequency $\omega \rightarrow \omega + i\partial/\partial t$. Then the equation for the perturbed distribution may be iteratively solved up to third order in electric field. The solution is then inserted into Eq. (3.12) and, under the assumption that there are random phases associated with the fluctuations, we take the appropriated ensembles averages. This procedure results in the nonlinear spectral balance equation. At this point, according to the two-time approximation, the slow time derivative is reintroduced [52]. We then obtain the nonlinear spectral balance equation³

$$\begin{aligned}
& \frac{i}{2} \frac{\partial \epsilon(\mathbf{k}, \omega)}{\partial \omega} \frac{\partial \langle \delta E^2 \rangle_{\mathbf{k}, \omega}}{\partial t} + \text{Re } \epsilon(\mathbf{k}, \omega) \langle \delta E^2 \rangle_{\mathbf{k}, \omega} + i \text{Im } \epsilon(\mathbf{k}, \omega) \langle \delta E^2 \rangle_{\mathbf{k}, \omega} \\
& - \frac{2}{\pi} \frac{1}{k^2 \epsilon^*(\mathbf{k}, \omega)} \sum_a e_a^2 \int d\mathbf{v} \delta(\omega - \mathbf{k} \cdot \mathbf{v}) F_a(\mathbf{v}) \\
= & -2 \int d\mathbf{k}' \int d\omega' \left\{ \left[\chi^{(2)}(\mathbf{k}', \omega' | \mathbf{k} - \mathbf{k}', \omega - \omega') \right]^2 \left[\frac{\langle \delta E^2 \rangle_{\mathbf{k}-\mathbf{k}', \omega-\omega'}}{\epsilon(\mathbf{k}', \omega')} \right. \right. \\
& \left. \left. + \frac{\langle \delta E^2 \rangle_{\mathbf{k}', \omega'}}{\epsilon(\mathbf{k} - \mathbf{k}', \omega - \omega')} \right] - \bar{\chi}^{(3)}(\mathbf{k}', \omega | -\mathbf{k}', -\omega' | \mathbf{k}, \omega) \langle \delta E^2 \rangle_{\mathbf{k}', \omega'} \right\} \langle \delta E^2 \rangle_{\mathbf{k}, \omega} \\
& + 2 \int d\mathbf{k}' \int d\omega' \frac{|\chi^{(2)}(\mathbf{k}', \omega' | \mathbf{k} - \mathbf{k}', \omega - \omega')|^2}{\epsilon^*(\mathbf{k}, \omega)} \langle \delta E^2 \rangle_{\mathbf{k}', \omega'} \langle \delta E^2 \rangle_{\mathbf{k}-\mathbf{k}', \omega-\omega'} \\
& - \frac{4}{\pi} \int d\mathbf{k}' \int d\omega' \frac{1}{k^2 |\epsilon(\mathbf{k}', \omega')|^2} \left[\frac{[\chi^{(2)}(\mathbf{k}', \omega' | \mathbf{k} - \mathbf{k}', \omega - \omega')]^2}{\epsilon(\mathbf{k} - \mathbf{k}', \omega - \omega')} \right] \langle \delta E^2 \rangle_{\mathbf{k}, \omega} \\
& - \frac{|\chi^{(2)}(\mathbf{k}', \omega' | \mathbf{k} - \mathbf{k}', \omega - \omega')|^2}{\epsilon^*(\mathbf{k}, \omega)} \left[\langle \delta E^2 \rangle_{\mathbf{k}-\mathbf{k}', \omega-\omega'} \right] \sum_a e_a^2 \int d\mathbf{v} \delta(\omega' - \mathbf{k} \cdot \mathbf{v}) F_a(\mathbf{v}) \\
& - \frac{4}{\pi} \int d\mathbf{k}' \int d\omega' \frac{1}{|\mathbf{k} - \mathbf{k}'|^2 |\epsilon(\mathbf{k} - \mathbf{k}', \omega - \omega')|^2} \left[\frac{[\chi^{(2)}(\mathbf{k}', \omega' | \mathbf{k} - \mathbf{k}', \omega - \omega')]^2}{\epsilon(\mathbf{k}', \omega')} \right] \langle \delta E^2 \rangle_{\mathbf{k}, \omega} \\
& - \frac{|\chi^{(2)}(\mathbf{k}', \omega' | \mathbf{k} - \mathbf{k}', \omega - \omega')|^2}{\epsilon^*(\mathbf{k}, \omega)} \left[\langle \delta E^2 \rangle_{\mathbf{k}', \omega'} \right] \sum_a e_a^2 \int d\mathbf{v} \delta(\omega - \omega' - (\mathbf{k} - \mathbf{k}') \cdot \mathbf{v}) F_a(\mathbf{v})
\end{aligned} \tag{3.13}$$

where on the left-hand side we have the expressions that correspond to the linear equation and on the right-hand side are the nonlinear expressions. The term

$$\epsilon(\mathbf{k}, \omega) = 1 + \sum_a \chi_a(\mathbf{k}, \omega) \tag{3.14}$$

is the linear dielectric response function.

In the above equations, $\sum_a \chi_a(\mathbf{k}, \omega)$ is the linear dielectric susceptibility, $\sum_a \chi_a^{(2)}(\mathbf{k}_1, \omega_1 | \mathbf{k}_2, \omega_2)$ is the second order nonlinear dielectric susceptibility and $\sum_a \bar{\chi}_a^{(3)}(\mathbf{k}_1, \omega_1 | \mathbf{k}_2, \omega_2 | \mathbf{k}_3, \omega_3)$ is the partial third-order nonlinear dielectric susceptibility. For particles of species a , the dielectric

³Equation (3.13) is not in the same form that appears in Refs. [22, 81]. The reason for this choice (see Eq. 2.59 of Ref. [52]), will become clear in the next chapter.

susceptibilities are respectively given by

$$\chi_a(\mathbf{k}, \omega) = -\frac{4\pi e_a \hat{n}_a}{k^2} \int d^3v \mathbf{k} \cdot \mathbf{g}_{\mathbf{k}, \omega} F_a, \quad (3.15)$$

$$\begin{aligned} \chi_a^{(2)}(\mathbf{k}_1, \omega_1 | \mathbf{k}_2, \omega_2) &= -\frac{1}{2} \frac{4\pi i e_a \hat{n}_a}{k_1 k_2 |\mathbf{k}_1 + \mathbf{k}_2|} \\ &\times \int d^3v \mathbf{g}_{\mathbf{k}_1 + \mathbf{k}_2, \omega_1 + \omega_2} [\mathbf{k}_1 (\mathbf{k}_2 \cdot \mathbf{g}_{\mathbf{k}_2, \omega_2}) + \mathbf{k}_2 (\mathbf{k}_1 \cdot \mathbf{g}_{\mathbf{k}_1, \omega_1})] F_a, \end{aligned} \quad (3.16)$$

$$\begin{aligned} \bar{\chi}_a^{(3)}(\mathbf{k}_1, \omega_1 | \mathbf{k}_2, \omega_2 | \mathbf{k}_3, \omega_3) &= -\frac{1}{2} \frac{4\pi i e_a \hat{n}_a}{k_1 k_2 k_3 |\mathbf{k}_1 + \mathbf{k}_2 + \mathbf{k}_3|} \\ &\times \int d^3v (\mathbf{g}_{\mathbf{k}_1 + \mathbf{k}_2 + \mathbf{k}_3, \omega_1 + \omega_2 + \omega_3} \cdot \mathbf{k}_1) \mathbf{g}_{\mathbf{k}_2 + \mathbf{k}_3, \omega_2 + \omega_3} \cdot [\mathbf{k}_2 (\mathbf{k}_3 \cdot \mathbf{g}_{\mathbf{k}_3, \omega_3}) + \mathbf{k}_3 (\mathbf{k}_2 \cdot \mathbf{g}_{\mathbf{k}_2, \omega_2})] F_a, \end{aligned} \quad (3.17)$$

where $\mathbf{g}_{\mathbf{k}, \omega}$ is a differential operator:

$$\mathbf{g}_{\mathbf{k}, \omega} \equiv -\frac{e_a}{m_a} \frac{1}{\omega - \mathbf{k} \cdot \mathbf{v} + i0} \frac{\partial}{\partial \mathbf{v}}. \quad (3.18)$$

Equation (3.13) is a general expression. The usual approach in plasma kinetic theory is to assume $|\text{Im } \epsilon(\mathbf{k}, \omega)| \ll |\text{Re } \epsilon(\mathbf{k}, \omega)|$. Then, the imaginary part of (3.13) leads to the wave kinetic equation, while the real part leads to the wave dispersion equation, whose solutions are the wave dispersion relations.

For the generalized particle kinetic equation is used a similar procedure. In this work, however, we use only the quasilinear approximation for the particle kinetic equation. Therefore, the nonlinear particle equation will be omitted here⁴. Then, in the quasilinear approximation, the particle kinetic equation is given by the following expression⁵ [52]

$$\begin{aligned} \frac{\partial F_a}{\partial t} &= \frac{\pi e_a^2}{m_a^2} \int d\mathbf{k} \int d\omega \left(\frac{\mathbf{k}}{k} \cdot \frac{\partial}{\partial \mathbf{v}} \right) \delta(\omega - \mathbf{k} \cdot \mathbf{v}) \\ &\times \left[\text{Im} \frac{m_a \epsilon(\mathbf{k}, \omega)}{2\pi^3 k |\epsilon(\mathbf{k}, \omega)|^2} F_a + \langle \delta E^2 \rangle_{\mathbf{k}, \omega} \left(\frac{\mathbf{k}}{k} \frac{\partial F_a}{\partial \mathbf{v}} \right) \right]. \end{aligned} \quad (3.19)$$

3.1.1 Wave kinetic equation for linear eigenmodes

Following the standard weak turbulence theory procedure, we assume slow wave amplification, which means that the wave growing process does not affect the plasma dynamics. Hence, the normal modes of oscillation are determined only by the linear response of the plasma, while the interactions among waves and particles are, in general, described by the nonlinear wave and particle kinetic equations. Thus, we have a theory that depicts nonlinear interactions between linear eigenmodes. The dispersion relations for linear normal modes are given by the solutions

⁴The generalized form can be seen at Refs. [22, 81]

⁵Equation (3.19) is not in the same form that appears in Refs. [22, 81]. The reason for this choice, which is based in Ref. [52], will become clear in the next chapter.

of the real part of the first term in Eq. (3.13)

$$0 = \operatorname{Re} \epsilon(\mathbf{k}, \omega) \langle \delta E^2 \rangle_{\mathbf{k}, \omega}. \quad (3.20)$$

Let us assume $\omega = \omega_{\mathbf{k}, \omega}^\alpha$ is the solution of the above expression. Once the dispersion relation has been calculated, we may write the spectral wave amplitude as follows

$$\langle \delta E^2 \rangle_{\mathbf{k}, \omega} = \sum_{\alpha} [I_{\mathbf{k}}^{+\alpha} \delta(\omega - \omega_{\mathbf{k}}^\alpha) + I_{\mathbf{k}}^{-\alpha} \delta(\omega + \omega_{\mathbf{k}}^\alpha)], \quad (3.21)$$

where the \pm signs represent the propagation direction of their respective normal modes, denoted by α . The eigenmodes will be given by the oscillation modes that satisfy the following condition

$$\epsilon(\mathbf{k}, \pm \omega_{\mathbf{k}, \omega}^\alpha) \approx 0. \quad (3.22)$$

In an unmagnetized plasma, there are two possible electrostatic eigenmodes: the Langmuir ($\alpha = L$) and ion-sound ($\alpha = S$) waves. Therefore, after careful considerations and extensive algebraic manipulations, the following kinetic equation for these waves is obtained⁶ [22, 23]

$$\begin{aligned} \frac{\partial I_{\mathbf{k}}^\alpha}{\partial t} = & - \frac{2\operatorname{Im} \epsilon(\mathbf{k}, \sigma\omega_{\mathbf{k}}^\alpha)}{\epsilon'(\mathbf{k}, \sigma\omega_{\mathbf{k}}^\alpha)} I_{\mathbf{k}}^\alpha + \sum_{a=e,i} \frac{4e^2}{k^2 [\epsilon'(\mathbf{k}, \sigma\omega_{\mathbf{k}}^\alpha)]^2} \int d\mathbf{v} \delta(\sigma\omega_{\mathbf{k}}^\alpha - \mathbf{k} \cdot \mathbf{v}) f_a(\mathbf{v}) \\ & - \sum_{\alpha, \beta} \sum_{\sigma'=\pm 1} \int d\mathbf{k}' A_{\alpha, \beta}(\mathbf{k}, \mathbf{k}') I_{\mathbf{k}'}^\beta I_{\mathbf{k}}^\alpha - \sum_{a=e,i} \frac{16e_a^2}{\epsilon'(\mathbf{k}, \sigma\omega_{\mathbf{k}}^\alpha)} \sum_{\sigma'=\pm 1} \sum_{\beta=L,S} \\ & \times \int d\mathbf{v} \int d\mathbf{k}' \frac{|\chi^{(2)}(\mathbf{k}', \sigma'\omega_{\mathbf{k}'}^\beta | \mathbf{k} - \mathbf{k}', \sigma\omega_{\mathbf{k}}^\alpha - \sigma'\omega_{\mathbf{k}'}^\beta)|^2}{|\mathbf{k} - \mathbf{k}'|^2 |\epsilon(\mathbf{k} - \mathbf{k}', \sigma\omega_{\mathbf{k}}^\alpha - \sigma'\omega_{\mathbf{k}'}^\beta)|^2} \\ & \times \left[\frac{I_{\mathbf{k}}^{\sigma\alpha}}{\epsilon(\mathbf{k}', \sigma'\omega_{\mathbf{k}'}^\beta)} - \frac{I_{\mathbf{k}'}^{\sigma'\beta}}{\epsilon'(\mathbf{k}, \sigma\omega_{\mathbf{k}}^\alpha)} \right] \delta[\sigma\omega_{\mathbf{k}}^\alpha - \sigma'\omega_{\mathbf{k}'}^\beta - (\mathbf{k} - \mathbf{k}') \cdot \mathbf{v}] f_a(\mathbf{v}) \\ & - 4\pi \sum_{\alpha, \beta, \gamma} \sum_{\sigma''=\pm 1} \int d\mathbf{k}' \frac{|\chi^{(2)}(\mathbf{k}', \sigma'\omega_{\mathbf{k}'}^\beta | \mathbf{k} - \mathbf{k}', \sigma''\omega_{\mathbf{k}-\mathbf{k}'}^\gamma)|^2}{\epsilon'(\mathbf{k}, \sigma\omega_{\mathbf{k}}^\alpha)} \\ & \times \left(\frac{I_{\mathbf{k}-\mathbf{k}'}^\gamma I_{\mathbf{k}}^\alpha}{\epsilon'(\mathbf{k}', \sigma'\omega_{\mathbf{k}'}^\beta)} + \frac{I_{\mathbf{k}'}^\beta I_{\mathbf{k}}^\alpha}{\epsilon'(\mathbf{k} - \mathbf{k}', \sigma''\omega_{\mathbf{k}-\mathbf{k}'}^\gamma)} - \frac{I_{\mathbf{k}'}^\beta I_{\mathbf{k}-\mathbf{k}'}^\gamma}{\epsilon'(\mathbf{k}, \sigma\omega_{\mathbf{k}}^\alpha)} \right) \delta(\sigma\omega_{\mathbf{k}}^\alpha - \sigma'\omega_{\mathbf{k}'}^\beta - \sigma''\omega_{\mathbf{k}-\mathbf{k}'}^\gamma), \end{aligned} \quad (3.23)$$

where the coefficient $A_{\alpha, \beta}(\mathbf{k}, \mathbf{k}')$ is given by

$$\begin{aligned} A_{\alpha, \beta}(\mathbf{k}, \mathbf{k}') = & \frac{4}{\epsilon'(\mathbf{k}, \sigma\omega_{\mathbf{k}}^\alpha)} \operatorname{Im} \left(2 \left[\chi^{(2)}(\mathbf{k}', \sigma'\omega_{\mathbf{k}'}^\beta | \mathbf{k} - \mathbf{k}', \sigma\omega_{\mathbf{k}}^\alpha - \sigma'\omega_{\mathbf{k}'}^\beta) \right]^2 \right. \\ & \left. \times \mathcal{P} \frac{1}{\epsilon(\mathbf{k} - \mathbf{k}', \sigma\omega_{\mathbf{k}}^\alpha - \sigma'\omega_{\mathbf{k}'}^\beta)} - \bar{\chi}^{(3)}(\mathbf{k}', \sigma'\omega_{\mathbf{k}'}^\beta | -\mathbf{k}', -\sigma'\omega_{\mathbf{k}'}^\beta | \mathbf{k}, \sigma\omega_{\mathbf{k}}^\alpha) \right), \end{aligned} \quad (3.24)$$

⁶Equation (3.23) is not in the same form that appears in Refs. [22, 81]. The reason for this choice, which is based in Ref. [52], will become clear in the next chapter.

and \mathcal{P} is the principal value of the integral where the coefficient belongs. In both expressions the following short-hand notation has been used

$$\epsilon'(\mathbf{k}, \sigma\omega_{\mathbf{k}}^{\alpha}) = \frac{\partial \text{Re } \epsilon(\mathbf{k}, \sigma\omega_{\mathbf{k}}^{\alpha})}{\partial \sigma\omega_{\mathbf{k}}^{\alpha}}. \quad (3.25)$$

On the right hand side of (3.23), in the first two terms we have the quasilinear wave-particle interaction, responsible for the induced and spontaneous emission processes. The third and fourth terms are nonlinear wave-particle interactions accounting for the induced and spontaneous scattering processes. The last term is the nonlinear wave-wave interaction describing the induced and spontaneous three wave-decay processes.

3.2 Weak turbulence equations for Langmuir and ion-sound waves

The further evaluation of Eq. (3.23) demands a careful analysis of the resonance conditions for each process and will not be addressed here⁷. In the following equations we show the complete wave kinetic equation for both (L) and (S) waves, in which the term describing the effects of spontaneous emission is already included.

For (L) waves we have:

$$\begin{aligned} \frac{\partial}{\partial t} \frac{I_{\mathbf{k}}^{\sigma L}}{\mu_{\mathbf{k}}^L} &= \mu_{\mathbf{k}}^L \frac{\omega_{pe}^2}{k^2} \int d^3 v \delta(\sigma\omega_{\mathbf{k}}^L - \mathbf{k} \cdot \mathbf{v}) \left(\hat{n} e^2 F_e(\mathbf{v}) + \pi (\sigma\omega_{\mathbf{k}}^L) \mathbf{k} \cdot \frac{\partial F_e(\mathbf{v})}{\partial \mathbf{v}} \frac{I_{\mathbf{k}}^{\sigma L}}{\mu_{\mathbf{k}}^L} \right) \\ &\quad - \pi \sigma \mu_{\mathbf{k}}^L \omega_{\mathbf{k}}^L \frac{e^2}{2T_e^2} \sum_{\sigma', \sigma''} \int d^3 k' \frac{\mu_{\mathbf{k}'}^L \mu_{\mathbf{k}-\mathbf{k}'}^S (\mathbf{k} \cdot \mathbf{k}')^2}{k^2 k'^2 |\mathbf{k} - \mathbf{k}'|^2} \left(\sigma' \omega_{\mathbf{k}'}^L \frac{I_{\mathbf{k}-\mathbf{k}'}^{\sigma'' S}}{\mu_{\mathbf{k}-\mathbf{k}'}^S} \frac{I_{\mathbf{k}}^{\sigma L}}{\mu_{\mathbf{k}}^L} \right. \\ &\quad \left. + \sigma'' \omega_{\mathbf{k}-\mathbf{k}'}^L \frac{I_{\mathbf{k}'}^{\sigma' L}}{\mu_{\mathbf{k}'}^L} \frac{I_{\mathbf{k}}^{\sigma L}}{\mu_{\mathbf{k}}^L} - \sigma \omega_{\mathbf{k}}^L \frac{I_{\mathbf{k}'}^{\sigma' L}}{\mu_{\mathbf{k}'}^L} \frac{I_{\mathbf{k}-\mathbf{k}'}^{\sigma'' S}}{\mu_{\mathbf{k}-\mathbf{k}'}^S} \right) \delta(\sigma\omega_{\mathbf{k}}^L - \sigma' \omega_{\mathbf{k}'}^L - \sigma'' \omega_{\mathbf{k}-\mathbf{k}'}^S) \\ &\quad + \sigma \omega_{\mathbf{k}}^L \frac{e^2}{m_e^2 \omega_{pe}^2} \sum_{\sigma'} \int d^3 k' \int d^3 v \frac{\mu_{\mathbf{k}}^L \mu_{\mathbf{k}'}^L (\mathbf{k} \cdot \mathbf{k}')^2}{k^2 k'^2} \delta[\sigma\omega_{\mathbf{k}}^L - \sigma' \omega_{\mathbf{k}'}^L - (\mathbf{k} - \mathbf{k}') \cdot \mathbf{v}] \\ &\quad \times \left[\hat{n} e^2 \left(\sigma \omega_{\mathbf{k}}^L \frac{I_{\mathbf{k}'}^{\sigma' L}}{\mu_{\mathbf{k}'}^L} - \sigma' \omega_{\mathbf{k}'}^L \frac{I_{\mathbf{k}}^{\sigma L}}{\mu_{\mathbf{k}}^L} \right) [F_e(\mathbf{v}) + F_i(\mathbf{v})] + \pi \frac{m_e}{m_i} \frac{I_{\mathbf{k}'}^{\sigma' L}}{\mu_{\mathbf{k}'}^L} \frac{I_{\mathbf{k}}^{\sigma L}}{\mu_{\mathbf{k}}^L} (\mathbf{k} - \mathbf{k}') \cdot \frac{\partial F_i(\mathbf{v})}{\partial \mathbf{v}} \right]. \end{aligned} \quad (3.26)$$

In the first line on the right-hand side of (3.26), one may recognize the quasilinear resonance condition $\delta(\sigma\omega_{\mathbf{k}}^L - \mathbf{k} \cdot \mathbf{v})$, which is responsible for the spontaneous emission process and the induced emission process, respectively. In the second and third lines we have the three wave-decay process, which can be recognized by the wave-wave resonance condition

⁷A comprehensive description of this process can be seen in subsection 3.2.3 and section 3.3 of [81].

$\delta(\sigma\omega_{\mathbf{k}}^L - \sigma'\omega_{\mathbf{k}'}^L - \sigma''\omega_{\mathbf{k}-\mathbf{k}'}^S)$ at the end of the third line. Inside the parenthesis, the first two terms depicts the induced wave-decay process, and the third term describes the spontaneous wave-decay process. In the last two lines we have the equations for the induced and spontaneous scattering processes. At the end of the fourth line is the nonlinear wave-particle resonance condition $\delta[\sigma\omega_{\mathbf{k}}^L - \sigma'\omega_{\mathbf{k}'}^L - (\mathbf{k} - \mathbf{k}') \cdot \mathbf{v}]$ and, in the last line, are the terms of spontaneous and induced scattering, respectively.

For (*S*) waves we have the same effects, in the same order:

$$\begin{aligned}
\frac{\partial}{\partial t} \frac{I_{\mathbf{k}}^{\sigma S}}{\mu_{\mathbf{k}}^S} &= \mu_{\mathbf{k}}^S \frac{\omega_{pe}^2}{k^2} \int d^3 v \delta(\sigma\omega_{\mathbf{k}}^S - \mathbf{k} \cdot \mathbf{v}) \left[\hat{n} e^2 [F_e(\mathbf{v}) + F_i(\mathbf{v})] \right. \\
&\quad \left. + \pi (\sigma\omega_{\mathbf{k}}^L) \left(\mathbf{k} \cdot \frac{\partial F_e(\mathbf{v})}{\partial \mathbf{v}} + \frac{m_e}{m_i} \mathbf{k} \cdot \frac{\partial F_i(\mathbf{v})}{\partial \mathbf{v}} \right) \frac{I_{\mathbf{k}}^{\sigma S}}{\mu_{\mathbf{k}}^S} \right] \\
&- \pi\sigma\omega_{\mathbf{k}}^L \frac{e^2}{4T_e^2} \sum_{\sigma',\sigma''} \int d^3 k' \frac{\mu_{\mathbf{k}}^S \mu_{\mathbf{k}'}^L \mu_{\mathbf{k}-\mathbf{k}'}^L [\mathbf{k}' \cdot (\mathbf{k} - \mathbf{k}')]^2}{k^2 k'^2 |\mathbf{k} - \mathbf{k}'|^2} \left(\sigma' \omega_{\mathbf{k}'}^L \frac{I_{\mathbf{k}-\mathbf{k}'}^{\sigma'' L}}{\mu_{\mathbf{k}-\mathbf{k}'}^L} \frac{I_{\mathbf{k}}^{\sigma S}}{\mu_{\mathbf{k}}^S} \right. \\
&\quad \left. + \sigma'' \omega_{\mathbf{k}-\mathbf{k}'}^L \frac{I_{\mathbf{k}'}^{\sigma' L} I_{\mathbf{k}}^{\sigma S}}{\mu_{\mathbf{k}'}^L \mu_{\mathbf{k}}^S} - \sigma\omega_{\mathbf{k}}^L \frac{I_{\mathbf{k}'}^{\sigma' L} I_{\mathbf{k}-\mathbf{k}'}^{\sigma'' L}}{\mu_{\mathbf{k}'}^L \mu_{\mathbf{k}-\mathbf{k}'}^L} \right) \delta(\sigma\omega_{\mathbf{k}}^S - \sigma'\omega_{\mathbf{k}'}^L - \sigma''\omega_{\mathbf{k}-\mathbf{k}'}^L) \quad (3.27) \\
&+ \sigma\omega_{\mathbf{k}}^L \frac{e^2}{m_e^2 \omega_{pe}^2} \sum_{\sigma'} \int d^3 k' \int d^3 v \frac{\mu_{\mathbf{k}}^S \mu_{\mathbf{k}'}^S (\mathbf{k} \cdot \mathbf{k}')^2}{k^4 k'^4 \lambda_{De}^4} \delta[\sigma\omega_{\mathbf{k}}^S - \sigma'\omega_{\mathbf{k}'}^S - (\mathbf{k} - \mathbf{k}') \cdot \mathbf{v}] \\
&\quad \times \left[\frac{\hat{n} e^2}{\omega_{pe}^2} W_{\mathbf{k},\mathbf{k}'} \left(\sigma\omega_{\mathbf{k}}^L \frac{I_{\mathbf{k}'}^{\sigma' S}}{\mu_{\mathbf{k}'}^S} - \sigma'\omega_{\mathbf{k}'}^L \frac{I_{\mathbf{k}}^{\sigma S}}{\mu_{\mathbf{k}}^S} \right) [F_e(\mathbf{v}) + F_i(\mathbf{v})] \right. \\
&\quad \left. + \pi \frac{m_e}{m_i} \left(W_{\mathbf{k},\mathbf{k}'} + \sigma \sigma' \frac{k'}{k} \right) \frac{I_{\mathbf{k}'}^{\sigma' S} I_{\mathbf{k}}^{\sigma S}}{\mu_{\mathbf{k}'}^S \mu_{\mathbf{k}}^S} (\mathbf{k} - \mathbf{k}') \cdot \frac{\partial F_i(\mathbf{v})}{\partial \mathbf{v}} \right].
\end{aligned}$$

In the scattering term we have

$$W_{\mathbf{k},\mathbf{k}'} = \left(1 + \frac{1}{\xi^2} \right)^2 \frac{1}{|\mathbf{k} - \mathbf{k}'|^4 \lambda_{De}^4 |\epsilon_{\parallel}(\mathbf{k} - \mathbf{k}', \sigma\omega_{\mathbf{k}}^S - \sigma'\omega_{\mathbf{k}'}^S)|^2}, \quad (3.28)$$

where

$$\epsilon_{\parallel}(\mathbf{k} - \mathbf{k}', \sigma\omega_{\mathbf{k}}^S - \sigma'\omega_{\mathbf{k}'}^S) = 1 + \frac{2(\mathbf{k} \cdot \mathbf{k}' - \sigma\sigma' k' k)}{|\mathbf{k} - \mathbf{k}'|^2 (k - \sigma\sigma' k')^2 \lambda_{De}^2} \quad (3.29)$$

$$+ i \left(\frac{\pi m_e}{2 m_i} \right)^{1/2} \left[\exp \left(-\frac{m_e \xi}{m_i} \frac{\pi}{2} \right) + \left(\frac{m_i T_e^3}{m_e T_i^3} \right)^{1/2} \exp \left(-\frac{T_e \xi}{T_i} \frac{\pi}{2} \right) \right],$$

with

$$\xi = \frac{(\sigma k - \sigma' k')^2}{|\mathbf{k} - \mathbf{k}'|^2}. \quad (3.30)$$

Though Eq. (3.27) depicts the full wave kinetic equation for ion-sound waves, the scattering term has always been neglected and will not be considered in this work as well. The reason for that is that the scattering of ion-sound waves caused by other ion-sound waves evolves

in a very slow time-scale. Indeed, we are interested in describing collisional processes, which act in a long evolution time. However, one must take one step at a time, and we do not discard including ion-sound scattering in future analysis.

The particle kinetic equation is given by

$$\begin{aligned} \frac{\partial F_a(\mathbf{v})}{\partial t} = & \frac{\pi e_a^2}{m_a^2} \sum_{\sigma} \sum_{\alpha=L,S} \int d^3k \left(\frac{\mathbf{k}}{k} \cdot \frac{\partial}{\partial \mathbf{v}} \right) \mu_{\mathbf{k}}^{\alpha} \delta(\sigma \omega_{\mathbf{k}}^{\alpha} - \mathbf{k} \cdot \mathbf{v}) \\ & \times \left(\frac{m_a}{4\pi^2} \frac{\sigma \omega_{\mathbf{k}}^L}{k} F_a(\mathbf{v}) + \frac{I_{\mathbf{k}}^{\sigma\alpha}}{\mu_{\mathbf{k}}^{\alpha}} \frac{\mathbf{k}}{k} \cdot \frac{\partial F_a(\mathbf{v})}{\partial \mathbf{v}} \right), \end{aligned} \quad (3.31)$$

where $a = i$ for ions and $a = e$ for electrons, and $\alpha = L, S$.

The following approximations and definitions were used to write the above equations

$$\begin{aligned} \frac{1}{\epsilon'_{\parallel}(\mathbf{k}, \sigma \omega_{\mathbf{k}}^L)} &= \frac{\sigma \mu_{\mathbf{k}}^L \omega_{\mathbf{k}}^L}{2}, & \frac{1}{\epsilon'_{\parallel}(\mathbf{k}, \sigma \omega_{\mathbf{k}}^S)} &= \frac{\sigma \mu_{\mathbf{k}}^S \omega_{\mathbf{k}}^L}{2}, \\ \mu_{\mathbf{k}}^L &= 1, & \mu_{\mathbf{k}}^S &= |k|^3 \lambda_{De}^3 \left(\frac{m_e}{m_i} \right)^{1/2} \left(1 + \frac{3T_i}{T_e} \right)^{1/2}. \end{aligned}$$

Chapter 4

Weak turbulence for collisional plasmas

In Chapter 3 we made a brief review of the standard weak turbulence theory procedure. Such procedure takes into account only the contributions from the linear eigenmodes. The basic premise of this conventional approach claims that only frequencies $\omega = \omega_{\mathbf{k}}$ that satisfy the dispersion relations are considered significant, even if the general electrostatic fluctuations $\langle \delta E^2 \rangle_{\mathbf{k},\omega}$ are characterized by all \mathbf{k} and ω . Therefore, the fluctuations with $\omega \neq \omega_{\mathbf{k}}$, which characterize the noneigenmodes, are ignored. In Ref. [52] the authors present a generalization of this customary approach, where, besides the traditional inclusion of the normal modes, it is also taken into account the contribution from the noneigenmode fluctuations. The result is a generalized expression for the spectral energy density of the waves, with some remarkable consequences for the wave and particle kinetic equations.

The generalized spectral energy density, which contains the noneigenmode contribution, is the central factor of this new kinetic turbulence theory for collisional plasmas. When it is substituted in the nonlinear terms of the nonlinear spectral balance equation, three new terms appear in the wave kinetic equation. The first term is an extension for the spontaneous scattering equation. The second term is a new, rigorous expression for the collisional damping rate of plasma waves. The third term depicts a hitherto unknown process of electrostatic radiation emission, in the eigenmode frequency range, due to particle scattering. This underlying electrostatic form of braking radiation was called *electrostatic bremsstrahlung* [52]. For the particle kinetic equation, the application of this generalized expression is responsible for the arising of the Balescu-Lenard collision integral, without any *ad hoc* addition.

In this chapter, we provide a basic outline of the elaborated demonstration imparted by the authors of [52]. We start by showing how the noneigenmodes contribution is included in the spectral energy density of the waves. Then we show that the inclusion of the noneigenmodes does not affect the quasilinear wave kinetic equation. In the next two subsections, we exhibit, without entering in details, the effects of the new contribution to the particle kinetic equation

and the nonlinear particle kinetic equation.

4.1 Inclusion of noneigenmodes

Let us start considering the linear part of the spectral balance equation, which corresponds to the left-hand side of Eq. (3.13)

$$\begin{aligned} \frac{1}{2} \frac{\partial \operatorname{Re} \epsilon(\mathbf{k}, \omega)}{\partial \omega} \frac{\partial \langle \delta E^2 \rangle_{\mathbf{k}, \omega}}{\partial t} + \operatorname{Re} \epsilon(\mathbf{k}, \omega) \langle \delta E^2 \rangle_{\mathbf{k}, \omega} + i \operatorname{Im} \epsilon(\mathbf{k}, \omega) \langle \delta E^2 \rangle_{\mathbf{k}, \omega} \\ = \frac{2}{\pi} \frac{1}{k^2 \epsilon^*(\mathbf{k}, \omega)} \sum_a e_a^2 \int d\mathbf{v} \delta(\omega - \mathbf{k} \cdot \mathbf{v}) f_a(\mathbf{v}), \end{aligned} \quad (4.1)$$

where the dielectric constant is given by

$$\epsilon(\mathbf{k}, \omega) = \sum_a \frac{4\pi e_a^2}{m_a k^2} \int d\mathbf{v} \frac{\mathbf{k} \cdot \partial f_a / \partial \mathbf{v}}{\omega - \mathbf{k} \cdot \mathbf{v} + i0}. \quad (4.2)$$

Then, taking the real part of (4.1), we have

$$\operatorname{Re} \epsilon(\mathbf{k}, \omega) \left[\langle \delta E^2 \rangle_{\mathbf{k}, \omega} - \frac{2}{\pi} \frac{1}{k^2 |\epsilon(\mathbf{k}, \omega)|^2} \sum_a e_a^2 \int d\mathbf{v} \delta(\omega - \mathbf{k} \cdot \mathbf{v}) f_a(\mathbf{v}) \right] = 0. \quad (4.3)$$

In the above equation we have two possibilities for the wave-number frequency space. If one is interested in the region of (\mathbf{k}, ω) in which $|\epsilon(\mathbf{k}, \omega)|^2 \neq 0$, then the left- and right-hand sides of (4.3) may be balanced by writing

$$\langle \delta E^2 \rangle_{\mathbf{k}, \omega} = \langle \delta E^2 \rangle_{\mathbf{k}, \omega}^0, \quad (4.4)$$

where

$$\langle \delta E^2 \rangle_{\mathbf{k}, \omega}^0 \equiv \frac{2}{\pi} \frac{1}{k^2 |\epsilon(\mathbf{k}, \omega)|^2} \sum_a e_a^2 \int d\mathbf{v} \delta(\omega - \mathbf{k} \cdot \mathbf{v}) f_a(\mathbf{v}). \quad (4.5)$$

It is clear that the solution of (4.4) depends on the denominator $|\epsilon(\mathbf{k}, \omega)|^2$ not being zero. For eigenmodes, however, $\epsilon(\mathbf{k}, \omega_k^\alpha) = 0$, meaning the denominator remains nonzero only if $\omega \neq \omega_k^\alpha$, i.e., if ω does not satisfy the dispersion relation. Hence, the electric field fluctuation $\langle \delta E^2 \rangle_{\mathbf{k}, \omega}^0$ must represent noneigenmodes contribution. As exposed in Section 3.1 the standard theory is concerned only with the normal oscillation modes, which are the solutions of the dispersion relations, calculated in the vicinity of the zeros of $\operatorname{Re} \epsilon(\mathbf{k}, \omega)$.

Therefore, we have two distinct situations. One is the situation in which collective modes are not important, and the electric field energy can be expressed by Eq. (4.4) with the electric field fluctuation $\langle \delta E^2 \rangle_{\mathbf{k}, \omega}^0$ given by (4.5). The other is standard situation, in which collective

modes are important, and the wave electric field is determined by

$$\begin{aligned} \langle \delta E^2 \rangle_{\mathbf{k}, \omega} - \langle \delta E^2 \rangle_{\mathbf{k}, \omega}^0 &= \sum_{\sigma=\pm 1} \sum_{\alpha=L, S} I_{\mathbf{k}}^{\sigma \alpha} \delta(\omega - \sigma \omega_{\mathbf{k}}^{\alpha}) \\ \operatorname{Re} \epsilon(\mathbf{k}, \sigma \omega_{\mathbf{k}}^{\alpha}) &= 0. \end{aligned} \quad (4.6)$$

The theory that we are analyzing is a generalization of the standard weak turbulence theory, in which both the eigenmode and noneigenmode are included by defining the following quantity

$$\Psi_{\mathbf{k}, \omega} \equiv \langle \delta E^2 \rangle_{\mathbf{k}, \omega} - \langle \delta E^2 \rangle_{\mathbf{k}, \omega}^0. \quad (4.7)$$

Thus, the function $\Psi_{\mathbf{k}, \omega}$ becomes the total eigenfunction of Eq. (4.3):

$$\operatorname{Re} \epsilon(\mathbf{k}, \omega) \Psi_{\mathbf{k}, \omega} = 0, \quad (4.8)$$

where $\Psi_{\mathbf{k}, \omega}$ can be expressed as

$$\Psi_{\mathbf{k}, \omega} = \sum_{\sigma=\pm 1} \sum_{\alpha=L, S} I_{\mathbf{k}}^{\sigma \alpha} \delta(\omega - \sigma \omega_{\mathbf{k}}^{\alpha}), \quad (4.9)$$

with the eigenvalue $\sigma \omega_{\mathbf{k}}^{\alpha}$ satisfying

$$\operatorname{Re} \epsilon(\mathbf{k}, \sigma \omega_{\mathbf{k}}^{\alpha}) = 0. \quad (4.10)$$

The procedure described above encompasses the two possibilities under analysis in this work by generalizing Eq. (3.21) to take into account the noneigenmode contribution, given by Eq. (4.5), along with Eq. (4.9) for the collective modes that satisfy the eigenmode condition, resulting in the following expression

$$\langle \delta E^2 \rangle_{\mathbf{k}, \omega} = \langle \delta E^2 \rangle_{\mathbf{k}, \omega}^0 + \sum_{\sigma=\pm 1} \sum_{\alpha=L, S} I_{\mathbf{k}}^{\sigma \alpha} \delta(\omega - \sigma \omega_{\mathbf{k}}^{\alpha}). \quad (4.11)$$

4.1.1 Absence of noneigenmode contribution to quasilinear wave kinetic equation

Let us start by including the noneigenmode term in the quasilinear wave kinetic equation. Substituting Eq. (4.11) in the imaginary part of Eq. (4.1), we have

$$\begin{aligned} &\frac{\partial \operatorname{Re} \epsilon(\mathbf{k}, \omega)}{\partial \omega} \frac{\partial \langle \delta E^2 \rangle_{\mathbf{k}, \omega}^0}{\partial t} + 2 \operatorname{Im} \epsilon(\mathbf{k}, \omega) \langle \delta E^2 \rangle_{\mathbf{k}, \omega}^0 + \sum_{\sigma=\pm 1} \sum_{\alpha} \left[\frac{\partial \operatorname{Re} \epsilon(\mathbf{k}, \sigma \omega_{\mathbf{k}}^{\alpha})}{\partial (\sigma \omega_{\mathbf{k}}^{\alpha})} \frac{\partial I_{\mathbf{k}}^{\sigma \alpha}}{\partial t} \right. \\ &\left. + 2 \operatorname{Im} \epsilon(\mathbf{k}, \sigma \omega_{\mathbf{k}}^{\alpha}) I_{\mathbf{k}}^{\sigma \alpha} \right] \delta(\omega - \sigma \omega_{\mathbf{k}}^{\alpha}) = \operatorname{Im} \frac{4}{\pi k^2 \epsilon^*(\mathbf{k}, \omega)} \sum_a e_a^2 \int d\mathbf{v} \delta(\omega - \mathbf{k} \cdot \mathbf{v}) f_a(\mathbf{v}). \end{aligned} \quad (4.12)$$

Making use of

$$\begin{aligned}\frac{1}{\epsilon(\mathbf{k}, \omega)} &= \mathcal{P} \frac{1}{\epsilon(\mathbf{k}, \omega)} - \sum_{\sigma=\pm 1} \sum_{\alpha=L,S} \frac{i\pi\delta(\omega - \sigma\omega_{\mathbf{k}}^{\alpha})}{\epsilon'(\mathbf{k}, \omega)} \\ \frac{1}{\epsilon^*(\mathbf{k}, \omega)} &= \mathcal{P} \frac{1}{\epsilon^*(\mathbf{k}, \omega)} + \sum_{\sigma=\pm 1} \sum_{\alpha=L,S} \frac{i\pi\delta(\omega - \sigma\omega_{\mathbf{k}}^{\alpha})}{\epsilon'(\mathbf{k}, \omega)},\end{aligned}\quad (4.13)$$

where

$$\epsilon'(\mathbf{k}, \omega) = \partial \operatorname{Re} \epsilon(\mathbf{k}, \omega) / \partial \omega,$$

we obtain

$$\begin{aligned}\epsilon'(\mathbf{k}, \omega) \frac{\partial \langle \delta E^2 \rangle_{\mathbf{k}, \omega}^0}{\partial t} + \operatorname{Im} \frac{4}{\pi k^2 \epsilon^*(\mathbf{k}, \omega)} \sum_a e_a^2 \int d\mathbf{v} \delta(\omega - \mathbf{k} \cdot \mathbf{v}) f_a(\mathbf{v}) \\ + \sum_{\sigma=\pm 1} \sum_{\alpha} \left[\epsilon'(\mathbf{k}, \sigma\omega_{\mathbf{k}}^{\alpha}) \frac{\partial I_{\mathbf{k}}^{\sigma\alpha}}{\partial t} + 2 \operatorname{Im} \epsilon(\mathbf{k}, \sigma\omega_{\mathbf{k}}^{\alpha}) I_{\mathbf{k}}^{\sigma\alpha} \right] \delta(\omega - \sigma\omega_{\mathbf{k}}^{\alpha}) \\ = \operatorname{Im} \mathcal{P} \frac{4}{\pi k^2 \epsilon^*(\mathbf{k}, \omega)} \sum_a e_a^2 \int d\mathbf{v} \delta(\omega - \mathbf{k} \cdot \mathbf{v}) f_a(\mathbf{v}) \\ + \sum_{\sigma=\pm 1} \sum_{\alpha} \frac{4\delta(\omega - \mathbf{k} \cdot \mathbf{v})}{k^2 \epsilon'(\mathbf{k}, \sigma\omega_{\mathbf{k}}^{\alpha})} \sum_a e_a^2 \int d\mathbf{v} \delta(\omega - \mathbf{k} \cdot \mathbf{v}) f_a(\mathbf{v}).\end{aligned}\quad (4.14)$$

According to the definition (4.5), the argument of the dielectric constant excludes the eigenmodes. Hence, the second term on the left-hand side of Eq. (4.14) is implicitly taken with the principal value, which means it cancels out the first term of the right-hand side. Thus, by assuming $\partial \langle \delta E^2 \rangle_{\mathbf{k}, \omega}^0 / \partial t = 0$, and removing the common factor $\sum_{\sigma=\pm 1} \sum_{\alpha} \delta(\omega - \sigma\omega_{\mathbf{k}}^{\alpha})$, we are left with

$$\epsilon'(\mathbf{k}, \sigma\omega_{\mathbf{k}}^{\alpha}) \frac{\partial I_{\mathbf{k}}^{\sigma\alpha}}{\partial t} + 2 \operatorname{Im} \epsilon(\mathbf{k}, \sigma\omega_{\mathbf{k}}^{\alpha}) I_{\mathbf{k}}^{\sigma\alpha} = \frac{4}{k^2 \epsilon'(\mathbf{k}, \sigma\omega_{\mathbf{k}}^{\alpha})} \sum_a e_a^2 \int d\mathbf{v} \delta(\omega - \mathbf{k} \cdot \mathbf{v}) f_a(\mathbf{v}). \quad (4.15)$$

And, rearranging Eq. (4.15), we obtain

$$\frac{\partial I_{\mathbf{k}}^{\sigma\alpha}}{\partial t} = -\frac{2 \operatorname{Im} \epsilon(\mathbf{k}, \sigma\omega_{\mathbf{k}}^{\alpha})}{\epsilon'(\mathbf{k}, \sigma\omega_{\mathbf{k}}^{\alpha})} I_{\mathbf{k}}^{\sigma\alpha} + \frac{4}{k^2 [\epsilon'(\mathbf{k}, \sigma\omega_{\mathbf{k}}^{\alpha})]^2} \sum_a e_a^2 \int d\mathbf{v} \delta(\omega - \mathbf{k} \cdot \mathbf{v}) f_a(\mathbf{v}), \quad (4.16)$$

that is equivalent to the first two terms of Eq. (3.23), which describe the effects of spontaneous and induced emissions, respectively. Both processes are determined by the linear wave-particle resonance conditions $\sigma\omega_{\mathbf{k}}^{\alpha} - \mathbf{k} \cdot \mathbf{v} = 0$. Therefore, we may conclude that noneigenmodes do not alter the quasilinear wave kinetic equation.

4.1.2 Noneigenmode contribution to particle kinetic equation

For the particle kinetic equation, however, the outcome is different. In this case, the inclusion of noneigenmode field fluctuations leads to the rigorous Balescu-Lenard collision

integral, resulting in the merge of two essential formulations of the plasma kinetic theory, without any *ad hoc* addition. The procedure starts by inserting the generalized wave electric field intensity, given by Eq. (4.11), in Eq. (3.19)

$$\begin{aligned} \frac{\partial f_a}{\partial t} = & \frac{\pi e_a^2}{m_a^2} \int d\mathbf{k} \int d\omega \left(\frac{\mathbf{k}}{k} \cdot \frac{\partial}{\partial \mathbf{v}} \right) \delta(\omega - \mathbf{k} \cdot \mathbf{v}) \left[\text{Im} \mathcal{P} \frac{m_a}{2\pi^3 k \epsilon^*(\mathbf{k}, \omega)} f_a(\mathbf{v}) \right. \\ & + \frac{2}{\pi k^2 |\epsilon(\mathbf{k}, \omega)|^2} \sum_b e_b^2 \int d\mathbf{v}' \delta(\omega - \mathbf{k} \cdot \mathbf{v}') f_b(\mathbf{v}') \left(\frac{\mathbf{k}}{k} \cdot \frac{\partial f_a(\mathbf{v})}{\partial \mathbf{v}} \right) \\ & \left. + \sum_{\sigma} \sum_{\alpha} \frac{\pi m_a \delta(\omega - \sigma \omega_{\mathbf{k}}^{\alpha})}{2\pi^3 k \epsilon'(\mathbf{k}, \sigma \omega_{\mathbf{k}}^{\alpha})} f_a(\mathbf{v}) + \sum_{\sigma} \sum_{\alpha} I_{\mathbf{k}}^{\sigma\alpha} \delta(\omega - \sigma \omega_{\mathbf{k}}^{\alpha}) \left(\frac{\mathbf{k}}{k} \cdot \frac{\partial f_a(\mathbf{v})}{\partial \mathbf{v}} \right) \right]. \end{aligned} \quad (4.17)$$

Proceeding with the ω integration, we redefine the velocity distribution function by taking the ambient density factor out

$$f_a(\mathbf{v}) = \hat{n} F_a(\mathbf{v}), \quad \int d^3 v F_a(\mathbf{v}) = 1, \quad (4.18)$$

and, making explicit use of the definition for $\text{Im} \epsilon(\mathbf{k}, \omega)$:

$$\text{Im} \epsilon(\mathbf{k}, \omega) = -\pi \sum_{\alpha} \frac{4\hat{n}\pi e_a^2}{m_a k^2} \int d\mathbf{v} \mathbf{k} \cdot \frac{\partial F_a}{\partial \mathbf{v}} \delta(\omega - \mathbf{k} \cdot \mathbf{v}),$$

we obtain the following form of the generalized particle kinetic equation including both the eigenmode and noneigenmode contributions [52]

$$\begin{aligned} \frac{\partial F_a(\mathbf{v})}{\partial t} = & \sum_b \frac{2e_a^2 e_b^2 n_b}{m_a} \frac{\partial}{\partial v_i} \int d\mathbf{k} \int d\mathbf{v}' \frac{k_i k_j}{k^4} \frac{\delta(\mathbf{k} \cdot \mathbf{v} - \mathbf{k} \cdot \mathbf{v}')}{|\epsilon(\mathbf{k}, \mathbf{k} \cdot \mathbf{v})|^2} \\ & \times \left(\frac{\partial}{\partial v_j} - \frac{m_a}{m_b} \frac{\partial}{\partial v'_j} \right) F_a(\mathbf{v}) F_b(\mathbf{v}') \\ & + \frac{\pi e_a^2}{m_a^2} \sum_{\sigma} \sum_{\alpha=L,S} \int d\mathbf{k} \left(\frac{\mathbf{k}}{k} \cdot \frac{\partial}{\partial \mathbf{v}} \right) \delta(\sigma \omega_{\mathbf{k}}^{\alpha} - \mathbf{k} \cdot \mathbf{v}) \\ & \times \left(\frac{m_a}{2\pi^2 k \epsilon'(\mathbf{k}, \sigma \omega_{\mathbf{k}}^L)} F_a(\mathbf{v}) + I_{\mathbf{k}}^{\sigma\alpha} \frac{\mathbf{k}}{k} \cdot \frac{\partial F_a(\mathbf{v})}{\partial \mathbf{v}} \right), \end{aligned} \quad (4.19)$$

where the first term on the right-hand side is the contribution of the noneigenmode inclusion in the particle kinetic equation and, as mentioned before, corresponds to the Balescu-Lenard collision integral. The other term is the usual quasilinear particle equation, which contains the velocity friction term, related with the spontaneous emission process, and the velocity space diffusion term.

In Eq. (4.19), the linear response $|\epsilon(\mathbf{k}, \mathbf{k} \cdot \mathbf{v})|^2$ in the denominator of the Balescu-Lenard integral can be approximated under the assumption that the most important contributions to the noneigenmode fluctuations is in the region around $v = 0$, i.e., the region with the highest

concentration of particles in the velocity distribution function. Therefore, we may treat these various angular frequency arguments as if they have the basic form of $\mathbf{k} \cdot \mathbf{v} \approx 0$ and approximate the collision integral as

$$\epsilon(\mathbf{k}, \mathbf{k} \cdot \mathbf{v}) \approx \epsilon(\mathbf{k}, 0) = 1 + \sum_a \frac{2\omega_{pa}^2}{k^2 v_{Ta}^2} = 1 + \frac{2\omega_{pe}^2}{k^2 v_{Te}^2} \left(1 + \frac{T_e}{T_i}\right), \quad (4.20)$$

where $\omega_{pe} = \sqrt{4\pi n_e e^2 / m_e}$ is the plasma frequency, $v_{Te} = \sqrt{2T_e / m_e}$ is the electron thermal velocity, and T_e and T_i are, respectively, the electron and ion temperature expressed in units of energy. This leads to

$$\begin{aligned} \frac{\partial F_a(\mathbf{v})}{\partial t} &= \sum_b \frac{2e_a^2 e_b^2 n_b}{m_a} \frac{\partial}{\partial v_i} \int d\mathbf{k} \int d\mathbf{v}' \frac{k_i k_j \lambda_{De}^4 \delta(\mathbf{k} \cdot \mathbf{v} - \mathbf{k} \cdot \mathbf{v}')}{|1 + T_e/T_i + k^2 \lambda_{De}^2|^2} \\ &\quad \times \left(\frac{\partial}{\partial v_j} - \frac{m_a}{m_b} \frac{\partial}{\partial v'_j} \right) F_a(\mathbf{v}) F_b(\mathbf{v}') \\ &+ \frac{\pi e_a^2}{m_a^2} \sum_{\sigma} \sum_{\alpha=L,S} \int d\mathbf{k} \left(\frac{\mathbf{k}}{k} \cdot \frac{\partial}{\partial \mathbf{v}} \right) \delta(\sigma \omega_{\mathbf{k}}^{\alpha} - \mathbf{k} \cdot \mathbf{v}) \\ &\quad \times \left(\frac{m_a}{2\pi^2 k \epsilon'(\mathbf{k}, \sigma \omega_{\mathbf{k}}^L)} F_a(\mathbf{v}) + I_{\mathbf{k}}^{\sigma \alpha} \frac{\mathbf{k}}{k} \cdot \frac{\partial F_a(\mathbf{v})}{\partial \mathbf{v}} \right), \end{aligned} \quad (4.21)$$

where $\lambda_{De} = \sqrt{T_e / 4\pi n_e e^2}$ is the Debye length.

The collision integral also has a further approximation where, assuming $2[\omega_{pe}/kv_{Te}]^2 \ll 1$, the linear response function can be written as $\epsilon(\mathbf{k}, \mathbf{k} \cdot \mathbf{v}) \approx 1$. In such case, the wave number range of noneigenmode fluctuations must be restricted to the short wavelength regime, $k^2 \lambda_{De}^2 \gg 1$. This approximation leads to the well known Landau collision integral, which is the approximation used in Refs. [45, 78]. A very detailed discussion about the limits and assumptions of the weak coupling approximation, which leads to the Landau collision integral, can be seen in Chapter 4 of Ref. [81]. In Ref. [81] the Balescu-Lenard collision integral was obtained through the Klimontovich statistical formalism [2, 79], which is also the starting point for the derivation of the weak turbulence theory [52] and the basis of the simplified approach presented in Section 3.1. The implementation depicted in Ref. [81] did not make any mention about the connection of the eigenmode and noneigenmode contributions to each term of the particle kinetic equation. However, the final result was exactly the same, which means that the real novelty here are not the equations, but it is this eigenmode/noneigenmode relationship with collective and collisional processes, respectively. The truly innovative outcome regarding new equations and the inclusion of noneigenmode fluctuations will appear in the wave dynamics, as will become clear in the next section.

4.2 Noneigenmode contribution to nonlinear wave kinetic equation

For the nonlinear wave kinetic equation, the implementation is far more extensive and complicated than the two previous cases. In this text, we provide a brief explanation of the method, which is not very different from the quasilinear case, though it is way more complex, and present some critical remarks regarding the inclusion of noneigenmodes in the nonlinear wave equation. It is worth to mention again, that a more detailed description of the procedure for the inclusion of the noneigenmode contribution in the weak turbulence's equations can be seen in [52].

Now, let us consider all terms in Eq. (3.13). On the left-hand side, we have the quasilinear equations that, as discussed before, are not altered by the inclusion of the noneigenmode fluctuations. Thus, we can call the left-hand side as “*NL*”, and work only with the nonlinear part, on right-hand side of (3.13), and substitute the total electric field fluctuation, given by Eq. (4.11), in these terms. Moreover, we are interested in how the noneigenmode contribution affects the emissions in the eigenmode frequency range, i.e., $\omega = \sigma\omega_{\mathbf{k}}$. Therefore, all the noneigenmode fluctuations $\langle\delta E^2\rangle_{\mathbf{k},\omega}^0$, with superscript 0 and subscript \mathbf{k},ω to be more specific, can be neglected at this point since, by definition, they are excluded from the region that satisfies the $\omega = \sigma\omega_{\mathbf{k}}$ condition. The noneigenmode fluctuations with different arguments ($\langle\delta E^2\rangle_{\mathbf{k}',\omega'}^0$ and $\langle\delta E^2\rangle_{\mathbf{k}-\mathbf{k}',\omega-\omega'}^0$), though, must be retained. After all these considerations, we have a generalized form of Eq. (3.13):

$$\begin{aligned} \text{NL} = & -2 \int d\mathbf{k}' \int d\omega' \left\{ \left[\chi^{(2)}(\mathbf{k}', \omega' | \mathbf{k} - \mathbf{k}', \omega - \omega') \right]^2 \right. \\ & \times \left[\frac{\langle\delta E^2\rangle_{\mathbf{k}-\mathbf{k}',\omega-\omega'}^0 + \sum_{\sigma''} \sum_{\gamma} I_{\mathbf{k}-\mathbf{k}'}^{\sigma''\gamma} \delta(\omega - \omega' - \sigma''\omega_{\mathbf{k}-\mathbf{k}'}^{\gamma})}{\epsilon(\mathbf{k}', \omega')} \right. \\ & + \left. \frac{\langle\delta E^2\rangle_{\mathbf{k}',\omega'}^0 + \sum_{\sigma'} \sum_{\beta} I_{\mathbf{k}'}^{\sigma'\beta} \delta(\omega' - \sigma'\omega_{\mathbf{k}'}^{\beta})}{\epsilon(\mathbf{k} - \mathbf{k}', \omega - \omega')} \right] - \bar{\chi}^{(3)}(\mathbf{k}', \omega | -\mathbf{k}', -\omega' | \mathbf{k}, \omega) \\ & \times \left. \left[\langle\delta E^2\rangle_{\mathbf{k}',\omega'}^0 + \sum_{\sigma'} \sum_{\beta} I_{\mathbf{k}'}^{\sigma'\beta} \delta(\omega' - \sigma'\omega_{\mathbf{k}'}^{\beta}) \right] \right\} \sum_{\sigma} \sum_{\alpha} I_{\mathbf{k}}^{\sigma\alpha} \delta(\omega - \sigma\omega_{\mathbf{k}}^{\alpha}) \\ & + 2 \int d\mathbf{k}' \int d\omega' \frac{|\chi^{(2)}(\mathbf{k}', \omega' | \mathbf{k} - \mathbf{k}', \omega - \omega')|^2}{\epsilon^*(\mathbf{k}, \omega)} \left[\langle\delta E^2\rangle_{\mathbf{k}',\omega'}^0 + \sum_{\sigma'} \sum_{\beta} I_{\mathbf{k}'}^{\sigma'\beta} \delta(\omega' - \sigma'\omega_{\mathbf{k}'}^{\beta}) \right] \\ & \times \left[\langle\delta E^2\rangle_{\mathbf{k}-\mathbf{k}',\omega-\omega'}^0 + \sum_{\sigma''} \sum_{\gamma} I_{\mathbf{k}-\mathbf{k}'}^{\sigma''\gamma} \delta(\omega - \omega' - \sigma''\omega_{\mathbf{k}-\mathbf{k}'}^{\gamma}) \right] \\ & - \frac{4}{\pi} \int d\mathbf{k}' \int d\omega' \frac{1}{k^2 |\epsilon(\mathbf{k}', \omega')|^2} \left\{ \frac{[\chi^{(2)}(\mathbf{k}', \omega' | \mathbf{k} - \mathbf{k}', \omega - \omega')]^2}{\epsilon(\mathbf{k} - \mathbf{k}', \omega - \omega')} \sum_{\sigma} \sum_{\alpha} I_{\mathbf{k}}^{\sigma\alpha} \delta(\omega - \sigma\omega_{\mathbf{k}}^{\alpha}) \right. \\ & \left. - \frac{|\chi^{(2)}(\mathbf{k}', \omega' | \mathbf{k} - \mathbf{k}', \omega - \omega')|^2}{\epsilon^*(\mathbf{k}, \omega)} \left[\langle\delta E^2\rangle_{\mathbf{k}-\mathbf{k}',\omega-\omega'}^0 + \sum_{\sigma''} \sum_{\gamma} I_{\mathbf{k}-\mathbf{k}'}^{\sigma''\gamma} \delta(\omega - \omega' - \sigma''\omega_{\mathbf{k}-\mathbf{k}'}^{\gamma}) \right] \right\} \end{aligned} \quad (4.22)$$

$$\begin{aligned}
& \times \sum_a e_a^2 \int d\mathbf{v} \delta(\omega' - \mathbf{k} \cdot \mathbf{v}) F_a(\mathbf{v}) \\
& - \frac{4}{\pi} \int d\mathbf{k}' \int d\omega' \frac{1}{|\mathbf{k} - \mathbf{k}'|^2 |\epsilon(\mathbf{k} - \mathbf{k}', \omega - \omega')|^2} \left\{ \frac{[\chi^{(2)}(\mathbf{k}', \omega' | \mathbf{k} - \mathbf{k}', \omega - \omega')]^2}{\epsilon(\mathbf{k}', \omega')} \right. \\
& \quad \times \sum_{\sigma} \sum_{\alpha} I_{\mathbf{k}}^{\sigma\alpha} \delta(\omega - \sigma \omega_{\mathbf{k}}^{\alpha}) - \frac{|\chi^{(2)}(\mathbf{k}', \omega' | \mathbf{k} - \mathbf{k}', \omega - \omega')|^2}{\epsilon^*(\mathbf{k}, \omega)} \\
& \quad \times \left. \left[\langle \delta E^2 \rangle_{\mathbf{k}', \omega'}^0 + \sum_{\sigma'} \sum_{\beta} I_{\mathbf{k}'}^{\sigma'\beta} \delta(\omega' - \sigma' \omega_{\mathbf{k}'}^{\beta}) \right] \right\} \sum_a e_a^2 \int d\mathbf{v} \delta(\omega - \omega' - (\mathbf{k} - \mathbf{k}') \cdot \mathbf{v}) F_a(\mathbf{v}).
\end{aligned}$$

In the above equation, the noneigenmode fluctuations are represented by the terms $\langle \delta E^2 \rangle_{\mathbf{k}', \omega'}^0$, and $\langle \delta E^2 \rangle_{\mathbf{k}-\mathbf{k}', \omega-\omega'}^0$. It is important to reinforce that if one is interested only in nonlinear terms related to collective and spontaneous fluctuations in the eigenmode frequency range, then all of these terms might be ignored. In such case, we are back to the standard weak turbulence theory.

After an extensive algebraic manipulation that involves making explicit use of definition (4.5) in the noneigenmode field fluctuations, carrying out the ω' integrations, then using Eq. (4.13) to decompose the denominators $1/\epsilon(\mathbf{k} - \mathbf{k}', \sigma \omega_{\mathbf{k}}^{\alpha} - \mathbf{k}' \cdot \mathbf{v})$ and $1/\epsilon^*(\mathbf{k}, \omega)$ into principal parts and imaginary terms, and taking the imaginary part of the resulting equation, we finally obtain the noneigenmode corrections to the nonlinear wave kinetic equation:

$$\begin{aligned}
\text{corr} = & - \sum_{\sigma'} \sum_{\beta} \sum_a 8\pi e_a^2 \int d\mathbf{k}' \int d\mathbf{v} \frac{|\chi^{(2)}(\mathbf{k}', \sigma' \omega_{\mathbf{k}'}^{\beta} | \mathbf{k} - \mathbf{k}', (\mathbf{k} - \mathbf{k}') \cdot \mathbf{v})|^2}{|\mathbf{k} - \mathbf{k}'|^2 |\epsilon(\mathbf{k} - \mathbf{k}', \mathbf{k} - \mathbf{k}', (\mathbf{k} - \mathbf{k}') \cdot \mathbf{v})|^2} \\
& \times \left[\frac{I_{\mathbf{k}}^{\sigma\alpha}}{\epsilon'(\mathbf{k}', \sigma' \omega_{\mathbf{k}'}^{\beta})} - \frac{I_{\mathbf{k}'}^{\sigma'\beta}}{\epsilon'(\mathbf{k}, \sigma \omega_{\mathbf{k}}^{\alpha})} \right] \delta[\sigma \omega_{\mathbf{k}}^{\alpha} - \sigma' \omega_{\mathbf{k}'}^{\beta} - (\mathbf{k} - \mathbf{k}') \cdot \mathbf{v}] f_a(\mathbf{v}) \\
& - \sum_a \frac{4e_a^2}{\pi} \int d\mathbf{k}' \int d\mathbf{v} \text{Im} \left[\mathcal{P} \frac{2[\chi^{(2)}(\mathbf{k}', \mathbf{k}' \cdot \mathbf{v} | \mathbf{k} - \mathbf{k}', \sigma \omega_{\mathbf{k}}^{\alpha} - \mathbf{k}' \cdot \mathbf{v})]^2}{\epsilon(\mathbf{k} - \mathbf{k}', \sigma \omega_{\mathbf{k}}^{\alpha} - \mathbf{k}' \cdot \mathbf{v})} \right. \\
& \quad \left. - \bar{\chi}^{(3)}(\mathbf{k}', \mathbf{k}' \cdot \mathbf{v} | -\mathbf{k}', -\mathbf{k}' \cdot \mathbf{v} | \mathbf{k}, \sigma \omega_{\mathbf{k}}^{\alpha}) \right] \frac{I_{\mathbf{k}}^{\sigma\alpha}}{k'^2 |\epsilon(\mathbf{k}', \mathbf{k}' \cdot \mathbf{v})|^2} f_a(\mathbf{v}) \\
& + \sum_a \sum_b \frac{24e_a^2 e_b^2}{\pi} \int d\mathbf{k}' \int d\mathbf{v} \int d\mathbf{v}' \frac{|\chi^{(2)}[\mathbf{k}', \mathbf{k}' \cdot \mathbf{v}' | \mathbf{k} - \mathbf{k}', (\mathbf{k} - \mathbf{k}') \cdot \mathbf{v}]|^2}{k'^2 |\mathbf{k} - \mathbf{k}'|^2 |\epsilon(\mathbf{k}', \mathbf{k}' \cdot \mathbf{v}')|^2 |\epsilon(\mathbf{k} - \mathbf{k}', (\mathbf{k} - \mathbf{k}') \cdot \mathbf{v})|^2} \\
& \quad \times \frac{\delta[\sigma \omega_{\mathbf{k}}^{\alpha} - \mathbf{k} \cdot \mathbf{v} + \mathbf{k}' \cdot (\mathbf{v} - \mathbf{v}')] f_a(\mathbf{v}) f_b(\mathbf{v}')}{\epsilon'(\mathbf{k}, \sigma \omega_{\mathbf{k}}^{\alpha})}.
\end{aligned} \tag{4.23}$$

At this point, we have to define an approximation for the various response functions with the angular frequency replaced by $\mathbf{k} \cdot \mathbf{v}$, appearing in the denominator of the correction terms. To do so, we must remember that waves are not subjected to Debye screening, therefore we cannot assume $k^2 \lambda_{De}^2 \gg 1$, that would lead to the same approximation $\epsilon(\mathbf{k}, 0) \approx 1$, which reduces the Balescu-Lenard collision integral to the Landau collision integral. Instead, we make use of Eq. (4.20), $\epsilon(\mathbf{k}, \mathbf{k} \cdot \mathbf{v}) \approx \epsilon(\mathbf{k}, 0) = 1 + (2\omega_{pe}^2/k^2 v_{Te}^2) (1 + T_e/T_i)$, which is the same we

applied to the collision integral in the previous subsection. Thus, applying this approximation and then adding the right-hand side of (4.23) to the right-hand side of Eq. (3.23), we obtain a generalized wave kinetic equation, which includes both the eigenmode and noneigenmode fluctuations:

$$\begin{aligned}
\frac{\partial I_{\mathbf{k}}^{\alpha}}{\partial t} = & -\frac{2\text{Im } \epsilon(\mathbf{k}, \sigma\omega_{\mathbf{k}}^{\alpha})}{\epsilon'(\mathbf{k}, \sigma\omega_{\mathbf{k}}^{\alpha})} I_{\mathbf{k}}^{\alpha} + \sum_a \frac{4e^2}{k^2[\epsilon'(\mathbf{k}, \sigma\omega_{\mathbf{k}}^{\alpha})]^2} \int d\mathbf{v} \delta(\sigma\omega_{\mathbf{k}}^{\alpha} - \mathbf{k} \cdot \mathbf{v}) f_a(\mathbf{v}) \\
& - 4\pi \sum_{\alpha, \beta, \gamma} \sum_{\sigma', \sigma''} \int d\mathbf{k}' \frac{|\chi^{(2)}(\mathbf{k}', \sigma'\omega_{\mathbf{k}'}^{\beta} | \mathbf{k} - \mathbf{k}', \sigma''\omega_{\mathbf{k}-\mathbf{k}'}^{\gamma})|^2}{\epsilon'(\mathbf{k}, \sigma\omega_{\mathbf{k}}^{\alpha})} \\
& \times \left(\frac{I_{\mathbf{k}-\mathbf{k}'}^{\gamma} I_{\mathbf{k}}^{\alpha}}{\epsilon'(\mathbf{k}', \sigma'\omega_{\mathbf{k}'}^{\beta})} + \frac{I_{\mathbf{k}'}^{\beta} I_{\mathbf{k}}^{\alpha}}{\epsilon'(\mathbf{k} - \mathbf{k}', \sigma''\omega_{\mathbf{k}-\mathbf{k}'}^{\gamma})} - \frac{I_{\mathbf{k}'}^{\beta} I_{\mathbf{k}-\mathbf{k}'}^{\gamma}}{\epsilon'(\mathbf{k}, \sigma\omega_{\mathbf{k}}^{\alpha})} \right) \delta(\sigma\omega_{\mathbf{k}}^{\alpha} - \sigma'\omega_{\mathbf{k}'}^{\beta} - \sigma''\omega_{\mathbf{k}-\mathbf{k}'}^{\gamma}) \\
& - \sum_{\alpha, \beta} \sum_{\sigma'} \int d\mathbf{k}' A_{\alpha, \beta}(\mathbf{k}, \mathbf{k}') I_{\mathbf{k}'}^{\beta} I_{\mathbf{k}}^{\alpha} - \sum_a \frac{16e_a^2}{\epsilon'(\mathbf{k}, \sigma\omega_{\mathbf{k}}^{\alpha})} \sum_{\sigma'} \sum_{\beta} \\
& \times \int d\mathbf{v} \int d\mathbf{k}' \frac{|\chi^{(2)}(\mathbf{k}', \sigma'\omega_{\mathbf{k}'}^{\beta} | \mathbf{k} - \mathbf{k}', \sigma\omega_{\mathbf{k}}^{\alpha} - \sigma'\omega_{\mathbf{k}'}^{\beta})|^2}{|\mathbf{k} - \mathbf{k}'|^2 |\epsilon(\mathbf{k} - \mathbf{k}', \sigma\omega_{\mathbf{k}}^{\alpha} - \sigma'\omega_{\mathbf{k}'}^{\beta})|^2} \\
& \times \left[\frac{I_{\mathbf{k}}^{\sigma\alpha}}{\epsilon(\mathbf{k}', \sigma'\omega_{\mathbf{k}'}^{\beta})} - \frac{I_{\mathbf{k}'}^{\sigma'\beta}}{\epsilon'(\mathbf{k}, \sigma\omega_{\mathbf{k}}^{\alpha})} \right] \delta[\sigma\omega_{\mathbf{k}}^{\alpha} - \sigma'\omega_{\mathbf{k}'}^{\beta} - (\mathbf{k} - \mathbf{k}') \cdot \mathbf{v}] f_a(\mathbf{v}) \\
& - \sum_a \frac{16e_a^2}{\epsilon'(\mathbf{k}, \sigma\omega_{\mathbf{k}}^{\alpha})} \sum_{\sigma'} \sum_{\beta} \int d\mathbf{k}' \int d\mathbf{v} \frac{|\mathbf{k} - \mathbf{k}'|^2 \lambda_{De}^4 |\chi^{(2)}(\mathbf{k}', \sigma'\omega_{\mathbf{k}'}^{\beta} | \mathbf{k} - \mathbf{k}', 0)|^2}{|1 + T_e/T_i + |\mathbf{k} - \mathbf{k}'|^2 \lambda_{De}^2|^2} \\
& \times \left[\frac{I_{\mathbf{k}}^{\sigma\alpha}}{\epsilon'(\mathbf{k}', \sigma'\omega_{\mathbf{k}'}^{\beta})} - \frac{I_{\mathbf{k}'}^{\sigma'\beta}}{\epsilon'(\mathbf{k}, \sigma\omega_{\mathbf{k}}^{\alpha})} \right] \delta[\sigma\omega_{\mathbf{k}}^{\alpha} - \sigma'\omega_{\mathbf{k}'}^{\beta} - (\mathbf{k} - \mathbf{k}') \cdot \mathbf{v}] f_a(\mathbf{v}) \\
& - \sum_a \frac{8e_a^2}{\pi} \int d\mathbf{k}' \int d\mathbf{v} \frac{k'^2 \lambda_{De}^4}{|1 + T_e/T_i + k'^2 \lambda_{De}^2|^2} \\
& \times \text{Im} \left[\mathcal{P} \frac{2[\chi^{(2)}(\mathbf{k}', 0 | \mathbf{k} - \mathbf{k}', \sigma\omega_{\mathbf{k}}^{\alpha})]^2}{\epsilon(\mathbf{k} - \mathbf{k}', \sigma\omega_{\mathbf{k}}^{\alpha})} - \bar{\chi}^{(3)}(\mathbf{k}', 0 | -\mathbf{k}', 0 | \mathbf{k}, \sigma\omega_{\mathbf{k}}^{\alpha}) \right] I_{\mathbf{k}}^{\sigma\alpha} f_a(\mathbf{v}) \\
& + \sum_a \sum_b \frac{48e_a^2 e_b^2}{\pi [\epsilon'(\mathbf{k}, \sigma\omega_{\mathbf{k}}^{\alpha})]^2} \int d\mathbf{k}' \int d\mathbf{v} \int d\mathbf{v}' \frac{k'^2 |\chi^{(2)}(\mathbf{k}', 0 | \mathbf{k} - \mathbf{k}', 0)|^2}{|1 + T_e/T_i + k^2 \lambda_{De}^2|^2} \\
& \times \frac{|\mathbf{k} - \mathbf{k}'|^2 \lambda_{De}^8}{|1 + T_e/T_i + |\mathbf{k} - \mathbf{k}'|^2 \lambda_{De}^2|^2} \delta[\sigma\omega_{\mathbf{k}}^{\alpha} - \mathbf{k} \cdot \mathbf{v} + \mathbf{k}' \cdot (\mathbf{v} - \mathbf{v}')] f_a(\mathbf{v}) f_b(\mathbf{v}'), \quad (4.24)
\end{aligned}$$

where the coefficient $A_{\alpha, \beta}(\mathbf{k}, \mathbf{k}')$ is given by Eq. (3.24).

Above, looking at the first noneigenmode term, in blue, one may notice the extreme similarity with its previous expression, which describes the spontaneous scattering process. In fact, this term is nothing but a *correction* to the spontaneous scattering process. Colored in dark-green is the new, rigorous expression for the *collisional damping*. The pink equation in the end, depicts the so-far unknown *electrostatic bremsstrahlung* process. The final expressions for the three new contributions to the wave kinetic equation are given below.

Correction for the spontaneous scattering

The blue term in Eq. (4.24), which depicts the correction for the spontaneous scattering term is:

$$\begin{aligned} \frac{\partial I_{\mathbf{k}}^{\sigma L}}{\partial t} \Big|_{\text{corr}} &= -4\hat{n}e^2 \sum_{\sigma'} \int d\mathbf{k}' \int d\mathbf{v} \frac{|\mathbf{k} - \mathbf{k}'|^2 \lambda_{De}^4 |\chi^{(2)}(\mathbf{k}', \sigma' \omega_{\mathbf{k}'}^L | \mathbf{k} - \mathbf{k}', 0)|^2}{|1 + T_e/T_i + |\mathbf{k} - \mathbf{k}'|^2 \lambda_{De}^2|^2} \\ &\quad \times \sigma \omega_{\mathbf{k}}^L (\sigma' \omega_{\mathbf{k}'}^L I_{\mathbf{k}}^{\sigma L} - \sigma \omega_{\mathbf{k}}^L I_{\mathbf{k}'}^{\sigma' L}) \delta[\sigma \omega_{\mathbf{k}}^L - \sigma' \omega_{\mathbf{k}'}^L - (\mathbf{k} - \mathbf{k}') \cdot \mathbf{v}] [F_e(\mathbf{v}) + F_i(\mathbf{v})], \\ \frac{\partial I_{\mathbf{k}}^{\sigma S}}{\partial t} \Big|_{\text{corr}} &= -4\hat{n}e^2 \mu_{\mathbf{k}} \mu_{\mathbf{k}'} \sigma \omega_{\mathbf{k}}^L \sum_{\sigma'} \int d\mathbf{k}' \int d\mathbf{v} \frac{|\mathbf{k} - \mathbf{k}'|^2 \lambda_{De}^4 |\chi^{(2)}(\mathbf{k}', \sigma' \omega_{\mathbf{k}'}^S | \mathbf{k} - \mathbf{k}', 0)|^2}{|1 + T_e/T_i + |\mathbf{k} - \mathbf{k}'|^2 \lambda_{De}^2|^2} \\ &\quad \times (\sigma' \omega_{\mathbf{k}'}^S I_{\mathbf{k}}^{\sigma S} - \sigma \omega_{\mathbf{k}}^S I_{\mathbf{k}'}^{\sigma' S}) \delta[\sigma \omega_{\mathbf{k}}^S - \sigma' \omega_{\mathbf{k}'}^S - (\mathbf{k} - \mathbf{k}') \cdot \mathbf{v}] [F_e(\mathbf{v}) + F_i(\mathbf{v})], \end{aligned} \quad (4.25)$$

where $\mu_{\mathbf{k}} = |k|^3 \lambda_{De}^3 (m_e/m_i)^{1/2} (1 + 3T_i/T_e)^{1/2}$.

After a careful analysis on the second order susceptibility, we have the following expressions for L and S waves

$$\begin{aligned} u_{k,k'}^{L(\text{corr})} &= -\frac{\hat{n}e^2}{m_e^2 \omega_{pe}^4} \sigma \omega_{\mathbf{k}}^L \sum_{\sigma'} \int d\mathbf{k}' \int d\mathbf{v} \frac{(\mathbf{k} - \mathbf{k}')^2}{k^2 k'^2 |1 + T_e/T_i + (\mathbf{k} - \mathbf{k}')^2 \lambda_{De}^2|^2} \\ &\quad \times (\sigma' \omega_{\mathbf{k}'}^L I_{\mathbf{k}}^{\sigma L} - \sigma \omega_{\mathbf{k}}^L I_{\mathbf{k}'}^{\sigma' L}) \delta[\sigma \omega_{\mathbf{k}}^L - \sigma' \omega_{\mathbf{k}'}^L - (\mathbf{k} - \mathbf{k}') \cdot \mathbf{v}] [F_e(\mathbf{v}) + F_i(\mathbf{v})], \end{aligned} \quad (4.26)$$

$$\begin{aligned} u_{k,k'}^{S(\text{corr})} &= -\frac{\hat{n}e^2}{m_e^2 \omega_{pe}^4} \mu_{\mathbf{k}} \mu_{\mathbf{k}'} \sigma \omega_{\mathbf{k}}^L \sum_{\sigma'} \int d\mathbf{k}' \int d\mathbf{v} \frac{1}{k^2 k'^2 \lambda_{De}^4} \left(1 - \frac{T_e}{T_i} \frac{\mathbf{k} \cdot \mathbf{k}'}{k'^2}\right)^2 \left[1 + \frac{T_e}{T_i} + (\mathbf{k} - \mathbf{k}')^2 \lambda_{De}^2\right]^{-2} \\ &\quad \times (\sigma' \omega_{\mathbf{k}'}^S I_{\mathbf{k}}^{\sigma S} - \sigma \omega_{\mathbf{k}}^S I_{\mathbf{k}'}^{\sigma' S}) \delta[\sigma \omega_{\mathbf{k}}^S - \sigma' \omega_{\mathbf{k}'}^S - (\mathbf{k} - \mathbf{k}') \cdot \mathbf{v}] [F_e(\mathbf{v}) + F_i(\mathbf{v})]. \end{aligned} \quad (4.27)$$

The corrected expression for the spontaneous scattering of L and S waves are

$$\begin{aligned} u_{k,k'}^L &= \sigma \omega_{\mathbf{k}}^L \frac{\hat{n}e^4}{m_e^2 \omega_{pe}^4} \sum_{\sigma'} \int d\mathbf{k}' \int d\mathbf{v} \frac{(\mathbf{k} \cdot \mathbf{k}')^2}{k^2 k'^2} \delta[\sigma \omega_{\mathbf{k}}^L - \sigma' \omega_{\mathbf{k}'}^L - (\mathbf{k} - \mathbf{k}') \cdot \mathbf{v}] \\ &\quad \times (\sigma \omega_{\mathbf{k}}^L I_{\mathbf{k}'}^{\sigma' L} - \sigma' \omega_{\mathbf{k}'}^L I_{\mathbf{k}}^{\sigma L}) \left[1 + \frac{1}{|1 + T_e/T_i + (\mathbf{k} - \mathbf{k}')^2 \lambda_{De}^2|^2}\right] [F_e(\mathbf{v}) + F_i(\mathbf{v})], \end{aligned} \quad (4.28)$$

$$\begin{aligned} u_{k,k'}^S &= \sigma \omega_{\mathbf{k}}^L \frac{\hat{n}e^4}{m_e^2 \omega_{pe}^4} \frac{\mu_{\mathbf{k}} \mu_{\mathbf{k}'}}{k^2 \lambda_{De}^4} \sum_{\sigma'} \int \frac{d\mathbf{k}'}{k'^2} \int d\mathbf{v} \delta[\sigma \omega_{\mathbf{k}}^S - \sigma' \omega_{\mathbf{k}'}^S - (\mathbf{k} - \mathbf{k}') \cdot \mathbf{v}] \left(\sigma \omega_{\mathbf{k}}^L \frac{I_{\mathbf{k}'}^{\sigma' S}}{\mu_{\mathbf{k}'}} - \sigma' \omega_{\mathbf{k}'}^L \frac{I_{\mathbf{k}}^{\sigma S}}{\mu_{\mathbf{k}}}\right) \\ &\quad \times \left[\frac{(\mathbf{k} \cdot \mathbf{k}')^2}{k^2 k'^2} W_{\mathbf{k}, \mathbf{k}'} + \frac{\left(1 - \frac{T_e}{T_i} \frac{\mathbf{k} \cdot \mathbf{k}'}{k'^2}\right)^2}{|1 + T_e/T_i + (\mathbf{k} - \mathbf{k}')^2 \lambda_{De}^2|^2} \right] [F_e(\mathbf{v}) + F_i(\mathbf{v})], \end{aligned} \quad (4.29)$$

where the blue term is the noneigenmode contribution.

Collisional damping for L and S waves

The collisional damping expression is given by the dark-green term in Eq. (4.24):

$$\begin{aligned} \frac{\partial I_{\mathbf{k}}^{\sigma L}}{\partial t} \Big|_{\text{coll}} &= - \sum_a \frac{4\hat{n}e_a^2}{\pi} \sigma \omega_{\mathbf{k}}^L \int d\mathbf{k}' \frac{k'^2 \lambda_{De}^4}{|1 + T_e/T_i + k'^2 \lambda_{De}^2|^2} \\ &\quad \times \int d\mathbf{v} \text{Im} \left[\mathcal{P} \frac{2[\chi^{(2)}(\mathbf{k}', 0|\mathbf{k} - \mathbf{k}', \sigma\omega_{\mathbf{k}}^L)]^2}{\epsilon(\mathbf{k} - \mathbf{k}', \sigma\omega_{\mathbf{k}}^L)} - \bar{\chi}^{(3)}(\mathbf{k}', 0|-\mathbf{k}', 0|\mathbf{k}, \sigma\omega_{\mathbf{k}}^L) \right] F_a(\mathbf{v}) I_{\mathbf{k}}^{\sigma L}, \\ \frac{\partial I_{\mathbf{k}}^{\sigma S}}{\partial t} \Big|_{\text{coll}} &= - \sum_a \frac{4\hat{n}e_a^2}{\pi} \sigma \mu_{\mathbf{k}} \omega_{\mathbf{k}}^L \int d\mathbf{k}' \frac{k'^2 \lambda_{De}^4}{|1 + T_e/T_i + k'^2 \lambda_{De}^2|^2} \\ &\quad \times \int d\mathbf{v} \text{Im} \left[\mathcal{P} \frac{2[\chi^{(2)}(\mathbf{k}', 0|\mathbf{k} - \mathbf{k}', \sigma\omega_{\mathbf{k}}^S)]^2}{\epsilon(\mathbf{k} - \mathbf{k}', \sigma\omega_{\mathbf{k}}^S)} - \bar{\chi}^{(3)}(\mathbf{k}', 0|-\mathbf{k}', 0|\mathbf{k}, \sigma\omega_{\mathbf{k}}^S) \right] F_a(\mathbf{v}) I_{\mathbf{k}}^{\sigma S}. \end{aligned} \quad (4.30)$$

With the appropriate approximations for the second order and partial third order susceptibilities carefully analyzed [52], we obtain the following expressions for L and S waves

$$\begin{aligned} \gamma_{\mathbf{k}}^{\sigma L (\text{coll})} &= \sigma \omega_{\mathbf{k}}^L \frac{4\hat{n}e^4 \omega_{pe}^2}{T_e^2} \int d\mathbf{k}' \frac{(\mathbf{k} \cdot \mathbf{k}')^2 \lambda_{De}^4}{k^2 k'^4 |\epsilon(\mathbf{k}', \sigma\omega_{\mathbf{k}}^L)|^2} \\ &\quad \times \left(1 + \frac{T_e}{T_i} + (\mathbf{k} - \mathbf{k}')^2 \lambda_{De}^2 \right)^{-2} \int d\mathbf{v} \mathbf{k}' \cdot \frac{\partial F_e(\mathbf{v})}{\partial \mathbf{v}} \delta[\sigma\omega_{\mathbf{k}}^L - \mathbf{k}' \cdot \mathbf{v}] \end{aligned} \quad (4.31)$$

$$\begin{aligned} \gamma_{\mathbf{k}}^{\sigma S (\text{coll})} &= \sigma \mu_{\mathbf{k}} \omega_{\mathbf{k}}^L \frac{\hat{n}e^4 \omega_{pe}^2}{T_e^2} \int d\mathbf{k}' \frac{1}{k^2 k'^4 |\epsilon(\mathbf{k}', \sigma\omega_{\mathbf{k}}^S)|^2} \\ &\quad \times \left(1 + \frac{T_e}{T_i} + (\mathbf{k} - \mathbf{k}')^2 \lambda_{De}^2 \right)^{-2} \left(1 + \frac{2T_e}{T_i} \frac{\mathbf{k} \cdot \mathbf{k}'}{k^2} \right) \\ &\quad \times \int d\mathbf{v} \mathbf{k}' \cdot \frac{\partial}{\partial \mathbf{v}} \left(F_e(\mathbf{v}) + \frac{m_e}{m_i} F_i(\mathbf{v}) \right) \delta[\sigma\omega_{\mathbf{k}}^S - \mathbf{k}' \cdot \mathbf{v}]. \end{aligned} \quad (4.32)$$

Electrostatic bremsstrahlung for L and S waves

The electrostatic bremsstrahlung equations are given by the pink term in Eq. (4.24):

$$\begin{aligned} \frac{\partial I_{\mathbf{k}}^{\sigma L}}{\partial t} \Big|_{\text{brem}} &= \sum_{a,b} \frac{12n_e e_a^2 e_b^2 \omega_{pe}^2}{\pi} \int d\mathbf{k}' \int d\mathbf{v} \int d\mathbf{v}' \frac{|\chi^{(2)}(\mathbf{k}', 0|\mathbf{k} - \mathbf{k}', 0)|^2}{k'^2 |\mathbf{k} - \mathbf{k}'|^2 |\epsilon(\mathbf{k}', 0)|^2 |\epsilon(\mathbf{k} - \mathbf{k}', 0)|^2} \\ &\quad \times \delta[\sigma\omega_{\mathbf{k}}^L - \mathbf{k} \cdot \mathbf{v} + \mathbf{k}' \cdot (\mathbf{v} - \mathbf{v}')] F_a(\mathbf{v}) F(\mathbf{v}'), \end{aligned} \quad (4.33)$$

$$\begin{aligned} \frac{\partial}{\partial t} \frac{I_{\mathbf{k}}^{\sigma S}}{\mu_{\mathbf{k}}} \Big|_{\text{brem}} &= \sum_{a,b} \frac{12n_e e_a^2 e_b^2 \omega_{pe}^2}{\pi} \int d\mathbf{k}' \int d\mathbf{v} \int d\mathbf{v}' \frac{|\chi^{(2)}(\mathbf{k}', 0|\mathbf{k} - \mathbf{k}', 0)|^2}{k'^2 |\mathbf{k} - \mathbf{k}'|^2 |\epsilon(\mathbf{k}', 0)|^2 |\epsilon(\mathbf{k} - \mathbf{k}', 0)|^2} \\ &\quad \times \delta[\sigma\omega_{\mathbf{k}}^S - \mathbf{k} \cdot \mathbf{v} + \mathbf{k}' \cdot (\mathbf{v} - \mathbf{v}')] F_a(\mathbf{v}) F(\mathbf{v}'). \end{aligned} \quad (4.34)$$

In Ref. [52], the following approximation for the second order susceptibility of both L

and S waves was employed

$$\chi^{(2)}(\mathbf{k}', 0 | \mathbf{k} - \mathbf{k}', 0) = -i \sum_a \frac{e_a}{T_a} \frac{\omega_{pa}^2}{kk'|\mathbf{k} - \mathbf{k}'|} \frac{1}{v_{Ta}^2} = \frac{ie}{T_e} \frac{1}{v_{Te}^2} \left(1 - \frac{T_e^2}{T_i^2} \frac{\omega_{pe}^2}{kk'|\mathbf{k} - \mathbf{k}'|} \right). \quad (4.35)$$

In the present work, however, we have revisited the subject, and found that an improved approximation could be employed for the L waves. The derivation of this alternative approach, where we basically make the same assumption $\mathbf{k} \cdot \mathbf{v} \approx 0$, $\mathbf{k}' \cdot \mathbf{v}' \approx 0$ and $\mathbf{k}' \cdot \mathbf{v} \approx 0$ but a few steps later, is detailed in Appendix A. For the S waves we keep the original approximation. Then, after applying the respective approximation for the second order susceptibility for the L and S waves, we have

$$\begin{aligned} P_{\mathbf{k}}^{\sigma L} &= \frac{3e^2}{4\pi^3} \frac{1}{(\omega_{\mathbf{k}}^L)^2} \left(1 - \frac{m_e T_e}{m_i T_i} \right)^2 \frac{v_e^4}{k^2} \int d\mathbf{k}' k'^2 |\mathbf{k} - \mathbf{k}'|^2 \left(1 + \frac{T_e}{T_i} + (\mathbf{k} - \mathbf{k}')^2 \lambda_D^2 \right)^{-2} \\ &\times \left(1 + \frac{T_e}{T_i} + k'^2 \lambda_D^2 \right)^{-2} \int d\mathbf{v} \int d\mathbf{v}' \delta[\sigma \omega_{\mathbf{k}}^L - \mathbf{k} \cdot \mathbf{v} + \mathbf{k}' \cdot (\mathbf{v} - \mathbf{v}')] \sum_a F_a(\mathbf{v}) \sum_b F_b(\mathbf{v}') \end{aligned} \quad (4.36)$$

$$\begin{aligned} P_{\mathbf{k}}^{\sigma S} &= \mu_{\mathbf{k}} \frac{3e^2 T_e}{16\pi^3 m_e} \left(1 - \frac{T_e^2}{T_i^2} \right)^2 \frac{1}{k^2 \lambda_D^2} \int d\mathbf{k}' \left(1 + \frac{T_e}{T_i} + (\mathbf{k} - \mathbf{k}')^2 \lambda_D^2 \right)^{-2} \\ &\times \left(1 + \frac{T_e}{T_i} + k'^2 \lambda_D^2 \right)^{-2} \int d\mathbf{v} \int d\mathbf{v}' \delta[\sigma \omega_{\mathbf{k}}^S - \mathbf{k} \cdot \mathbf{v} + \mathbf{k}' \cdot (\mathbf{v} - \mathbf{v}')] \sum_a F_a(\mathbf{v}) \sum_b F_b(\mathbf{v}'). \end{aligned} \quad (4.37)$$

4.2.1 Generalized wave kinetic equation for L and S waves

Adding Eqs. (4.31) and (4.36) to Eq. (3.26), and Eqs. (4.32) and (4.37) to Eq. (3.27), and then substituting the spontaneous scattering term of both equations with their respective corrected expressions, (4.28) and (4.29), we obtain the following generalized wave kinetic equations for L and S waves, respectively:

$$\begin{aligned} \frac{\partial I_{\mathbf{k}}^{\sigma L}}{\partial t} &= \frac{\omega_{pe}^2}{k^2} \int d\mathbf{v} \delta(\sigma \omega_{\mathbf{k}}^L - \mathbf{k} \cdot \mathbf{v}) \left(\hat{n} e^2 F_e(\mathbf{v}) + \pi (\sigma \omega_{\mathbf{k}}^L) \mathbf{k} \cdot \frac{\partial F_e(\mathbf{v})}{\partial \mathbf{v}} I_{\mathbf{k}}^{\sigma L} \right) \\ &- \pi \sigma \omega_{\mathbf{k}}^L \frac{e^2}{2T_e^2} \sum_{\sigma', \sigma''} \int d\mathbf{k}' \frac{\mu_{\mathbf{k}-\mathbf{k}'}^S (\mathbf{k} \cdot \mathbf{k}')^2}{k^2 k'^2 |\mathbf{k} - \mathbf{k}'|^2} \left(\sigma' \omega_{\mathbf{k}'}^L \frac{I_{\mathbf{k}-\mathbf{k}'}^{\sigma'' S}}{\mu_{\mathbf{k}-\mathbf{k}'}^S} I_{\mathbf{k}}^{\sigma L} \right. \\ &\left. + \sigma'' \omega_{\mathbf{k}-\mathbf{k}'}^L I_{\mathbf{k}'}^{\sigma' L} I_{\mathbf{k}}^{\sigma L} - \sigma \omega_{\mathbf{k}}^L I_{\mathbf{k}'}^{\sigma' L} \frac{I_{\mathbf{k}-\mathbf{k}'}^{\sigma'' S}}{\mu_{\mathbf{k}-\mathbf{k}'}^S} \right) \delta(\sigma \omega_{\mathbf{k}}^L - \sigma' \omega_{\mathbf{k}'}^L - \sigma'' \omega_{\mathbf{k}-\mathbf{k}'}^S) \\ &+ \sigma \omega_{\mathbf{k}}^L \frac{e^2}{m_e^2 \omega_{pe}^2} \sum_{\sigma'} \int d\mathbf{k}' \int d\mathbf{v} \frac{(\mathbf{k} \cdot \mathbf{k}')^2}{k^2 k'^2} \delta[\sigma \omega_{\mathbf{k}}^L - \sigma' \omega_{\mathbf{k}'}^L - (\mathbf{k} - \mathbf{k}') \cdot \mathbf{v}] \\ &\times \left\{ \frac{\hat{n} e^2}{\omega_{pe}^2} \left(\sigma \omega_{\mathbf{k}}^L I_{\mathbf{k}'}^{\sigma' L} - \sigma' \omega_{\mathbf{k}'}^L I_{\mathbf{k}}^{\sigma L} \right) \left[1 + \frac{1}{|1 + T_e/T_i + (\mathbf{k} - \mathbf{k}')^2 \lambda_{De}^2|^2} \right] [F_e(\mathbf{v}) + F_i(\mathbf{v})] \right. \\ &\left. + \pi \frac{m_e}{m_i} I_{\mathbf{k}'}^{\sigma' L} I_{\mathbf{k}}^{\sigma L} (\mathbf{k} - \mathbf{k}') \cdot \frac{\partial F_i(\mathbf{v})}{\partial \mathbf{v}} \right\} + 2I_{\mathbf{k}}^{\sigma L} \gamma_{\mathbf{k}}^{\sigma L} + P_{\mathbf{k}}^{\sigma L}, \end{aligned} \quad (4.38)$$

$$\begin{aligned}
\frac{\partial}{\partial t} \frac{I_{\mathbf{k}}^{\sigma S}}{\mu_{\mathbf{k}}^S} &= \mu_{\mathbf{k}}^S \frac{\omega_{pe}^2}{k^2} \int d\mathbf{v} \delta(\sigma\omega_{\mathbf{k}}^S - \mathbf{k} \cdot \mathbf{v}) \left[\hat{n} e^2 [F_e(\mathbf{v}) + F_i(\mathbf{v})] \right. \\
&\quad + \pi (\sigma\omega_{\mathbf{k}}^L) \left(\mathbf{k} \cdot \frac{\partial F_e(\mathbf{v})}{\partial \mathbf{v}} + \frac{m_e}{m_i} \mathbf{k} \cdot \frac{\partial F_i(\mathbf{v})}{\partial \mathbf{v}} \right) \frac{I_{\mathbf{k}}^{\sigma S}}{\mu_{\mathbf{k}}^S} \Big] \\
&\quad - \pi\sigma\omega_{\mathbf{k}}^L \frac{e^2}{4T_e^2} \sum_{\sigma',\sigma''} \int d\mathbf{k}' \frac{\mu_{\mathbf{k}}^S [\mathbf{k}' \cdot (\mathbf{k} - \mathbf{k}')]^2}{k^2 k'^2 |\mathbf{k} - \mathbf{k}'|^2} \left(\sigma' \omega_{\mathbf{k}'}^L I_{\mathbf{k}-\mathbf{k}'}^{\sigma'' L} \frac{I_{\mathbf{k}}^{\sigma S}}{\mu_{\mathbf{k}}^S} \right. \\
&\quad + \sigma'' \omega_{\mathbf{k}-\mathbf{k}'}^L I_{\mathbf{k}'}^{\sigma' L} \frac{I_{\mathbf{k}}^{\sigma S}}{\mu_{\mathbf{k}}^S} - \sigma \omega_{\mathbf{k}}^L I_{\mathbf{k}'}^{\sigma' L} I_{\mathbf{k}-\mathbf{k}'}^{\sigma'' L} \Big) \delta(\sigma\omega_{\mathbf{k}}^S - \sigma'\omega_{\mathbf{k}'}^L - \sigma''\omega_{\mathbf{k}-\mathbf{k}'}^L) \\
&\quad + \frac{e^2}{m_e^2 \omega_{pe}^2} \frac{\mu_{\mathbf{k}}^S \mu_{\mathbf{k}'}^S}{\lambda_{De}^4} \sigma \omega_{\mathbf{k}}^L \sum_{\sigma'} \int \frac{d\mathbf{k}'}{k^2 k'^2} \int d\mathbf{v} \delta[\sigma\omega_{\mathbf{k}}^S - \sigma'\omega_{\mathbf{k}'}^S - (\mathbf{k} - \mathbf{k}') \cdot \mathbf{v}] \\
&\quad \times \left\{ \left[\frac{\hat{n} e^2 (\mathbf{k} \cdot \mathbf{k}')^2}{\omega_{pe}^2 k^2 k'^2} W_{\mathbf{k},\mathbf{k}'} + \frac{\left(1 - \frac{T_e \mathbf{k} \cdot \mathbf{k}'}{T_i k'^2} \right)^2}{|1 + T_e/T_i + (\mathbf{k} - \mathbf{k}')^2 \lambda_{De}^2|^2} \right] \right. \\
&\quad \times \left(\sigma \omega_{\mathbf{k}}^L \frac{I_{\mathbf{k}'}^{\sigma' S}}{\mu_{\mathbf{k}'}^S} - \sigma' \omega_{\mathbf{k}'}^L \frac{I_{\mathbf{k}}^{\sigma S}}{\mu_{\mathbf{k}}^S} \right) [F_e(\mathbf{v}) + F_i(\mathbf{v})] \\
&\quad \left. + \frac{m_e \pi (\mathbf{k} \cdot \mathbf{k}')^2}{m_i k^2 k'^2} \left(W_{\mathbf{k},\mathbf{k}'} + \sigma \sigma' \frac{k'}{k} \right) \frac{I_{\mathbf{k}'}^{\sigma' S}}{\mu_{\mathbf{k}'}^S} \frac{I_{\mathbf{k}}^{\sigma S}}{\mu_{\mathbf{k}}^S} (\mathbf{k} - \mathbf{k}') \cdot \frac{\partial F_i(\mathbf{v})}{\partial \mathbf{v}} \right\} + 2I_{\mathbf{k}}^{\sigma S} \gamma_{\mathbf{k}}^{\sigma S} + P_{\mathbf{k}}^{\sigma S},
\end{aligned} \tag{4.39}$$

where the coefficient W is given by Eq. (3.28).

Chapter 5

Weakly turbulent processes in the presence of collisional interactions

The generalization introduced in [52] and summarized in Chapter 4, is an innovative approach, in which the contribution of the usually neglected noneigenmode fluctuations is taken into account along with the well-known eigenmodes contribution. The outcome of this new formulation is a first principles theory that combines both collective and non-collective processes, assuming the propagation of electrostatic oscillations in unmagnetized plasmas, without any *ad hoc* addition. Such theory is the basis of the present research, in which the primary objective is performing numerical analysis of the generalized weak turbulence equations, and then investigate its applications on the description and interpretation of space plasma phenomena. More specifically, the solar plasma, where the results of the first two studies [78, 82] have shown a promising perspective.

From the three new terms presented in the last chapter, we analyzed two: the collisional damping [82] and electrostatic bremsstrahlung [78]. The third term is a correction for the spontaneous scattering effect, which is a nonlinear process. The first study, however, analyses only the intensity of the collisional damping spectrum for L and S waves by numerically integrating Eqs. (4.31) and (4.32), respectively. Regarding the second study, the time evolution analysis was made using quasilinear approximation, which does not involve nonlinear wave-particle interaction, like the scattering effect. Besides that, a small correction to a nonlinear term does not seem to justify a whole study dedicated only to it.

In this chapter, we discuss some essential aspects regarding the results obtained in both studies mentioned above. The results are presented in the form of appended papers, using chronological order, in Sections 5.1 and 5.2.

5.1 Collisional damping rates for plasma waves

In this first analysis, presented in Ref. [82], we have numerically integrated Eqs. (4.31) for L waves, and (4.32) for S waves, considering Maxwellian velocity distribution function for the particles, without including the new effects in the time evolution subroutine. The main objective here was to comprehend important aspects of this so-far unknown expressions, how they relate to other equivalent plasma processes and with the heuristic Spitzer formula, for collisional damping. The main question was: “Are they equivalent?”, more specifically, “Are their magnitudes, at least, in the same order of magnitude?”. The answer was no. We found out that the Spitzer formula overestimates the collisional damping effect in several orders of magnitude in comparison with the new expression. Further, the insignificance of the collisional damping became even more evident when we compared its damping rate with the collisionless (Landau) damping rate in the same figure.

The following paper is fairly self-sustained regarding the theory and methods applied. All important equations are there, including their normalized form and the normalization constants.

Collisional damping rates for plasma waves

S. F. Tigik,^{1,a)} L. F. Ziebell,^{1,b)} and P. H. Yoon^{2,3,c)}

¹*Instituto de Física, Universidade Federal do Rio Grande do Sul, 91501-970 Porto Alegre, Rio Grande do Sul, Brazil*

²*Institute for Physical Science and Technology, University of Maryland, College Park, Maryland 20742, USA*

³*School of Space Research, Kyung Hee University, Yongin, Gyeonggi 446-701, South Korea*

(Received 22 May 2016; accepted 31 May 2016; published online 14 June 2016)

The distinction between the plasma dynamics dominated by collisional transport versus collective processes has never been rigorously addressed until recently. A recent paper [P. H. Yoon *et al.*, Phys. Rev. E **93**, 033203 (2016)] formulates for the first time, a unified kinetic theory in which collective processes and collisional dynamics are systematically incorporated from first principles. One of the outcomes of such a formalism is the rigorous derivation of collisional damping rates for Langmuir and ion-acoustic waves, which can be contrasted to the heuristic customary approach. However, the results are given only in formal mathematical expressions. The present brief communication numerically evaluates the rigorous collisional damping rates by considering the case of plasma particles with Maxwellian velocity distribution function so as to assess the consequence of the rigorous formalism in a quantitative manner. Comparison with the heuristic (“Spitzer”) formula shows that the accurate damping rates are much lower in magnitude than the conventional expression, which implies that the traditional approach over-estimates the importance of attenuation of plasma waves by collisional relaxation process. Such a finding may have a wide applicability ranging from laboratory to space and astrophysical plasmas. *Published by AIP Publishing.*

[<http://dx.doi.org/10.1063/1.4953802>]

In a recently published paper,¹ the formalism of plasma kinetic theory was revisited, and a set of coupled equations were derived, which describe the dynamical evolution of the velocity distribution functions of plasma particles and the spectral wave energy densities associated with electrostatic waves. Reference 1 follows the standard weak turbulence perturbative ordering, except that unlike the textbook approaches, which take into account only the collective eigenmodes in the linear and nonlinear wave-particle interactions, the new formalism includes the effects of non-collective fluctuations emitted by thermal particles. It is shown that the non-collective fluctuations, which had been largely ignored in the literature hitherto, are responsible for collisional effects in both the particle and wave equations. Specifically, Ref. 1 demonstrates that the inclusion of non-collective part of thermal fluctuations leads to the collision integral, while the collective eigenmodes are responsible for the usual quasi-linear diffusion (plus the velocity friction) term(s) in the particle kinetic equation. As for the collectively excited waves, which satisfy the dispersion relations, and are thus eigenmodes, the influence of non-collective thermal fluctuations rigorously lead to the collisional wave damping of the collective waves, as well as the emission of these waves by particle collisions (i.e., bremsstrahlung emission of electrostatic eigenmodes). Such a derivation, without any *ad hoc* additions, was done for the first time.

If one is interested only in the collisional relaxation for collision-dominated plasmas, then transport processes can be legitimately discussed solely on the basis of well-known collisional kinetic equation.^{2,3} Collisional transport is important for high density plasmas such as in the solar interior. In the opposite limit, if one’s concern is only on relaxation processes that involve collective oscillations and waves, then various nonlinear theories of plasma turbulence may be employed.^{4–7} Collective processes dominate rarefied plasmas, which characterize most of the heliosphere, interstellar, and intergalactic environments.

It is the dichotomy that separates the purely collisional versus purely collective descriptions that had not been rigorously bridged until the recent work.¹ There are intermediate situations where both collisional and collective processes must be treated together, such as the solar x ray bremsstrahlung radiation sources,^{8–10} or in the Earth’s ionospheric plasma where collisional conductivity becomes important.¹¹ (Note that for the Earth’s ionosphere, the dominant collisional process is the charged particle collisions with the neutrals, however.) For such situations, there was a general lack of satisfactory theories, which one may bring to bear in order to address the necessary physics, until recently. Instead, it had been a common practice to introduce collisional damping in the wave evolution as an indirect effect of assuming a collisional operator in the particle equation, and define an effective collision frequency.^{8–10,12–16} However, such a procedure is tantamount to inserting the collisional dissipation by hand, as it were, to the governing microscopic equation which describes fundamentally collision-free situation.

^{a)}Electronic mail: sabrina.tigik@ufrgs.br

^{b)}Electronic mail: luiz.ziebell@ufrgs.br

^{c)}Electronic mail: yoonp@umd.edu

Consequently, strictly speaking, the method is at best, heuristic. Nevertheless, such an *ad hoc* prescription is widely practiced in the plasma physics literature.

Thus, in the literature, often a governing equation is adopted

$$\left[\frac{\partial}{\partial t} + \mathbf{v} \cdot \nabla + e_a \left(\mathbf{E} + \frac{\mathbf{v}}{c} \times \mathbf{B} \right) \cdot \frac{\partial}{\partial \mathbf{p}} \right] f_a = C_a(f_a), \quad (1)$$

where $C_a(f_a)$ represents the collision integral and a denotes particle species ($a=e$ for electrons, $a=i$ for ions). If f_a , \mathbf{E} and \mathbf{B} in the above represent the averaged one-particle distribution function and average fields, then Eq. (1) represents the correct collisional kinetic equation.^{2,3} However, if these represent the total (average plus fluctuation), then they become microscopic one-particle distribution function and microscopic fields. For such a case, the right-hand side of Eq. (1) should be zero, since microscopic equations are reversible. As shown in Ref. 1, the irreversibility (signified by collision operator on the right-hand side) enters the problem only as a result of statistical averages and the loss of information. Nonetheless, the standard procedure in the literature is to interpret f_a and field vectors as microscopic quantities, and employ expansion for small-amplitude perturbations. Upon replacing the collision operator by an effective collision frequency, $C_a(f_a) \approx -\nu_{\text{coll}} f_a$, the effective particle collision frequency is absorbed into the wave-particle resonance condition, and ends up as part of the imaginary part of the wave frequency, corresponding to a damping effect on the waves. As a consequence of the above-described recipe, known as the “Spitzer approximation” in the literature, one may obtain the collisional damping rate for Langmuir waves, given by

$$\gamma_{\text{coll}} = -\frac{\pi n_e e^4 \ln \Lambda}{m_e^2 v_{Te}^3}, \quad (2)$$

where $v_{Te} = (2T_e/m_e)^{1/2}$ is the electron thermal speed and $\Lambda = \lambda_{De} T_e / e^2 = 4\pi n_e \lambda_{De}^3$ is a constant. Note that Λ represents the total number of electrons in a sphere whose radius is equal to the Debye length, $\lambda_{De} = [T_e/(4\pi n_e e^2)]^{1/2}$. Here, m_e , T_e , and n_e stand for electron mass, electron temperature (in the unit of energy), and electron density, respectively. Note that Eq. (2) implies that the collisional damping rate is constant and does not depend on wave vector (or wave frequency).

Reference 1, in contrast, shows that the accurate collisional damping rates for plasma waves, that is, Langmuir (L) and ion-acoustic (S) waves, are much more complicated than is indicated by the approximate formula (2) in that the correct formulae exhibit dependence on wave number (and thus, frequency). However, the final results were given only in terms of formal expressions so that it is difficult to assess the consequence of the new formulation. The purpose of the present brief communication is to carry out numerical analysis so that one may understand the significance, or lack thereof, of the new findings in a quantitative way.

We start with the formal and rigorous expression for the collisional damping rates for L and S waves, as given by Eq. (4.44) in Ref. 1

$$\begin{aligned} \gamma_{\mathbf{k}}^{L(\text{coll})} &= \omega_{\mathbf{k}}^L \frac{4n_e e^4 \omega_{pe}^2}{T_e^2} \int d\mathbf{k}' \frac{(\mathbf{k} \cdot \mathbf{k}')^2 \lambda_{De}^4}{k^2 k'^4 |\epsilon(\mathbf{k}', \omega_{\mathbf{k}}^L)|^2} \\ &\times \left(1 + \frac{T_e}{T_i} + (\mathbf{k} - \mathbf{k}')^2 \lambda_{De}^2 \right)^{-2} \\ &\times \int d\mathbf{v} \mathbf{k}' \cdot \frac{\partial F_e(\mathbf{v})}{\partial \mathbf{v}} \delta(\omega_{\mathbf{k}}^L - \mathbf{k}' \cdot \mathbf{v}), \end{aligned} \quad (3)$$

$$\begin{aligned} \gamma_{\mathbf{k}}^{S(\text{coll})} &= \mu_{\mathbf{k}} \omega_{\mathbf{k}}^L \frac{n_e e^4 \omega_{pe}^2}{T_e^2} \int d\mathbf{k}' \frac{1}{k^2 k'^4 |\epsilon(\mathbf{k}', \omega_{\mathbf{k}}^S)|^2} \\ &\times \left(1 + \frac{T_e}{T_i} + (\mathbf{k} - \mathbf{k}')^2 \lambda_{De}^2 \right)^{-2} \\ &\times \left(1 + \frac{2T_e \mathbf{k} \cdot \mathbf{k}'}{T_i k^2} \right) \int d\mathbf{v} \delta(\omega_{\mathbf{k}}^S - \mathbf{k}' \cdot \mathbf{v}) \\ &\times \mathbf{k}' \cdot \frac{\partial}{\partial \mathbf{v}} \left(F_e(\mathbf{v}) + \frac{m_e}{m_i} F_i(\mathbf{v}) \right). \end{aligned} \quad (4)$$

In the above equations, $\omega_{\mathbf{k}}^L = \omega_{pe} \left(1 + \frac{3}{2} k^2 \lambda_{De}^2 \right)$ and $\omega_{\mathbf{k}}^S = \omega_{pe} k \lambda_{De} \sqrt{\frac{m_e}{m_i} \frac{1+3T_i/T_e}{1+k^2 \lambda_{De}^2}}$ designate Langmuir and ion-sound mode dispersion relations, respectively, m_i and T_i being the ion (proton) mass and temperature, respectively, and $\omega_{pe} = (4\pi n_e e^2 / m_e)^{1/2}$ is the plasma frequency. The ensemble-averaged one-particle distribution function $F_a(\mathbf{v})$ is normalized to unity, $\int d\mathbf{v} F_a(\mathbf{v}) = 1$. The quantity $\mu_{\mathbf{k}}$ is defined by $\mu_{\mathbf{k}} = k^3 \lambda_{De}^3 \sqrt{\frac{m_e}{m_i} \left(1 + \frac{3T_i}{T_e} \right)}$, and $\epsilon(\mathbf{k}, \omega_{\mathbf{k}}^L)$ and $\epsilon(\mathbf{k}, \omega_{\mathbf{k}}^S)$ are the dielectric constants

$$\epsilon(\mathbf{k}, \omega) = 1 + \sum_a \frac{\omega_{pa}^2}{k^2} \int d\mathbf{v} \frac{\mathbf{k} \cdot \partial F_a / \partial \mathbf{v}}{\omega - \mathbf{k} \cdot \mathbf{v} + i0}.$$

Evidently, Eqs. (3) and (4) are far more sophisticated than the simple expression (2). The question is what is the actual implication of these results? Specifically, to what extent does the approximation (2) conform with the rigorous results (3) and (4), and if not, what is the extent of the discrepancy?

In order to quantitatively analyze Eqs. (3) and (4), it is advantageous to introduce suitable dimensionless quantities

$$\mathbf{u} = \frac{\mathbf{v}}{v_{Te}}, \quad z = \frac{\omega}{\omega_{pe}}, \quad \mathbf{q} = \frac{\mathbf{k} v_{Te}}{\omega_{pe}} = \mathbf{k} \sqrt{2} \lambda_{De} \quad (5)$$

and rewrite the collisional damping rates (3) and (4) in normalized form

$$\begin{aligned} \gamma_{\mathbf{q}}^{L(\text{coll})} &\equiv \frac{\gamma_{\mathbf{k}}^{L(\text{coll})}}{\omega_{pe}} = \frac{2g z_{\mathbf{q}}^L}{q^2} \int d\mathbf{q}' \frac{(\mathbf{q} \cdot \mathbf{q}')^2}{q'^4 |\epsilon(\mathbf{q}', z_{\mathbf{q}}^L)|^2} \\ &\times \left(1 + \frac{T_e}{T_i} + \frac{(\mathbf{q} - \mathbf{q}')^2}{2} \right)^{-2} \\ &\times \int d\mathbf{u} \mathbf{q}' \cdot \frac{\partial \Phi_e(\mathbf{u})}{\partial \mathbf{u}} \delta(z_{\mathbf{q}}^L - \mathbf{q}' \cdot \mathbf{u}), \end{aligned} \quad (6)$$

$$\gamma_{\mathbf{q}}^{S(\text{coll})} \equiv \frac{\gamma_{\mathbf{q}}^{S(\text{coll})}}{\omega_{pe}} = \frac{2g z_{\mathbf{q}}^L}{q^2} \int \frac{d\mathbf{q}'}{q'^4 |\epsilon(\mathbf{q}', z_{\mathbf{q}}^S)|^2} \\ \times \left(1 + \frac{T_e}{T_i} + \frac{(\mathbf{q} - \mathbf{q}')^2}{2}\right)^{-2} \\ \times \left(1 + \frac{2T_e}{T_i} \frac{\mathbf{q} \cdot \mathbf{q}'}{q^2}\right) \int d\mathbf{u} \delta(z_{\mathbf{q}}^S - \mathbf{q}' \cdot \mathbf{u}) \\ \times \mathbf{q}' \cdot \frac{\partial}{\partial \mathbf{u}} \left(\Phi_e(\mathbf{u}) + \frac{m_e}{m_i} \Phi_i(\mathbf{u})\right), \quad (7)$$

where in dimensionless form, the dispersion relations are given by $z_{\mathbf{q}}^L = 1 + \frac{3q^2}{4}$ and $z_{\mathbf{q}}^S = q \sqrt{\frac{m_e}{m_i} \frac{1+3T_i/T_e}{2+q^2}}$. In Eqs. (6) and (7), the quantity g is defined by

$$g = \frac{1}{2^{3/2}(4\pi)^2 n_e \lambda_{De}^3} = \frac{1}{2^{3/2}(4\pi\Lambda)}, \quad (8)$$

which is related to the parameter Λ discussed earlier. The quantity g is an effective “plasma parameter” in that it is related to the inverse of the number of particles in a “Debye sphere.”

Let us assume that ions and electrons have isotropic Maxwellian velocity distributions

$$\Phi_a(\mathbf{u}) = v_e^3 F_a(\mathbf{v}) = \frac{1}{\pi^{3/2}} \left(\frac{m_a T_e}{m_e T_a}\right)^{3/2} \exp\left(-\frac{m_a T_e}{m_e T_a} u^2\right). \quad (9)$$

Then the dielectric constants appearing in the denominators of Eqs. (3) and (4) are given by the following:

$$\epsilon(\mathbf{q}', z_{\mathbf{q}}^L) = 1 + \frac{2}{q'^2} \left[1 + \frac{z_{\mathbf{q}}^L}{q'} Z\left(\frac{z_{\mathbf{q}}^L}{q'}\right)\right], \quad (10)$$

$$\epsilon(\mathbf{q}', z_{\mathbf{q}}^S) = 1 + \frac{2}{q'^2} \left[1 + \frac{z_{\mathbf{q}}^S}{q'} Z\left(\frac{z_{\mathbf{q}}^S}{q'}\right)\right] \\ + \frac{T_e}{T_i} \frac{2}{q'^2} \left\{1 + \left(\frac{m_i T_e}{m_e T_i}\right)^{1/2} \frac{z_{\mathbf{q}}^S}{q'} Z\left[\left(\frac{m_i T_e}{m_e T_i}\right)^{1/2} \frac{z_{\mathbf{q}}^S}{q'}\right]\right\}. \quad (11)$$

For Maxwellian velocity distribution (9), the velocity integral $\int d\mathbf{u}$ in Eqs. (6) and (7) can be carried out analytically upon making use of the resonance delta function conditions. One may also perform the angular integration associated with the \mathbf{q}' vector integral, which reduces Eqs. (6) and (7) in the form that involves a single q' integration

$$\gamma_{\mathbf{q}}^{L(\text{coll})} = -(16\pi^{1/2} g) \frac{(z_{\mathbf{q}}^L)^2}{q^2} \int_0^\infty \frac{dq'}{|\epsilon(q', z_{\mathbf{q}}^L)|^2} \\ \times \left(\frac{2B^2 - A^2}{B^2 - A^2} - \frac{B}{A} \ln \frac{B+A}{B-A}\right) \frac{1}{q'^3} \exp\left(-\frac{(z_{\mathbf{q}}^L)^2}{q'^2}\right), \quad (12)$$

$$\gamma_{\mathbf{q}}^{S(\text{coll})} = -(16\pi^{1/2} g) \frac{\mu_{\mathbf{q}} z_{\mathbf{q}}^L z_{\mathbf{q}}^S}{q^2} \int_0^\infty \frac{dq'}{|\epsilon(q', z_{\mathbf{q}}^S)|^2} \\ \times \left[\frac{4}{B^2 - A^2} - \frac{T_e}{T_i} \frac{q'}{q^2 q'^2} \frac{1}{q'^3} \left(\frac{2AB}{B^2 - A^2} - \ln \frac{B+A}{B-A}\right)\right] \\ \times \sum_{a=e,i} \frac{T_e}{T_a} \left(\frac{m_a T_e}{m_e T_a}\right)^{1/2} \frac{1}{q'^3} \exp\left(-\frac{m_a T_e}{m_e T_a} \frac{(z_{\mathbf{q}}^S)^2}{q'^2}\right), \quad (13)$$

where we have defined

$$A = -2qq', \quad (14)$$

$$B = 2\left(1 + \frac{T_e}{T_i}\right) + q^2 + q'^2.$$

For reference, the customary heuristic collisional damping rate (2), derived under the “Spitzer approximation,” which is applicable for Langmuir wave, is given in normalized form by

$$\bar{\gamma}_{\text{coll}} \equiv \frac{\gamma_{\text{coll}}}{\omega_{pe}} = -\frac{\pi n_e e^4 \ln \Lambda}{m_e^2 v_e^3 \omega_{pe}} = -\pi g \ln\left(\frac{1}{2^{3/2}(4\pi g)}\right). \quad (15)$$

For comparison, we also discuss the collisionless damping, also known as Landau damping, which is well-known. From Eq. (3.24) of Ref. 1, we have the Landau damping rates for L and S waves

$$\gamma_{\mathbf{k}}^L = \frac{\pi \omega_{\mathbf{k}}^L \omega_{pe}^2}{2k^2} \int d\mathbf{v} \mathbf{k} \cdot \frac{\partial F_e(\mathbf{v})}{\partial \mathbf{v}} \delta(\omega_{\mathbf{k}}^L - \mathbf{k} \cdot \mathbf{v}),$$

$$\gamma_{\mathbf{k}}^S = \frac{\pi \mu_{\mathbf{k}} \omega_{\mathbf{k}}^L \omega_{pe}^2}{2k^2} \int d\mathbf{v} \mathbf{k} \cdot \frac{\partial}{\partial \mathbf{v}} \left(F_e(\mathbf{v}) + \frac{m_e}{m_i} F_i(\mathbf{v})\right) \delta(\omega_{\mathbf{k}}^S - \mathbf{k} \cdot \mathbf{v}), \quad (16)$$

which are textbook results. Making use of dimensionless variables, the above expressions are rewritten as

$$\gamma_{\mathbf{q}}^L = -\frac{\pi^{1/2} (z_{\mathbf{q}}^L)^2}{q^3} \exp\left(-\frac{(z_{\mathbf{q}}^L)^2}{q^2}\right),$$

$$\gamma_{\mathbf{q}}^S = -\frac{\pi^{1/2} \mu_{\mathbf{q}} z_{\mathbf{q}}^L z_{\mathbf{q}}^S}{q^3} \sum_{a=e,i} \frac{T_e}{T_a} \left(\frac{m_a T_e}{m_e T_a}\right)^{1/2} \exp\left(-\frac{m_a T_e}{m_e T_a} \frac{(z_{\mathbf{q}}^S)^2}{q^2}\right). \quad (17)$$

In Fig. 1, we plot the normalized collisional L mode damping rate divided by g , $\gamma_q^{L(\text{coll})}/g$, as a function of dimensionless wave number q , for three values of the temperature ratio $T_e/T_i = 10$ (red), 7 (black), and 4 (blue). It is shown that for the range of temperature ratios considered, the damping rate is maximum for q between 5 and 9, approximately, and that the growth rate increases with decreasing temperature ratio T_e/T_i , for the entire range of wavelengths. In contrast, the approximate collisional damping rate divided by g , $\bar{\gamma}_{\text{coll}}/g = \pi \ln[2^{3/2}(4\pi g)]$, is independent of the normalized wave number q , but the result depends on g . In general, the

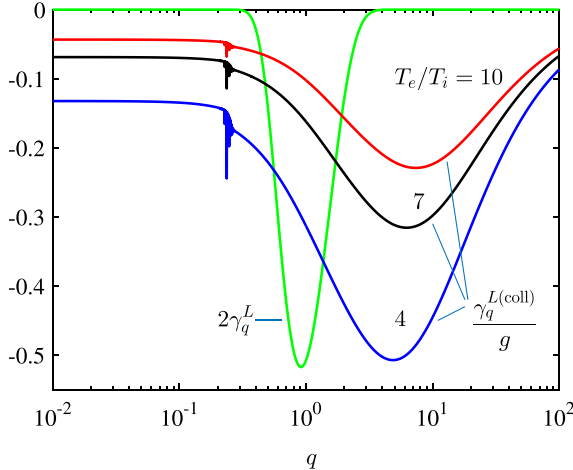


FIG. 1. Normalized collisional damping for L waves, $\gamma_q^{L(\text{coll})}/g$, vs normalized wavenumber q , for three values of the ratio T_e/T_i . The dimensionless Landau damping rate $2\gamma_q^L$ is also plotted in green. Note that the Landau damping rate is *not* divided by the factor g . The factor 2, which multiplies γ_q^L is for the sake of visual presentation.

plasma parameter g must be small by definition, so we consider several different choices, $g = 10^{-10}, 10^{-8}, 10^{-6}$, and 10^{-4} . For these choices, we find that $\bar{\gamma}_{\text{coll}}/g \sim -61.12, -46.6524, -32.1849$, and -17.7173 , which are all far higher in absolute value than those depicted in Fig. 1. This shows that the use of incorrect collisional damping rate may greatly over-estimate the actual damping rate.

We also superpose in Fig. 1, the collisionless (Landau) damping rate for Langmuir wave [i.e., the first equation in (17)] vs q (green). We multiplied the damping rate by factor 2 for visual reason. Note that the Landau damping rate is *not* divided by the plasma parameter g , so that the actual magnitude of the “collisionless” damping rate will greatly exceed that of the “collisional” damping rate by factor $1/g \gg 1$. This shows that over the range of wave numbers over which the most important linear and nonlinear wave-particle interactions are expected to take place, the collisional damping of the Langmuir wave will be practically ignorable. However, it is interesting to note that for small wave number domain ($q \ll 1$) for which the Landau damping rate becomes negligible, the collisional damping rate remains finite. In the collisionless plasmas, the undamped Langmuir waves in the long wavelength regime are supposed to lead to the so-called condensation phenomenon, where the wave energy accumulates without undergoing Landau damping. Over a long time period, the Zakharov strong turbulence effect is supposed to come into play in order to dissipate the accumulated wave energy.¹⁷ However, the present finding suggests that the collisional damping may contribute to the dissipation of the Langmuir wave energy in such a wavelength regime. We also note that for large q , the collisionless (Landau) damping rate eventually becomes exponentially weak. In contrast, the collisional damping rate may overcome the Landau damping rate, which makes sense, since for extremely short wavelength the binary collisions may lead to the damping of plasma waves.

Before we close and for the sake of completeness, we plot in Fig. 2 the normalized collisional damping for S waves

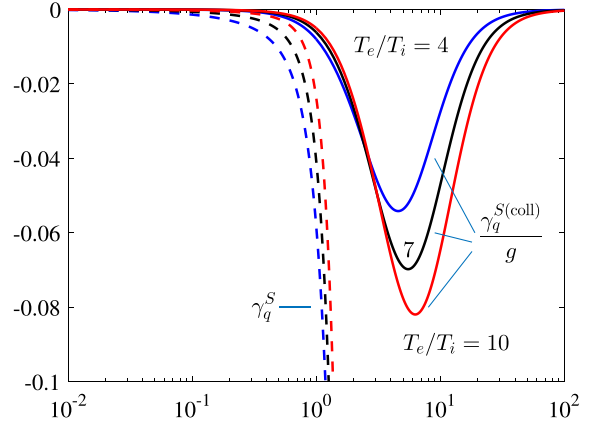


FIG. 2. Normalized collisional damping for S waves, $\gamma_q^{S(\text{coll})}/g$, vs normalized wavenumber q , for three values of the ratio T_e/T_i .

divided by g , $\gamma_q^{S(\text{coll})}/g$, as a function of wave number q , for the same three values of the temperature ratio considered in Fig. 1, that is, $T_e/T_i = 4, 7$, and 10 . The same color scheme is used to indicate the three cases. Unlike the case of L mode, the collisional damping rate for S mode does not asymptotically approach a finite value for $q \rightarrow 0$. We also superpose the collisionless (Landau) damping rates for S waves vs q , but since γ_q^S depends on T_e/T_i , we use the same color scheme to indicate the three difference choices of T_e/T_i , except that we plot the collisionless damping rate with dashes. Again, we note that γ_q^S is *not* divided by g , so that the actual damping rate is much higher in magnitude than the collisional damping rate $\gamma_q^{S(\text{coll})}$. In the case of S mode, it becomes evident that the collisional damping plays no significant role whatsoever when compared against the collisionless damping, and thus the dynamical role of collisions on the dissipation of ion-sound mode damping becomes totally negligible.

In the present brief communication, we have investigated the formal collisional damping rates derived in Ref. 1, by numerical means. It is found that the collisional damping rates for Langmuir and ion-acoustic waves are much smaller than the conventional expressions, which means that the collisional damping has been over-estimated in the literature. While the collisional damping for ion-sound wave is totally negligible, the same for Langmuir wave becomes finite, albeit small, in the region of infinite wave length regime where collisionless Landau damping rate vanishes. Such a property may potentially provide the necessary dissipation mechanism in order to prevent the unchecked accumulation of wave energy for the long wavelength regime, known as the Langmuir condensation problem.

The importance of the present work is quite obvious. There are many physical situations where collisional and collective effects are both important, both in laboratory and space applications. The present analysis is based upon the recent work,¹ which makes a simplifying assumption of electrostatic interaction in field-free plasmas. For more realistic applications, electromagnetic interaction in magnetized plasmas must be considered within the framework of the collisional weak turbulence theory. Reference 1 and the present work may represent the beginning of a new research paradigm.

This work has been partially supported by CNPq (Brazil). P.H.Y. acknowledges support by NSF Grant Nos. AGS1147759 and AGS1550566 to the University of Maryland. The research at Kyung Hee University was supported by the BK21-Plus grant from the National Research Foundation (NRF), Korea. P.H.Y. also acknowledges the Science Award Grant from the GFT Foundation to the University of Maryland.

¹P. H. Yoon, L. F. Ziebell, E. P. Kontar, and R. Schlickeiser, *Phys. Rev. E* **93**, 033203 (2016).

²P. Helander and D. J. Sigmar, *Collisional Transport in Magnetized Plasmas* (Cambridge University Press, New York, 2002).

³G. P. Zank, *Transport Processes in Space Physics and Astrophysics* (Springer, New York, 2014).

⁴A. G. Sitenko, *Fluctuations & Non-linear Wave Interactions in Plasmas* (Pergamon, New York, 1982).

⁵D. B. Melrose, *Instabilities in Space and Laboratory Plasmas* (Cambridge University Press, New York, 1986).

⁶R. Balescu, *Aspects of Anomalous Transport in Plasmas* (Institute of Physics Publishing, Philadelphia, 2005).

⁷R. A. Treumann and W. Baumjohann, *Advanced Space Plasma Physics* (Imperial College Press, London, 2001).

⁸K. G. McClements, *Astron. Astrophys.* **175**, 255 (1987).

⁹I. G. Hannah, E. P. Kontar, and O. K. Sirenko, *Astrophys. J. Lett.* **707**, L45 (2009).

¹⁰H. Ratcliffe and E. P. Kontar, *Astron. Astrophys.* **562**, A57 (2014).

¹¹M. C. Kelley, *The Earth's Ionosphere* (Academic Press, New York, 1989).

¹²G. G. Comisar, *Phys. Fluids* **6**, 76 (1963).

¹³W. P. Wood and B. W. Ninham, *Aust. J. Phys.* **22**, 453 (1969).

¹⁴D. B. Melrose, *Plasma Astrophysics* (Gordon and Breach, New York, 1980).

¹⁵A. O. Benz, *Plasma Astrophysics* (Kluwer, Dordrecht, 2002).

¹⁶E. M. Lifshitz and L. P. Pitaevskii, *Physical Kinetics* (Pergamon, New York, 1981).

¹⁷V. E. Zakharov, *Sov. Phys. JETP* **35**, 908 (1972).

5.2 Generation of suprathermal electrons by collective processes in collisional plasmas

For the analysis of the electrostatic bremsstrahlung, the simple integration of Eqs. (4.36) and (4.37) was not very clarifying since we did not have any equivalent effect for comparison. So we had to perform the time evolution of the system and analyze the outcome. However, in order to put in evidence the action of the new effect, is useful to start with the simplest possible situation. Therefore, instead of using the complete set of nonlinear weak turbulence equations given by Eqs. (4.38) and (4.39), we restrict our analysis to the quasilinear formalism, which includes single particle spontaneous emission and wave-particle induced emission, and add the collisional damping and electrostatic bremsstrahlung effects. The particle kinetic equation is given by the usual quasilinear equation, where we included the Landau collision integral (the same used in [45]). After a long evolution period, the system reaches a steady state where the electron velocity distribution strongly resembles a core-halo distribution. An interesting and surprising detail is that this suprathermal electron population grows even in the presence of binary collisions. In the next two subsections we provide some helpful information regarding the equations and methods employed in [78].

Furthermore, an extra result is presented in Appendix B, where we compare the stationary state of the L waves spectrum obtained after the time evolution (using the results discussed in [45]), with the asymptotic Langmuir spectrum generated by a theoretical core-halo distribution, composed 95% by a Maxwellian core and 5% by a kappa tail, in the presence and in the absence of bremsstrahlung emission, for several values of the κ index. It is shown that the asymptotic spectra obtained in the case of distributions with low κ indexes are less affected by the electrostatic bremsstrahlung emission than the spectra generated in the presence of higher κ indexes, and in the Maxwellian case. These findings suggest that core-halo distributions may represent the asymptotic equilibrium when the electrostatic bremsstrahlung is taken into account.

5.2.1 Dimensionless equations

In order to simplify the numerical analysis, it is convenient to write the equations in terms of dimensionless variables. Thus, let us start by some important definitions

$$\begin{aligned} z &\equiv \frac{\omega}{\omega_{pe}}, & \tau &\equiv \omega_{pe}t, & \mathbf{q} &\equiv \frac{\mathbf{k}v_e}{\omega_{pe}}, & \mathbf{u} &\equiv \frac{\mathbf{v}}{v_e}, \\ \mu_{\mathbf{q}}^L &= 1, & \mu_{\mathbf{q}}^S &= \frac{q^3}{2^{3/2}} \sqrt{\frac{m_e}{m_i}} \left(1 + \frac{3T_i}{T_e}\right)^{1/2}, \end{aligned}$$

$$\Phi_a(\mathbf{u}) = v_e^3 F_a(\mathbf{u}), \quad \mathcal{E}_{\mathbf{q}}^{\sigma\alpha} = \frac{(2\pi)^2 g}{m_e v_e^2} \frac{I_{\mathbf{k}}^{\sigma\alpha}}{\mu_{\mathbf{k}}^{\alpha}}, \quad P_{\mathbf{k}}^{\alpha} = \frac{m_e v_e^2}{(2\pi)^2 g} \omega_{pe} P_{\mathbf{q}}^{\alpha},$$

where $g = 1/[2^{3/2} (4\pi)^2 \hat{n} \lambda_{De}^3]$ is the plasma parameter, $\lambda_{De} = T_e/(4\pi \hat{n} e^2) = v_e^2/(2\omega_{pe}^2)$, $v_e = (2T_e/m_e)^{1/2}$ is the electron thermal velocity and T_e is the electron temperature.

In terms of the normalized variables and quantities, the equations for L and S waves, including the contributions from non-eigenmode fluctuations, become

$$\begin{aligned} \frac{\partial \mathcal{E}_{\mathbf{q}}^{\sigma L}}{\partial \tau} &= \mu_{\mathbf{q}}^L \frac{\pi}{q^2} \int d\mathbf{u} \delta(\sigma z_{\mathbf{q}}^L - \mathbf{q} \cdot \mathbf{u}) \\ &\times \left(g \Phi_e(\mathbf{u}) + (\sigma z_{\mathbf{q}}^L) \mathbf{q} \cdot \frac{\partial \Phi_e(\mathbf{u})}{\partial \mathbf{u}} \mathcal{E}_{\mathbf{q}}^{\sigma L} \right) + 2\mathcal{E}_{\mathbf{q}}^{\sigma L} \gamma_{\mathbf{q}}^{\sigma L} + P_{\mathbf{q}}^{\sigma L}, \end{aligned} \quad (5.1)$$

$$\begin{aligned} \frac{\partial \mathcal{E}_{\mathbf{q}}^{\sigma S}}{\partial \tau} &= \mu_{\mathbf{q}}^S \frac{\pi}{q^2} \int d\mathbf{u} \delta(\sigma z_{\mathbf{q}}^S - \mathbf{q} \cdot \mathbf{u}) \left[g[\Phi_e(\mathbf{u}) + \Phi_i(\mathbf{u})] \right. \\ &\left. + (\sigma z_{\mathbf{q}}^S) \left(\mathbf{q} \cdot \frac{\partial \Phi_e(\mathbf{u})}{\partial \mathbf{u}} + \frac{m_e}{m_i} \mathbf{q} \cdot \frac{\partial \Phi_i(\mathbf{u})}{\partial \mathbf{u}} \right) \mathcal{E}_{\mathbf{q}}^{\sigma S} \right] + 2\mathcal{E}_{\mathbf{q}}^{\sigma S} \gamma_{\mathbf{q}}^{\sigma S} + P_{\mathbf{q}}^{\sigma S}, \end{aligned} \quad (5.2)$$

where $\gamma_{\mathbf{q}}^{\sigma L}$ and $\gamma_{\mathbf{q}}^{\sigma S}$ are the dimensionless form of Eqs. (4.31) and (4.32), which describe the collisional damping rate for L and S waves, respectively

$$\begin{aligned} \gamma_{\mathbf{q}}^{\sigma L} &= \frac{2g z_{\mathbf{q}}^L}{q^2} \int d\mathbf{q}' \frac{(\mathbf{q} \cdot \mathbf{q}')^2}{q'^4 |\epsilon(\mathbf{q}', z_{\mathbf{q}}^L)|^2} \left(1 + \frac{T_e}{T_i} + \frac{(\mathbf{q} - \mathbf{q}')^2}{2} \right)^{-2} \\ &\times \int d\mathbf{u} \mathbf{q}' \cdot \frac{\partial \Phi_e(\mathbf{u})}{\partial \mathbf{u}} \delta(z_{\mathbf{q}}^L - \mathbf{q}' \cdot \mathbf{u}), \end{aligned} \quad (5.3)$$

$$\begin{aligned} \gamma_{\mathbf{q}}^{\sigma S} &= \frac{2g z_{\mathbf{q}}^S}{q^2} \int \frac{d\mathbf{q}'}{q'^4 |\epsilon(\mathbf{q}', z_{\mathbf{q}}^S)|^2} \left(1 + \frac{T_e}{T_i} + \frac{(\mathbf{q} - \mathbf{q}')^2}{2} \right)^{-2} \left(1 + \frac{2T_e}{T_i} \frac{\mathbf{q} \cdot \mathbf{q}'}{q^2} \right) \\ &\times \int d\mathbf{u} \mathbf{q}' \cdot \frac{\partial}{\partial \mathbf{u}} \left(\Phi_e(\mathbf{u}) + \frac{m_e}{m_i} \Phi_i(\mathbf{u}) \right) \delta(z_{\mathbf{q}}^S - \mathbf{q}' \cdot \mathbf{u}). \end{aligned} \quad (5.4)$$

The terms $P_{\mathbf{q}}^{\sigma L}$ and $P_{\mathbf{q}}^{\sigma S}$ are the normalized versions of Eqs. (4.36) and (4.37), that depict the electrostatic bremsstrahlung effect for L and S waves, and are respectively given by

$$\begin{aligned} P_{\mathbf{q}}^{\sigma L} &= \frac{12e^2}{\pi^3} \frac{1}{q^2} \frac{1}{(z_{\mathbf{q}}^L)^2} \left(1 - \frac{m_e}{m_i} \frac{T_e}{T_i} \right)^2 \frac{\omega_{pe}^2}{v_e} \int d\mathbf{q}' q'^2 |\mathbf{q} - \mathbf{q}'|^2 \\ &\times \left[2 \left(1 + \frac{T_e}{T_i} \right) + q'^2 \right]^{-2} \left[2 \left(1 + \frac{T_e}{T_i} \right) + |\mathbf{q} - \mathbf{q}'|^2 \right]^{-2} \\ &\times \int d\mathbf{u} \int d\mathbf{u}' \delta \left[\sigma z_{\mathbf{q}}^L - \mathbf{q} \cdot \mathbf{u} + \mathbf{q}' \cdot (\mathbf{u} - \mathbf{u}') \right] \sum_a \Phi_a(\mathbf{u}) \sum_b \Phi_b(\mathbf{u}'), \end{aligned} \quad (5.5)$$

$$\begin{aligned}
P_{\mathbf{q}}^{\sigma S} = & \mu_{\mathbf{q}} \frac{3e^2 T_e}{16\pi^3 m_e} \left(1 - \frac{T_e^2}{T_i^2}\right)^2 \frac{32 \omega_{pe}^2}{q^2 v_e^3} \int d\mathbf{q}' \\
& \times \left[2 \left(1 + \frac{T_e}{T_i}\right) + q'^2\right]^{-2} \left[2 \left(1 + \frac{T_e}{T_i}\right) + (\mathbf{q} - \mathbf{q}')^2\right]^{-2} \\
& \times \int d\mathbf{u} \int d\mathbf{u}' \delta[\sigma z_{\mathbf{q}}^L - \mathbf{q}' \cdot \mathbf{u}' - (\mathbf{q} - \mathbf{q}') \cdot \mathbf{u}] \sum_a \Phi_a(\mathbf{u}) \sum_b \Phi_b(\mathbf{u}').
\end{aligned} \tag{5.6}$$

The dimensionless form of the particle kinetic equation has the following form

$$\begin{aligned}
\frac{\partial \Phi_a(\mathbf{u})}{\partial \tau} = & \frac{e_a^2 m_e^2}{e^2 m_a^2} \sum_{\sigma} \sum_{\alpha=L,S} \int d\mathbf{q} \left(\frac{\mathbf{q}}{q} \cdot \frac{\partial}{\partial \mathbf{u}} \right) \mu_{\mathbf{q}}^{\alpha} \delta(\sigma z_{\mathbf{q}}^{\alpha} - \mathbf{q} \cdot \mathbf{u}) \\
& \times \left(g \frac{m_a}{m_e} \frac{\sigma z_{\mathbf{q}}^L}{q} \Phi_a(\mathbf{u}) + \mathcal{E}_{\mathbf{q}}^{\sigma \alpha} \frac{\mathbf{q}}{q} \cdot \frac{\partial \Phi_a(\mathbf{u})}{\partial \mathbf{u}} \right) + \sum_b \theta_{ab}(\Phi_a, \Phi_b),
\end{aligned} \tag{5.7}$$

where $\theta_{ab}(\Phi_a, \Phi_b)$ is the linearized Landau collision integral, which, for $a = e$, is given by

$$\begin{aligned}
\sum_b \theta_{eb}(\Phi_e, \Phi_b) = & \sum_b \Gamma_{eb} \left\{ \frac{\partial}{\partial \mathbf{u}} \cdot \left(2 \frac{m_e}{m_b} \Psi(u_{eb}) \frac{\mathbf{u}}{u^3} \Phi_e \right) \right. \\
& + \frac{\partial}{\partial \mathbf{u}} \cdot \left\{ \left[\left(\Phi(u_{eb}) - \frac{1}{2u_{eb}^2} \Psi(u_{eb}) \right) \frac{\partial^2 u}{\partial \mathbf{u} \partial \mathbf{u}} \right] \cdot \frac{\partial \Phi_e}{\partial \mathbf{u}} \right\} \\
& \left. + \frac{\partial}{\partial \mathbf{u}} \cdot \left[\left(\frac{1}{u_{eb}^2} \Psi(u_{eb}) \frac{\mathbf{u} \mathbf{u}}{u^3} \right) \cdot \frac{\partial \Phi_e}{\partial \mathbf{u}} \right] \right\},
\end{aligned} \tag{5.8}$$

where $u_{eb} \equiv u(v_{te}/v_{tb})$, $u = v/v_{te}$, with v_{te} and v_{tb} representing the thermal velocity of electrons and the particles of species b , with $b = e, i$. The quantity $\Psi(x) \equiv \Phi(x) - x\Phi'(x)$ is an auxiliary function [83], in which $\Phi(x) \equiv \frac{2}{\sqrt{\pi}} \int_0^x e^{-t^2} dt$ is the error function and $\Phi'(x) = \frac{2}{\sqrt{\pi}} e^{-x^2}$ is its derivative. The factor Γ_{eb} is given by $\Gamma_{eb} = 2\pi g Z_b^2 \ln \Lambda$, where $g = 1/[2^{3/2}(4\pi)^2 \hat{n} \lambda_{De}^3]$ is the plasma parameter, $\ln \Lambda$ is Coulomb logarithm, and $Z_{b=e,i}$ is the charge number of ions and electrons, with $Z_e = 1$. The dispersion relations for L and S waves in dimensionless form are given by

$$z_{\mathbf{q}}^L = \left(1 + \frac{3}{2} q^2\right)^{1/2}, \quad z_{\mathbf{q}}^S = \frac{q A}{(1 + q^2/2)^{1/2}}, \quad A = \frac{1}{\sqrt{2}} \left(\frac{m_e}{m_i}\right)^{1/2} \left(1 + 3 \frac{T_i}{T_e}\right)^{1/2}.$$

The above set of integro-differential equations was numerically solved in 2D wave-number space and 2D velocity space, respectively. For the wave kinetic equations, it was used a fourth-order Runge-Kutta method and, for the partial differential equation describing the electron dynamics, we employed the splitting algorithm. In both cases we used fixed time step $\Delta\tau = 0.1$. The wave number space grid has been assumed with 71×71 points in k_{\perp} and k_{\parallel} , with $0 < k_{\perp} v_e / \omega_{pe} < 0.6$ and $0 < k_{\parallel} v_e / \omega_{pe} < 0.6$. In the velocity space, the grid configuration was 71×141 for v_{\perp}/v_e and v_{\parallel}/v_e , with velocity range $0 < v_{\perp}/v_e < 16$ and $-16 < v_{\parallel}/v_e < 16$.



Generation of Suprathermal Electrons by Collective Processes in Collisional Plasma

S. F. Tigik¹ , L. F. Ziebell¹ , and P. H. Yoon^{2,3,4}

¹ Instituto de Física, Universidade Federal do Rio Grande do Sul, 91501-970 Porto Alegre, RS, Brazil; sabrina.tigik@ufrgs.br, luiz.ziebell@ufrgs.br

² Institute for Physical Science & Technology, University of Maryland, College Park, MD 20742, USA; yoonp@umd.edu

³ School of Space Research, Kyung Hee University, Yongin, Korea

⁴ Korea Astronomy and Space Science Institute, Daejeon, Korea

Received 2017 August 31; revised 2017 October 8; accepted 2017 October 20; published 2017 November 8

Abstract

The ubiquity of high-energy tails in the charged particle velocity distribution functions (VDFs) observed in space plasmas suggests the existence of an underlying process responsible for taking a fraction of the charged particle population out of thermal equilibrium and redistributing it to suprathermal velocity and energy ranges. The present Letter focuses on a new and fundamental physical explanation for the origin of suprathermal electron velocity distribution function (EVDF) in a collisional plasma. This process involves a newly discovered electrostatic bremsstrahlung (EB) emission that is effective in a plasma in which binary collisions are present. The steady-state EVDF dictated by such a process corresponds to a Maxwellian core plus a quasi-inverse power-law tail, which is a feature commonly observed in many space plasma environments. In order to demonstrate this, the system of self-consistent particle- and wave-kinetic equations are numerically solved with an initially Maxwellian EVDF and Langmuir wave spectral intensity, which is a state that does not reflect the presence of EB process, and hence not in force balance. The EB term subsequently drives the system to a new force-balanced steady state. After a long integration period it is demonstrated that the initial Langmuir fluctuation spectrum is modified, which in turn distorts the initial Maxwellian EVDF into a VDF that resembles the said core-suprathermal VDF. Such a mechanism may thus be operative at the coronal source region, which is characterized by high collisionality.

Key words: solar wind – Sun: corona – Sun: particle emission

1. Introduction

Inverse power-law velocity or energy distributions of charged particles are either directly observed or inferred in various regions of the universe accessible to either direct or remote observations, which includes 4–5 MeV protons accelerated at the heliospheric termination shock and detected by the *Voyager 1* and 2 spacecraft (Stone et al. 2008), tens of MeV electrons energized at the magnetic-field loop-top X-ray sources during solar flares (Krucker & Battaglia 2014; Oka et al. 2015), energetic ions and electrons measured in the geomagnetic tail region during disturbed conditions (Christon et al. 1991), etc. The solar wind is also replete with background populations of protons and electrons featuring inverse power-law tail distributions even in extremely quiet conditions (Vasyliunas 1968; Feldman et al. 1975; Lin 1998; Gloeckler 2003; Fisk & Gloeckler 2012).

In particular, the solar wind electron velocity distribution function (EVDF) is composed of a Maxwellian core ($\gtrsim 95\%$ of the total density), with energies around 10 eV, a tenuous ($4 \sim 5\%$) high-energy halo with energies up to $10^2 \sim 10^3$ eV, and a highly energetic “superhalo” population with the density ratio of $10^{-9} \sim 10^{-6}$ and with energies up to ~ 100 keV (Lin 1998). For fast wind, sometimes a narrow beam-like structure called the *strahl*, which is aligned with the magnetic field and streaming in the anti-sunward direction, is also measured (Feldman et al. 1976, 1978; Pierrard et al. 1999).

Given the prevalence of non-thermal distributions in nature, the study of the charged particle acceleration mechanisms that produce such distributions is of obvious importance and has a wide-ranging applicability across different sub-disciplines in astrophysical and space plasma physics. One of the first kinetic models on how suprathermal electron populations are generated involves the assumption that a sub-population of suprathermal

electrons in low coronal regions exists, which is “selected” by Coulomb collisions and interacts with the thermal core and the surrounding environment in order to form the power-law EVDF at 1 au (Scudder & Olbert 1979a, 1979b). Later improved models generally rely on Coulomb collisional dynamics at the coronal base and phase-space mapping along inhomogeneous solar magnetic field lines (Lie-Svendsen et al. 1997; Pierrard et al. 1999, 2001). Collisional effects, however, become rather insignificant for solar altitudes higher than, say, 10 solar radii. In order to explain the observed quasi-isotropic nature of EVDF near 1 au, wave-particle resonant interaction must be important. Thus, the collective effects on the EVDF have been considered with or without other global features (Vocks et al. 2005; Vocks 2012; Pavan et al. 2013; Seough et al. 2015; Kim et al. 2016).

An outstanding issue is whether the suprathermal EVDFs are generated at the coronal source region in the first place. This issue may have important ramifications on the coronal heat flux and inverted temperature profile. If an enhanced number of high-energy particles is assumed to be present in the low transition region of the Sun, more particles are capable of escaping the gravitational potential, unleashing the so-called “velocity filtration effect,” which is shown to produce the observed temperature inversion in the solar corona, a feature that may be relevant to the coronal heating (Scudder 1992a, 1992b; Teles et al. 2015). In this regard, Che & Goldstein (2014) proposed a scenario in which electron streams accelerated by nanoflares can lead to the two-stream instability, and ultimately produce a core-halo distribution in the inner corona. According to their model, the core-halo population is simply convected outward along open field lines while preserving the phase-space properties.

In this Letter we propose an alternative mechanism. This is not an acceleration in the traditional sense, but rather it is a mechanism that relies on a new fundamental plasma process involving the wave-particle interaction in a collisional plasma. Our theory is based on a recent paper by Yoon et al. (2016), where the kinetic theory of collective processes in collisional plasmas was formulated. The problem of combined collisional dissipation and collective processes had not been rigorously investigated from first principles in the literature. This is not to say that collisional dissipation processes or collective processes are not understood separately. On the contrary, each process is well understood. Indeed, if one is interested in the situation where the binary collisional relaxation is dominant, then transport processes can be legitimately discussed solely on the basis of the well-known collisional kinetic equation (Helander & Sigmar 2002; Zank 2014). Conversely, if one's concern is only on relaxation processes that involve collective oscillations, waves, and instabilities, there exists a vast amount of literature on linear and nonlinear theories of plasma waves, instabilities, and turbulence. It is the dichotomy that separates the purely collisional versus purely collective descriptions that had not been rigorously bridged until Yoon et al. (2016).

Among the findings of Yoon et al. (2016) is a hitherto-unknown effect that came out without any ad hoc assumption. The first principle equation of this new effect depicts the emission of electrostatic fluctuations, in the eigenmode frequency range, caused by particle scattering. This electrostatic form of “braking radiation” was appropriately named electrostatic bremsstrahlung (EB) by the authors of Yoon et al. (2016), which is not to be confused with a process sometimes known in the literature by the same terminology. In the literature, the process of relativistic electrons scattering Langmuir waves into transverse radiation is also called the “electrostatic bremsstrahlung” (Gailitis & Tsytovich 1964; Colgate 1967; Melrose 1971; Windsor & Kellogg 1974; Akopyan & Tsytovich 1977; Schlickeiser 2003), which is actually an induced scattering of transverse radiation off of relativistic electrons mediated by Langmuir waves. The “electrostatic bremsstrahlung” of Yoon et al. (2016) is the emission of electrostatic eigenmodes by collisional process, which is analogous to but distinct from the emission of transverse electromagnetic radiation by collisional process.

As will be demonstrated subsequently, the combined effects of Langmuir wave-electron resonant interaction in the presence of the new EB process leads to the self-consistent formation of the core-halo EVDF, which is a process that may be operative pervasively in the lower coronal environment. We thus suggest that the present mechanism may be the most widely operative process that is responsible for the formation of non-thermal EVDFs, not only in the solar environment, but also in other astrophysical environments. In the rest of this Letter, we detail the present finding.

2. Theoretical Formulation

The essential idea behind the new process responsible for taking a fraction of the electron population out of thermal equilibrium and redistributing it to suprathermal velocity and energy ranges is that the presence of the EB emission term (as well as the collisional damping term) in the wave-kinetic equation, combined with the particle kinetic equation, leads to a new steady-state electron distribution function, which corresponds to a Maxwellian core plus a quasi-inverse power-law

tail. Conceptually, such a state is a new quasi-equilibrium that is distinct from thermodynamic equilibrium. In such a state, enhanced electrostatic fluctuations coexist with a population of charged particles while maintaining a dynamical steady state. In order to demonstrate this process, we numerically solve the system of particle- and wave-kinetic equations of the generalized weak turbulence theory (Yoon et al. 2016), starting with an initially Maxwellian electron velocity distribution and Langmuir wave spectral intensity that reflects the presence of only the customary spontaneous and induced emissions, but not the EB or the collisional damping. Of course, such an initial state is out of force balance. The EB and collisional damping terms subsequently drive the system to a new force-balanced steady state for the wave intensity. The initial Langmuir fluctuation spectrum is thus significantly modified as a result of the additional terms in the wave-kinetic equation. The modified Langmuir wave spectrum in turn distorts the initial Maxwellian electron distribution, and transforms it into a new quasi-steady-state velocity distribution function (VDF) that superficially resembles the core-suprathermal velocity distribution function. In what follows, we discuss the details of this numerical demonstration.

We perform the self-consistent numerical analysis on the EB emission in the Langmuir (L) electrostatic eigenmode frequency range by including the new mechanism in the wave-kinetic equation. Instead of making use of the complete set of nonlinear weak turbulence equations presented in Yoon et al. (2016), we restrict our analysis to the quasi-linear formalism, which includes single-particle spontaneous emission and wave-particle induced emission. We also take into account in the wave equations the effects of collisional damping. Such a simplified approach allows the study of the time evolution of the system, and puts in evidence the new mechanisms that have been introduced in Yoon et al. (2016). Besides, in the absence of free-energy sources, with which the present Letter is not concerned, the nonlinear mode-coupling terms are not expected to play any important dynamical roles. The equation describing the dynamics of L waves is therefore given by

$$\begin{aligned} \frac{\partial I_k^{\sigma L}}{\partial t} = & \frac{\pi \omega_p^2}{k^2} \int d\mathbf{v} \delta(\sigma \omega_k^L - \mathbf{k} \cdot \mathbf{v}) \\ & \times \left(\frac{n_0 e^2}{\pi} F_e(\mathbf{v}) + \sigma \omega_k^L I_k^{\sigma L} \mathbf{k} \cdot \frac{\partial F_e(\mathbf{v})}{\partial \mathbf{v}} \right) \\ & + 2\gamma_k^{\sigma L} I_k^{\sigma L} + P_k^{\sigma L}, \end{aligned} \quad (1)$$

where $I_k^{\sigma L}$ is the wave intensity associated with the Langmuir wave defined via $E_{k,\omega}^2 = \sum_{\sigma=\pm} I_k^{\sigma L} \delta(\omega - \sigma \omega_k^L)$, $E_{k,\omega}$ is the spectral component of the wave electric field, and the dispersion relation is given by $\omega_k^L = \omega_{pe} \left(1 + \frac{3}{2} k^2 \lambda_D^2 \right)$. Here, $\omega_{pe} = \sqrt{4\pi n_0 e^2 / m_e}$ and $\lambda_D = \sqrt{T_e / (4\pi n_0 e^2)}$ stand for the plasma frequency and Debye length, respectively, and n_0 , e , m_e , and T_e are the ambient density, unit electric charge, electron mass, and electron temperature, respectively.

The first term on the right-hand side of Equation (1) contains two contributions: the first term within the large parenthesis, proportional to the EVDF, $F_e(\mathbf{v})$, represents the discrete-particle effect of spontaneous emission; the second term, proportional to the derivative, $\partial F_e(\mathbf{v}) / \partial \mathbf{v}$, represents the induced emission. The second line of Equation (1) on the right-hand side includes

the collisional wave damping rate, $\gamma_k^{\sigma L}$, obtained in the same context as the EB (Yoon et al. 2016), and numerically analyzed and discussed in Tigik et al. (2016a). The collisional damping is defined by

$$\begin{aligned} \gamma_k^{\sigma L} = & \omega_k^L \frac{4n_e e^4 \omega_{pe}^2}{T_e^2} \int d\mathbf{k}' \frac{(\mathbf{k} \cdot \mathbf{k}')^2 \lambda_D^4}{k'^4 |\epsilon(\mathbf{k}', \omega_k^L)|^2} \\ & \times \left(1 + \frac{T_e}{T_i} + (\mathbf{k} - \mathbf{k}')^2 \lambda_D^2\right)^{-2} \\ & \times \int d\mathbf{v} \mathbf{k}' \cdot \frac{\partial F_e(\mathbf{v})}{\partial \mathbf{v}} \delta(\omega_k^L - \mathbf{k}' \cdot \mathbf{v}), \end{aligned} \quad (2)$$

where T_i is the proton temperature, and $\epsilon(\mathbf{k}, \omega)$ is the linear dielectric-response function. In the literature, the collisional damping rate of plasma waves are often computed by heuristic means. That is, the collisional operator is simply added to the exact Vlasov (or Klimontovich) equation by hand, as it were, and the small-amplitude wave analysis is carried out, leading to the so-called Spitzer formula for the collisional damping rate (Lifshitz & Pitaevskii 1981). A similar heuristic and ad hoc recipe is also applied even for a turbulent plasma (Makhankov & Tsytovich 1968). Such approaches are at best heuristic and, strictly speaking, incorrect, as the collisionality represents dissipation and irreversibility, whereas the Vlasov or Klimontovich equation exactly preserves the phase-space information, and thus is reversible. In the non-equilibrium statistical mechanics it is well known that the irreversibility enters the problem only as a result of statistical averages and the subsequent loss of information. The authors of Yoon et al. (2016) carried out the rigorous analysis of introducing the collisionality starting from the exact Klimontovich equation and taking ensemble averages. The collisional damping rate that emerged, namely Equation (2), is the correct expression that replaces the heuristic Spitzer formula, and it was found in Tigik et al. (2016a) that the heuristic Spitzer collisional damping rate grossly overestimates the actual rate.

The term $P_k^{\sigma L}$ in Equation (1) describes the EB emission process, which is new and is the subject of this Letter. In Yoon et al. (2016) a specific approximate form of $P_k^{\sigma L}$ was derived. In this Letter we have revisited the approximation procedure, and find that a more appropriate form is given by

$$\begin{aligned} P_k^{\sigma L} = & \frac{3e^2}{4\pi^3} \frac{1}{(\omega_k^L)^2} \left(1 - \frac{m_e T_e}{m_i T_i}\right)^2 \frac{v_e^4}{k^2} \int d\mathbf{k}' k'^2 |\mathbf{k} - \mathbf{k}'|^2 \\ & \times \left(1 + \frac{T_e}{T_i} + k'^2 \lambda_D^2\right)^{-2} \left(1 + \frac{T_e}{T_i} + (\mathbf{k} - \mathbf{k}')^2 \lambda_D^2\right)^{-2} \\ & \times \int d\mathbf{v} \int d\mathbf{v}' \sum_{a,b} F_a(\mathbf{v}) F_b(\mathbf{v}') \\ & \times \delta[\sigma \omega_k^L - \mathbf{k} \cdot \mathbf{v} + \mathbf{k}' \cdot (\mathbf{v} - \mathbf{v}')], \end{aligned} \quad (3)$$

where m_i is the proton mass and $v_e = \sqrt{2T_e/m_e}$ stands for electron thermal speed. The detailed derivation of the above-improved formula is reserved for another full-length article, as it is too lengthy for the present Letter.

The dynamical equation for EVDF $F_e(\mathbf{v})$ is given by the particle kinetic equation, which includes the Coulomb collision

operator written in the form of the velocity-space Fokker-Planck equation,

$$\begin{aligned} \frac{\partial F_a(\mathbf{v})}{\partial t} = & \frac{\partial}{\partial \mathbf{v}_i} \left(A_i(\mathbf{v}) F_a(\mathbf{v}) + D_{ij}(\mathbf{v}) \frac{\partial F_a(\mathbf{v})}{\partial \mathbf{v}_j} \right) \\ & + \sum_b \theta_{ab}(F_a, F_b), \\ A_i(\mathbf{v}) = & \frac{e^2}{4\pi m_e} \int d\mathbf{k} \frac{k_i}{k^2} \sum_{\sigma=\pm 1} \sigma \omega_k^L \delta(\sigma \omega_k^L - \mathbf{k} \cdot \mathbf{v}), \\ D_{ij}(\mathbf{v}) = & \frac{\pi e^2}{m_e^2} \int d\mathbf{k} \frac{k_i k_j}{k^2} \sum_{\sigma=\pm 1} \delta(\sigma \omega_k^L - \mathbf{k} \cdot \mathbf{v}) I_k^{\sigma L}, \end{aligned} \quad (4)$$

where the coefficient $A_i(\mathbf{v})$ represents the velocity-space friction, and the coefficient $D_{ij}(\mathbf{v})$ describes the velocity diffusion. The distribution functions, $F_a(\mathbf{v})$ and $F_b(\mathbf{v})$, are both normalized to unity, $\int d\mathbf{v} F_{a,b}(\mathbf{v}) = 1$, where $a = e, i$ and $b = e, i$ represent the interacting particles. The term $\theta_{ab}(F_a, F_b)$ depicts the effects of Coulomb collisions between particles of species a and b .

For the present analysis, we adopt a linearized form of the Landau collision integral for $\theta_{ab}(F_a, F_b)$, in which it is assumed that the evolving EVDF collides with a Maxwellian background distribution. This assumption relies on the fact that the growing tail population of the EVDF has a much lower density than the core electrons, so that the effects of collisions between the tail electrons with the background EVDF are more significant than the effects of collisions among electrons of the tail population. The lengthy linearization procedure can be found in detail in Tigik et al. (2016b) and will not be repeated here for the sake of space economy. In short, the linearized collision operator is given by

$$\begin{aligned} \theta_{ab} (f_a, f_b) = & \Gamma_{ab} \left[\frac{\partial}{\partial \mathbf{v}_a} \cdot \left(2 \frac{m_a}{m_b} \Psi(x_{ab}) \frac{\mathbf{v}_a}{v_a^3} f_a \right) \right. \\ & + \frac{\partial}{\partial \mathbf{v}_a} \cdot \left\{ \left[\left(\Phi(x_{ab}) - \frac{1}{2x_{ab}^2} \Psi(x_{ab}) \right) \frac{\partial^2 v_a}{\partial \mathbf{v}_a \partial \mathbf{v}_a} \right] \cdot \frac{\partial f_a}{\partial \mathbf{v}_a} \right\} \\ & \left. + \frac{\partial}{\partial \mathbf{v}_a} \cdot \left[\left(\frac{1}{x_{ab}^2} \Psi(x_{ab}) \frac{\mathbf{v}_a \mathbf{v}_a}{v_a^3} \right) \cdot \frac{\partial f_a}{\partial \mathbf{v}_a} \right] \right], \end{aligned} \quad (5)$$

where $x_{ab} \equiv v_a/v_{tb}$, v_{tb} is the thermal velocity of the particles of species b , $\Gamma = 4\pi n e^4 \ln \Lambda / m_e^2$, and $\Psi(x) \equiv \Phi(x) - x\Phi'(x)$ is an auxiliary function (Gaffey 1976), in which $\Phi(x_{ab}) \equiv \frac{2}{\sqrt{\pi}} \int_0^x e^{-t^2} dt$ is the error function and $\Phi'(x_{ab}) = \frac{2}{\sqrt{\pi}} e^{-x^2}$ is its derivative.

3. Numerical Analysis

The set of integro-differential equations for waves and particles, (1) and (4), was numerically solved in 2D wave-number space and 2D velocity space, respectively. The purpose of the numerical analysis is to demonstrate that the coupled system of equations leads to an asymptotically steady-state EVDF that resembles the core-halo distribution, regardless of how the solution is initiated. As a concrete example, we assumed an initial state of isotropic Maxwellian VDF for both

ions and electrons, given by

$$F_a(v) = \frac{1}{\pi^{3/2} v_a^3} \exp\left(-\frac{v^2}{v_a^2}\right), \quad (6)$$

where $v_a = (2T_a/m_a)^{1/2}$, with $a = i, e$. The ion VDF is assumed to be constant along the time evolution, which is a reasonable assumption as we are working in the much-faster timescale of electron-ion interactions. The electron-ion temperature ratio of $T_e/T_i = 7.0$ is adopted, and the plasma parameter of $(n_0 \lambda_D^3)^{-1} = 5 \times 10^{-3}$ is used. This choice represents a relatively high collisionality. For the coronal-base source region, at the point where the plasma becomes fully ionized, the electron density is of the order 10^9 – 10^{11} cm $^{-3}$ and the electron temperature may reach $\sim 10^4$ – 10^6 K (Aschwanden 2005) [or equivalently, $\sim 10^0$ – 10^2 eV]. If we assume a central value for the density and the temperature, 10^{10} cm $^{-3}$ and 10^5 K, for instance, the corresponding plasma parameter would be $(n_0 \lambda_D^3)^{-1} \approx 10^{-5}$, more than two orders of magnitude below the value, which we have used for the numerical analysis. Such a higher value was purposely utilized in order to reduce the computational time necessary to obtain the results. The final outcome of the time evolution, however, is not affected by the inflated plasma parameter.

The initial Langmuir wave intensity was chosen by balancing only the spontaneous- and induced-emission processes in the equations for the wave amplitudes, namely,

$$I_k^{\sigma L}(0) = \frac{T_e}{4\pi^2} (1 + 3k^2 \lambda_D^2). \quad (7)$$

Because the VDF and the Langmuir spectrum have azimuthal symmetry, we plot the results of numerical solution by using a 1D projection on the parallel direction of the velocity and wave number.

It is important to note that the initial electron distribution and Langmuir wave spectral intensity, (6) and (7), do not satisfy the steady-state condition $\partial/\partial t = 0$ in the particle- and wave-kinetic Equations (4) and (1), respectively. This is purposeful, since our aim is to demonstrate that the set of Equations (4) and (1) do not permit the electron distribution and Langmuir wave spectral intensity, (6) and (7), respectively, as the legitimate steady-state solution, and so the equations will force the initial state to make a transition to a new steady state or, equivalently, a new quasi-equilibrium state.

For the numerical analysis, we take into account the new effects of collisional damping and EB, starting from the above initial condition. With the addition of these new terms, the initial wave spectrum is no longer in equilibrium with the particle distribution, triggering an interesting evolution. Let us define normalized Langmuir wave intensity

$$\mathcal{E}_q^{\sigma L} = \frac{(2\pi)^2 g}{m_e v_e^2} I_k^{\sigma \alpha},$$

where $g = [2^{3/2} (4\pi)^2 n_e \lambda_D^3]^{-1}$. We also define the normalized temporal variable, $\tau = \omega_{pe} t$, and the normalized wave number $k v_e / \omega_{pe}$. Figure 1 shows the time evolution of $\mathcal{E}_q^{\sigma L}$. It is seen that the bremsstrahlung radiation emitted in the frequency range corresponding to L waves alters the spectrum, creating a modification that starts at $q \approx 0.4$ and ends in a peak around

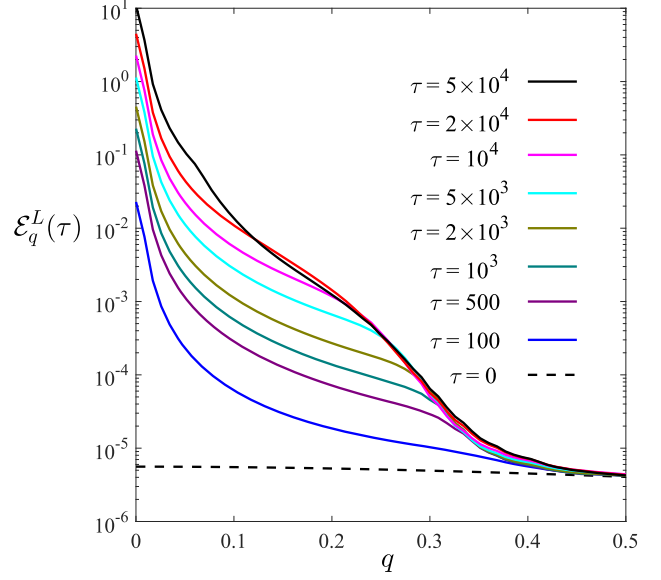


Figure 1. Time evolution of the Langmuir spectrum, taking into account the influence of the bremsstrahlung emission.

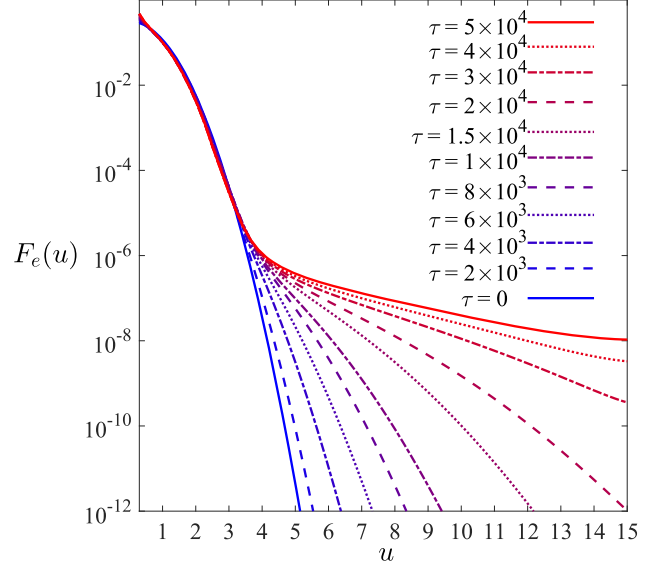


Figure 2. Time evolution of the electron velocity distribution function.

$q = 0$. The wave growth appears early in the time evolution and evolves rapidly, as can be seen in Figure 1. After $\tau = 5000$, the shape of the curve starts to change and the wave growth becomes slower. At $\tau = 50,000$, the Langmuir spectrum appears to be very close to an asymptotic state.

The early stages of the time evolution of the EVDF are quite gradual, but the first signs of modification start to appear around $\tau = 2000$ and are almost imperceptible. In Figure 2, the earliest indication of change is shown at $\tau = 4000$. At this time an energized tail becomes apparent. The demarcation between the core and tail occurs around $u = v/v_e \approx 4.6$. The velocity spectrum associated with the energetic tail population continues to harden as time progresses, while the core defined for $u \lesssim 4.6$ remains essentially unchanged. In short, we have demonstrated that the initial Maxwellian electron distribution

(6) has made a transition to a new quasi-equilibrium state in which the electron distribution function bears a superficial resemblance to the Maxwellian core plus a quasi-inverse power-law tail population.

4. Final Remarks

The results obtained suggest that, in the presence of EB emission, the wave-particle system attains a state of asymptotic equilibrium, in which the EVDF possesses a feature of core-halo distribution that is highly reminiscent of the solar wind EVDF. We thus conclude that the present mechanism of the collective wave-particle interaction process that takes place in a collisional environment, such as the coronal source region, may be a highly efficient and common process in many astrophysical environments. Before we close, we note that we have also analyzed the particle kinetic equation in which the collisional operator is not present on the right-hand side of (4). The result (not shown) is not very different from the present result, which indicates that the mechanism of generating the suprathermal electrons mainly comes from the wave dynamics that operate in a collisional environment.

We have also checked the overall energy budget of the system. Since the initial state, comprised of Maxwellian distribution and Langmuir spectral intensity that does not reflect the bremsstrahlung emission, is not in force balance, there is a transfer of energy between the particles and waves early on, but over a longer time period the system enters a state where the net exchange between the particles and waves gradually settles down to a minimal level. Note that in terms of the total energy content, the tail portion of the EVDF contains a relatively low proportion of the net energy, as the number density is several orders of magnitude lower than the core distribution. Although it is not so easy to verify by visual means, there is a slight cooling associated with the core part of the EVDF. This shows that the present process is not an acceleration mechanism, but rather involves the redistribution of particle population in velocity or energy space in order to form a new quasi-equilibrium.

S.F.T. acknowledges a PhD fellowship from CNPq (Brazil). L.F.Z. acknowledges support from CNPq (Brazil), grant No. 304363/2014-6. P.H.Y. acknowledges NSF grant AGS1550566 to the University of Maryland, and the BK21 plus program from the National Research Foundation (NRF), Korea, to Kyung Hee University.

ORCID iDs

- S. F. Tigik [ID](https://orcid.org/0000-0002-5968-9637)
L. F. Ziebell [ID](https://orcid.org/0000-0003-0279-0280)
P. H. Yoon [ID](https://orcid.org/0000-0001-8134-3790)

References

- Akopyan, A. V., & Tsytovich, V. N. 1977, *Afz*, **13**, 717
Aschwanden, M. J. 2005, Physics of the Solar Corona (2nd ed.; Chichester: Praxis)
Che, H., & Goldstein, M. L. 2014, *ApJL*, **795**, L38
Christon, S. P., Williams, D. J., Mitchell, D. G., Huang, C. Y., & Frank, L. A. 1991, *JGR*, **96**, 1
Colgate, S. A. 1967, *ApJ*, **150**, 163
Feldman, W. C., Asbridge, J. R., Bame, S. J., & Gosling, J. T. 1976, *JGR*, **81**, 5054
Feldman, W. C., Asbridge, J. R., Bame, S. J., Gosling, J. T., & Lemons, D. S. 1978, *JGR*, **83**, 5285
Feldman, W. C., Asbridge, J. R., Bame, S. J., Montgomery, M. D., & Gary, S. P. 1975, *JGR*, **80**, 4181
Fisk, L. A., & Gloeckler, G. 2012, *SSRv*, **173**, 433
Gaffey, J. D., Jr. 1976, *JPIP*, **16**, 149
Gailitis, A. K., & Tsytovich, V. N. 1964, *SvA*, **8**, 359
Gloeckler, G. 2003, in AIP Conf. Ser. 679, Solar Wind Ten, ed. M. Velli et al. (Melville, NY: AIP), 583
Helander, P., & Sigmar, D. J. 2002, Collisional Transport in Magnetized Plasmas (Cambridge: Cambridge Univ. Press)
Kim, S., Yoon, P. H., Choe, G. S., & Moon, Y.-J. 2016, *ApJ*, **828**, 60
Krucker, S., & Battaglia, M. 2014, *ApJ*, **780**, 107
Lie-Svendsen, Ø., Hansteen, V. H., & Leer, E. 1997, *JGR*, **102**, 4701
Lifshitz, E. M., & Pitaevskii, L. P. 1981, Physical Kinetics (Oxford: Pergamon Press)
Lin, R. P. 1998, *SSRv*, **86**, 61
Makhankov, V. G., & Tsytovich, V. N. 1968, *JETP*, **26**, 1023
Melrose, D. B. 1971, *Ap&SS*, **10**, 197
Oka, M., Hugh, H. S., & Saint-Hilaire, P. 2015, *ApJ*, **799**, 1920
Pavan, J., Viñas, A. F., Yoon, P. H., Ziebell, L. F., & Gaelzer, R. 2013, *ApJL*, **769**, L30
Pierrard, V., Maksimovic, M., & Lemaire, J. 1999, *JGR*, **104**, 17021
Pierrard, V., Maksimovic, M., & Lemaire, J. 2001, *JGR*, **106**, 29305
Schlickeiser, R. 2003, *A&A*, **410**, 397
Scudder, J. D. 1992a, *ApJ*, **398**, 299
Scudder, J. D. 1992b, *ApJ*, **398**, 319
Scudder, J. D., & Olbert, S. 1979a, *JGR*, **84**, 2755
Scudder, J. D., & Olbert, S. 1979b, *JGR*, **84**, 6603
Seough, J., Nariyuki, Y., Yoon, P. H., & Saito, S. 2015, *ApJL*, **811**, L7
Stone, E. C., Cummings, A. C., McDonald, F. B., et al. 2008, *Natur*, **454**, 71
Teles, T. N., Gupta, S., Di Cintio, P., & Casetti, L. 2015, *PhRvE*, **92**, 020101
Tigik, S. F., Ziebell, L. F., & Yoon, P. H. 2016a, *PhPl*, **23**, 064504
Tigik, S. F., Ziebell, L. F., Yoon, P. H., & Kontar, E. P. 2016b, *A&A*, **586**, A19
Vasyliunas, V. M. 1968, *JGR*, **73**, 2839
Vocks, C. 2012, *SSRv*, **172**, 303
Vocks, C., Salem, C., Lin, R. P., & Mann, G. 2005, *ApJ*, **627**, 540
Windsor, R. A., & Kellogg, P. J. 1974, *ApJ*, **190**, 167
Yoon, P. H., Ziebell, L. F., Kontar, E. P., & Schlickeiser, R. 2016, *PhRvE*, **93**, 033203
Zank, G. P. 2014, *LNP*, **877**

Chapter 6

Final remarks

In this thesis, we have presented the results of the first analyses of a new theory, depicted in Chapter 4, which combines collective processes (eigenmodes) and collisional interactions (noneigenmodes), for Langmuir and ion-sound waves, without any *ad hoc* addition. The importance of this formalism, became clear right in the first study, presented in Section 5.1, where it was shown that the collisional damping rate calculated with the heuristic Spitzer formula, that is independent of the wave-number, is highly overestimated when compared with the rigorous expression, which has to be integrated in the wave-number space. The Spitzer approximation is largely applied to the modeling and interpretation of several solar phenomena observed by space-probes [38, 39, 42, 76, 84–86], a fact that emphasizes the necessity of the development of a mathematically rigorous theory able to describe hybrid situations involving collective oscillations and collisional interactions.

The second study, discussed in Section 5.2, focused on the consequences of including the hitherto unknown effect of electrostatic bremsstrahlung in the time evolution of a Maxwellian electron velocity distribution, under the quasilinear regime. The unexpected outcome of this analysis revealed an underlying process responsible for taking the electron velocity distribution out of its initial equilibrium state, leading it to a new quasi-equilibrium state that is satisfied by a velocity distribution composed by a Maxwellian core with a suprathermal tail. Such velocity distributions are pervasively observed in space plasmas [87–97]. However, until these days, despite several attempts of explaining how they form and why space plasmas are particularly prone to develop a suprathermal tail while retaining the thermal core, no existing theory is capable of describing self-consistently its origin and evolution. Again, the relevance of this research becomes evident.

The ubiquity of inverse power-law velocity distribution in space plasmas indicates the action of a fundamental physical process that might -or might not- be the electrostatic bremsstrahlung. For instance, the possibility of the formation of suprathermal electron veloc-

ity distributions in a mildly collisional environment, as demonstrated in [78], has a positive correlation with the velocity filtration model, which relies on the existence of a high energy electron population in the solar transition region, located between the chromosphere and the solar corona, to explain the temperature inversion observed in the solar corona [75, 98–104].

It is important to emphasize the fundamental aspect of the theory presented in Ref. [52]. The rigorous analysis performed during this doctoral research, suggests that collisional interactions involving charged particles enfold physical processes that go beyond the Coulomb collisions effects. An enthralling prospect of this study lies in the possibility of these underlying kinetic processes being connected to unexplained phenomena observed in space plasmas. On that regard, the electrostatic weak turbulence theory for collisional plasmas is a first step towards a more accurate description of the microscopic physics of plasmas. Further development should extend this formalism to include electromagnetic waves and, in the long term, the influence of ambient magnetic field.

These efforts on improving the theoretical description of kinetic processes in plasmas and numerically analyzing the equations are just in time with current technological progress in the resolution capability of spacecraft measurement equipment. A great example of this new trend is NASA’s Magnetospheric Multiscale (MMS) mission that investigates the physics of magnetic reconnection in the Earth’s magnetosphere. Equipped with high-precision instruments [105, 106], MMS was capable of directly measure wave-particle energy exchange process in the ion kinetic scale [107], for the first time. Therefore, it is becoming evident that the kinetic scale is the next frontier in observational plasma physics, and this will require a more accurate and comprehensive theory.

Appendix A

Improved approximation for the second order susceptibility

In this appendix, we present two different approximations applied to the second-order susceptibility in the electrostatic bremsstrahlung equation for Langmuir waves. Initially, for comparison, we show the original simplification used in Ref. [52]. In the sequence, we introduce an improved approximation for the same expression, highlighting the main differences. This new version, though, is only suitable for fast-waves, which is the case of Langmuir oscillations, but does not apply to the case of ion-sound waves. Moreover, the results for ion-sound waves are quite well behaved with the original approximation, which is the same that was initially used for L waves in Ref. [52]. Therefore, S waves will be considered only in Appendix A.1, while Appendix A.2 will be directed solely to the expression for L waves.

A.1 Original approximation

The initial expressions for L and S waves, still in terms of the second order susceptibility are given by:

$$\frac{\partial I_{\mathbf{k}}^{\sigma L}}{\partial t} \Big|_{\text{brem}} = \sum_{a,b} \frac{12n_e e_a^2 e_b^2 \omega_{pe}^2}{\pi} \int d\mathbf{k}' \int d\mathbf{v} \int d\mathbf{v}' \frac{|\chi^{(2)}(\mathbf{k}', 0 | \mathbf{k} - \mathbf{k}', 0)|^2}{k'^2 |\mathbf{k} - \mathbf{k}'|^2 |\epsilon(\mathbf{k}', 0)|^2 |\epsilon(\mathbf{k} - \mathbf{k}', 0)|^2} \\ \times \delta [\sigma \omega_{\mathbf{k}}^L - \mathbf{k} \cdot \mathbf{v} + \mathbf{k}' \cdot (\mathbf{v} - \mathbf{v}')] F_a(\mathbf{v}) F(\mathbf{v}'), \quad (\text{A1})$$

$$\frac{\partial}{\partial t} \frac{I_{\mathbf{k}}^{\sigma S}}{\mu_{\mathbf{k}}} \Big|_{\text{brem}} = \sum_{a,b} \frac{12n_e e_a^2 e_b^2 \omega_{pe}^2}{\pi} \int d\mathbf{k}' \int d\mathbf{v} \int d\mathbf{v}' \frac{|\chi^{(2)}(\mathbf{k}', 0 | \mathbf{k} - \mathbf{k}', 0)|^2}{k'^2 |\mathbf{k} - \mathbf{k}'|^2 |\epsilon(\mathbf{k}', 0)|^2 |\epsilon(\mathbf{k} - \mathbf{k}', 0)|^2} \\ \times \delta [\sigma \omega_{\mathbf{k}}^S - \mathbf{k} \cdot \mathbf{v} + \mathbf{k}' \cdot (\mathbf{v} - \mathbf{v}')] F_a(\mathbf{v}) F(\mathbf{v}'). \quad (\text{A2})$$

Assuming that the most important contribution comes from the region where $\mathbf{k} \cdot \mathbf{v} \simeq 0$,

$\mathbf{k}' \cdot \mathbf{v}' \simeq 0$, and $\mathbf{k}' \cdot \mathbf{v} \simeq 0$,

$$\begin{aligned} \chi_a^{(2)}[\mathbf{k}', \mathbf{k}' \cdot \mathbf{v}' | \mathbf{k} - \mathbf{k}', (\mathbf{k} - \mathbf{k}') \cdot \mathbf{v}] &\simeq -\frac{2\pi i e_a^3}{kk'|\mathbf{k} - \mathbf{k}'|m_a^2 T_a^2} \int d\mathbf{v}'' \\ &\left[-\frac{T_a}{m_a} \frac{\mathbf{k}' \cdot (\mathbf{k} - \mathbf{k}')}{(-\mathbf{k} \cdot \mathbf{v}'' + i0)} \frac{(\mathbf{k} - \mathbf{k}') \cdot \mathbf{v}''}{[-(\mathbf{k} - \mathbf{k}') \cdot \mathbf{v}'' + i0]^2} + \frac{1}{(-\mathbf{k} \cdot \mathbf{v}'' + i0)} \frac{(\mathbf{k}' \cdot \mathbf{v}'')((\mathbf{k} - \mathbf{k}') \cdot \mathbf{v}'')}{(-(\mathbf{k} - \mathbf{k}') \cdot \mathbf{v}'' + i0)} \right. \\ &\left. - \frac{T_a}{m_a} \frac{(\mathbf{k} - \mathbf{k}') \cdot \mathbf{k}'}{(-\mathbf{k} \cdot \mathbf{v}'' + i0)} \frac{\mathbf{k}' \cdot \mathbf{v}''}{(-\mathbf{k}' \cdot \mathbf{v}'' + i0)^2} + \frac{1}{(-\mathbf{k} \cdot \mathbf{v}'' + i0)} \frac{((\mathbf{k} - \mathbf{k}') \cdot \mathbf{v}'')(\mathbf{k}' \cdot \mathbf{v}'')}{(-\mathbf{k}' \cdot \mathbf{v}'' + i0)} \right] f_a(\mathbf{v}'') \end{aligned} \quad (\text{A3})$$

$$\begin{aligned} \chi_a^{(2)}[\mathbf{k}', \mathbf{k}' \cdot \mathbf{v}' | \mathbf{k} - \mathbf{k}', (\mathbf{k} - \mathbf{k}') \cdot \mathbf{v}] &\simeq -\frac{2\pi i e_a^3}{kk'|\mathbf{k} - \mathbf{k}'|m_a^2 T_a^2} \int d\mathbf{v}'' \\ &\times \left[-\frac{T_a}{m_a} \frac{\mathbf{k}' \cdot (\mathbf{k} - \mathbf{k}')}{(-\mathbf{k} \cdot \mathbf{v}'' + i0)} \frac{(\mathbf{k} - \mathbf{k}') \cdot \mathbf{v}''}{[-(\mathbf{k} - \mathbf{k}') \cdot \mathbf{v}''][-(\mathbf{k} - \mathbf{k}') \cdot \mathbf{v}'' + i0]} + \frac{1}{(-\mathbf{k} \cdot \mathbf{v}'' + i0)} \frac{(\mathbf{k}' \cdot \mathbf{v}'')((\mathbf{k} - \mathbf{k}') \cdot \mathbf{v}'')}{[-(\mathbf{k} - \mathbf{k}') \cdot \mathbf{v}'' + i0]} \right. \\ &\left. - \frac{T_a}{m_a} \frac{(\mathbf{k} - \mathbf{k}') \cdot \mathbf{k}'}{(-\mathbf{k} \cdot \mathbf{v}'' + i0)} \frac{\mathbf{k}' \cdot \mathbf{v}''}{(-\mathbf{k}' \cdot \mathbf{v}'')(-\mathbf{k}' \cdot \mathbf{v}'' + i0)} + \frac{1}{(-\mathbf{k} \cdot \mathbf{v}'' + i0)} \frac{((\mathbf{k} - \mathbf{k}') \cdot \mathbf{v}'')(\mathbf{k}' \cdot \mathbf{v}'')}{(-\mathbf{k}' \cdot \mathbf{v}'' + i0)} \right] f_a(\mathbf{v}'') \end{aligned} \quad (\text{A4})$$

Simplifying, and writing the coefficient in front of the expression in a different way,

$$\begin{aligned} \chi_a^{(2)}[\mathbf{k}', \mathbf{k}' \cdot \mathbf{v}' | \mathbf{k} - \mathbf{k}', (\mathbf{k} - \mathbf{k}') \cdot \mathbf{v}] &\simeq -i \frac{e_a}{T_a} \frac{\omega_{pa}^2}{kk'|\mathbf{k} - \mathbf{k}'|} \frac{1}{v_a^2} \\ &\times \int d\mathbf{v}'' \left\{ \frac{T_a}{m_a} \frac{\mathbf{k}' \cdot (\mathbf{k} - \mathbf{k}')}{\mathbf{k} \cdot \mathbf{v}''} \left[\frac{1}{(\mathbf{k} - \mathbf{k}') \cdot \mathbf{v}''} + \frac{1}{(\mathbf{k}' \cdot \mathbf{v}'')} \right] \right. \\ &\left. + \underbrace{\frac{\mathbf{k}' \cdot \mathbf{v}''}{\mathbf{k} \cdot \mathbf{v}''} + \frac{(\mathbf{k} - \mathbf{k}') \cdot \mathbf{v}''}{\mathbf{k} \cdot \mathbf{v}''}}_{=1} \right\} F_a(\mathbf{v}'') + i \operatorname{Im} \chi^{(2)}, \end{aligned} \quad (\text{A5})$$

$$\begin{aligned} \chi_a^{(2)}[\mathbf{k}', \mathbf{k}' \cdot \mathbf{v}' | \mathbf{k} - \mathbf{k}', (\mathbf{k} - \mathbf{k}') \cdot \mathbf{v}] &\simeq -i \frac{e_a}{T_a} \frac{\omega_{pa}^2}{kk'|\mathbf{k} - \mathbf{k}'|} \frac{1}{v_a^2} \\ &\times \int d\mathbf{v}'' \left[\frac{T_a}{m_a} \frac{\mathbf{k}' \cdot (\mathbf{k} - \mathbf{k}')}{(\mathbf{k} - \mathbf{k}') \cdot \mathbf{v}''} + 1 \right] F_a(\mathbf{v}'') \end{aligned} \quad (\text{A6})$$

where we have used $f_a = \hat{n}F_a$.

The term containing \mathbf{v}'' vanishes, for distribution function which depends only on the absolute value of the velocity, like the Maxwellian distribution. Therefore,

$$\chi_a^{(2)}[\mathbf{k}', \mathbf{k}' \cdot \mathbf{v}' | \mathbf{k} - \mathbf{k}', (\mathbf{k} - \mathbf{k}') \cdot \mathbf{v}] \simeq -i \frac{e_a}{T_a} \frac{\omega_{pa}^2}{kk'|\mathbf{k} - \mathbf{k}'|} \frac{1}{v_a^2} \quad (\text{A7})$$

Defining $e_i = e$, $e_e = -e$ and assuming $n_e = n_i = \bar{n}$, we have

$$\begin{aligned}
\chi^{(2)}[\mathbf{k}', \mathbf{k}' \cdot \mathbf{v}' | \mathbf{k} - \mathbf{k}', (\mathbf{k} - \mathbf{k}') \cdot \mathbf{v}] &= \sum_a \chi_a^{(2)}[\mathbf{k}', \mathbf{k}' \cdot \mathbf{v}' | \mathbf{k} - \mathbf{k}', (\mathbf{k} - \mathbf{k}') \cdot \mathbf{v}] \\
&\simeq ie \frac{1}{kk'|\mathbf{k} - \mathbf{k}'|} \left(\frac{\omega_{pe}^2}{T_e v_e^2} - \frac{\omega_{pi}^2}{T_i v_i^2} \right) \\
&= ie \frac{\omega_{pe}^2}{kk'|\mathbf{k} - \mathbf{k}'|} \left(\frac{m_e}{T_e 2T_e} - \frac{m_e}{m_i} \frac{m_i}{T_i 2T_i} \right) \\
&= i \frac{e}{T_e} \frac{\omega_{pe}^2}{kk'|\mathbf{k} - \mathbf{k}'|} \frac{1}{v_e^2} \left(1 - \frac{m_e}{m_i} \frac{2T_e^2}{m_e} \frac{m_i}{2T_i^2} \right) \\
&= i \frac{e}{T_e} \frac{\omega_{pe}^2}{kk'|\mathbf{k} - \mathbf{k}'|} \frac{1}{v_e^2} \left(1 - \frac{T_e^2}{T_i^2} \right).
\end{aligned} \tag{A8}$$

Finally we have the original approximation:

$$\chi^{(2)}[\mathbf{k}', \mathbf{k}' \cdot \mathbf{v}' | \mathbf{k} - \mathbf{k}', (\mathbf{k} - \mathbf{k}') \cdot \mathbf{v}] = i \frac{e}{2T_e} \frac{1}{kk'|\mathbf{k} - \mathbf{k}'| \lambda_{De}^2} \left(1 - \frac{T_e^2}{T_i^2} \right), \tag{A9}$$

and the resulting expressions

$$\begin{aligned}
P_{\mathbf{k}}^{\sigma L} &= \frac{3e^2 T_e}{16\pi^3 m_e} \left(1 - \frac{T_e^2}{T_i^2} \right)^2 \frac{1}{k^2 \lambda_{De}^2} \int d\mathbf{k}' \left(1 + \frac{T_e}{T_i} + k'^2 \lambda_{De}^2 \right)^{-2} \left(1 + \frac{T_e}{T_i} + (\mathbf{k} - \mathbf{k}')^2 \lambda_{De}^2 \right)^{-2} \\
&\times \int d\mathbf{v} \int d\mathbf{v}' \delta[\sigma \omega_{\mathbf{k}}^L - \mathbf{k} \cdot \mathbf{v} + \mathbf{k}' \cdot (\mathbf{v} - \mathbf{v}')] \sum_a F_a(\mathbf{v}) \sum_b F_b(\mathbf{v}'),
\end{aligned} \tag{A10}$$

$$\begin{aligned}
P_{\mathbf{k}}^{\sigma S} &= \mu_{\mathbf{k}} \frac{3e^2 T_e}{16\pi^3 m_e} \left(1 - \frac{T_e^2}{T_i^2} \right)^2 \frac{1}{k^2 \lambda_{De}^2} \int d\mathbf{k}' \left(1 + \frac{T_e}{T_i} + k'^2 \lambda_{De}^2 \right)^{-2} \left(1 + \frac{T_e}{T_i} + (\mathbf{k} - \mathbf{k}')^2 \lambda_{De}^2 \right)^{-2} \\
&\times \int d\mathbf{v} \int d\mathbf{v}' \delta[\sigma \omega_{\mathbf{k}}^S - \mathbf{k} \cdot \mathbf{v} + \mathbf{k}' \cdot (\mathbf{v} - \mathbf{v}')] \sum_a F_a(\mathbf{v}) \sum_b F_b(\mathbf{v}').
\end{aligned} \tag{A11}$$

A.2 Alternative approach

From Eq.(4.24) in Ref. [52] we have

$$\begin{aligned}
&\sum_{a,b} \frac{48e_a^2 e_b^2}{\pi} \frac{1}{[\epsilon'(\mathbf{k}, \sigma \omega_{\mathbf{k}}^\alpha)]^2} \int d\mathbf{k}' \int d\mathbf{v} \int d\mathbf{v}' \delta[\sigma \omega_{\mathbf{k}}^\alpha - \mathbf{k} \cdot \mathbf{v} + \mathbf{k}' \cdot (\mathbf{v} - \mathbf{v}')] \\
&\times \frac{|\chi^{(2)}[\mathbf{k}', \mathbf{k}' \cdot \mathbf{v}' | \mathbf{k} - \mathbf{k}', (\mathbf{k} - \mathbf{k}') \cdot \mathbf{v}]|^2}{k'^2 |\mathbf{k} - \mathbf{k}'|^2 |\epsilon(\mathbf{k}', \mathbf{k}' \cdot \mathbf{v}')|^2 |\epsilon[\mathbf{k} - \mathbf{k}', (\mathbf{k} - \mathbf{k}') \cdot \mathbf{v}]|^2} f_a(\mathbf{v}) f_b(\mathbf{v}'),
\end{aligned} \tag{A12}$$

which depends on the second-order susceptibility, defined as follows,

$$\chi_a^{(2)}(q_1 | q_2) = -\frac{4\pi i e_a}{k_1 k_2 |\mathbf{k}_1 + \mathbf{k}_2|} \int d\mathbf{v}'' \alpha_a^{(2)}(\mathbf{v}''; q_1 | q_2) f_a(\mathbf{v}''), \tag{A13}$$

with $\alpha_a^{(2)}$ given by,

$$\alpha_a^{(2)}(\mathbf{v}''; q_1|q_2) f_a(\mathbf{v}'') = \frac{1}{2} \left[(\mathbf{k}_1 \cdot \mathbf{g}_{q_1+q_2}^a)(\mathbf{k}_2 \cdot g_{q_2}^a) + (\mathbf{k}_2 \cdot \mathbf{g}_{q_1+q_2}^a)(\mathbf{k}_1 \cdot g_{q_1}^a) \right], \quad (\text{A14})$$

and g_q^a given by,

$$g_{\mathbf{k},\omega}^a = -\frac{e_a}{m_a} \frac{1}{\omega - \mathbf{k} \cdot \mathbf{v}'' + i0} \frac{\partial}{\partial \mathbf{v}''}. \quad (\text{A15})$$

Notice that we used variable \mathbf{v}'' , since \mathbf{v} and \mathbf{v}' already appear in Eq. (A13).

Therefore, using Eq. (A14) in Eq. (A13),

$$\begin{aligned} \chi_a^{(2)}[\mathbf{k}', \mathbf{k}' \cdot \mathbf{v}' | \mathbf{k} - \mathbf{k}', (\mathbf{k} - \mathbf{k}') \cdot \mathbf{v}] &= -\frac{4\pi ie_a}{kk'|\mathbf{k} - \mathbf{k}'|} \frac{1}{2} \int d\mathbf{v}'' \left[(\mathbf{k}' \cdot \mathbf{g}_{\mathbf{k}, \mathbf{k}' \cdot \mathbf{v}' + (\mathbf{k} - \mathbf{k}') \cdot \mathbf{v}}^a)((\mathbf{k} - \mathbf{k}') \cdot \mathbf{g}_{\mathbf{k} - \mathbf{k}', (\mathbf{k} - \mathbf{k}') \cdot \mathbf{v}}^a) \right. \\ &\quad \left. + ((\mathbf{k} - \mathbf{k}') \cdot \mathbf{g}_{\mathbf{k}, \mathbf{k}' \cdot \mathbf{v}' + (\mathbf{k} - \mathbf{k}') \cdot \mathbf{v}}^a)(\mathbf{k}' \cdot \mathbf{g}_{\mathbf{k}', \mathbf{k}' \cdot \mathbf{v}'}^a) \right] f_a(\mathbf{v}'') \end{aligned} \quad (\text{A16})$$

By using Eq. (A15),

$$\begin{aligned} \chi_a^{(2)}[\mathbf{k}', \mathbf{k}' \cdot \mathbf{v}' | \mathbf{k} - \mathbf{k}', (\mathbf{k} - \mathbf{k}') \cdot \mathbf{v}] &= -\frac{2\pi ie_a^3}{kk'|\mathbf{k} - \mathbf{k}'| m_a^2} \int d\mathbf{v}'' \\ &\times \left\{ \left[\frac{\mathbf{k}' \cdot \partial_{\mathbf{v}''}}{[\mathbf{k}' \cdot \mathbf{v}' + (\mathbf{k} - \mathbf{k}') \cdot \mathbf{v} - \mathbf{k} \cdot \mathbf{v}'' + i0]} \frac{(\mathbf{k} - \mathbf{k}') \cdot \partial_{\mathbf{v}''}}{[(\mathbf{k} - \mathbf{k}') \cdot \mathbf{v} - (\mathbf{k} - \mathbf{k}') \cdot \mathbf{v}'' + i0]} \right. \right. \\ &\left. \left. + \frac{(\mathbf{k} - \mathbf{k}') \cdot \partial_{\mathbf{v}''}}{[\mathbf{k}' \cdot \mathbf{v}' + (\mathbf{k} - \mathbf{k}') \cdot \mathbf{v} - \mathbf{k} \cdot \mathbf{v}'' + i0]} \frac{\mathbf{k}' \cdot \partial_{\mathbf{v}''}}{[\mathbf{k}' \cdot \mathbf{v}' - \mathbf{k}' \cdot \mathbf{v}'' + i0]} \right\} f_a(\mathbf{v}'') \right. \end{aligned} \quad (\text{A17})$$

$$\begin{aligned} \chi_a^{(2)}[\mathbf{k}', \mathbf{k}' \cdot \mathbf{v}' | \mathbf{k} - \mathbf{k}', (\mathbf{k} - \mathbf{k}') \cdot \mathbf{v}] &= -\frac{2\pi ie_a^3}{kk'|\mathbf{k} - \mathbf{k}'| m_a^2} \int d\mathbf{v}'' \\ &\times \left\{ \left[\frac{\mathbf{k}' \cdot (\mathbf{k} - \mathbf{k}')}{[\mathbf{k}' \cdot \mathbf{v}' + (\mathbf{k} - \mathbf{k}') \cdot \mathbf{v} - \mathbf{k} \cdot \mathbf{v}'' + i0]} \frac{(\mathbf{k} - \mathbf{k}') \cdot \partial_{\mathbf{v}''}}{[(\mathbf{k} - \mathbf{k}') \cdot \mathbf{v} - (\mathbf{k} - \mathbf{k}') \cdot \mathbf{v}'' + i0]^2} \right. \right. \\ &\left. \left. + \frac{1}{[\mathbf{k}' \cdot \mathbf{v}' + (\mathbf{k} - \mathbf{k}') \cdot \mathbf{v} - \mathbf{k} \cdot \mathbf{v}'' + i0]} \frac{\mathbf{k}' \cdot \partial_{\mathbf{v}''} (\mathbf{k} - \mathbf{k}') \cdot \partial_{\mathbf{v}''}}{[(\mathbf{k} - \mathbf{k}') \cdot \mathbf{v} - (\mathbf{k} - \mathbf{k}') \cdot \mathbf{v}'' + i0]} \right. \right. \\ &\left. \left. + \frac{(\mathbf{k} - \mathbf{k}') \cdot \mathbf{k}'}{[\mathbf{k}' \cdot \mathbf{v}' + (\mathbf{k} - \mathbf{k}') \cdot \mathbf{v} - \mathbf{k} \cdot \mathbf{v}'' + i0]} \frac{\mathbf{k}' \cdot \partial_{\mathbf{v}''}}{[\mathbf{k}' \cdot \mathbf{v}' - \mathbf{k}' \cdot \mathbf{v}'' + i0]^2} \right. \right. \\ &\left. \left. + \frac{1}{[\mathbf{k}' \cdot \mathbf{v}' + (\mathbf{k} - \mathbf{k}') \cdot \mathbf{v} - \mathbf{k} \cdot \mathbf{v}'' + i0]} \frac{(\mathbf{k} - \mathbf{k}') \cdot \partial_{\mathbf{v}''} \mathbf{k}' \cdot \partial_{\mathbf{v}''}}{[\mathbf{k}' \cdot \mathbf{v}' - \mathbf{k}' \cdot \mathbf{v}'' + i0]} \right\} f_a(\mathbf{v}'') \right. \end{aligned} \quad (\text{A18})$$

Assuming a Maxwellian velocity distribution function

$$\begin{aligned} \chi_a^{(2)}[\mathbf{k}', \mathbf{k}' \cdot \mathbf{v}' | \mathbf{k} - \mathbf{k}', (\mathbf{k} - \mathbf{k}') \cdot \mathbf{v}] = & -\frac{2\pi i e_a^3}{kk'|\mathbf{k} - \mathbf{k}'|m_a^2 T_a^2} \int d\mathbf{v}'' \\ & \times \left\{ -\frac{T_a}{m_a} \frac{\mathbf{k}' \cdot (\mathbf{k} - \mathbf{k}')}{[\mathbf{k}' \cdot \mathbf{v}' + (\mathbf{k} - \mathbf{k}') \cdot \mathbf{v} - \mathbf{k} \cdot \mathbf{v}'' + i0]} \frac{(\mathbf{k} - \mathbf{k}') \cdot \mathbf{v}''}{[(\mathbf{k} - \mathbf{k}') \cdot \mathbf{v} - (\mathbf{k} - \mathbf{k}') \cdot \mathbf{v}'' + i0]^2} \right. \\ & + \frac{1}{[\mathbf{k}' \cdot \mathbf{v}' + (\mathbf{k} - \mathbf{k}') \cdot \mathbf{v} - \mathbf{k} \cdot \mathbf{v}'' + i0]} \frac{(\mathbf{k}' \cdot \mathbf{v}'')((\mathbf{k} - \mathbf{k}') \cdot \mathbf{v}'')}{[(\mathbf{k} - \mathbf{k}') \cdot \mathbf{v} - (\mathbf{k} - \mathbf{k}') \cdot \mathbf{v}'' + i0]} \\ & - \frac{T_a}{m_a} \frac{(\mathbf{k} - \mathbf{k}') \cdot \mathbf{k}'}{[\mathbf{k}' \cdot \mathbf{v}' + (\mathbf{k} - \mathbf{k}') \cdot \mathbf{v} - \mathbf{k} \cdot \mathbf{v}'' + i0]} \frac{\mathbf{k}' \cdot \mathbf{v}''}{[\mathbf{k}' \cdot \mathbf{v}' - \mathbf{k}' \cdot \mathbf{v}'' + i0]^2} \\ & \left. + \frac{1}{[\mathbf{k}' \cdot \mathbf{v}' + (\mathbf{k} - \mathbf{k}') \cdot \mathbf{v} - \mathbf{k} \cdot \mathbf{v}'' + i0]} \frac{((\mathbf{k} - \mathbf{k}') \cdot \mathbf{v}'')(\mathbf{k}' \cdot \mathbf{v}'')}{[\mathbf{k}' \cdot \mathbf{v}' - \mathbf{k}' \cdot \mathbf{v}'' + i0]} \right\} f_a(\mathbf{v}'') \end{aligned} \quad (\text{A19})$$

Here, instead of making the early assumption that $\mathbf{k} \cdot \mathbf{v} \simeq 0$, $\mathbf{k}' \cdot \mathbf{v}' \simeq 0$ and $\mathbf{k}' \cdot \mathbf{v} \simeq 0$, we take into account the fact that Eq. (A12) contains a delta function:

$$\mathbf{k}' \cdot \mathbf{v}' + (\mathbf{k} - \mathbf{k}') \cdot \mathbf{v} = \sigma \omega_{\mathbf{k}}^{\alpha}. \quad (\text{A20})$$

With this small change we obtain a quite different expression than that obtained at the same point in the previous approach:

$$\begin{aligned} \chi_a^{(2)}[\mathbf{k}', \mathbf{k}' \cdot \mathbf{v}' | \mathbf{k} - \mathbf{k}', (\mathbf{k} - \mathbf{k}') \cdot \mathbf{v}] = & -\frac{2\pi i e_a^3}{kk'|\mathbf{k} - \mathbf{k}'|m_a^2 T_a^2} \int d\mathbf{v}'' \\ & \times \left\{ -\frac{T_a}{m_a} \frac{\mathbf{k}' \cdot (\mathbf{k} - \mathbf{k}')}{[\sigma \omega_{\mathbf{k}}^{\alpha} - \mathbf{k} \cdot \mathbf{v}'' + i0]} \frac{(\mathbf{k} - \mathbf{k}') \cdot \mathbf{v}''}{[\sigma \omega_{\mathbf{k}}^{\alpha} - \mathbf{k}' \cdot \mathbf{v}' - (\mathbf{k} - \mathbf{k}') \cdot \mathbf{v}'' + i0]^2} \right. \\ & + \frac{1}{[\sigma \omega_{\mathbf{k}}^{\alpha} - \mathbf{k} \cdot \mathbf{v}'' + i0]} \frac{(\mathbf{k}' \cdot \mathbf{v}'')((\mathbf{k} - \mathbf{k}') \cdot \mathbf{v}'')}{[\sigma \omega_{\mathbf{k}}^{\alpha} - \mathbf{k}' \cdot \mathbf{v}' - (\mathbf{k} - \mathbf{k}') \cdot \mathbf{v}'' + i0]} \\ & - \frac{T_a}{m_a} \frac{(\mathbf{k} - \mathbf{k}') \cdot \mathbf{k}'}{[\sigma \omega_{\mathbf{k}}^{\alpha} - \mathbf{k} \cdot \mathbf{v}'' + i0]} \frac{\mathbf{k}' \cdot \mathbf{v}''}{[\sigma \omega_{\mathbf{k}}^{\alpha} - (\mathbf{k} - \mathbf{k}') \cdot \mathbf{v}' - \mathbf{k}' \cdot \mathbf{v}'' + i0]^2} \\ & \left. + \frac{1}{[\sigma \omega_{\mathbf{k}}^{\alpha} - \mathbf{k} \cdot \mathbf{v}'' + i0]} \frac{((\mathbf{k} - \mathbf{k}') \cdot \mathbf{v}'')(\mathbf{k}' \cdot \mathbf{v}'')}{[\sigma \omega_{\mathbf{k}}^{\alpha} - (\mathbf{k} - \mathbf{k}') \cdot \mathbf{v}' - \mathbf{k}' \cdot \mathbf{v}'' + i0]} \right\} f_a(\mathbf{v}''). \end{aligned} \quad (\text{A21})$$

And it is just after the previous assumption that we assume that the most important

contribution comes from the region where $\mathbf{k} \cdot \mathbf{v} \simeq 0$, $\mathbf{k}' \cdot \mathbf{v}' \simeq 0$, and $\mathbf{k}' \cdot \mathbf{v} \simeq 0$, then

$$\begin{aligned} \chi_a^{(2)}[\mathbf{k}', \mathbf{k}' \cdot \mathbf{v}' | \mathbf{k} - \mathbf{k}', (\mathbf{k} - \mathbf{k}') \cdot \mathbf{v}] &= -\frac{2\pi i e_a^3}{kk'|\mathbf{k} - \mathbf{k}'|m_a^2 T_a^2} \int d\mathbf{v}'' \\ &\times \left\{ -\frac{T_a}{m_a} \frac{\mathbf{k}' \cdot (\mathbf{k} - \mathbf{k}')}{[\sigma\omega_{\mathbf{k}}^\alpha - \mathbf{k} \cdot \mathbf{v}'' + i0]} \frac{(\mathbf{k} - \mathbf{k}') \cdot \mathbf{v}''}{[\sigma\omega_{\mathbf{k}}^\alpha - (\mathbf{k} - \mathbf{k}') \cdot \mathbf{v}'' + i0]^2} \right. \\ &+ \frac{1}{[\sigma\omega_{\mathbf{k}}^\alpha - \mathbf{k} \cdot \mathbf{v}'' + i0]} \frac{(\mathbf{k}' \cdot \mathbf{v}'')((\mathbf{k} - \mathbf{k}') \cdot \mathbf{v}'')}{[\sigma\omega_{\mathbf{k}}^\alpha - (\mathbf{k} - \mathbf{k}') \cdot \mathbf{v}'' + i0]} \\ &- \frac{T_a}{m_a} \frac{(\mathbf{k} - \mathbf{k}') \cdot \mathbf{k}'}{[\sigma\omega_{\mathbf{k}}^\alpha - \mathbf{k} \cdot \mathbf{v}'' + i0]} \frac{\mathbf{k}' \cdot \mathbf{v}''}{[\sigma\omega_{\mathbf{k}}^\alpha - \mathbf{k}' \cdot \mathbf{v}'' + i0]^2} \\ &\left. + \frac{1}{[\sigma\omega_{\mathbf{k}}^\alpha - \mathbf{k} \cdot \mathbf{v}'' + i0]} \frac{((\mathbf{k} - \mathbf{k}') \cdot \mathbf{v}'')(\mathbf{k}' \cdot \mathbf{v}'')}{[\sigma\omega_{\mathbf{k}}^\alpha - \mathbf{k}' \cdot \mathbf{v}'' + i0]} \right\} f_a(\mathbf{v}'') \end{aligned} \quad (\text{A22})$$

For L waves, we can assume that the factor $\sigma\omega_{\mathbf{k}}^L$ is dominant on the denominators,

$$\begin{aligned} \chi_a^{(2)}[\mathbf{k}', \mathbf{k}' \cdot \mathbf{v}' | \mathbf{k} - \mathbf{k}', (\mathbf{k} - \mathbf{k}') \cdot \mathbf{v}] &= -\frac{2\pi i e_a^3}{kk'|\mathbf{k} - \mathbf{k}'|m_a^2 T_a^2} \int d\mathbf{v}'' \\ &\times \left[-\frac{T_a}{m_a} [\mathbf{k}' \cdot (\mathbf{k} - \mathbf{k}')] \frac{(\mathbf{k} - \mathbf{k}') \cdot \mathbf{v}''}{(\sigma\omega_{\mathbf{k}}^L)^3} + \frac{(\mathbf{k}' \cdot \mathbf{v}'')((\mathbf{k} - \mathbf{k}') \cdot \mathbf{v}'')}{(\sigma\omega_{\mathbf{k}}^L)^2} \right. \\ &\left. - \frac{T_a}{m_a} [(\mathbf{k} - \mathbf{k}') \cdot \mathbf{k}'] \frac{\mathbf{k}' \cdot \mathbf{v}''}{(\sigma\omega_{\mathbf{k}}^L)^3} + \frac{((\mathbf{k} - \mathbf{k}') \cdot \mathbf{v}'')(\mathbf{k}' \cdot \mathbf{v}'')}{(\sigma\omega_{\mathbf{k}}^L)^2} \right] f_a(\mathbf{v}'') \end{aligned} \quad (\text{A23})$$

Due to their asymmetry, the terms which are linear in \mathbf{v}'' will vanish when integrated, leading to the following expression

$$\begin{aligned} \chi_a^{(2)}[\mathbf{k}', \mathbf{k}' \cdot \mathbf{v}' | \mathbf{k} - \mathbf{k}', (\mathbf{k} - \mathbf{k}') \cdot \mathbf{v}] &= -\frac{2\pi i e_a^3}{kk'|\mathbf{k} - \mathbf{k}'|m_a^2 T_a^2} \frac{m_a^2}{2} \\ &\times \int d\mathbf{v}'' \left[2 \frac{(\mathbf{k}' \cdot \mathbf{v}'')((\mathbf{k} - \mathbf{k}') \cdot \mathbf{v}'')}{(\sigma\omega_{\mathbf{k}}^L)^2} \right] f_a(\mathbf{v}''). \end{aligned} \quad (\text{A24})$$

As an approximation, we write

$$\begin{aligned} \chi_a^{(2)}[\mathbf{k}', \mathbf{k}' \cdot \mathbf{v}' | \mathbf{k} - \mathbf{k}', (\mathbf{k} - \mathbf{k}') \cdot \mathbf{v}] &= -\frac{2\pi i e_a^3}{kk'|\mathbf{k} - \mathbf{k}'|m_a^2 T_a^2} \frac{m_a^2}{2} \frac{k'|\mathbf{k} - \mathbf{k}'|}{(\sigma\omega_{\mathbf{k}}^L)^2} \int d\mathbf{v}'' |\mathbf{v}''|^2 f_a(\mathbf{v}'') \\ &= -\frac{2\pi i e_a^3}{km_a^2 T_a^2} \frac{m_a^2}{2} \frac{2}{(\sigma\omega_{\mathbf{k}}^L)^2} \frac{2T_a}{m_a} \bar{n} \\ &= -i \frac{e_a}{m_a} \frac{\omega_{pa}^2}{k(\sigma\omega_{\mathbf{k}}^L)^2} \frac{m_a^2}{T_a^2} \frac{2T_a}{m_a} \end{aligned}$$

which leads to

$$\chi_a^{(2)}[\mathbf{k}', \mathbf{k}' \cdot \mathbf{v}' | \mathbf{k} - \mathbf{k}', (\mathbf{k} - \mathbf{k}') \cdot \mathbf{v}] \simeq -i4 \frac{e_a}{m_a} \frac{\omega_{pa}^2}{(\omega_{\mathbf{k}}^L)^2} \frac{1}{kv_a^2} \quad (\text{A25})$$

Defining $e_i = e$ and $e_e = -e$, and assuming $n_e = n_i = \bar{n}$, we have

$$\chi^{(2)}[\mathbf{k}', \mathbf{k}' \cdot \mathbf{v}' | \mathbf{k} - \mathbf{k}', (\mathbf{k} - \mathbf{k}') \cdot \mathbf{v}] = \sum_a \chi_a^{(2)}[\mathbf{k}', \mathbf{k}' \cdot \mathbf{v}' | \mathbf{k} - \mathbf{k}', (\mathbf{k} - \mathbf{k}') \cdot \mathbf{v}] \quad (\text{A26})$$

$$\begin{aligned} \sum_a \chi_a^{(2)}[\mathbf{k}', \mathbf{k}' \cdot \mathbf{v}' | \mathbf{k} - \mathbf{k}', (\mathbf{k} - \mathbf{k}') \cdot \mathbf{v}] &\simeq -4i \frac{e}{k(\omega_{\mathbf{k}}^L)^2} \left(\frac{\omega_{pe}^2}{m_e v_e^2} - \frac{\omega_{pi}^2}{m_i v_i^2} \right) \\ &= -4i \frac{e}{k(\omega_{\mathbf{k}}^L)^2} \left(\frac{\omega_{pe}^2}{m_e v_e^2} - \frac{(m_e/m_i)\omega_{pe}^2}{m_i v_i^2} \right) \\ &= -4ie \frac{\omega_{pe}^2}{k(\omega_{\mathbf{k}}^L)^2} \frac{1}{m_e v_e^2} \left(1 - \frac{m_e^2}{m_i^2} \frac{v_e^2}{v_i^2} \right) \\ &= -4ie \frac{\omega_{pe}^2}{k(\omega_{\mathbf{k}}^L)^2} \frac{m_e}{m_e 2T_e} \left(1 - \frac{m_e^2}{m_i^2} \frac{2T_e}{m_e} \frac{m_i}{2T_i} \right) \\ &= -i \frac{2e}{T_e} \frac{\omega_{pe}^2}{k(\omega_{\mathbf{k}}^L)^2} \left(1 - \frac{m_e}{m_i} \frac{T_e}{T_i} \right) \end{aligned} \quad (\text{A27})$$

$$\chi^{(2)}[\mathbf{k}', \mathbf{k}' \cdot \mathbf{v}' | \mathbf{k} - \mathbf{k}', (\mathbf{k} - \mathbf{k}') \cdot \mathbf{v}] \simeq i \frac{2e}{T_e} \frac{\omega_{pe}^2}{k(\omega_{\mathbf{k}}^L)^2} \left(1 - \frac{m_e}{m_i} \frac{T_e}{T_i} \right) \quad (\text{A28})$$

Therefore, the resulting expression for the electrostatic bremsstrahlung of L waves in the new approximation is

$$\begin{aligned} P_{\mathbf{k}}^{\sigma L} &= \frac{3e^2}{4\pi^3} \frac{1}{(\omega_{\mathbf{k}}^L)^2} \left(1 - \frac{m_e}{m_i} \frac{T_e}{T_i} \right)^2 \frac{v_e^4}{k^2} \int d\mathbf{k}' k'^2 |\mathbf{k} - \mathbf{k}'|^2 \left(1 + \frac{T_e}{T_i} + (\mathbf{k} - \mathbf{k}')^2 \lambda_D^2 \right)^{-2} \\ &\times \left(1 + \frac{T_e}{T_i} + k'^2 \lambda_D^2 \right)^{-2} \int d\mathbf{v} \int d\mathbf{v}' \delta[\sigma \omega_{\mathbf{k}}^L - \mathbf{k} \cdot \mathbf{v} + \mathbf{k}' \cdot (\mathbf{v} - \mathbf{v}')] \sum_a F_a(\mathbf{v}) \sum_b F_b(\mathbf{v}') \end{aligned} \quad (\text{A29})$$

Since this approximation assumes that the dominant frequency range on the denominators is given by the dispersion relation of Langmuir waves (see Eq. (A23)), which are high frequency oscillations near the electron plasma frequency, it is not suitable for use in the bremsstrahlung expression for S waves.

Appendix B

Asymptotic equilibrium

The results presented in Ref. [78] suggest that in the presence of electrostatic bremsstrahlung emission, the wave-particle system evolves to a state of asymptotic equilibrium, in which the velocity distribution resembles the ubiquitous core-halo velocity distribution. To test this assumption, we search for the steady state solution of the kinetic equation for Langmuir waves, taking into account the effects of collisional damping and electrostatic bremsstrahlung, in addition to the spontaneous and induced emission processes,

$$\frac{\partial \mathcal{E}_{\mathbf{q}}^{\sigma L}}{\partial \tau} = \mu_{\mathbf{q}}^L \frac{\pi}{q^2} \int d\mathbf{u} \delta(\sigma z_{\mathbf{q}}^L - \mathbf{q} \cdot \mathbf{u}) \left(g \Phi_e(\mathbf{u}) + \sigma z_{\mathbf{q}}^L \mathcal{E}_{\mathbf{q}}^{\sigma L} \mathbf{q} \cdot \frac{\partial \Phi_e}{\partial \mathbf{u}} \right) + P_{\mathbf{q}}^{\sigma L} + 2\gamma_{\mathbf{q}}^{\sigma L} \mathcal{E}_{\mathbf{q}}^{\sigma L} \approx 0, \quad (\text{A1})$$

For use in this asymptotic equation, let us assume isotropic distributions for ions and electrons, which are the summation of Maxwellian and kappa distributions. In terms of dimensionless variables, we have

$$f_{\beta}(\mathbf{u}) = \left(1 - \frac{n_{\kappa\beta}}{n_e}\right) \frac{1}{\pi^{3/2} u_{\beta}^3} \exp\left(-\frac{u^2}{u_{\beta}^2}\right) + \frac{n_{\kappa\beta}}{n_e} \frac{1}{\pi^{3/2} \kappa_{\beta}^{3/2} u_{\beta,\kappa}^3} \frac{\Gamma(\kappa_{\beta} + 1)}{\Gamma(\kappa_{\beta} - 1/2)} \left(1 + \frac{u^2}{\kappa_{\beta} u_{\beta,\kappa}^2}\right)^{-(\kappa_{\beta} + 1)}. \quad (\text{A2})$$

where

$$u_{\beta,\kappa} = \frac{v_{\beta,\kappa}}{v_e}, \quad u_{\beta} = \frac{v_{\beta}}{v_e}, \quad u_{\beta,\kappa}^2 = \frac{\kappa_{\beta} - 3/2}{\kappa_{\beta}} u_{\beta}^2. \quad (\text{A3})$$

The equilibrium is obtained setting expression (A1) equal to zero, leading to

$$\mathcal{E}_{\mathbf{q}}^{\sigma L} = \frac{g}{2(z_{\mathbf{q}}^L)^2} \frac{\left(1 - \frac{n_{\kappa e}}{n_e}\right) I_M^{eL} + \frac{n_{\kappa}}{n_e} I_1^{eL} + \frac{1}{\mu_{\mathbf{q}}^L g} \frac{q^2}{\pi} P_q^{\sigma L}}{\left(1 - \frac{n_{\kappa e}}{n_e}\right) I_M^{eL} + \frac{u_{\beta,\kappa}^2}{u_{\beta,\kappa}^2} \frac{(\kappa_e + 1)}{\kappa_e} \frac{n_{\kappa e}}{n_e} I_2^{eL} - \frac{1}{\mu_{\mathbf{q}}^L} \frac{q^2}{\pi} \frac{1}{(\sigma z_q^L)^2} \gamma_{\mathbf{q}}^{\sigma L(\text{coll})}}, \quad (\text{A4})$$

where

$$I_M^{\beta\alpha} = \int d^3 u \Phi_{\beta,M}(u) \delta(\sigma z_{\mathbf{q}}^{\alpha} - \mathbf{q} \cdot \mathbf{u}), \quad (\text{A5})$$

$$I_1^{\beta\alpha} = \int d^3u \Phi_{\beta,\kappa}(u)\delta(\sigma z_q^\alpha - \mathbf{q} \cdot \mathbf{u}), \quad (\text{A6})$$

$$I_2^{\beta\alpha} = \int d^3u \left(1 + \frac{u^2}{\kappa_\beta u_{\beta,\kappa}^2}\right)^{-1} \Phi_{\beta,\kappa}(u)\delta(\sigma z_q^\alpha - \mathbf{q} \cdot \mathbf{u}). \quad (\text{A7})$$

The integrals $I_M^{\beta\alpha}$, $I_1^{\beta\alpha}$ and $I_2^{\beta\alpha}$ can be evaluated analytically, resulting in

$$\begin{aligned} I_M^{\beta\alpha} &= \frac{1}{\pi^{1/2} u_\beta} \frac{1}{q} \exp\left(-\frac{(z_q^\alpha/q)^2}{u_\beta^2}\right), \\ I_1^{\beta\alpha} &= \frac{1}{\pi^{1/2} \kappa_\beta^{1/2} u_{\beta,\kappa}} \frac{\Gamma(\kappa_\beta)}{\Gamma(\kappa_\beta - 1/2)} \frac{1}{q} \left(1 + \frac{(z_q^\alpha/q)^2}{\kappa_\beta u_{\beta,\kappa}^2}\right)^{-\kappa_\beta}, \\ I_2^{\beta\alpha} &= \frac{1}{\pi^{1/2} \kappa_\beta^{1/2} u_{\beta,\kappa}} \frac{\Gamma(\kappa_\beta)}{\Gamma(\kappa_\beta - 1/2)} \frac{\kappa_\beta}{\kappa_\beta + 1} \frac{1}{q} \left(1 + \frac{(z_q^\alpha/q)^2}{\kappa_\beta u_{\beta,\kappa}^2}\right)^{-(\kappa_\beta+1)}. \end{aligned} \quad (\text{A8})$$

Using the expressions given by the equations (A8), the numerator of the expression for the asymptotic wave spectrum becomes

$$\left(1 - \frac{n_{\kappa e}}{n_e}\right) \frac{1}{\pi^{1/2} u_e} \frac{1}{q} \exp\left(-\frac{(z_q^L/q)^2}{u_e^2}\right) + \frac{n_{\kappa e}}{n_e} \frac{1}{\pi^{1/2} \kappa_e^{1/2} u_{e,\kappa}} \frac{\Gamma(\kappa_e)}{\Gamma(\kappa_e - 1/2)} \frac{1}{q} \left(1 + \frac{(z_q^L/q)^2}{\kappa_e u_{e,\kappa}^2}\right)^{-(\kappa_e)} + \frac{1}{\mu_q^L g} \frac{q^2}{\pi} P_q^{\sigma L}.$$

Proceeding in the same way, the expression at the denominator of the expression for the asymptotic wave spectrum becomes

$$\begin{aligned} &\left(1 - \frac{n_{\kappa e}}{n_e}\right) \frac{1}{\pi^{1/2} u_e} \frac{1}{q} \exp\left(-\frac{(z_q^L/q)^2}{u_e^2}\right) + \frac{u_e^2}{u_{e,\kappa}^2} \frac{n_{\kappa e}}{n_e} \frac{1}{\pi^{1/2} \kappa_e^{1/2} u_{e,\kappa}} \\ &\times \frac{\Gamma(\kappa_e)}{\Gamma(\kappa_e - 1/2)} \frac{1}{q} \left(1 + \frac{(z_q^L/q)^2}{\kappa_e u_{e,\kappa}^2}\right)^{-(\kappa_e+1)} - \frac{1}{\mu_q^L} \frac{q^2}{\pi} \frac{T_e}{T_*} \frac{1}{(\sigma z_q^L)^2} \gamma_q^{\sigma L(\text{coll})}. \end{aligned}$$

Therefore,

$$\begin{aligned} \mathcal{E}_q^{\sigma L} &= \frac{g}{2(z_q^L)^2} \left[\left(1 - \frac{n_{\kappa e}}{n_e}\right) \exp\left(-\frac{(z_q^L/q)^2}{u_e^2}\right) \right. \\ &+ \frac{n_{\kappa e}}{n_e} \frac{1}{(\kappa_e - 3/2)^{1/2}} \frac{\Gamma(\kappa_e)}{\Gamma(\kappa_e - 1/2)} \left(1 + \frac{(z_q^L/q)^2}{\kappa_e - 3/2}\right)^{-\kappa_e} + \hat{P}_q^{\sigma L} \Big] \\ &\times \left[\left(1 - \frac{n_{\kappa e}}{n_e}\right) \exp\left(-\frac{(z_q^L/q)^2}{u_e^2}\right) \right. \\ &+ \frac{n_{\kappa e}}{n_e} \frac{1}{(\kappa_e - 3/2)^{3/2}} \frac{\Gamma(\kappa_e + 1)}{\Gamma(\kappa_e - 1/2)} \left(1 + \frac{(z_q^L/q)^2}{\kappa_e - 3/2}\right)^{-(\kappa_e+1)} - 2\hat{\gamma}_q^{\sigma L(\text{coll})} \Big]^{-1}, \end{aligned} \quad (\text{A9})$$

where

$$\hat{P}_q^{\sigma L} = \frac{u_e}{\mu_q^L g} \frac{q^3}{\pi^{1/2}} P_q^{\sigma L}, \quad (\text{A10})$$

$$\hat{\gamma}_{\mathbf{q}}^{\sigma L(\text{coll})} = \frac{u_e}{\mu_q^L} \frac{q^3}{\pi^{1/2}} \frac{1}{2(\sigma z_q^L)^2} \gamma_{\mathbf{q}}^{\sigma L(\text{coll})}. \quad (\text{A11})$$

[Figure B.1](#) shows the normalized value of the asymptotic spectrum of L waves, obtained with the use of Eq. (A9), considering a plasma in which the ion population is described by a Maxwellian velocity distribution, and the electron population is described by a distribution as defined in equation (A2), with $n_{ke}/n_e = 0.05$. That is, the electron distribution is a core-halo distribution, with 5% of the particles in the halo population. For the evaluation of the collisional damping and electrostatic bremsstrahlung terms, appearing in Eq. (A9), we used Eqs. (5.3) and (5.5), taking into account only the Maxwellian distribution, which is a reasonable approximation due to the smallness of the halo population. [Figure B.1\(a\)](#) shows the spectra obtained considering several values of the index κ_e , from $\kappa_e = 2.5$ to $\kappa_e = 40$. It is seen that the wave amplitude increases at the region of small values of q , with the increase of κ_e . It is also seen that in the case of fairly large value of κ_e , as $\kappa_e = 40$, the spectrum obtained in the case of a core-halo distribution is very close to the spectrum obtained in the case of a purely Maxwellian electron distribution, which can be obtained from equation (A9) by taking $n_{ke} = 0$. It is also seen that in the case of small values of κ_e the asymptotic spectrum is qualitatively very similar to the spectrum obtained after the time evolution of the system, taking into account the new effects of electrostatic bremsstrahlung and collisional damping, shown in Figure 1 of Ref. [78]. For comparison, we show in figure [Figure B.1\(b\)](#) the asymptotic spectrum of L waves which would be obtained by neglecting the new effects, of collisional bremsstrahlung and collisional damping.

The equations presented in this appendix and, more important, the ideas about the asymptotic state of the eigenmodes of an unmagnetized plasma considering several values of the kappa coefficient, were developed in parallel with another work, which slightly deviates from the main subject of this PhD research, but had a big contribution on the development of the work presented in Ref. [78]. The work in question, whose title is “Weakly turbulent plasma processes in the presence of inverse power-law velocity tail population” [108], investigates the modifications on the spectra of the Langmuir, ion-sound and transverse waves caused by different kappa indexes in a core-halo velocity distribution function. The full article can be seen in Appendix C.

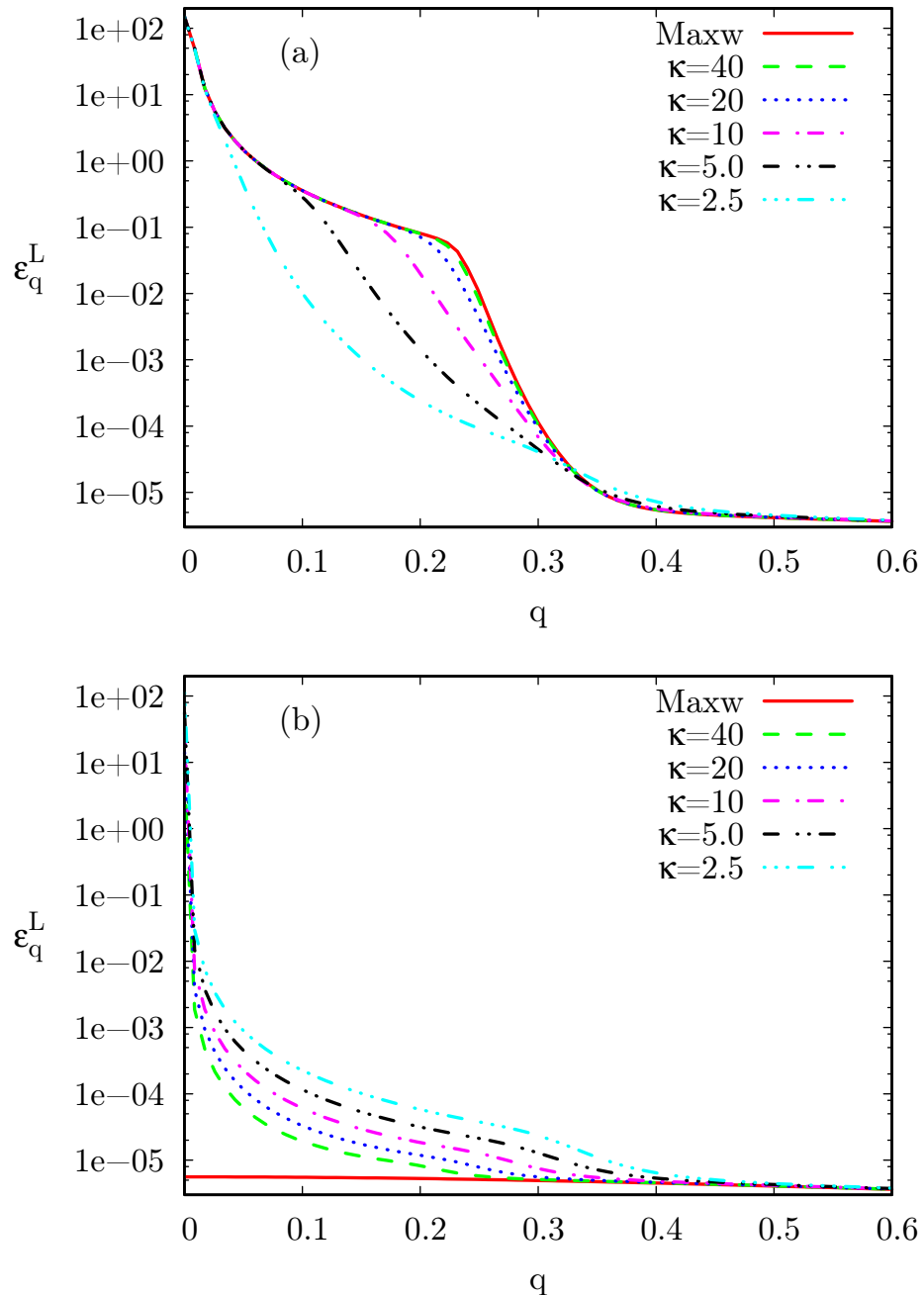


Figure B.1: Asymptotic spectrum of Langmuir waves for several values of κ index and Maxwellian distribution. (a) With electrostatic bremsstrahlung emission and collisional damping. (b) Without bremsstrahlung emission and collisional damping.

Appendix C

Extra publication

This publication is mainly related with the results presented in Ref. [78]. We can say that most of the ideas about the physical processes occurring in [78], regarding the formation of the core-halo velocity distribution and the fact that the electrostatic bremsstrahlung could be the underlying process behind the ubiquity of such velocity distribution in the space environment, came from the analysis of the results presented in [108].

Weakly turbulent plasma processes in the presence of inverse power-law velocity tail population

S. F. Tigik,^{1,a)} L. T. Petruzzellis,^{1,b)} L. F. Ziebell,^{1,c)} P. H. Yoon,^{2,3,4,d)} and R. Gaelzer^{1,e)}

¹*Instituto de Física, Universidade Federal do Rio Grande do Sul, 91501-970 Porto Alegre, RS, Brazil*

²*Korea Astronomy and Space Science Institute, Daejeon, South Korea*

³*Institute for Physical Science & Technology, University of Maryland, College Park, Maryland 20742, USA*

⁴*School of Space Research, Kyung Hee University, Yongin, Gyeonggi 446-701, South Korea*

(Received 20 October 2017; accepted 3 November 2017; published online 27 November 2017)

Observations show that plasma particles in the solar wind frequently display power-law velocity distributions, which can be isotropic or anisotropic. Particularly, the velocity distribution functions of solar wind electrons are frequently modeled as a combination of a background Maxwellian distribution and a non-thermal distribution which is known as the “halo” distribution. For fast solar wind conditions, highly anisotropic field-aligned electrons, denominated as the “strahl” distribution, are also present. Motivated by these observations, the present paper considers a tenuous plasma with Maxwellian ions, and electrons described by a summation of an isotropic Maxwellian distribution and an isotropic Kappa distribution. The formalism of weak turbulence theory is utilized in order to discuss the spectra of electrostatic waves that must be present in such a plasma, satisfying the conditions of quasi-equilibrium between the processes of spontaneous fluctuations and of induced emission. The kappa index and relative density of the Kappa electron distribution are varied. By taking into account the effects due to electromagnetic waves into the weak turbulence formalism, we investigate the electromagnetic spectra that satisfy the conditions of “turbulent equilibrium,” and also the time evolution of the wave spectra and of the electron distribution, which occurs in the case of the presence of an electron beam in the electron distribution. Published by AIP Publishing. <https://doi.org/10.1063/1.5009931>

I. INTRODUCTION

Observations made in the space environment consistently show plasma particles with velocity distributions that have non-thermal tails, and frequently with anisotropies.^{1–6} Characteristically, observed solar wind electrons are modeled by a combination of the Maxwellian core population (with energy in the range of tens of eV) and a tenuous but energetic *halo* distribution that contains a power-law velocity distribution in the suprathermal range ($\sim 10^2$ – 10^3 eV). For energy range even higher than that of the halo population, that is, for ~ 20 – 200 keV range, *superhalo* electrons are also observed.⁷ The halo and superhalo distributions are often modeled by the *Kappa distribution*.^{7–15} For the fast solar wind condition,¹⁶ a field-aligned electron beam called the *strahl* is often observed to stream away from the Sun. The *strahl* is characterized by the similar energy range as that of the halo electrons. Observations show that the number density of *strahl* decreases as one moves away from the Sun while the halo density increases,¹⁷ but their combined density remains constant, being $\sim 4\%$ – 5% of the total density. The energetic superhalo electrons contribute very little to the net electron content, as their number density amounts to not more than 10^{-6} of the total electron density, but owing to their high

energy, their presence is evident in the velocity or energy spectrum. The observations thus suggest that the *strahl* electrons are but a field aligned portion of the halo population, which are gradually pitch-angle scattered/diffused back to the isotropic halo by some unknown processes, of which the whistler wave fluctuations are the prime candidate.^{15,18}

The Kappa distribution was introduced to phenomenologically describe the non-thermal feature of the electron velocity distribution,⁸ but appears nowadays in the literature in a framework of non-extensive thermo-statistical equilibrium.¹⁹ Possibly the first time that a Kappa distribution was mentioned in such a context was about 20 years ago, in Ref. 20. A family of Kappa distributions is used in the literature, which include isotropic or anisotropic Kappa models. Isotropic Kappa distributions are usually written in terms of two different forms, one which can be found in Refs. 8–10 and the other which can be found in Refs. 13 and 14. These two different forms of Kappa distributions have been used by the plasma physics community and have been the subject of a number of theoretical discussions in recent years.^{21–25} In the present paper, we use a generic form of Kappa distribution, which, in particular cases, can reproduce the two widely used forms mentioned earlier, and use such a distribution to describe the *halo* distribution in the electron population.

Velocity distributions with power-law tails also appear mentioned in the context of turbulence theory, as in the pioneering work of Ref. 26, dealing with the velocity distributions in the presence of a superthermal radiation field. Recently, one of us put forth a rigorous theory of Kappa

^{a)}Electronic mail: sabrina.tigik@ufrgs.br

^{b)}Electronic mail: larissa.petruzzellis@ufrgs.br

^{c)}Electronic mail: luiz.ziebell@ufrgs.br

^{d)}Electronic mail: yoonp@umd.edu

^{e)}Electronic mail: rudi.gaelzer@ufrgs.br

distribution from the viewpoint of weak turbulence theory, rather than treating the Kappa distribution as simply a phenomenological tool.^{27,28} In such a theory, it was shown that a quasi-stationary state of electrons and a spectrum of electrostatic Langmuir fluctuations form a self-consistent pair of solutions of the stationary weak turbulence kinetic equations. A rather remarkable finding is that such a solution permits only the Kappa distribution as the legitimate solution, but nothing else, if the nonlinear interaction terms in the wave kinetic equation are considered. This finding may explain the physical origin of the pervasive Kappa-like electron distribution functions observed in the space environment. The accompanying Langmuir fluctuation spectrum, according to the above-referenced papers,^{27,28} is significantly modified from the thermal equilibrium form of the spectrum in that the long wavelength regime of the fluctuation spectrum exhibits an inverse power-law behavior, $\propto k^{-2}$, while for high k , the spectrum approaches a constant value. These findings and discussions were, however, carried out on the basis of the simplifying assumption of a single electron species. This was done for the sake of simplicity. For the actual situation, as overviewed earlier, the solar wind electrons are composed of several components, typically a quasi isotropic Maxwellian core plus a quasi isotropic halo population, which is often modeled by a Kappa distribution. In view of this, it is timely and appropriate to revisit the problem of solar wind such as electron distribution and the associated Langmuir fluctuation spectrum for multi- or, at least, a two-component electron plasma.

Ideally, one must obtain the electron distribution *and* the Langmuir fluctuation spectrum in a self-consistent manner without making any assumption at the outset. This is possible if one makes a simplifying assumption of single component electrons.^{27,28} However, if one is to consider multiple (or two component) electrons, then the situation becomes rather complex. Even if one ignores the nonlinear coupling term, the self-consistent solution for *both* electron distribution *and* the Langmuir spectrum must be obtained by numerical iteration scheme.²⁹ In the present analysis, we are interested in revisiting the approach taken in Ref. 29 but within the context of the analytical method. In order to reduce the complexity of the problem to some extent, we approach the problem by allowing a two component electron distribution function model and seeking the Langmuir spectrum intensity, which is consistent with the model electron distribution function.

Thus, in the first part of the present analysis, we will investigate the spectral form of the electrostatic fluctuation intensity that exists in a plasma, satisfying equilibrium conditions between the processes related to spontaneous fluctuations and the processes induced by the waves themselves. The analysis is made in the framework of weak turbulence theory including spontaneous effects. We consider an unmagnetized plasma with plasma particles described by velocity distributions, which are a summation of an isotropic Maxwellian background and a “halo” characterized by isotropic Kappa distributions of generic form. The analysis to be made under the framework of weak turbulence theory shows that electrostatic waves, i.e., Langmuir (L) and ion-sound (S) waves, can be naturally occurring in a plasma as a

result of spontaneous and induced effects. Electromagnetic waves, i.e., transverse waves (T), cannot be generated by these mechanisms, but can appear due to nonlinear interactions involving other types of plasma waves.

In the second part of the present paper, we also investigate the generation of electromagnetic waves, and the possibility of an approximated asymptotic solution for the spectrum of transverse waves, obtained as the outcome of nonlinear processes described by weak turbulence theory. Investigations on the equilibrium spectra of electrostatic waves and on the spectrum of T waves at turbulent equilibrium have already been made in the case of Maxwellian plasmas, but to the best of our knowledge, they have not yet been made taking into account the presence of a tenuous but energetic population of Kappa distributed particles. In addition to the investigation of the equilibrium spectra, we also investigate using weak turbulence theory the time evolution of the wave-particle system when an electron beam is assumed to exist in the medium.

The equations of weak turbulence theory can be found in the literature and will not be reproduced here for brevity. For the present paper, we utilize the formalism as presented in Ref. 30, and only comment on the basic features of these equations, which will be useful for the analysis of the results appearing in the present paper. We start by commenting on the equation that describes the time evolution of L waves.

In the context of weak turbulence theory, the time evolution of L waves is ruled by terms associated with spontaneous and induced emission, three-wave decay, and spontaneous plus induced scattering. The emission terms satisfy the wave-particle resonance condition, $\sigma\omega_{\mathbf{k}}^L - \mathbf{k} \cdot \mathbf{v} = 0$, where $\omega_{\mathbf{k}}^L$ is the dispersion relation for L waves, and $\sigma = \pm 1$ represent forward or backward propagation of the waves. The three-wave decay processes involve interactions between different types of waves, satisfying the following resonance conditions: $\sigma\omega_{\mathbf{k}}^L - \sigma'\omega_{\mathbf{k}'}^L - \sigma''\omega_{\mathbf{k}-\mathbf{k}'}^S = 0$, $\sigma\omega_{\mathbf{k}}^L - \sigma'\omega_{\mathbf{k}'}^T - \sigma''\omega_{\mathbf{k}-\mathbf{k}'}^T = 0$, and $\sigma\omega_{\mathbf{k}}^L - \sigma'\omega_{\mathbf{k}'}^S - \sigma''\omega_{\mathbf{k}-\mathbf{k}'}^T = 0$, where $\omega_{\mathbf{k}}^S$ and $\omega_{\mathbf{k}}^T$ are the dispersion relations for ion-acoustic waves (S) and for transverse waves, respectively. The scattering processes involve waves with two different wavelengths and frequencies, interacting with plasma particles, satisfying the following resonance conditions: $\sigma\omega_{\mathbf{k}}^L - \sigma'\omega_{\mathbf{k}'}^L - (\mathbf{k} - \mathbf{k}') \cdot \mathbf{v} = 0$ and $\sigma\omega_{\mathbf{k}}^L - \sigma'\omega_{\mathbf{k}'}^T - (\mathbf{k} - \mathbf{k}') \cdot \mathbf{v} = 0$. Detailed expressions for these terms can be found, for instance, in Ref. 30.

The equation that describes the time evolution of S waves presents a similar structure, containing spontaneous and induced emission terms, which satisfy the resonance condition, $\sigma\omega_{\mathbf{k}}^S - \mathbf{k} \cdot \mathbf{v} = 0$; three-wave decay terms satisfying the resonance conditions, $\sigma\omega_{\mathbf{k}}^S - \sigma'\omega_{\mathbf{k}'}^L - \sigma''\omega_{\mathbf{k}-\mathbf{k}'}^L = 0$, and $\sigma\omega_{\mathbf{k}}^S - \sigma'\omega_{\mathbf{k}'}^L - \sigma''\omega_{\mathbf{k}-\mathbf{k}'}^T = 0$; and a scattering term that satisfies $\sigma\omega_{\mathbf{k}}^S - \sigma'\omega_{\mathbf{k}'}^L - (\mathbf{k} - \mathbf{k}') \cdot \mathbf{v} = 0$. The scattering processes are deemed to be extremely slow in the case of S waves and are usually neglected.³⁰

The equation for the T waves can be considered of a different nature, in the sense that the superluminal T waves do not satisfy the wave-particle resonance condition, and therefore, there is no emission terms, either spontaneous or

induced. The equation that describes the time evolution of T waves features three-wave decay terms with resonance conditions given by $\sigma\omega_{\mathbf{k}}^T - \sigma'\omega_{\mathbf{k}'}^L - \sigma''\omega_{\mathbf{k}-\mathbf{k}'}^L = 0$, $\sigma\omega_{\mathbf{k}}^T - \sigma'\omega_{\mathbf{k}'}^L - \sigma''\omega_{\mathbf{k}-\mathbf{k}'}^S = 0$, and $\sigma\omega_{\mathbf{k}}^T - \sigma'\omega_{\mathbf{k}'}^T - \sigma''\omega_{\mathbf{k}-\mathbf{k}'}^L = 0$, and a scattering term satisfying $\sigma\omega_{\mathbf{k}}^T - \sigma'\omega_{\mathbf{k}'}^L - (\mathbf{k} - \mathbf{k}') \cdot \mathbf{v} = 0$.³⁰

In addition to the wave equations, the set of weak turbulence equations also contains equations for the time evolution of the particle distribution functions. In collisionless plasmas, the equation for the time evolution of the particle distribution function is well-known [see, for instance, Eq. (1) of Ref. 30] and includes a quasilinear diffusion term and a term originated from spontaneous fluctuations, both satisfying the wave-particle resonance conditions $\sigma\omega_{\mathbf{k}}^\alpha - \mathbf{k} \cdot \mathbf{v} = 0$, where α can be L or S

$$\frac{\partial f_a(\mathbf{v})}{\partial t} = \frac{\pi e_a^2}{m_a^2} \sum_{\sigma=\pm 1} \sum_{\alpha=L,S} \int \frac{d\mathbf{k}}{k^2} \mathbf{k} \cdot \frac{\partial}{\partial \mathbf{v}} \delta(\sigma\omega_{\mathbf{k}}^\alpha - \mathbf{k} \cdot \mathbf{v}) \times \left(\frac{m_a \sigma \omega_{\mathbf{k}}^\alpha}{4\pi^2} f_a(\mathbf{v}) + I_{\mathbf{k}}^{\sigma\alpha} \mathbf{k} \cdot \frac{\partial f_a(\mathbf{v})}{\partial \mathbf{v}} \right). \quad (1)$$

In Eq. (1), $f_a(\mathbf{v})$ is the distribution function for particles of species a ($a=e$ for electrons and $a=i$ for ions), normalized as $\int d\mathbf{v} f_a(\mathbf{v}) = 1$.

The present paper is organized as follows: In Sec. II, we introduce a generic form of isotropic Kappa distribution and describe the distribution function for plasma particles, constituted by a summation of a Maxwellian distribution and an isotropic Kappa distribution, with much lower number density than the Maxwellian population. In Sec. III, we briefly derive the expressions that give the spectra of L and S waves and that satisfy equilibrium conditions. In doing so, we take into account the velocity distributions presented in Sec. II. In Sec. IV, we discuss the possibility of an asymptotic spectrum of transverse waves (T), which is the result of nonlinear interaction in the wave-particle system. We derive an expression, which approximately describes this asymptotic state. In Sec. V, we present some results that show the wave spectra, taking into account parameters which are compatible with conditions in the solar wind. We also present in Sec. V some results that show the time evolution of the wave spectra and of the particle distribution function, obtained by numerical solution of equations of weak turbulence theory. Section VI summarizes the results obtained.

II. THE VELOCITY DISTRIBUTIONS FOR PLASMA PARTICLES

Let us assume that isotropic distributions for ions and electrons are made of the summation of Maxwellian and Kappa distributions. In three dimensions (3D), considering a generic form for the Kappa distribution, we may write

$$f_\beta(\mathbf{v}) = \left(1 - \frac{n_{\kappa\beta}}{n_e} \right) f_{\beta,M}(\mathbf{v}) + \frac{n_{\kappa\beta}}{n_e} f_{\beta,\kappa}(\mathbf{v}), \quad (2)$$

where

$$f_{\beta,M}(\mathbf{v}) = \frac{1}{\pi^{3/2} v_\beta^3} \exp \left(-\frac{v^2}{v_\beta^2} \right), \quad (3)$$

$$f_{\beta,\kappa}(\mathbf{v}) = \frac{1}{\pi^{3/2} \kappa_\beta^{3/2} v_{\beta,\kappa}^3} \frac{\Gamma(\kappa_\beta + \alpha_\beta)}{\Gamma\left(\kappa_\beta + \alpha_\beta - \frac{3}{2}\right)} \left(1 + \frac{v^2}{\kappa_\beta v_{\beta,\kappa}^2} \right)^{-(\kappa_\beta + \alpha_\beta)}, \quad (4)$$

where $v_\beta = \sqrt{2T_\beta/m_\beta}$ is the thermal velocity of particle species labeled β , and $v_{\beta,\kappa}$ is a parameter with the same physical dimension as the particle thermal velocity, and reduces to the thermal velocity in the limit $\kappa_\beta \rightarrow \infty$. The distribution functions given by Eqs. (3) and (4) are normalized such that $\int d^3 v f_\beta = 1$.

Particular cases of the distribution (4) that correspond to the forms of Kappa distributions which are widely used in the literature can be obtained by a suitable choice of parameters α_β and $v_{\beta,\kappa}$. Namely, if $\alpha_\beta = 1$, and

$$v_{\beta,\kappa}^2 = \frac{\kappa_\beta - \frac{3}{2}}{\kappa_\beta} v_\beta^2, \quad (5)$$

then Eq. (4) becomes a form of isotropic Kappa distribution, which is widely used in the literature^{8–10}

$$f_\beta(\mathbf{v}) = \frac{1}{\pi^{3/2} \kappa_\beta^{3/2} v_{\beta,\kappa}^3} \frac{\Gamma(\kappa_\beta + 1)}{\Gamma\left(\kappa_\beta - \frac{1}{2}\right)} \left(1 + \frac{v^2}{\kappa_\beta v_{\beta,\kappa}^2} \right)^{-(\kappa_\beta + 1)}. \quad (6)$$

The average value of the kinetic energy, in the case of distribution (6), leads to the usual notion of temperature, since it is easily obtained that

$$\left\langle \frac{1}{2} m v^2 \right\rangle_\beta = \frac{3T_\beta}{2}. \quad (7)$$

In the above, $\langle \dots \rangle_\beta = \int d\mathbf{v} \dots f_\beta$.

Another customary choice is to take $\alpha_\beta = 0$ and $v_{\beta,\kappa} = v_\beta$. This corresponds to the case in which Eq. (4) becomes the isotropic Kappa distribution, which is used, for instance, in Refs. 13 and 14

$$f_\beta(\mathbf{v}) = \frac{1}{\pi^{3/2} \kappa_\beta^{3/2} v_\beta^3} \frac{\Gamma(\kappa_\beta)}{\Gamma\left(\kappa_\beta - \frac{3}{2}\right)} \left(1 + \frac{v^2}{\kappa_\beta v_\beta^2} \right)^{-\kappa_\beta}. \quad (8)$$

For distribution function (8), the average value of the kinetic energy does not lead to the usual notion of temperature, since it is easy to obtain that

$$\left\langle \frac{1}{2} m v^2 \right\rangle_\beta = \frac{3T_\beta}{2} \frac{\kappa_\beta}{\kappa_\beta - 5/2}. \quad (9)$$

It can also be noticed that the distribution given by (8) can be obtained as a result of the use of the non-extensive statistical mechanics as formulated in Refs. 13, 31, and 32, while the distribution function given by (6) results from a modified approach to non-extensive statistical mechanics, which utilizes the so-called escort probability functions.^{33,34}

For convenience, we define dimensionless velocities, by division of the velocity by the electron thermal velocity v_e ,

$\mathbf{u} = \mathbf{v}/v_e$, the normalized wavenumber $\mathbf{q} = \mathbf{k}v_e/\omega_{pe}$, the normalized wave frequency for waves of type α , $z_{\mathbf{q}}^{\alpha} = \omega_{\mathbf{q}}^{\alpha}/\omega_{pe}$ (where $\alpha = L, S$, or T), and the dimensionless time variable, $\tau = \omega_{pe}t$, with $\omega_{pe} = \sqrt{4\pi n_e e^2/m_e}$ being the electron plasma frequency. We also define the normalized wave intensity for waves of type α

$$\mathcal{E}_{\mathbf{q}}^{\sigma\alpha} = \frac{(2\pi)^2 g I_{\mathbf{k}}^{\sigma\alpha}}{m_e v_e^2 \mu_{\mathbf{k}}^{\alpha}}, \quad (10)$$

and introduce other useful dimensionless quantities

$$\begin{aligned} u &= \frac{v}{v_e}, & u_{\beta,\kappa} &= \frac{v_{\beta,\kappa}}{v_e}, & u_{\beta} &= \frac{v_{\beta}}{v_e}, \\ \mu &= \frac{m_e}{m_i}, & \delta_e &= \frac{n_{ke}}{n_e}, & \delta_i &= \frac{n_{ki}}{n_e}. \end{aligned} \quad (11)$$

In terms of the dimensionless variables, the dispersion relations for the waves and the velocity distribution functions become

$$z_{\mathbf{q}}^L = \left(1 + \frac{3}{2} q^2\right)^{1/2}, \quad (12)$$

$$z_{\mathbf{q}}^S = \frac{q}{\sqrt{2}} \left(\frac{m_e}{m_i}\right)^{1/2} \left(1 + 3 \frac{T_i}{T_e}\right)^{1/2} \left(1 + \frac{1}{2} q^2\right)^{-1/2}, \quad (13)$$

$$z_{\mathbf{q}}^T = \left(1 + \frac{c^2}{v_e^2} q^2\right)^{1/2}, \quad (14)$$

$$\Phi_{\beta,M}(\mathbf{u}) = \frac{1}{\pi^{3/2} u_{\beta}^3} \exp\left(-\frac{u^2}{u_{\beta}^2}\right), \quad (15)$$

$$\Phi_{\beta,\kappa}(\mathbf{u}) = \frac{1}{\pi^{3/2} \kappa_{\beta}^{3/2} u_{\beta,\kappa}^3} \frac{\Gamma(\kappa_{\beta} + \alpha_{\beta})}{\Gamma(\kappa_{\beta} + \alpha_{\beta} - \frac{3}{2})} \left(1 + \frac{u^2}{\kappa_{\beta} u_{\beta,\kappa}^2}\right)^{-(\kappa_{\beta} + \alpha_{\beta})}. \quad (16)$$

III. INITIAL L AND S WAVE INTENSITIES

Making use of the equations of weak turbulence theory, the spectra of electrostatic waves may be initialized by neglecting the nonlinear interactions and balancing the

spontaneous and induced emission terms, and by taking into account only the background populations. For the L waves, using the symbol $\Phi_e(\mathbf{u})$ for the electron distribution function in terms of normalized quantities, we utilize the wave equation without the nonlinear terms, written in terms of the dimensionless quantities

$$\begin{aligned} \frac{\partial}{\partial \tau} \mathcal{E}_{\mathbf{q}}^{\sigma L} &= \frac{\pi}{q^2} \int d\mathbf{u} \delta(\sigma z_{\mathbf{q}}^L - \mathbf{q} \cdot \mathbf{u}) \\ &\times \left(g \Phi_e(\mathbf{u}) + (\sigma z_{\mathbf{q}}^L) \mathbf{q} \cdot \frac{\partial \Phi_e(\mathbf{u})}{\partial \mathbf{u}} \mathcal{E}_{\mathbf{q}}^{\sigma L} \right). \end{aligned} \quad (17)$$

Using spherical coordinates in velocity space, with the z axis along \mathbf{q} , and considering distribution (2) written in terms of dimensionless variables, we obtain

$$\begin{aligned} \frac{\partial}{\partial \tau} \mathcal{E}_{\mathbf{q}}^{\sigma L} &= \frac{\pi}{q^2} \left\{ g [(1 - \delta_e) I_M^{\sigma L} + \delta_e I_1^{\sigma L}] \right. \\ &\left. - 2(\sigma z_{\mathbf{q}}^L)^2 \left[(1 - \delta_e) I_M^{\sigma L} + \frac{\delta_e u_e^2 (\kappa_e + \alpha_e)}{u_{e,\kappa}^2 \kappa_e} I_2^{\sigma L} \right] \mathcal{E}_{\mathbf{q}}^{\sigma L} \right\}, \end{aligned} \quad (18)$$

where

$$\begin{aligned} I_M^{\beta\alpha} &= \int d^3 u \Phi_{\beta,M}(u) \delta(\sigma z_{\mathbf{q}}^{\alpha} - \mathbf{q} \cdot \mathbf{u}), \\ I_1^{\beta\alpha} &= \int d^3 u \Phi_{\beta,\kappa}(u) \delta(\sigma z_{\mathbf{q}}^{\alpha} - \mathbf{q} \cdot \mathbf{u}), \\ I_2^{\beta\alpha} &= \int d^3 u \left(1 + \frac{u^2}{\kappa_{\beta} u_{\beta,\kappa}^2}\right)^{-1} \Phi_{\beta,\kappa}(u) \delta(\sigma z_{\mathbf{q}}^{\alpha} - \mathbf{q} \cdot \mathbf{u}). \end{aligned} \quad (19)$$

The equilibrium is obtained by setting the expression for the time derivative equal to zero, which leads to

$$\mathcal{E}_{\mathbf{q}}^{\sigma L} = \frac{g}{2(z_{\mathbf{q}}^L)^2} \frac{(1 - \delta_e) I_M^{\sigma L} + \delta_e I_1^{\sigma L}}{(1 - \delta_e) I_M^{\sigma L} + \frac{\delta_e u_e^2 (\kappa_e + \alpha_e)}{u_{e,\kappa}^2 \kappa_e} I_2^{\sigma L}}. \quad (20)$$

The integrals $I_M^{\beta\alpha}$, $I_1^{\beta\alpha}$, and $I_2^{\beta\alpha}$ can be evaluated analytically. For the case $\beta = e$, it is possible to obtain

$$\begin{aligned} \mathcal{E}_{\mathbf{q}}^{\sigma L} &= \frac{g}{2(z_{\mathbf{q}}^L)^2} \left[(1 - \delta_e) \exp(-\xi_e) + \frac{\delta_e u_e}{\kappa_e^{1/2} u_{e,\kappa}} \frac{\Gamma(\kappa_e + \alpha_e - 1)}{\Gamma(\kappa_e + \alpha_e - 3/2)} \frac{1}{(1 + \xi_{e,\kappa})^{\kappa_e + \alpha_e - 1}} \right] \\ &\times \left[(1 - \delta_e) \exp(-\xi_e) + \frac{\delta_e u_e^3}{\kappa_e^{3/2} u_{e,\kappa}^3} \frac{\Gamma(\kappa_e + \alpha_e)}{\Gamma(\kappa_e + \alpha_e - 3/2)} \frac{1}{(1 + \xi_{e,\kappa})^{\kappa_e + \alpha_e}} \right]^{-1}, \\ \xi_e &= \frac{(z_q^L/q)^2}{u_e^2}, \quad \xi_{e,\kappa} = \frac{(z_q^L/q)^2}{\kappa_e u_{e,\kappa}^2}. \end{aligned} \quad (21)$$

For the S waves, we obtain the following equation:

$$\frac{\partial}{\partial \tau} \mathcal{E}_{\mathbf{q}}^{\sigma S} = \mu_{\mathbf{q}}^S \frac{\pi}{q^2} \int d\mathbf{u} \delta(\sigma z_{\mathbf{q}}^S - \mathbf{q} \cdot \mathbf{u}) \left[g(\Phi_e(\mathbf{u}) + \Phi_i(\mathbf{u})) + (\sigma z_{\mathbf{q}}^L) \left(\mathbf{q} \cdot \frac{\partial \Phi_e(\mathbf{u})}{\partial \mathbf{u}} + \frac{m_e}{m_i} \mathbf{q} \cdot \frac{\partial \Phi_i(\mathbf{u})}{\partial \mathbf{u}} \right) \mathcal{E}_{\mathbf{q}}^{\sigma S} \right], \quad (22)$$

where

$$\mu_q^S = \frac{q^3}{2^{3/2}} \sqrt{\frac{m_e}{m_i}} \left(1 + \frac{3T_i}{T_e}\right)^{1/2}. \quad (23)$$

Following steps are similar to those employed in the case of L waves, and the initial spectrum of S waves is seen to obey the following expression:

$$\mathcal{E}_q^{\sigma S} = \frac{g}{2(z_q^L)(z_q^S)} \frac{N_s}{D_s}, \quad (24)$$

where

$$\begin{aligned} N_s &= (1 - \delta_e) I_M^{eS} + \delta_e I_1^{eS} + (1 - \delta_i) I_M^{iS} + \delta_i I_1^{iS}, \\ D_s &= (1 - \delta_e) I_M^{eS} + \frac{\delta_e u_e^2 (\kappa_e + \alpha_e)}{u_{e,\kappa}^2 \kappa_e} I_2^{eS} \\ &\quad + \mu (1 - \delta_i) \frac{u_e^2}{u_i^2} I_M^{iS} + \frac{\delta_i \mu u_e^2 (\kappa_i + \alpha_i)}{u_{i,\kappa}^2 \kappa_i} I_2^{iS}. \end{aligned}$$

After the evaluation of the $I_M^{\beta\alpha}$, $I_1^{\beta\alpha}$, and $I_2^{\beta\alpha}$ integrals, one obtains the following:

$$\begin{aligned} \mathcal{E}_q^{\sigma S} &= \frac{g}{2(z_q^L)(z_q^S)} \left[(1 - \delta_e) \exp(-\xi_e) + \frac{\delta_e u_e}{\kappa_e^{1/2} u_{e,\kappa}} \frac{\Gamma(\kappa_e + \alpha_e - 1)}{\Gamma(\kappa_e + \alpha_e - 3/2)} \frac{1}{(1 + \xi_{e,\kappa})^{\kappa_e + \alpha_e - 1}} \right. \\ &\quad + (1 - \delta_i) \exp(-\xi_i) + \frac{\delta_i u_e}{\kappa_i^{1/2} u_{i,\kappa}} \frac{\Gamma(\kappa_i + \alpha_i - 1)}{\Gamma(\kappa_i + \alpha_i - 3/2)} \frac{1}{(1 + \xi_{i,\kappa})^{\kappa_i + \alpha_i - 1}} \Big] \\ &\quad \times \left[(1 - \delta) \exp(-\xi_e) + \frac{\delta u_e^3}{\kappa_e^{3/2} u_{e,\kappa}^3} \frac{\Gamma(\kappa_e + \alpha_e)}{\Gamma(\kappa_e + \alpha_e - 3/2)} \frac{1}{(1 + \xi_{e,\kappa})^{\kappa_e + \alpha_e}} \right. \\ &\quad \left. + \mu (1 - \delta_i) \frac{u_e^3}{u_i^3} \exp(-\xi_i) + \frac{\delta_i \mu u_e^3}{\kappa_i^{3/2} u_{i,\kappa}^3} \frac{\Gamma(\kappa_i + \alpha_i)}{\Gamma(\kappa_i + \alpha_i - 3/2)} \frac{1}{(1 + \xi_i)^{\kappa_i + \alpha_i}} \right]^{-1}, \end{aligned} \quad (25)$$

where ξ_e and $\xi_{e,\kappa}$ are defined in (21) and

$$\xi_i = \frac{(z_q^L/q)^2}{u_i^2}, \quad \xi_{i,\kappa} = \frac{(z_q^L/q)^2}{\kappa_i u_{i,\kappa}^2}. \quad (26)$$

This brings a closure to the first part of the present paper, namely, to theoretically discuss the self-consistent form of electrostatic Langmuir and ion-sound wave fluctuation intensities that arise when the electron velocity distribution function is composed of a Maxwellian core plus a “halo” component given by a Kappa distribution. In Ref. 29, a similar problem was approached (minus the discussion of ion-acoustic wave intensity) by considering the iterative numerical solution of the self-consistent set of particle and wave kinetic equations. The present discussion complements Ref. 29 in that our approach has been within the context of an analytical method. The analytical solution, while less rigorous than the iterative solution obtained in Ref. 29, is nevertheless useful in the subsequent discussion of transverse wave intensity, which we turn to next.

IV. ASYMPTOTIC WAVE LEVEL FOR TRANSVERSE WAVES

The time evolution of transverse T waves, which are electromagnetic waves, is governed by an equation that contains the terms related to three wave decay involving a T wave and two L waves: a T wave, an L wave, and an S wave, and two T waves and a L wave, and also a scattering term involving a T wave, a L wave, and particles.³⁰ The evolution

equation does not feature a quasilinear term, such as those appearing in the equations for L and S waves, given by Eqs. (17) and (22), because the linear resonance condition with the particles is not satisfied by the superluminal T waves.³⁰

The occurrence of decay processes involving L and S waves, and also of scattering processes, has as a consequence that T waves are generated by these nonlinear mechanisms, even if they are not considered present as an initial condition. It is therefore pertinent to investigate the asymptotic state attained by the spectrum of T waves, due to the nonlinear processes. This asymptotic state characterizes what can be called a “turbulent equilibrium” and has already been investigated by us considering an equilibrium plasma in which the plasma particles are described by Maxwellian distributions.^{35,36} In the present investigation, we consider the case in which the velocity distributions of plasma particles contain a population described by Kappa distributions, as given by Eq. (2).

At the asymptotic state, it may be considered that the decay terms are not very effective in changing the wave level, since they do not involve particles and represent just an exchange of momentum and energy among different waves. The scattering term can therefore be considered to be the dominant term for late evolution of the system. This conjecture has already been used in the case of Maxwellian velocity distributions, and has been well supported by numerical analysis of the time evolution considering the complete weak turbulence equation for the T waves.^{35,36} Consequently, using this approximation and adopting normalized variables, the equation for late stages of the time evolution of T waves can be written as follows:³⁰

$$\begin{aligned} \frac{\partial}{\partial \tau} \mathcal{E}_{\mathbf{q}}^{\sigma T} &\simeq \sum_{\sigma'} \int d\mathbf{q}' \int d\mathbf{u} \frac{(\mathbf{q} \times \mathbf{q}')^2}{q^2 q'^2} \delta \left[\sigma z_{\mathbf{q}}^T - \sigma' z_{\mathbf{q}'}^L - (\mathbf{q} - \mathbf{q}') \cdot \mathbf{u} \right] \\ &\times \left[g(\sigma z_{\mathbf{q}}^T) \left(\sigma z_{\mathbf{q}}^T \mathcal{E}_{\mathbf{q}'}^{\sigma L} - \sigma' z_{\mathbf{q}'}^L \frac{\mathcal{E}_{\mathbf{q}}^{\sigma T}}{2} \right) (\Phi_e + \Phi_i) - \mathcal{E}_{\mathbf{q}'}^{\sigma L} \frac{\mathcal{E}_{\mathbf{q}}^{\sigma T}}{2} (\mathbf{q} - \mathbf{q}') \cdot \frac{\partial}{\partial \mathbf{u}} \left((\sigma z_{\mathbf{q}}^T - \sigma' z_{\mathbf{q}'}^L) \Phi_e - \frac{m_e}{m_i} (\sigma z_{\mathbf{q}}^T) \Phi_i \right) \right]. \end{aligned} \quad (27)$$

The asymptotic state is obtained by taking the time derivative equal to zero. Doing this, and using the distribution functions given by Eq. (2), we obtain

$$\begin{aligned} \sum_{\sigma'} \int d\mathbf{q}' \frac{(\mathbf{q} \times \mathbf{q}')^2}{q^2 q'^2} \left\{ g(\sigma z_{\mathbf{q}}^T) \left(\sigma' z_{\mathbf{q}'}^L \frac{\mathcal{E}_{\mathbf{q}}^{\sigma T}}{2} - \sigma z_{\mathbf{q}}^T \mathcal{E}_{\mathbf{q}'}^{\sigma L} \right) \left[(1 - \delta_e) I_M^e + \delta_e I_1^e + (1 - \delta_i) I_M^i + \delta_i I_1^i \right] \right. \\ + \frac{m_e}{m_i} \mathcal{E}_{\mathbf{q}'}^{\sigma L} \frac{\mathcal{E}_{\mathbf{q}}^{\sigma T}}{2} (\sigma z_{\mathbf{q}}^T - \sigma' z_{\mathbf{q}'}^L) (\sigma z_{\mathbf{q}}^T) \left[\frac{2}{u_i^2} (1 - \delta_i) I_M^i + \delta_i \frac{2}{u_{i,\kappa}^2} \frac{(\kappa_i + \alpha_i)}{\kappa_i} I_2^i \right] \\ \left. - \mathcal{E}_{\mathbf{q}'}^{\sigma L} \frac{\mathcal{E}_{\mathbf{q}}^{\sigma T}}{2} \left(\sigma z_{\mathbf{q}}^T - \sigma' z_{\mathbf{q}'}^L \right)^2 \left[\frac{2}{u_e^2} (1 - \delta_e) I_M^e + \delta_e \frac{2}{u_{e,\kappa}^2} \frac{(\kappa_e + \alpha_e)}{\kappa_e} I_2^e \right] \right\} = 0. \end{aligned} \quad (28)$$

Making use of the analytical expressions for the quantities I_M^β , I_1^β , and I_2^β , one arrives at the following:

$$\begin{aligned} \mathcal{E}_{\mathbf{q}}^{\sigma T} &= 2(\sigma z_{\mathbf{q}}^T)^2 \sum_{\sigma'} \int d\mathbf{q}' \frac{(\mathbf{q} \times \mathbf{q}')^2}{q'^2 |\mathbf{q} - \mathbf{q}'|} g \mathcal{E}_{\mathbf{q}'}^{\sigma' L} \sum_{\beta=e,i} \left(\frac{1 - \delta_\beta}{u_\beta} e^{-\zeta_\beta} + \frac{\delta_\beta}{\kappa_\beta^{1/2} u_{\beta,\kappa}} \frac{\Gamma(\kappa_\beta + \alpha_\beta - 1)}{\Gamma(\kappa_\beta + \alpha_\beta - 3/2)} \frac{1}{(1 + \zeta_\beta)^{\kappa_\beta + \alpha_\beta - 1}} \right) \\ &\times \left\{ \sum_{\sigma'} \int d\mathbf{q}' \frac{(\mathbf{q} \times \mathbf{q}')^2}{q'^2 |\mathbf{q} - \mathbf{q}'|} \left[g_*(\sigma z_{\mathbf{q}}^T)(\sigma' z_{\mathbf{q}'}^L) \sum_{\beta=e,i} \left(\frac{1 - \delta_\beta}{u_\beta} e^{-\zeta_\beta} + \frac{\delta_\beta}{\kappa_\beta^{1/2} u_{\beta,\kappa}} \frac{\Gamma(\kappa_\beta + \alpha_\beta - 1)}{\Gamma(\kappa_\beta + \alpha_\beta - 3/2)} \frac{1}{(1 + \zeta_{\beta,\kappa})^{\kappa_\beta + \alpha_\beta - 1}} \right) \right. \right. \\ &+ \mu \mathcal{E}_{\mathbf{q}'}^{\sigma' L} (\sigma z_{\mathbf{q}}^T - \sigma' z_{\mathbf{q}'}^L) (\sigma z_{\mathbf{q}}^T) \left(\frac{2(1 - \delta_i)}{u_i^3} e^{-\zeta_i} + \frac{2\delta_i}{\kappa_i^{3/2} u_{i,\kappa}^3} \frac{\Gamma(\kappa_i + \alpha_i)}{\Gamma(\kappa_i + \alpha_i - 3/2)} \frac{1}{(1 + \zeta_i)^{\kappa_i + \alpha_i}} \right) \\ &\left. \left. - \mathcal{E}_{\mathbf{q}'}^{\sigma' L} (\sigma z_{\mathbf{q}}^T - \sigma' z_{\mathbf{q}'}^L)^2 \left(\frac{2(1 - \delta_e)}{u_e^3} e^{-\zeta_e} + \frac{2\delta_e}{\kappa_e^{3/2} u_{e,\kappa}^3} \frac{\Gamma(\kappa_e + \alpha_e)}{\Gamma(\kappa_e + \alpha_e - 3/2)} \frac{1}{(1 + \zeta_{e,\kappa})^{\kappa_e + \alpha_e}} \right) \right] \right\}^{-1}, \\ \zeta_\beta &= \frac{(\sigma z_{\mathbf{q}}^T - \sigma' z_{\mathbf{q}'}^L)^2}{u_\beta^2 |\mathbf{q} - \mathbf{q}'|^2}, \quad \zeta_{\beta,\kappa} = \frac{(\sigma z_{\mathbf{q}}^T - \sigma' z_{\mathbf{q}'}^L)^2}{\kappa_\beta u_{\beta,\kappa}^2 |\mathbf{q} - \mathbf{q}'|^2}, \quad (\beta = e, i). \end{aligned} \quad (29)$$

This is a fairly complex expression. However, one notices that the contributions due to the Maxwellian population feature an exponential factor, which is very peaked with maximum occurring for $\sigma' = \sigma$ and $q' \simeq q_m$, the value of q for which $z_{q'}^L = z_q^T$. The contributions due to the Kappa distribution are also proportional to a factor which is unity for $\sigma' = \sigma$ and $q' \simeq q_m$, and decrease rapidly away from this point. As a consequence, the terms corresponding to the induced scattering can be neglected, since they are proportional to $(\sigma z_{\mathbf{q}}^T - \sigma' z_{\mathbf{q}'}^L)$, and the asymptotic spectrum of T waves can be approximated by the following:

$$\begin{aligned} \mathcal{E}_{\mathbf{q}}^{\sigma T} &\simeq 2(\sigma z_{\mathbf{q}}^T)^2 \sum_{\sigma'} \int d\mathbf{q}' \frac{(\mathbf{q} \times \mathbf{q}')^2}{q'^2 |\mathbf{q} - \mathbf{q}'|} g \mathcal{E}_{\mathbf{q}_m}^{\sigma' L} \sum_{\beta=e,i} \left(\frac{1 - \delta_\beta}{u_\beta} e^{-\zeta_\beta} + \frac{\delta_\beta}{\kappa_\beta^{1/2} u_{\beta,\kappa}} \frac{\Gamma(\kappa_\beta + \alpha_\beta - 1)}{\Gamma(\kappa_\beta + \alpha_\beta - 3/2)} \frac{1}{(1 + \zeta_{\beta,\kappa})^{\kappa_\beta + \alpha_\beta - 1}} \right) \\ &\times \left[\sum_{\sigma'} \int d\mathbf{q}' \frac{(\mathbf{q} \times \mathbf{q}')^2}{q'^2 |\mathbf{q} - \mathbf{q}'|} g_*(\sigma z_{\mathbf{q}}^T)^2 \sum_{\beta=e,i} \left(\frac{1 - \delta_\beta}{u_\beta} e^{-\zeta_\beta} + \frac{\delta_\beta}{\kappa_\beta^{1/2} u_{\beta,\kappa}} \frac{\Gamma(\kappa_\beta + \alpha_\beta - 1)}{\Gamma(\kappa_\beta + \alpha_\beta - 3/2)} \frac{1}{(1 + \zeta_{\beta,\kappa})^{\kappa_\beta + \alpha_\beta - 1}} \right) \right]^{-1}. \end{aligned} \quad (30)$$

As a result of these approximations, and assuming that in the absence of particle beams, the spectrum of L waves remains nearly the same as in the initial state, and is therefore symmetrical, $\mathcal{E}_{q_m}^{-L} = \mathcal{E}_{q_m}^{+L}$, it is seen that the asymptotic spectrum of T waves can be simplified by

$$\mathcal{E}_{\mathbf{q}}^{\sigma T} \simeq 2\mathcal{E}_{\mathbf{q}_m}^{\sigma L}, \quad q_m = \sqrt{\frac{2}{3}} \frac{c}{v_e} q. \quad (31)$$

To sum up the second part of the present analysis, by making use of the equations of electromagnetic weak turbulence, we have derived the asymptotic form of the

transverse wave intensity, which is given in terms of the Langmuir wave intensity. The Langmuir wave fluctuation intensity, however, was already discussed in Sec. III so that we may readily obtain the explicit form of the transverse wave intensity.

V. NUMERICAL RESULTS

In order to illustrate the effects of the presence of a Kappa population of electrons on the spectrum of waves, which satisfy the conditions of equilibrium with the particle distribution, we consider that the electron population is described by distribution function (2), with $\alpha=1$, and $u_{e,\kappa}^2 = u_e^2(\kappa_e - 3/2)/\kappa_e$. The ion distribution is assumed to be described by an isotropic Maxwellian distribution, i.e., we assume $\delta_i=0$. Finally, we use $T_e/T_i=2$, a value for the electron and ion temperature ratio which is within the range of values observed in the solar wind.³⁷

In Fig. 1, we show the initial spectrum of electrostatic waves divided by g , as a function of normalized wavenumber $q=kv_e/\omega_{pe}$, for several values of the index κ_e . We assume that the electron population described by a Kappa distribution constitute 10% of the electron population, i.e., $\delta_e=0.1$. Figures 1(a) and 1(b) show the initial spectra of L and S waves, obtained using Eqs. (21) and (25), respectively. The spectra obtained in the case of purely Maxwellian distribution, with $n_{ke}/n_e=0.0$, are also shown in Figs. 1(a) and 1(b), for reference. In Figs. 1(a) and 1(b) are shown the curves corresponding to several values of κ_e ($\kappa_e=40, 20, 10, 5$, and 2.5).

Figure 1(a) shows that the value of $\mathcal{E}_q^L(0)$ in the case of the presence of Kappa population is higher than the value obtained in the case of a purely Maxwellian distribution, with a difference that is already noticeable in the scale of the figure even for the upper limit shown, $q=0.6$, and increases for smaller values of q , featuring a peak that diverges for $q \rightarrow 0$. For larger values of κ_e , the shape of the L spectrum is similar to the shape exhibited in the case of small values of κ_e , but the magnitude of the spectrum at a given value of q is smaller for increasing values of κ_e . It is noticed, however, that the peak at $q \rightarrow 0$ is present even for large values of κ_e .

The presence of the peak in the L spectrum, for $q \rightarrow 0$, can be understood by the analysis of Eq. (21). In the

presence of a population of kappa electrons, even for a small value of n_{ke}/n_e , it is seen that for a sufficiently small value of q the contribution due to the Maxwellian population vanishes, due to the factor $\exp(-(z_q^L/q)^2/u_e^2)$. For the region of q values where this occurs, the contribution of the Kappa population is dominant, and the equilibrium spectrum can be given by the approximated expression

$$\mathcal{E}_q^{\sigma L} \simeq \frac{g}{2(z_q^L)^2} \frac{u_{e,\kappa}^2}{u_e^2} \left(1 + \frac{(z_q^L/q)^2}{\kappa_e u_{e,\kappa}^2} \right). \quad (32)$$

In the case of $\kappa_e \rightarrow \infty$, this expression reduces to $g/(2(z_q^L)^2)$, which is the expression obtained in the Maxwellian case, as expected. However, for finite values of κ_e , no matter how large, Eq. (32) is seen to diverge at $q \rightarrow 0$. The explanation for this is as follows: For large values of κ_e , the Kappa distribution coincides with a Maxwellian distribution, in the region of velocity space with significant electron population. However, the initial spectra of waves are obtained from Eq. (17), which for equilibrium requires a balance between the term associated with spontaneous fluctuations, which is proportional to the distribution function, and the term associated with induced emission, which is proportional to the velocity derivative of the distribution function and to the value of the wave spectra at the resonant velocity. For $q \rightarrow 0$, the resonant velocity becomes progressively larger. Since for very large velocities the derivative of the Kappa distribution is smaller than the derivative of the Maxwellian distribution, the wave spectra for small q have to be higher in the case of Kappa distribution than in the case of Maxwellian distribution, in order to satisfy the equilibrium condition.

Figure 1(b) shows the values of $\mathcal{E}_q^S(0)/g$ vs. $q=kv_e/\omega_{pe}$. In fact, the figure shows the values of $\mathcal{E}_q^S(0)$ multiplied by μ_q^S , but we continue to denote the quantity as $\mathcal{E}_q^S(0)$, for simplicity. The figure displays the results obtained for several values of κ_e , but the different curves cannot be distinguished in the scale of the figure. It is seen that the kappa index of the Kappa distribution is not relevant for the initial spectrum of S waves, while it was seen to be relevant for the initial spectrum of L waves.

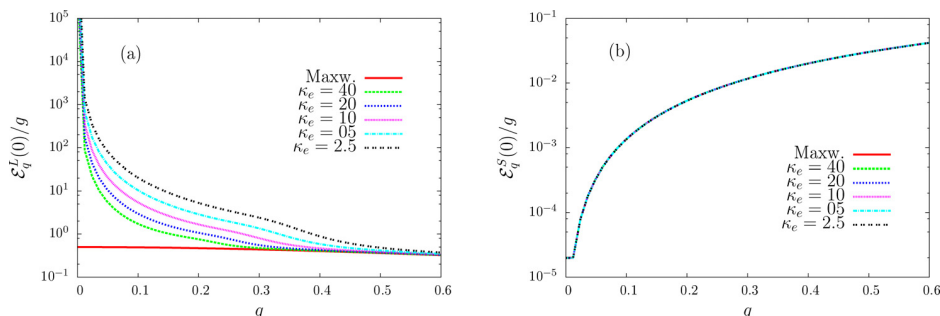


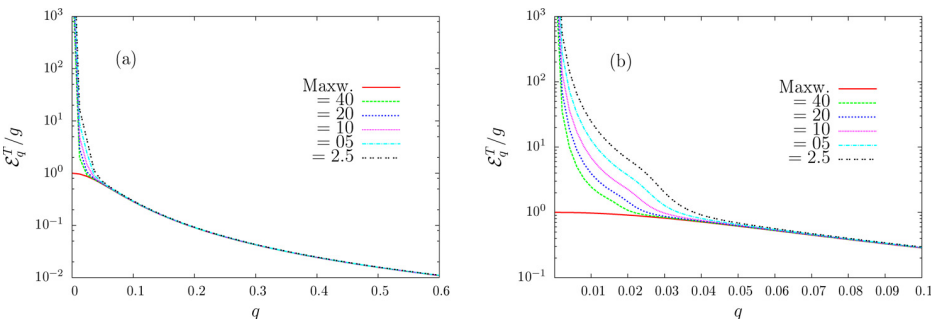
FIG. 1. Initial spectrum of electrostatic waves divided by g , as a function of normalized wavenumber $q=kv_e/\omega_{pe}$, for several values of the index κ_e . The case of Maxwellian distribution, $n_{ke}/n_e=0.0$, is also shown for reference. (a) L waves and (b) S waves. For S waves, all curves overlap. Electron distribution given by Eq. (2), with $\alpha_e=1$ and $u_{\beta,\kappa}^2 = u_\beta^2(\kappa_e - 3/2)/\kappa_e$, for $n_{ke}/n_e=0.1$. The ion distribution is an isotropic Maxwellian, and $T_e/T_i=2$. The spectra of L and S waves are given by Eqs. (21) and (25).

We have also obtained the initial spectrum of electrostatic waves by assuming a fixed value of the index κ_e and considering different values of the relative number density of the Kappa population, n_{ke}/n_e . The results obtained, both for large and for small values of κ_e , show that the spectra obtained for L and S waves are almost independent of the value of the number density of the Kappa population, as long as it is not zero. These results are not shown here for the sake of brevity, since the curves obtained for different values of n_{ke}/n_e are basically the same as the curves shown in Fig. 1, for each value of κ_e . The important point to be emphasized is that the presence of a small population of electrons described by a Kappa population is sufficient to significantly affect the equilibrium spectrum of L waves in the region of small wave numbers, leading to the formation of the peaked feature at $q \simeq 0$.

Figure 2 displays the asymptotic spectrum of T waves, obtained using Eq. (31). Figure 2(a) shows \mathcal{E}_q^T/g as a function of normalized wavenumber, for $n_{ke}/n_e = 0.1$, and several values of κ_e , and also present a curve obtained considering a purely Maxwellian electron distribution, obtained with $n_{ke}/n_e = 0$. The conditions and parameters are the same as those used to obtain the spectrum of L waves in Fig. 1. Let us first comment on the result obtained considering $n_{ke}/n_e = 0$, given by the red line in Fig. 2(a). This result is explained by the analysis of Eq. (31), which shows that the spectrum of T waves is proportional to the spectrum of L waves, given by Eq. (21), evaluated at $q = q_m$. If the Kappa population is vanishing, $n_{ke}/n_e = 0$, the Kappa contributions vanishes in Eq. (21), and the contributions due to the Maxwellian population in the numerator and in the denominator cancel out, and the spectrum turns out to be given by

$$\mathcal{E}_q^{T,0} \simeq 2 \frac{g}{2(z_{q_m}^L)^2} = \frac{g}{2 + 3q_m^2}.$$

At $q = 0$, the amplitude of the spectrum of T waves in the case of Maxwellian electron distribution is therefore twice the magnitude of the spectrum of L waves, but decays faster for larger values of q , since $q_m \gg q$. With the presence of a population described by a Kappa distribution, Fig. 2(a) shows that the spectrum of T waves is modified in the region of small wave numbers, in comparison with the spectrum obtained in the Maxwellian case. In the scale of the figure, the modification is noticeable for normalized wavenumber $q < 0.1$, with a difference that increases with the decrease in



the κ_e index, i.e., increases with the increase in the non-thermal character of the electron distribution. The spectrum features divergent behavior for $q \rightarrow 0$, as already noticed for the L waves in Fig. 1.

Figure 2(b) shows an expanded view of the region of small values of q , for the conditions that have been discussed in Fig. 2(a). The expanded view clearly shows the increase in the magnitude of the T wave spectrum at small values of q . For instance, it is seen that for $q \simeq 0.02$, the intensity of the spectrum of T waves in the case of $\kappa_e = 2.5$ is about one order of magnitude above the intensity displayed in the case of $\kappa_e = 40$.

We have also investigated the dependence of the T spectrum on the relative number density n_{ke}/n_e , for a fixed value of κ_e . The results obtained have shown that the T wave spectrum obtained in the presence of a Kappa distribution is almost independent of the number density of the Kappa population. The only noticeable feature in the spectra is the presence of the peak around $q = 0$, which occurs for any finite value of n_{ke}/n_e , and vanishes in the purely Maxwellian case ($n_{ke}/n_e = 0$).

In addition to these results concerning the initial spectra of electrostatic waves and the asymptotic spectrum of transverse waves, we also present some results which show the time evolution of the wave-particle system, comparing a situation in which the background electron velocity distribution is a Maxwellian distribution with a situation in which an “halo” population described by an isotropic Kappa distribution is also present.

For the study of the time evolution of the system, we utilize the set of weak turbulence equations, with some additional approximations. Regarding the plasma particles, we assume that the ion velocity distribution remains constant along the evolution and that in the case of the equation for the electron distribution, the quasilinear diffusion due to S waves can be neglected in comparison with the diffusion caused by the L waves. Regarding the waves, we describe the evolution of the L waves by including the spontaneous and induced emission processes, the three-wave decay processes involving L and S waves, and the scattering process involving two L waves and the particles. Nonlinear interaction involving T waves are neglected in the equation for the time evolution of the L waves, for simplicity, which is common practice in the literature. The evolution of S waves is described in the present analysis by taking into account the emission terms and the three-wave decay term involving L

FIG. 2. Asymptotic spectrum of T waves, \mathcal{E}_q^T , characterizing a state of “turbulent equilibrium,” vs normalized wavenumber q . (a) \mathcal{E}_q^T for $n_{ke}/n_e = 0.1$, and several values of κ_e . The case of Maxwellian distribution, $n_{ke}/n_e = 0.0$, is also shown for reference; (b) expanded view of the region of small values of q in Fig. 3(a). Other parameters and conditions are as in Fig. 1.

and S waves, and neglecting the effect of the decay term involving S , L , and T waves, and also the scattering term. In the equation for the T waves, however, which contains only nonlinear effects, we keep all the terms that have already been described in Sec. I, namely, the decay involving a T wave and two L waves, the decay involving a T wave, a L wave, and a S wave, the decay involving two T waves and a L wave, and the scattering term.

We utilize a two-dimensional approximation (2D), considering a grid of 51×101 points in (u_{\perp}, u_z) space, with $0 \leq u_{\perp} \leq 12$ and $-12 \leq u_z \leq 12$, a grid of 51×51 points in (q_{\perp}, q_z) space for L and S waves, and a grid of 71×71 points in (q_{\perp}, q_z) space for the T waves, which develop fine features that require a better resolution than the L and S waves, considering the evolution in the interval $0 \leq q_{\perp} \leq 0.6$ and $0 \leq q_z \leq 0.6$ for all waves. The normalized time step has been adopted as $\Delta\tau = 0.1$, and the equations were solved using a fourth-order Runge-Kutta procedure for the wave equations and the splitting method for the equation describing the time evolution of the electrons.

As starting conditions, we assume that the background electron population is described by distribution function (2), with the 2D versions of Eqs. (3) and (4), with the Kappa distribution defined using $\alpha = 1$ and $u_{e,\kappa}^2 = u_e^2(\kappa_e - 1)/\kappa_e$, which is the proper value of $u_{e,\kappa}^2$ for 2D distributions. We assume that the ion distribution is described by an isotropic Maxwellian distribution, with $T_e/T_i = 2$. We also assume that the plasma parameter is $(n\lambda_D^3)^{-1} = 5.0 \times 10^{-3}$, and $v_e^2/c^2 = 4.0 \times 10^{-3}$, values that have already been used in the analyses of the plasma emission without taking into account the presence of a Kappa distribution.^{36,38}

A further approximation is made for the numerical analysis, regarding the initial wave spectra. As already discussed in the initial paragraphs of this section on numerical results [see Eq. (32) and the accompanying comments], in the presence of a Kappa distribution, the initial spectrum of L diverges for $q \rightarrow 0$. This divergence, although consistent with the non-relativistic approach, is not appropriate for the numerical analysis. In our numerical implementation of the formalism, the initial spectrum of L waves is given by Eq. (21) down to the value of q such the resonant velocity becomes equal to c , i.e., the value of q for which $z_q^L/q = c/v_e$. It is assumed that for values of q smaller than this value, the initial L wave spectrum is given by the same value obtained at the limit value of the resonant q . With such approximation, when a Kappa distribution is assumed to be present, the initial spectrum of L has significant growth in

the region of small values of q , in comparison with the spectrum in the case of a Maxwellian plasma background, but the divergence is avoided. The initial spectrum of L waves is therefore given by Eq. (21), with an approximation in the region of small values of q , and the spectrum of S is given by Eq. (25). The T waves are assumed not present at initial time.

Figure 3 shows one dimensional (1D) representations of the spectrum of T waves, i.e., obtained after integration of \mathcal{E}_q^T along the perpendicular component of normalized wavenumber, q_{\perp} . The spectra are shown for different values of τ and show the evolution of the T wave spectrum. Figure 3(a) displays the wave spectra obtained in the case of purely Maxwellian electron distribution, i.e., $n_{ke}/n_e = 0.0$. Figure 3(b) depicts the wave spectra obtained when the electron distribution contains a Kappa population, with $n_{ke}/n_e = 5.0 \times 10^{-2}$, and $\kappa_e = 5.0$. In panel (a), it is seen that the amplitude of the waves increases for all values of q_z and gradually evolves toward the asymptotic solution described by Eq. (31) in the case of $n_{ke} = 0.0$, and which appears as the red lines in Fig. 2. The situation depicted in Fig. 3(a) corresponds to the initial stages of the evolution, which is displayed up to a longer time in Fig. 2 of Ref. 36. In the presence of a small Kappa population, the spectrum of T waves evolves as shown in Fig. 3(b). The spectrum grows for all values of q_z , much as seen in Fig. 3(a), but there is a difference. A peak is seen to appear near $q_z = 0$ and grows in time. What is seen in Fig. 3(b) are some steps in the time evolution of the spectrum that is asymptotically given by Eq. (31), and represented in Fig. 2. It must be noticed that the peak near $q_z = 0$ in Fig. 3(b) has a finite height. It does not diverge as the peaks appearing in 2, because for the numerical analysis of the equation which describes the time evolution, we have assumed that the L wave spectrum saturates for sufficiently small value of q , instead of growing infinitely for $q \rightarrow 0$.

The growth of the peak near $q = 0$ in the T wave spectrum can be explained as follows. The dominant process for the formation of background spectrum of T is the scattering involving L waves. The scattering effect is maximum for wavelengths which satisfy $z_q^T = z_{q'}^L$, which means $q' = q_m$, where q_m is defined by Eq. (31). As seen in Fig. 1(a), in the case of a small population described by a Kappa distribution, the spectrum of L waves is above the spectra obtained in the purely Maxwellian case for $q' \leq 0.2$. The scattering process is therefore most effective to generate T waves with $q \leq 0.02$, for the value of v_e/c which we have assumed. The

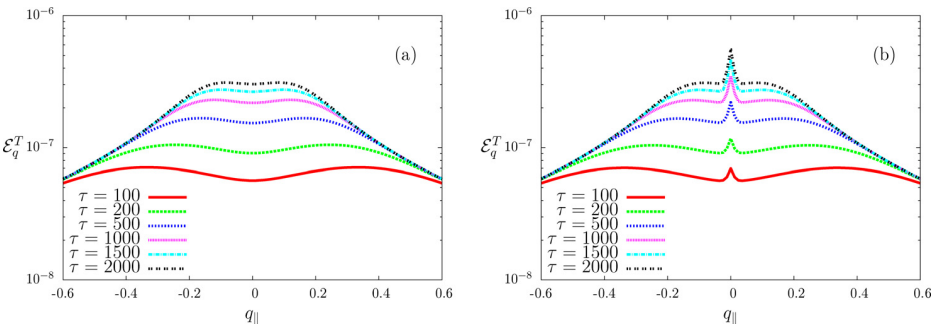


FIG. 3. (a) 1D spectrum of T waves vs. q_{\parallel} , for several values of τ , for $n_{ke}/n_e = 0.0$; (b) 1D spectrum of T waves vs. q_{\parallel} , for several values of τ , for $n_{ke}/n_e = 5.0 \times 10^{-2}$ and $\kappa_e = 5.0$. Other parameters and conditions are as in Fig. 1.

scattering of L waves is mainly responsible for the formation of the spectrum of T waves, and the peak for large wavelengths, which is seen in the L wave spectrum that occurs in the presence of Kappa distributed electrons, is the cause for the growth of the peak for large wavelengths in the T wave spectrum.

In what follows, we investigate the time evolution of the beam-plasma instability, comparing the situation in which the background electron distribution is purely Maxwellian with a case in which there is also a “halo” population described by a Kappa distribution. We assume a beam population described by a displaced Maxwellian distribution, with a normalized beam velocity $u_b = 6.0$, number density given by $n_b/n_e = 1.0 \times 10^{-3}$, and temperature $T_b = T_e$. Figure 4 shows 2D plots of the electron velocity distribution. Due to the presence of the beam, the background electron distribution is slightly displaced in velocity space so that the average velocity of the complete electron velocity distribution is zero.

Figure 4 shows 2D plots of the electron velocity distribution, the spectrum of L waves, and the spectrum of T waves, at $\tau = 500$. The spectrum of S waves remains very similar to the initial shape and is not shown. The three panels

at the left column were obtained considering that the background electron distribution is a Maxwellian distribution, i.e., considering $n_{ke}/n_e = 0.0$, and the panels at the right column were obtained assuming $n_{ke}/n_e = 0.05$, with $\kappa_e = 5.0$. For the parameters chosen, at such a point in the time evolution, the quasilinear process has already transferred a significant part of the energy available in the beam to the waves, creating a peak in the spectrum of L waves. The nonlinear processes are already operative, creating a ring-like structure in the spectrum of L waves, creating a spectrum of T waves over the whole grid of q values, and creating some peaked features for the T waves, in the region of small values of q . The situations depicted in Figs. 4(a), 4(c), and 4(e) correspond to those appearing in Figs. 1(b), 2(b), and 4(b) of Ref. 39, which is dedicated to the study of emission by nonlinear processes in a plasma with Maxwellian background distributions. It can be noticed in Figs. 4(a) and 4(b) that the region between the core of the velocity distribution and the peak of the beam distribution is already quite flattened, corresponding to the formation of the peak in the L spectrum which is centered at $(q_\perp, q_z) \simeq (0, 0.2)$ in Figs. 4(c) and 4(d).

The results appearing in Fig. 4 can be considered as representative of the time evolution of the wave-particle system.

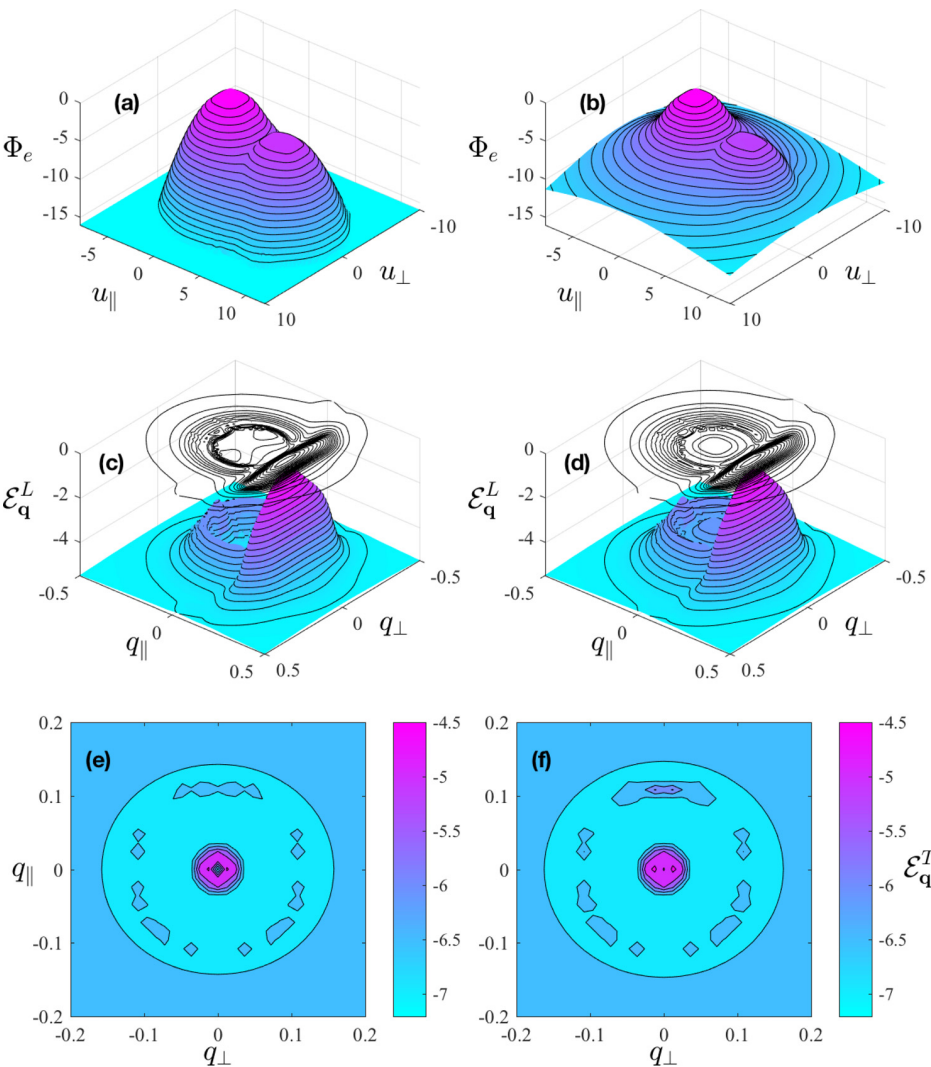


FIG. 4. (a) Electron distribution function at $\tau = 500$, vs. u_\parallel and u_\perp , for $n_{ke}/n_e = 0.0$; (b) electron distribution function at $\tau = 500$, vs. u_\parallel and u_\perp , for $n_{ke}/n_e = 5.0 \times 10^{-2}$; (c) spectrum of L waves at $\tau = 500$, vs. q_\parallel and q_\perp , for $n_{ke}/n_e = 0.0$; (d) spectrum of L waves at $\tau = 500$, vs. q_\parallel and q_\perp , for $n_{ke}/n_e = 5.0 \times 10^{-2}$; (e) spectrum of T waves at $\tau = 500$, vs. q_\parallel and q_\perp , for $n_{ke}/n_e = 0.0$; and (f) spectrum of T waves at $\tau = 500$, vs. q_\parallel and q_\perp , for $n_{ke}/n_e = 5.0 \times 10^{-2}$. Input parameters are as follows: $T_e/T_i = 2.0$, $T_b/T_e = 1.0$, $n_b/n_e = 1.0 \times 10^{-3}$, $v_b/v_e = 6.0$, $g = 5.0 \times 10^{-3}$, and $\kappa_e = 5.0$.

For further analysis of the time evolution, we show in Fig. 5 1D representations of the electron distribution and of the wave spectra, obtained after the integration of the 2D quantities, along u_{\perp} in the case of the velocity distribution and along q_{\perp} in the case of the wave spectra. As in Fig. 4, the left column displays the results obtained assuming $n_{ke}/n_e = 0.0$, and the right column shows the results obtained assuming $n_{ke}/n_e = 0.05$, with $\kappa_e = 5.0$. The electron distribution function in each case is shown in Figs. 5(a) and 5(b), respectively, for several values of τ , between $\tau = 100$ and $\tau = 2000$. In both panels, the gradual flattening of the peak of the beam distribution and the formation of a *plateau* in the region of velocities between the beam and the core distribution can be noticed. In Fig. 5(a), the appearance of a small population of backscattered electrons is also noticed, which

start to become distinguishable at $\tau \simeq 1000$. In panel 5(b), these backscattered electrons are not noticeable in the scale of the figure, because the Kappa distribution already had a sizeable population at that region of velocity space.

Figures 5(c) and 5(d) show a 1D projection of the L wave spectrum. In panel (c), one notices that at $\tau = 100$, the only distinctive feature in the spectrum is the primary peak generated at $q_z \simeq 0.2$, at the spectral region where the waves are in resonance with electrons in the region of positive velocity in the velocity distribution. At $\tau = 200$, there is already a hint of a backward peak, at $q_z \simeq -0.2$. At $\tau = 500$, and beyond that, the backward peak appears well developed, and there is a profile in the wave spectrum, continuous between the forward peak and the backward peak. This is only a 1D projection of the ring formed by scattering and

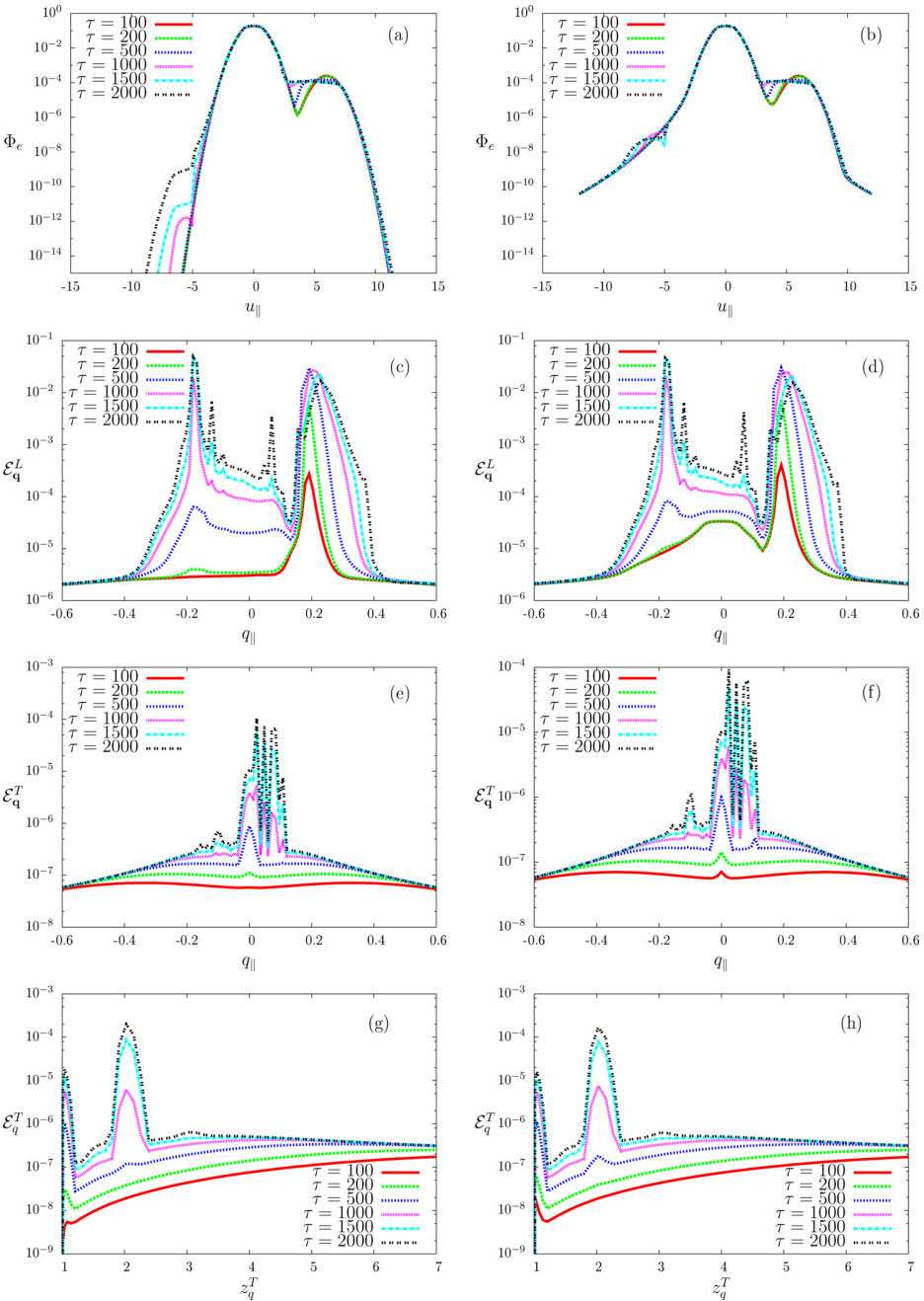


FIG. 5. (a) 1D electron distribution function vs. u_{\parallel} , for several values of τ , for $n_{ke}/n_e = 0.0$; (b) 1D electron distribution function vs. u_{\parallel} , for several values of $\tau = 500$, for $n_{ke}/n_e = 5.0 \times 10^{-2}$; (c) 1D spectrum of L waves vs. q_{\parallel} , for several values of τ , for $n_{ke}/n_e = 0.0$; (d) 1D spectrum of L waves vs. q_{\parallel} , for several values of τ , for $n_{ke}/n_e = 5.0 \times 10^{-2}$; (e) 1D spectrum of T waves vs. q_{\parallel} , for several values of τ , for $n_{ke}/n_e = 0.0$; (f) 1D spectrum of T waves vs. q_{\parallel} , for several values of τ , for $n_{ke}/n_e = 5.0 \times 10^{-2}$; (g) Spectrum of T waves vs. q , for several values of τ , for $n_{ke}/n_e = 0.0$; (h) Spectrum of T waves vs. q , for several values of τ , for $n_{ke}/n_e = 5.0 \times 10^{-2}$. The parameters are the same as those used in Fig. 4.

decay, which is seen in the 2D representation appearing in Fig. 4(c). On the other hand, when the electron distribution function features the presence of a Kappa distribution, the L wave spectrum at $\tau = 100$ features the peak generated by quasilinear effect at $q_z \simeq 0.2$, and also the peak around $q = 0$, characteristic of the spectrum at equilibrium in the presence of a Kappa distribution. Due to the approximation that we have adopted, of a limiting resonant velocity, the spectrum at $q = 0$ is finite instead of divergent. The 1D projection at Fig. 5(d) shows at $\tau = 200$, there is already a hint of the backward peak. At $\tau = 500$, and beyond, the 1D spectrum of Fig. 5(d) becomes similar to that appearing in Fig. 5(c), but this is only the effect of the 1D projection. The actual spectrum in the case of Fig. 5(d) is constituted by the primary and the back-scattered peaks, by the peak around $q = 0$, and by the ring structure formed by nonlinear effects, as shown in Fig. 4(d).

The 1D projection of the spectrum of T waves appears depicted in Figs. 5(e) and 5(f), for several values of τ . In both panels, the sequence of lines show initially the formation of a background spectrum of T waves, added of the growth of a wave peak around $q_z = 0$. Between $\tau = 500$ and $\tau = 1000$, other peaked structures appear in the 1D representations of Figs. 5(e) and 5(f), which are the projections of the narrow ring structure shown in Figs. 4(e) and 4(f). The 1D representations in Fig. 5, as well as the 2D representations in Fig. 4, show that the T wave spectrum obtained in the case of Maxwellian electron distribution is very similar to the T wave spectrum obtained in the case of the presence of a “halo” described by a Kappa distribution. The only noticeable difference is that the peaks appearing in the T wave spectrum are slightly higher in the case of $n_{ke} \neq 0$, panel (e), than in the case of $n_{ke} = 0$, panel (f), for the same value of τ .

Another representation of the T wave spectrum appears in Figs. 5(g) and 5(h), which display the spectrum of T waves after integration along the pitch angle. That is, Figs. 5(g) and 5(h) show the quantity

$$\mathcal{E}_q = \int_0^{2\pi} d\theta q \mathcal{E}_q^T$$

as a function of the normalized wave frequency. This representation clearly shows the early formation of the T wave background, then the onset of the primary peak of fundamental emission, with the frequency equal to the electron plasma frequency, and later on the onset of harmonic emission, with the peak of emission at $2\omega_{pe}$ clearly emerging between $\tau = 500$ and $\tau = 1000$. The comparison between Figs. 5(h) and 5(g) show that the curves obtained in both cases are qualitatively the same, with the sole difference that the peaks are slightly higher in the case of $n_{ke} \neq 0$, shown in Fig. 5(h).

VI. FINAL REMARKS

In the present paper, we have discussed the spectra of electrostatic and electromagnetic waves, which may be present at quiescent situation in plasmas whose particles have velocity distribution functions which are a combination of a thermal background and an energetic “halo” distribution.

The motivation for the study has been the abundance of measurements made in the solar wind environment, by satellites at different orbits, which show the occurrence of particle distribution functions with these characteristics. For the analysis presented in the paper, the electron velocity distribution has been represented as a summation of a Maxwellian distribution function and an isotropic Kappa distribution, with the fraction of population having the Kappa populations assumed as a free parameter.

The investigation has been conducted using the theoretical framework of weak turbulence theory. We have briefly discussed basic features of the equations of weak turbulence theory, and we have initially used these equations to obtain expressions for the spectra of electrostatic waves, obtained as the outcome of the balance between spontaneous fluctuations and induced emission. These equilibrium spectra, for high frequency Langmuir waves (L) and for low frequency ion-acoustic waves (S), have been routinely discussed in the literature for the case of Maxwellian plasmas, but this paper presents as a novel feature a description of the effects of the presence of a population of particles described by a Kappa velocity distribution. Theoretical expressions for the spectra of L and S waves have been obtained considering that both ions and electrons can be described by a combination of Maxwellian and Kappa distribution. Some numerical results have also been presented, considering the case of Maxwellian distribution for the ions and the combined distribution for electrons, and considering different values of the κ_e index. These results show that the effect of the presence of the Kappa distribution is noticeable in the spectrum of L waves in the region of large wavelengths, with difference relative to the spectrum obtained in the case of purely Maxwellian distribution which increases for decreasing values of the index κ_e in the energetic population. The distinctive feature, which exists even for very tenuous Kappa population, is the presence of a peak of wave intensity for very large wavelengths (wavenumber $k \rightarrow 0$).

We have also discussed the characteristics of the spectrum of electromagnetic waves (T), which is presented in the plasma as the outcome of nonlinear processes involving L and S waves, and particles. These spectra can be characterized as a state of “turbulent equilibrium.” The turbulent equilibrium spectra have already been discussed for the case of Maxwellian velocity distributions, and the present paper extends the discussion for the case in which an energetic “halo” described as a Kappa distribution is also present in the plasma. The results obtained show that the spectrum of T waves has the general features similar to those obtained in the case of Maxwellian distributions, with the effect of the presence of the Kappa population appearing as a peak of T waves in the large wavelength region, much narrower than the peak obtained in the spectrum of the L waves.

In addition to the results concerning the equilibrium spectra, we have also presented some results, which show the time evolution of the spectra of L and T waves, and the time evolution of the electron distribution function, as a result of the presence of a tenuous electron beam travelling in the plasma. We have followed the time evolution of the wave-particle system up to the formation of the *plateau* in

the electron distribution function, which indicates the saturation of the induced processes described by quasilinear theory. The results shown in the paper compared with the results obtained in the case in which the background electron population is described by a Maxwellian distribution, with the results obtained in the case of a background distribution described as a core population with Maxwellian distribution and a tenuous population with isotropic Kappa distribution. It is shown that the time evolution of the spectrum of L waves obtained in the presence of the “halo” distribution is qualitatively very similar to the spectrum obtained in the case of thermal background distribution, except for the occurrence of the enhanced wave intensity for $k \rightarrow 0$, characteristic of the presence of a Kappa population of particles. The spectra obtained for the T waves along the time evolution, in the two situations which have been considered, are also qualitatively very similar, with the difference that the peak corresponding to the harmonic emission is slightly more pronounced in the presence of a tenuous Kappa distribution, in comparison with harmonic emission obtained in the case of Maxwellian background population.

ACKNOWLEDGMENTS

S.F.T. and L.T.P. acknowledge Ph.D. fellowships from CNPq (Brazil). L.F.Z. acknowledges the support from CNPq (Brazil), Grant No. 304363/2014-6. R.G. acknowledges the support from CNPq (Brazil), Grant Nos. 478728/2012-3 and 307626/2015-6. P.H.Y. acknowledges NSF Grant No. AGS1550566 to the University of Maryland, the BK21 plus program from the National Research Foundation (NRF), Korea, to Kyung Hee University, and the Science Award Grant from the GFT, Inc., to the University of Maryland.

- ¹W. C. Feldman, J. R. Asbridge, S. J. Bame, M. D. Montgomery, and S. P. Gary, *J. Geophys. Res.* **80**, 4181, <https://doi.org/10.1029/JA080i031p04181> (1975).
- ²W. G. Philipp, H. Miggenrieder, M. D. Montgomery, K.-H. Mühlhäuser, H. Rosenbauer, and R. Schwenn, *J. Geophys. Res.* **92**, 1075, <https://doi.org/10.1029/JA092iA02p01075> (1987).
- ³R. P. Lin, K. A. Anderson, S. Ashford, C. Carlson, D. Curtis, R. Ergun, D. Larson, J. McFadden, M. McCarthy, G. K. Parks, H. Réme, J. M. Bosqued, J. Coutelier, F. Cotin, C. D'Uston, K.-P. Wenzel, T. R. Sanderson, J. Henrion, J. C. Ronnet, and G. Paschmann, *Space Sci. Rev.* **71**, 125 (1995).
- ⁴E. C. Stone, A. C. Cummings, and F. B. McDonald, *Nature* **454**, 71 (2008).
- ⁵S. Krucker and M. Battaglia, *Astrophys. J.* **780**, 107 (2014).
- ⁶M. Oka, S. Krucker, H. S. Hudson, and P. Saint-Hilaire, *Astrophys. J.* **799**, 129 (2015).

- ⁷L. Wang, R. P. Lin, C. Salem, M. Pulupa, D. E. Larson, P. H. Yoon, and J. G. Luhmann, *Astrophys. J. Lett.* **753**, L23 (2012).
- ⁸V. M. Vasiliunas, *J. Geophys. Res.* **73**, 2839, <https://doi.org/10.1029/JA073i009p02839> (1968).
- ⁹D. Summers and R. M. Thorne, *Phys. Fluids B* **3**, 1835 (1991).
- ¹⁰R. L. Mace and M. A. Hellberg, *Phys. Plasmas* **2**, 2098 (1995).
- ¹¹M. P. Leubner and N. Schupfer, *J. Geophys. Res.* **105**, 27387, <https://doi.org/10.1029/1999JA000447> (2000).
- ¹²M. P. Leubner and N. Schupfer, *J. Geophys. Res.* **106**, 12993, <https://doi.org/10.1029/2000JA000425> (2001).
- ¹³M. P. Leubner, *Astrophys. Space Sci.* **282**, 573 (2002).
- ¹⁴M. P. Leubner, *Astrophys. J.* **604**, 469 (2004).
- ¹⁵S. Kim, P. H. Yoon, G. S. Choe, and L. Wang, *Astrophys. J.* **806**, 32 (2015).
- ¹⁶D. J. McComas, H. A. Elliott, N. A. Schwadron, J. T. Gosling, R. M. Skoug, and B. E. Goldstein, *Geophys. Res. Lett.* **30**, 24, <https://doi.org/10.1029/2003GL017136> (2003).
- ¹⁷M. Maksimovic, I. Zouganelis, J.-Y. Chaufrey, K. Issautier, E. E. Scime, J. E. Littleton, E. Marsch, D. J. McComas, C. Salem, R. P. Lin, and H. Elliott, *J. Geophys. Res.* **110**, A09104, <https://doi.org/10.1029/2005JA011119> (2005).
- ¹⁸C. Vocks and G. Mann, *Astrophys. J.* **593**, 1134 (2003).
- ¹⁹E. G. Livadiotis, *Kappa Distributions* (Elsevier, Amsterdam, 2017).
- ²⁰R. Treumann, *Geophys. Res. Lett.* **24**, 1727, <https://doi.org/10.1029/97GL01760> (1997).
- ²¹M. A. Hellberg, R. L. Mace, T. K. Baluku, I. Kourakis, and N. S. Saini, *Phys. Plasmas* **16**, 094701 (2009).
- ²²M. Hapgood, C. Perry, J. Davies, and M. Denton, *Planet. Space Sci.* **59**, 618 (2011).
- ²³G. Livadiotis and D. J. McComas, *Space Sci. Rev.* **175**, 183 (2013).
- ²⁴G. Livadiotis, *J. Geophys. Res.* **120**, 1607, <https://doi.org/10.1002/2014JA020825> (2015).
- ²⁵M. Lazar, H. Fichtner, and P. H. Yoon, *Astron. Astrophys.* **589**, A39 (2016).
- ²⁶A. Hasegawa, K. Mima, and M. Duongvan, *Phys. Rev. Lett.* **54**, 2608 (1985).
- ²⁷P. H. Yoon, *Phys. Plasmas* **19**, 052301 (2012).
- ²⁸P. H. Yoon, *J. Geophys. Res.* **119**, 7074, <https://doi.org/10.1002/2014JA020353> (2014).
- ²⁹S. Kim, P. H. Yoon, G. S. Choe, and Y. J. Moon, *Astrophys. J.* **828**, 60 (2016).
- ³⁰P. H. Yoon, L. F. Ziebell, R. Gaelzer, and J. Pavan, *Phys. Plasmas* **19**, 102303 (2012).
- ³¹C. Tsallis, *J. Stat. Phys.* **52**, 479 (1988).
- ³²R. Silva, A. R. Plastino, and J. A. S. Lima, *Phys. Lett. A* **249**, 401 (1998).
- ³³C. Tsallis, R. S. Mendes, and A. R. Plastino, *Physica A* **261**, 534 (1998).
- ³⁴G. Livadiotis and D. J. McComas, *J. Geophys. Res.* **114**, A11105, <https://doi.org/10.1029/2009JA014352> (2009).
- ³⁵L. F. Ziebell, P. H. Yoon, F. J. R. Simões, Jr., R. Gaelzer, and J. Pavan, *Phys. Plasmas* **21**, 010701 (2014).
- ³⁶L. F. Ziebell, P. H. Yoon, R. Gaelzer, and J. Pavan, *Phys. Plasmas* **21**, 012306 (2014).
- ³⁷J. A. Newbury, C. T. Russell, J. L. Phillips, and S. P. Gary, *J. Geophys. Res.: Space Phys.* **103**, 9553, <https://doi.org/10.1029/98JA00067> (1998).
- ³⁸L. F. Ziebell, P. H. Yoon, R. Gaelzer, and J. Pavan, *Astrophys. J. Lett.* **795**, L32 (2014).
- ³⁹L. F. Ziebell, P. H. Yoon, L. T. Petruzzellis, R. Gaelzer, and J. Pavan, *Astrophys. J.* **806**, 237 (2015).

Appendix D

Two-dimensional time evolution of beam-plasma instability in the presence of binary collisions

The paper included in this appendix is the complete text of Ref. [45], which summarizes the outcomes of the Master's dissertation [81] that led to the current doctoral research. This text was included here with the intention to give the reader a complete view of the work developed during my graduate studies.

Two-dimensional time evolution of beam-plasma instability in the presence of binary collisions

S. F. Tigik¹, L. F. Ziebell¹, P. H. Yoon^{2,3}, and E. P. Kontar⁴

¹ Instituto de Física, Universidade Federal do Rio Grande do Sul, 91501-970 Porto Alegre, RS, Brazil

² Institute for Physical Science & Technology, University of Maryland, College Park, MD 20742, USA

³ School of Space Research, Kyung Hee University, Yongin, 446-701 Gyeonggi, South Korea

⁴ School of Physics and Astronomy, University of Glasgow, Glasgow G12 8QQ, UK

Received 29 August 2015 / Accepted 21 November 2015

ABSTRACT

Energetic electrons produced during solar flares are known to be responsible for generating solar type III radio bursts. The radio emission is a byproduct of Langmuir wave generation via beam-plasma interaction and nonlinear wave-wave and wave-particle interaction processes. In addition to type III radio bursts, electrons traveling downwards toward the chromosphere lead to the hard X-ray emission via electron-ion collisions. Recently, the role of Langmuir waves on the X-ray-producing electrons has been identified as important, because Langmuir waves may alter the electron distribution, thereby affecting the X-ray profile. Both Coulomb collisions and wave-particle interactions lead electrons to scattering and energy exchange that necessitates considering the two-dimensional (2D) problem in velocity space. The present paper investigates the influence of binary collisions on the beam-plasma instability development in 2D in order to elucidate the nonlinear dynamics of Langmuir waves and binary collisions. The significance of the present findings in the context of solar physics is discussed.

Key words. Sun: radio radiation – Sun: particle emission – methods: numerical

1. Introduction

The beam-plasma interaction between the energetic electrons produced during the solar flare and the background coronal plasma is a source of rich nonlinear phenomena. A number of solar radio bursts are associated with non-thermal electron populations and associated Langmuir waves. One of the most important and well-studied phenomena is the generation of solar type-III solar radio bursts (Wild & McCready 1950; Wild 1950). Fast electrons escaping from active regions in the Sun to the corona and interplanetary space generate Langmuir turbulence, which partially converts to radiation at the local plasma frequency and/or its harmonic(s). A nonlinear conversion process involves sophisticated wave decay and wave scattering. This is the well-known plasma emission, and it is the basic radio emission mechanism for type III radio bursts and for the reverse slope bursts (see, e.g., Tang & Moore 1982; Dennis et al. 1984).

The first theory of plasma emission was put forth by Ginzburg & Zhelezniakov (1958) and many modifications and improvements have been made over the past six decades (Tsytovich 1967; Kaplan & Tsytovich 1968; Zheleznyakov & Zaitsev 1970; Melrose 1982; Goldman & Dubois 1982; Goldman 1983; Cairns 1987; Robinson & Cairns 1998; Mel'Nik et al. 1999; Kontar 2001; Ledenev et al. 2004; Li et al. 2005, 2006a,b, 2008a,b; Li & Cairns 2013; Ratcliffe & Kontar 2014). Although the essential theoretical framework based upon EM weak turbulence theory, which describes the entire process starting from the beam-generated Langmuir turbulence to the radiation generation, was available, complete numerical solution of

the entire set of EM weak turbulence equations have not been done until quite recently, when Ziebell et al. (2014a,b,c, 2015) numerically solved the complete equations of EM weak turbulence theory for the first time. It should be mentioned that a few authors carried out direct EM particle-in-cell (PIC) simulations to characterize the nonlinear behavior of the plasma emission process (Kasaba et al. 2001; Karlický & Vandas 2007; Rhee et al. 2009a,b; Umeda 2010; Ganse et al. 2012a,b, 2014). The full numerical solution of the analytical EM weak turbulence equations by Ziebell et al. (2014a, 2015) complements these PIC simulation efforts.

The type III radio bursts are not the only process of importance associated with solar flares. For electrons traveling down to the chromosphere, they generate X-rays via bremsstrahlung when they collide with plasma. The approximate treatment of the electron dynamics by only considering the Coulomb collisions is known as the thick target model (e.g., Holman et al. 2011, as a recent review). Under such a simplifying assumption, Brown (1971) and Syrovatskii & Shmeleva (1972) analyzed the dynamics of electron distribution and the related bremsstrahlung X-ray spectrum from accelerated/injected electrons. In the literature, however, there are discussions of the importance of Langmuir wave generation on the underlying non-thermal electron energy distribution. Emslie & Smith (1984) first considered the effects of wave generation on the electron beam propagation toward the chromosphere. Hamilton & Petrosian (1987) and McClements (1987, 1989) reconsidered the same problem but found that the influence of wave-particle interactions was insignificant for

stationary electron injection. However, recent works by [Hannah et al. \(2009, 2013\)](#) and [Karlický & Kontar \(2012\)](#) demonstrate that the collective effects are sufficiently significant after all, especially for transient sources of nonthermal electrons, such that without these effects, the solar hard X-ray spectra measured by RHESSI spacecraft may not be interpreted correctly. [Zharkova & Siversky \(2011\)](#) also studied a similar problem. Moreover, [Kontar et al. \(2012\)](#) have shown that the presence of plasma inhomogeneity and/or nonlinear wave-wave interactions can lead to an overestimated number and energy of energetic electrons accelerated in the corona even in the case of stationary electron injection.

As noted above, the problem of flare-generated nonthermal electrons and X-ray emission from the same source that also generates type III radio bursts is a complicated one, which requires simultaneous time-dependent treatment of various processes that include Coulomb collisions, collective Langmuir wave generation, and nonlinear wave-wave interactions. In addition, the evolution of electrons not only in energy but also in collisional pitch-angle scattering is important for interpreting some X-ray observations (e.g., [MacKinnon 1991](#); [Jeffrey et al. 2014](#)).

The purpose of the present paper is not to revisit the plasma emission, which has recently been discussed by [Ziebell et al. \(2014a, 2015\)](#) and by [Ratcliffe & Kontar \(2014\)](#) in application to flaring loops, or to address the issue of the influence of collective processes on the X-ray generation by bremsstrahlung per se, which was addressed by [Hannah et al. \(2009\)](#) and [Kontar et al. \(2012\)](#). Instead, we address a fundamental 2D plasma physics problem that may be related to both the type-III-generating electrons and the X-ray-generating non-thermal electrons. That is, we consider the influence of both Coulomb collisions and the collective effects in two-dimensional (2D) electron beam-plasma interaction problem, taking only the evolution of the particle distribution and of the spectra of electrostatic waves into account, without incorporating the effects associated to electromagnetic oscillations.

Unlike previous works related to this type of analysis where the effects of Coulomb collisions have normally been ignored ([Ziebell et al. 2008](#)), the present paper includes electron-electron and electron-ion collisions. On the other hand, unlike the previous works related to the solar X-ray problem where, in addition to collisional effects, quasilinear effects are included considering one-dimensional (1D) wave excitation, we now consider the nonlinear dynamics associated with the wave scattering and decay in two dimensions, along with the collisional dynamics. The 2D evolution is particularly important since collisional scattering and collisional energy loss operate on the same time scales. Moreover, radioemission and Langmuir wave evolution depend on angular distribution of plasma waves. The objective with such relatively limited analysis that only includes electrostatic waves is to gather information about the effect of collisions on the time evolution of the beam-plasma system, on the relative roles of collisions and nonlinear mechanisms of three-wave decay and wave-particle scattering, and on the possibly different time scales of the different physical processes when evolving self-consistently. The information to be obtained with such study may be useful for future analysis of the time evolution of more complex processes, in which other nonlinear mechanisms have to be taken into account, such as the actual production of fundamental and harmonic emission that characterize type III emissions and the complicated interaction between energetic electrons, background plasma, and waves, which is associated to the solar X-ray emission.

The structure of the paper is as follows. In Sect. 2 we briefly describe the theoretical formulation and the setup for the numerical analysis. In Sect. 3 we present and discuss the results of the numerical analysis. Finally, in Sect. 4 we conclude the paper and comment on the results obtained.

2. Theoretical formulation and numerical setup

The wave kinetic equations for L and S waves that describe quasilinear process as well as nonlinear decay and scattering processes are given in terms of the spectral wave energy density, $I_k^{\sigma L} = \langle E_L^{\sigma 2}(\mathbf{k}) \rangle$ and $I_k^{\sigma S} = \langle E_S^{\sigma 2}(\mathbf{k}) \rangle$, where $E_L^\sigma(\mathbf{k})$ and $E_S^\sigma(\mathbf{k})$ represent the spectral electric field component associated with L and S waves, respectively, and where $\sigma = \pm 1$ stands for the sign of wave phase velocity. The wave kinetic equations for these waves are given by [Yoon \(2006\)](#) and [Ziebell et al. \(2008\)](#):

$$\begin{aligned} \frac{\partial I_k^{\sigma L}}{\partial t} = & \frac{\pi \omega_p^2}{k^2} \int d\mathbf{v} \delta(\sigma \omega_k^L - \mathbf{k} \cdot \mathbf{v}) \left(\frac{n_0 e^2}{\pi} F_e(\mathbf{v}) \right. \\ & \left. + \sigma \omega_k^L I_k^{\sigma L} \mathbf{k} \cdot \frac{\partial F_e(\mathbf{v})}{\partial \mathbf{v}} \right) + \frac{\pi e^2}{2 T_e^2} \sum_{\sigma', \sigma'' = \pm 1} \sigma \omega_k^L \\ & \times \int d\mathbf{k}' \frac{\mu_{\mathbf{k}-\mathbf{k}'} (\mathbf{k} \cdot \mathbf{k}')^2}{k^2 k'^2 |\mathbf{k} - \mathbf{k}'|^2} \delta(\sigma \omega_k^L - \sigma' \omega_{\mathbf{k}'}^L - \sigma'' \omega_{\mathbf{k}-\mathbf{k}'}^S) \\ & \times \left[\sigma \omega_k^L I_{\mathbf{k}'}^{\sigma' L} \frac{I_{\mathbf{k}-\mathbf{k}'}^{\sigma'' S}}{\mu_{\mathbf{k}-\mathbf{k}'}} - \left(\sigma' \omega_{\mathbf{k}'}^L \frac{I_{\mathbf{k}-\mathbf{k}'}^{\sigma'' S}}{\mu_{\mathbf{k}-\mathbf{k}'}} + \sigma'' \omega_{\mathbf{k}-\mathbf{k}'}^L I_{\mathbf{k}'}^{\sigma' L} \right) I_k^{\sigma L} \right] \\ & - \frac{\pi e^2}{m_e^2 \omega_p^2} \sum_{\sigma' = \pm 1} \int d\mathbf{k}' \int d\mathbf{v} \frac{(\mathbf{k} \cdot \mathbf{k}')^2}{k^2 k'^2} \delta[\sigma \omega_k^L - \sigma' \omega_{\mathbf{k}'}^L \\ & - (\mathbf{k} - \mathbf{k}') \cdot \mathbf{v}] \times \left(\frac{\hat{n} e^2}{\pi \omega_{pe}^2} \sigma \omega_k^L (\sigma' \omega_{\mathbf{k}'}^L I_k^{\sigma L} - \sigma \omega_k^L I_{\mathbf{k}'}^{\sigma' L}) F_i \right. \\ & \left. - \frac{m_e}{m_i} \sigma \omega_k^L I_{\mathbf{k}'}^{\sigma' L} I_k^{\sigma L} (\mathbf{k} - \mathbf{k}') \cdot \frac{\partial F_i}{\partial \mathbf{v}} \right), \end{aligned} \quad (1)$$

$$\begin{aligned} \frac{\partial I_k^{\sigma S}}{\partial t} = & \frac{\pi \mu_k \omega_p^2}{k^2} \int d\mathbf{v} \delta(\sigma \omega_k^S - \mathbf{k} \cdot \mathbf{v}) \left[\frac{n_0 e^2}{\pi} (F_e + F_i) \right. \\ & \left. + \sigma \omega_k^L \frac{I_k^{\sigma S}}{\mu_k} \mathbf{k} \cdot \frac{\partial}{\partial \mathbf{v}} \left(F_e + \frac{m_e}{m_i} F_i \right) \right] + \frac{\pi e^2}{4 T_e^2} \sum_{\sigma', \sigma'' = \pm 1} \sigma \omega_k^L \\ & \times \int d\mathbf{k}' \frac{\mu_k [\mathbf{k}' \cdot (\mathbf{k} - \mathbf{k}')]}{k^2 k'^2 |\mathbf{k} - \mathbf{k}'|^2} \delta(\sigma \omega_k^S - \sigma' \omega_{\mathbf{k}'}^L - \sigma'' \omega_{\mathbf{k}-\mathbf{k}'}^L) \\ & \times \left[\sigma \omega_k^L I_{\mathbf{k}'}^{\sigma' L} I_{\mathbf{k}-\mathbf{k}'}^{\sigma'' L} - \left(\sigma' \omega_{\mathbf{k}'}^L I_{\mathbf{k}-\mathbf{k}'}^{\sigma'' L} + \sigma'' \omega_{\mathbf{k}-\mathbf{k}'}^L I_{\mathbf{k}'}^{\sigma' L} \right) \frac{I_k^{\sigma S}}{\mu_k} \right], \end{aligned} \quad (2)$$

where $\omega_p = (4\pi n_0 e^2/m_e)^{1/2}$ is the electron plasma frequency, and e , m_e , and n_0 stand for the unit electric charge, electron mass, and the ambient particle number density, respectively. The dispersion relations for L and S modes are well-known:

$$\begin{aligned} \omega_k^L &= \omega_p \left(1 + \frac{3}{2} k^2 \lambda_D^2 \right), \\ \omega_k^S &= \omega_p \frac{k \lambda_D}{(1 + k^2 \lambda_D^2)^{1/2}} \left(\frac{m_e}{m_i} \right)^{1/2} \left(1 + \frac{3 T_i}{T_e} \right)^{1/2}, \end{aligned}$$

where $v_e = (2 T_e / m_e)^{1/2}$ is the electron thermal speed, and $\lambda_D = v_e / (\sqrt{2} \omega_p)$ is the electron Debye length, with T_e being

the electron temperature. In (1) and (2) we have also introduced a quantity

$$\mu_k = |k|^3 \lambda_D^3 \left(\frac{m_e}{m_i} \right)^{1/2} \left(1 + \frac{3T_i}{T_e} \right)^{1/2}.$$

The first terms on the righthand sides of (1) and (2) describe the spontaneous emission and quasilinear effects. The second terms contain the energy conservation condition, $\delta(\sigma\omega_k^L - \sigma'\omega_{k'}^L - \sigma''\omega_{k-k'}^S)$, for L mode and a similar three-wave resonance condition for S mode, and describe the three-wave decay processes. The third term in (1) contains the nonlinear wave-particle resonance condition $\delta[\sigma\omega_k^L - \sigma'\omega_{k'}^L - (\mathbf{k} - \mathbf{k}') \cdot \mathbf{v}]$, and it depicts the scattering of L waves by the ions. We have neglected the scattering effects for (2), which rules the evolution of S waves, since the scattering processes involving S waves are extremely slow processes.

For the time evolution of the particle distribution, we consider the effects of spontaneous fluctuation, the quasilinear diffusion effect, and the effect of binary collisions. The particle kinetic equation is thus given by

$$\begin{aligned} \frac{\partial F_a(\mathbf{v})}{\partial t} &= \frac{\partial}{\partial v_i} \left(A_i(\mathbf{v}) F_a(\mathbf{v}) + D_{ij}(\mathbf{v}) \frac{\partial F_a(\mathbf{v})}{\partial v_j} \right) + \sum_b \theta_{ab}(F_a, F_b), \\ A_i(\mathbf{v}) &= \frac{e_a^2}{4\pi m_a} \int d\mathbf{k} \frac{k_i}{k^2} \sum_{\sigma=\pm 1} \sigma \omega_k^L \delta(\sigma \omega_k^\alpha - \mathbf{k} \cdot \mathbf{v}), \\ D_{ij}(\mathbf{v}) &= \frac{\pi e_a^2}{m_a^2} \int d\mathbf{k} \frac{k_i k_j}{k^2} \sum_{\sigma=\pm 1} \delta(\sigma \omega_k^\alpha - \mathbf{k} \cdot \mathbf{v}) I_k^{\sigma\alpha}, \\ \theta_{ab}(F_a, F_b) &= -\frac{2\pi n_{0a} n_{0b} e_a^2 e_b^2 \ln \Lambda}{m_a} \frac{\partial}{\partial v_i} \\ &\quad \times \int d\mathbf{v}' U_{ij} \left(\frac{F_a(\mathbf{v})}{m_b} \frac{\partial F_b(\mathbf{v}')}{\partial v'_j} - \frac{F_b(\mathbf{v}')}{m_a} \frac{\partial F_a(\mathbf{v})}{\partial v_j} \right), \\ U_{ij} &= \frac{w^2 \delta_{ij} - w_i w_j}{w^3}, \quad \mathbf{w} = \mathbf{v} - \mathbf{v}'. \end{aligned} \quad (3)$$

The term with coefficient A_i describes the effects of spontaneous fluctuations, and the term with coefficient D_{ij} rules the quasilinear diffusion process. The symbol α represents either L or S , depending on whether the particle species a in the above particle kinetic equations stands for $a = e$ (electrons) or $a = i$ (ions). The quantity $\theta_{ab}(F_a, F_b)$ represents the binary collisions of particles of species a with particles of species b . The quantity $\ln \Lambda$ is the Coulomb logarithm.

In the set of wave kinetic Eqs. (1) and (2), we do not (yet) include a collisional damping term. The collisional effect is only incorporated through the particle kinetic equation (3), which contains the collision operator $\sum_b \theta_{ab}(F_a, F_b)$. Upon linearization of the governing particle kinetic equation and coupling to the wave equation, then the collision frequency ν_{coll} broadens (Dupree 1966; Ishihara & Hirose 1985; Bian et al. 2014; Pécseli 2014) the wave-particle resonance conditions, $\omega - \mathbf{k} \cdot \mathbf{v}$, where ν_{coll} is the effective collision frequency that is obtained from the particle equation. In this way, the collisional damping rate for the collective wave phenomena is calculated by the particle collision term in an indirect way. However, a more complete treatment should contain explicit collisional damping term for the wave kinetic equation. In a recently submitted work, Yoon et al. (2015) address this issue by reformulating the standard weak turbulence theory to include contributions from those electrostatic fluctuation spectra (ω, k) for which ω and k do not satisfy the plasma

wave dispersion relations. They show that these so-called “non-eigenmode” contributions, which are typically ignored in the literature, are not only responsible for the same collision integral $\sum_b \theta_{ab}(F_a, F_b)$ in the particle kinetic equation, as in Eq. (3), but also they lead to the collisional damping term, as well as the electrostatic analog of the bremsstrahlung. One could, however, include the collisional damping term heuristically, as in the recent paper by Ratcliffe & Kontar (2014).

We introduce the following dimensionless variables and definitions:

$$\begin{aligned} z &\equiv \frac{\omega}{\omega_{pe}}, \quad \tau \equiv \omega_{pe} t, \quad \mathbf{q} \equiv \frac{kv_{te}}{\omega_{pe}}, \quad \mathbf{u} \equiv \frac{\mathbf{v}}{v_{te}}, \\ \mu_q^L &= 1, \quad \mu_q^T = 1, \quad \mu_q^S = \frac{q^3}{2^{3/2}} \sqrt{\frac{m_e}{m_i}} \left(1 + \frac{3T_i}{T_e} \right)^{1/2}, \\ \lambda_{De}^2 &= \frac{T_e}{4\pi \hat{n} e^2} = \frac{v_{te}^2}{2\omega_{pe}^2}, \quad g = \frac{1}{2^{3/2} (4\pi)^2 \hat{n} \lambda_{De}^3}, \\ F_a(\mathbf{u}) &= v_{te}^3 f_a(\mathbf{u}), \quad \mathcal{E}_q^{\sigma\alpha} = \frac{(2\pi)^2 g I_k^{\sigma\alpha}}{m_e v_{te}^2 \mu_k^\alpha}. \end{aligned}$$

In terms of the normalized variables and quantities, the equation for Langmuir (L) waves is expressed as

$$\begin{aligned} \frac{\partial \mathcal{E}_q^{\sigma L}}{\partial \tau} &= \left\{ \mu_q^L \frac{\pi}{q^2} \int d\mathbf{u} \delta(\sigma z_q^L - \mathbf{q} \cdot \mathbf{u}) \right. \\ &\quad \times \left. \left(g F_e(\mathbf{u}) + (\sigma z_q^L) \mathbf{q} \cdot \frac{\partial F_e(\mathbf{u})}{\partial \mathbf{u}} \mathcal{E}_q^{\sigma L} \right) \right\}_{Lql} \\ &\quad + \left\{ 2\sigma \mu_q^L z_q^L \sum_{\sigma', \sigma''} \int d\mathbf{q}' \frac{\mu_{q'}^L \mu_{q-q'}^S (\mathbf{q} \cdot \mathbf{q}')^2}{q^2 q'^2 |\mathbf{q} - \mathbf{q}'|^2} \left(\sigma z_q^L \mathcal{E}_{q'}^{\sigma' L} \mathcal{E}_{q-q'}^{\sigma'' S} \right. \right. \\ &\quad \left. \left. - \sigma' z_{q'}^L \mathcal{E}_{q-q'}^{\sigma'' S} \mathcal{E}_q^{\sigma L} - \sigma'' z_{q-q'}^L \mathcal{E}_{q'}^{\sigma' L} \mathcal{E}_q^{\sigma L} \right) \right\}_{LdLS} \\ &\quad \times \left. \delta \left(\sigma z_q^L - \sigma' z_{q'}^L - \sigma'' z_{q-q'}^S \right) \right\}_{LdLS} + \left\{ \sigma z_q^L \sum_{\sigma'} \int d\mathbf{q}' \right. \\ &\quad \times \left. \frac{\mu_q^L \mu_{q'}^L (\mathbf{q} \cdot \mathbf{q}')^2}{q^2 q'^2} \delta[\sigma z_q^L - \sigma' z_{q'}^L - (\mathbf{q} - \mathbf{q}') \cdot \mathbf{u}] \right. \\ &\quad \times \left. \left[g \left(\sigma z_q^L \mathcal{E}_{q'}^{\sigma' L} - \sigma' z_{q'}^L \mathcal{E}_k^{\sigma L} \right) [F_e(\mathbf{u}) + F_i(\mathbf{u})] \right. \right. \\ &\quad \left. \left. + \frac{m_e}{m_i} \mathcal{E}_{q'}^{\sigma' L} \mathcal{E}_q^{\sigma L} (\mathbf{q} - \mathbf{q}') \cdot \frac{\partial F_i(\mathbf{u})}{\partial \mathbf{u}} \right] \right\}_{LsLL}. \end{aligned} \quad (4)$$

The equation for ion-acoustic (S) waves is likewise expressed in terms of dimensionless quantities,

$$\begin{aligned} \frac{\partial \mathcal{E}_q^{\sigma S}}{\partial \tau} &= \left\{ \mu_q^S \frac{\pi}{q^2} \int d\mathbf{u} \delta(\sigma z_q^S - \mathbf{q} \cdot \mathbf{u}) \left[g [F_e(\mathbf{u}) + F_i(\mathbf{u})] \right. \right. \\ &\quad + \left. \left(\sigma z_q^L \left(\mathbf{q} \cdot \frac{\partial F_e(\mathbf{u})}{\partial \mathbf{u}} + \frac{m_e}{m_i} \mathbf{q} \cdot \frac{\partial F_i(\mathbf{u})}{\partial \mathbf{u}} \right) \mathcal{E}_q^{\sigma S} \right) \right\}_{S_{ql}} \\ &\quad + \left\{ \sigma z_q^L \sum_{\sigma', \sigma''} \int d\mathbf{q}' \frac{\mu_q^S \mu_{q'}^L \mu_{q-q'}^L [\mathbf{q}' \cdot (\mathbf{q} - \mathbf{q}')]^2}{q^2 q'^2 |\mathbf{q} - \mathbf{q}'|^2} \right. \\ &\quad \times \left. \left(\sigma z_q^L \mathcal{E}_{q'}^{\sigma' L} \mathcal{E}_{q-q'}^{\sigma'' L} - \sigma' z_{q'}^L \mathcal{E}_{q-q'}^{\sigma' L} \mathcal{E}_q^{\sigma S} - \sigma'' z_{q-q'}^L \mathcal{E}_{q'}^{\sigma' L} \mathcal{E}_q^{\sigma S} \right) \right. \\ &\quad \times \left. \left. \delta \left(\sigma z_q^S - \sigma' z_{q'}^L - \sigma'' z_{q-q'}^L \right) \right\}_{S_{dLL}}. \right. \end{aligned} \quad (5)$$

The dimensionless particle kinetic equation is given by

$$\begin{aligned} \frac{\partial F_a(\mathbf{u})}{\partial \tau} = & \frac{e_a^2 m_e^2}{e^2 m_a^2} \sum_{\sigma} \sum_{\alpha=L,S} \int d\mathbf{q} \left(\frac{\mathbf{q}}{q} \cdot \frac{\partial}{\partial \mathbf{u}} \right) \mu_q^\alpha \delta(\sigma z_q^\alpha - \mathbf{q} \cdot \mathbf{u}) \\ & \times \left(g \frac{m_a}{m_e} \frac{\sigma z_q^L}{q} F_a(\mathbf{v}) + \mathcal{E}_q^{\sigma\alpha} \frac{\mathbf{q}}{q} \cdot \frac{\partial F_a(\mathbf{u})}{\partial \mathbf{u}} \right) \\ & + \sum_b \theta_{ab}(F_a, F_b). \end{aligned} \quad (6)$$

Finally, the dispersion relations in dimensionless form are given by

$$\begin{aligned} z_q^L &= \left(1 + \frac{3}{2} q^2 \right)^{1/2}, \\ z_q^S &= \frac{q A}{(1 + q^2/2)^{1/2}}, \quad A = \frac{1}{\sqrt{2}} \left(\frac{m_e}{m_i} \right)^{1/2} \left(1 + 3 \frac{T_i}{T_e} \right)^{1/2}, \end{aligned}$$

where $v_{te} = (2T_e/m_e)^{1/2}$ is the electron thermal speed, and λ_{De} is the electron Debye length, with T_e being the electron temperature.

For further reference, in the equation for the L waves, Eq. (5), the term that describes the spontaneous emission and the quasilinear effects has been denoted Lql , the term that describes the three-wave decay involving L and S waves has been denoted $LdLS$, and the term describing scattering involving L waves has been denoted $LsLL$. In the equation for the evolution of S waves, namely Eq. (6), the first term describes the spontaneous emission and quasilinear effects and is denoted Sql , and the second term describes the three-wave decay involving L waves and is denoted $SdLL$.

In the equation for the particle distribution functions (7), the term with g describes the effects of spontaneous fluctuations, and the term with the velocity derivative describes the quasilinear diffusion process.

For a detailed derivation of the above equations without the term that represents the collisional effects, the reader is referred to Yoon (2000, 2005, 2006). The collisional term is essentially the Landau collision integral, which is well known in the literature (e.g., Lifshitz & Pitaevskii 1981; Karney 1986; Jeffrey et al. 2014, see also Appendix A). Assuming that both ion and electron background distributions are Maxwellian distributions, the kinetic equation describing the evolution of electron distribution function F_a in fully ionized hydrogen plasma can be written in spherical coordinates (v, θ) ,

$$\begin{aligned} \sum_b \theta_{ab}(F_a, F_b) = & \frac{\Gamma}{2v^2} \left\{ \frac{\partial}{\partial v} \left(2v G(u) \frac{\partial f}{\partial v} + 4u^2 G(u) f \right) \right. \\ & + \frac{1}{v} \frac{\partial}{\partial \mu} \left((1 - \mu^2) \left[\text{erf}(u) - G(u) \right] \frac{\partial f}{\partial \mu} \right) \Big\} \\ & + \frac{\Gamma}{2v^3} \frac{\partial}{\partial \mu} \left((1 - \mu^2) \frac{\partial f}{\partial \mu} \right), \end{aligned} \quad (7)$$

where, $\mu = v_{||}/v = \cos(\theta)$, $u = \sqrt{mv^2/2k_B T_e}$, $\Gamma = 4\pi n e^4 \ln \Lambda / m_e^2$, $\text{erf}(u)$ is the error function, and $G(u)$ is the Chandrasekhar function, given by

$$G(u) = \frac{\text{erf}(u) - u \text{erf}'(u)}{2u^2}. \quad (8)$$

The first term on the righthand side of Eq. (7) describes electron-electron collisions, while the second is due to electron scattering by ions. One can combine the collisional terms (Eq. (7)) with the collective terms (Eq. (6)) and define generalized friction and diffusion coefficients.

The initial electron distribution function is assumed to be made of a Maxwellian background and a forward beam distribution with number density n_f . In 2D, the assumed distribution function is given as

$$\begin{aligned} F_e(\mathbf{v}, 0) = & \frac{1 - n_f/n_0}{\pi v_{te}^2} \exp \left(-\frac{v_\perp^2}{v_{te}^2} - \frac{(v_{||} - v_0)^2}{v_{te}^2} \right) \\ & + \frac{n_f/n_0}{\pi v_{tf}^2} \exp \left(-\frac{v_\perp^2}{v_{tf}^2} - \frac{(v_{||} - v_f)^2}{v_{tf}^2} \right). \end{aligned} \quad (9)$$

Here $v_{te}^2 = 2T_e/m_e$ and $v_{tf}^2 = 2T_f/m_e$ are the background and the beam thermal velocities squared, respectively. The quantities v_0 and v_f are the drift velocities of the background and forward beam, respectively. The background drift velocity v_0 is such that it guarantees zero net drift velocity for the electron distribution, i.e., $v_0 = -(v_f n_f)/(n_0 - n_f)$. The initial ion distribution in 2D is given by $F_i(\mathbf{v}) = (m_i/2\pi T_i) \exp[-m_i v^2/(2T_i)]$, where T_i and m_i are the ion temperature and the proton mass, respectively. For the present study, we assume that the ion distribution remains constant along the time evolution.

The intensities of L and S waves are initialized by balancing the spontaneous and induced emissions, taking the background population into account:

$$\begin{aligned} I_k^{\sigma L}(0) = & \frac{T_e}{4\pi^2} \frac{1}{1 + 3k^2 \lambda_D^2}, \\ I_k^{\sigma S}(0) = & \frac{T_e}{4\pi^2} k^2 \lambda_D^2 \sqrt{\frac{1 + k^2 \lambda_D^2}{1 + 3k^2 \lambda_D^2}} \\ & \times \frac{\int d\mathbf{v} \delta(\sigma \omega_k^S - \mathbf{k} \cdot \mathbf{v}) (F_e + F_i)}{\int d\mathbf{v} \delta(\sigma \omega_k^S - \mathbf{k} \cdot \mathbf{v}) [F_e + (T_e/T_i) F_i]}. \end{aligned} \quad (10)$$

3. Numerical analysis

The set of Eqs. (4), (5), and (8)–(10) have been solved in 2D wave number space and 2D velocity space by employing a splitting method with fixed time step for the equation for evolution of the electron distribution and a fourth-order Runge-Kutta method for the wave equations. The 2D version for the particle equation is shown by Eq. (A.11), with the coefficients coming from weak turbulence theory as given by (A.12), and the collision term given by Eqs. (A.9) and (A.10). Similar equations for the wave evolution can be obtained by converting Eqs. (4) and (5) to 2D coordinates. For all the cases, we have used $\Delta\tau = 0.1$. We employed a 51×51 grid for k_\perp and $k_{||}$ with $0 < k_\perp v_{te}/\omega_p < 0.6$, and $0 < k_{||} v_{te}/\omega_p < 0.6$. For the velocities, we used a 51×101 grid for v_\perp/v_{te} and $v_{||}/v_{te}$, covering the velocity range $0 < v_\perp/v_{te} < 12$ and $-12 < v_{||}/v_{te} < 12$. For the subsequent numerical solutions to be discussed, we assume a forward beam with the same temperature as the background population, $T_f/T_e = 1.0$, electron-to-ion temperature ratio $T_e/T_i = 7.0$, plasma parameter $(n_0 \lambda_D^3)^{-1} = 5.0 \times 10^{-3}$, and

electron temperature, such that $v_{te}^2/c^2 = 4.0 \times 10^{-3}$. We also assume $v_f/v_{te} = 5.0$ and $n_f/n_0 = 1.0 \times 10^{-3}$, a value that is relatively high for the case of solar wind beam electrons, but has been assumed in order to reduce the computational time required to obtain the numerical results.

The characteristics of the grids used for the numerical analyses were also chosen as a compromise between the resolution obtained and the performance of the numerical code. The grid used in wave number space resolves some fundamental details in the wave spectra, such as (a) the primary peak that grows due to quasilinear interaction between L waves and the beam particles in the region of the positive derivative of the distribution function and (b) the peak corresponding to backwardly propagating L waves, which are generated by nonlinear interaction between L and S waves. In velocity space, the grid used allows for a smooth description of the distribution function and of the beam, including the important region of transition between the core distribution and the beam. Even with use of the chosen grids, the code needs to run for a few days in a personal computer with updated technology. Owing to the 2D nature of the problem investigated, a twofold increase in resolution would require nearly a fourfold increase in computational time. We have reached the conclusion that such a costly enhanced resolution would not be needed to describe the relevant features of the time evolution of the system under investigation.

As one application of the numerical code, we studied the time evolution of the system in two situations. The first situation neglects the influence of collisions, which can be easily done just by turning off the collisional term in the equation for the evolution of the electron distribution function. In the second situation, we took the effect of binary collisions into account. For comparison, we also added some results that show the time evolution of the distribution function that is only subject to collisions.

Figure 1 shows the time evolution of electron velocity distribution function by plotting F_e in 2D velocity space at different time steps corresponding to $\omega_{pe}t = 500, 1000, 2000, 5000, 10^4, 1.5 \times 10^4$, and 2×10^4 . The lefthand panels depict solutions with only collisions; the middle panels correspond to the self-consistent solution without collisional effects, as in the type III beam case (Ziebell et al. 2008); and the righthand panels show solutions that contain both collisional effects and self-consistent Langmuir wave dynamics. As the lefthand panels show, the collisional relaxation of the beam leads to the systematic energy losses and isotropization of the beam. Eventually, the beam merges with the Maxwellian background. In contrast, collisionless quasilinear relaxation, appearing in the middle panels, shows that slowing down the beam proceeds via the velocity space plateau formation.

The total electron distribution undergoes some heating, but the overall shape of the distribution is quite different from the collision-only case. In these middle panels, it is noticeable that an X-shaped band of irregular features appears near the core of the distribution in the late stages of the time evolution. These irregular features in the distribution function are apparently connected with irregular features that appear near the edge of the grid representing the spectrum of L waves and must be due to accumulation of numerical imprecision. These irregular features do not spread and do not produce any perceptible effect on the relevant features of the distribution, such as the formation of the plateau joining the core and the beam distributions or the overall broadening of the velocity distribution.

In accordance with this interpretation, one sees that the irregular features do not appear in the left- and righthand panels, since they are washed out by the effect of collisions. At the end of the

computational period, it is seen that the net electron distribution is still anisotropic, with the 2D distribution elongated along the beam direction. In the case of collisions plus the Langmuir wave dynamics (the righthand panels), the early evolution is similar to the purely quasilinear case, but the later evolution is affected by the Coulomb collisional dynamics. Such a combined beam-plasma dynamical interaction showing the transition from the collective dynamics to collisional dynamics has not been done in the literature.

In the context of the solar applications, the third panels are similar to those considered (e.g., Hamilton & Petrosian 1987; McClements 1989; Hannah et al. 2009; Hannah & Kontar 2011; Zharkova & Siversky 2011), in that both the Coulomb collisional dynamics and self-consistent Langmuir wave dynamics are considered. The above references, however, also heuristically included collisional damping term for the Langmuir waves, whereas in the present approach, the collisional effects influence the Langmuir dynamics indirectly and only through the electron distribution function evolution. In spite of this caveat, however, our work is more general in the sense that we consider two-dimensional dynamics and also allow nonlinear wave processes, such as the decay interaction and nonlinear wave-particle scattering similar to Kontar et al. (2012) and Karlický & Kontar (2012). Also, the above references employed simplified Coulomb collisional integral for the particles, whereas our numerical solution is based upon the Landau operator. In the context of solar X-ray, however, inhomogeneity effects is important. In addition, for the solar X-ray problem different initial electron velocity distributions should be adopted, such as the power-law distribution. We do not have inhomogeneity effects (see, e.g., Kontar & Péceli 2002), and our choice of initial electron distribution is a simple Gaussian core plus a drifting beam. As such, our calculation is not meant to represent the solar X-ray problem. Instead, our interest has been on understanding the 2D evolution.

Figure 2 shows the spectrum of Langmuir (L) waves, as a function of normalized components of a wave vector in 2D space for several values of the normalized time between $\tau = 500$ and $\tau = 20\,000$. Since the purely collisional dynamics involves no waves by default, the Langmuir spectrum is absent in that case. As such, Fig. 2 only shows two situations. The lefthand panels show Langmuir wave spectra when only self-consistent collective effects are considered without the collisional terms in the particle equation, and the righthand panels solutions that contain both collisional dynamics and self-consistent wave dynamics in the particle kinetic equations. Of course, for both cases, the ion-sound wave intensity is also self-consistently calculated, but the results are not shown. Both cases exhibit similar early-time dynamics of the Langmuir wave time evolution.

The forward-propagating “primary” Langmuir waves are the direct result of bump-on-tail instability by the electron beam. For $\omega_{pe}t = 500$, the nonlinear decay and scattering off thermal ions (these are nonlinear processes depicted in the wave kinetic equations) already begin to produce weak backward-traveling Langmuir waves. These “backscattered” Langmuir waves form a semi-arc shaped spectra as time proceeds, eventually distributing the wave momentum in the quasi circular area in 2D wave number space. For later dynamics, such as beyond $\omega_{pe} = 15\,000$, however, the evolution of the wave spectra for two cases are quite distinct. In the pure collective dynamic case, one notices that there is an appreciable gap along the parallel wave number; in contrast, in the general case where both collective dynamics and collisions are included, the primary Langmuir waves undergo spreading at a wave vector azimuthal angle so that the

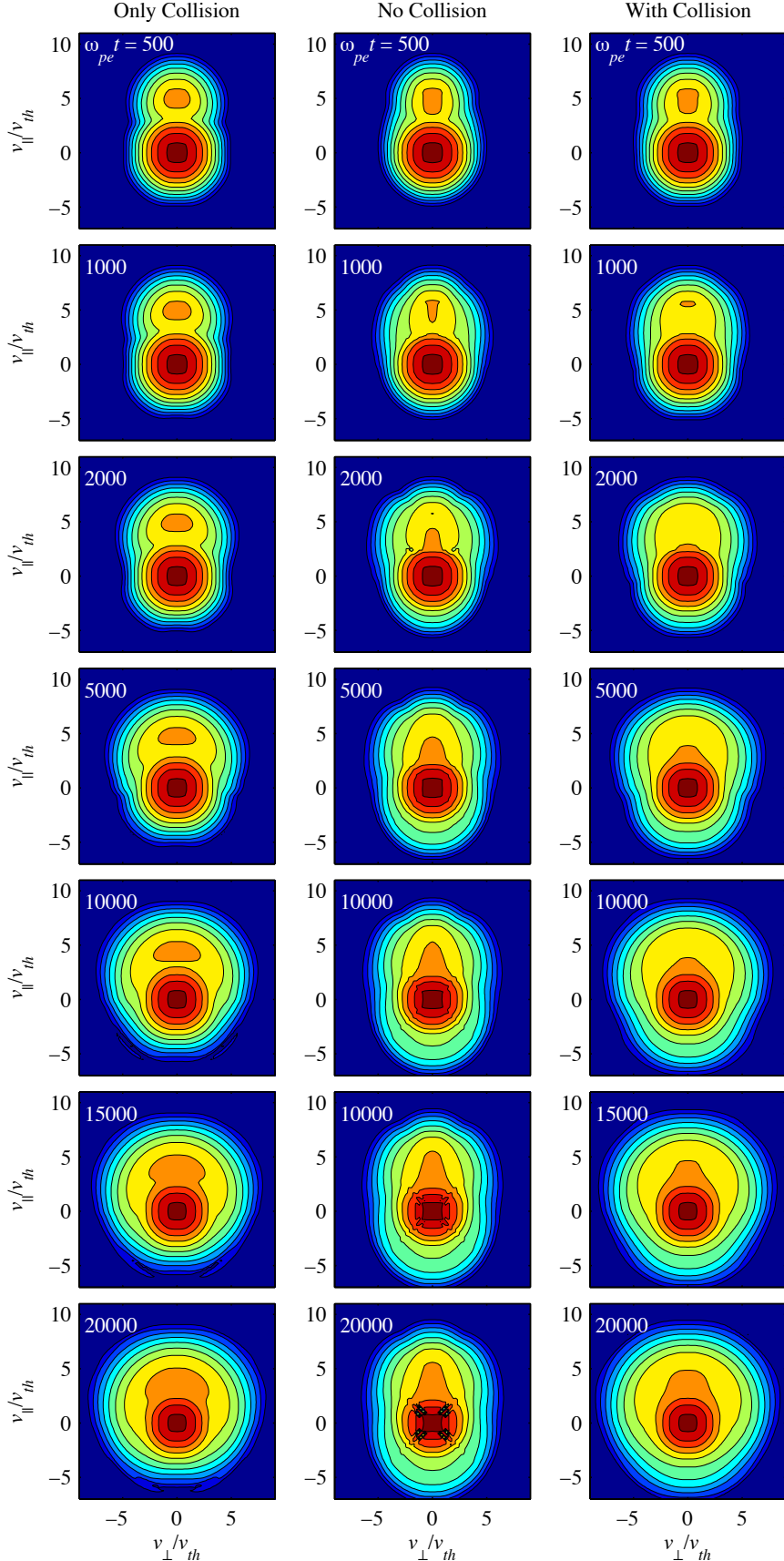


Fig. 1. Time evolution of electron velocity distribution function is shown in 2D velocity space plot at different time steps. The *lefthand panels* depict solutions with only collisions (as in the thick target approximation), the *middle panels* correspond to the self-consistent solution without collisional effects (as in the type III beam case), and the *right panels* show solutions that contain both collisional dynamics and self-consistent Langmuir wave dynamics.

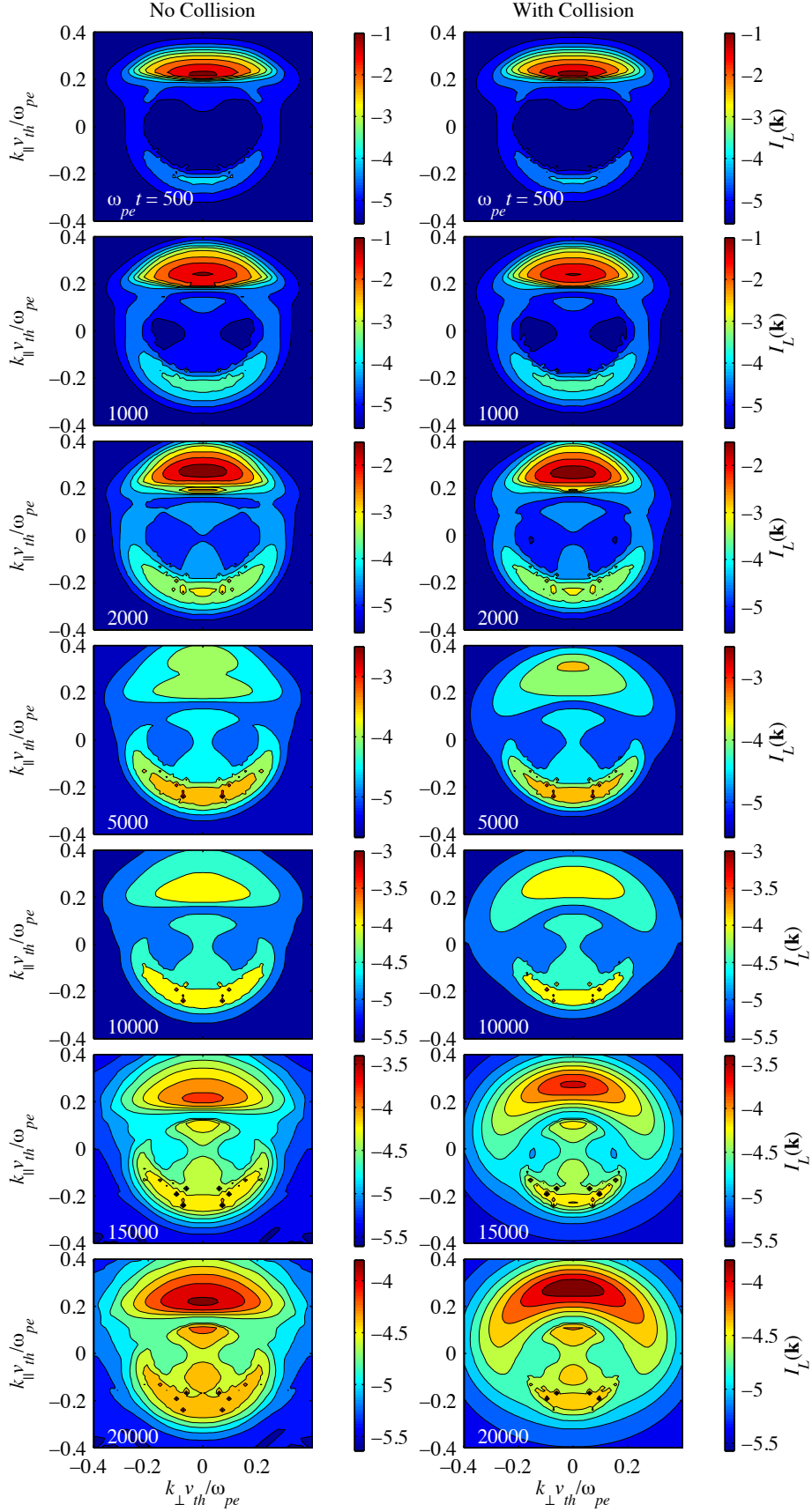


Fig. 2. Time evolution of Langmuir wave spectrum as a 2D wave number space plot at different time steps. The *lefthand panels* depict solutions with only self-consistent collective effects without the collisional terms in the particle equation, and the *right ones* show solutions that contain both collisional dynamics and self-consistent wave dynamics.

wave spectrum appears to be much more symmetric throughout the semi-circular area.

In the context of solar applications, Hamilton & Petrosian (1987), McClements (1989), Hannah et al. (2009), Hannah & Kontar (2011), and Zharkova & Siversky (2011), solved self-consistent Langmuir wave kinetic equations. Kontar et al. (2012) also demonstrate numerically that nonlinear wave-wave interactions are important. However, since these authors did not consider nonlinear mode coupling physics in 2D, the Langmuir spectrum in such a scheme does not give the wave vector pitch angle evolution. The evolution in pitch angle affects the level of Langmuir waves and generally reduces peak values of spectral energy density of plasma waves.

4. Final remarks

The energetic electrons produced during the solar flare lead to the generation of solar type III solar radio bursts and/or reverse slope bursts when the fast electrons escape the acceleration region. Electrons propagating downwards are responsible for reverse slope bursts (e.g., Tang & Moore 1982) that generate Langmuir waves in collisional plasma. These electrons traveling down towards the chromosphere are responsible for X-rays emitted via bremsstrahlung (see, e.g., Holman et al. 2011). There have been recent discussions (Hannah et al. 2009; Hannah & Kontar 2011; Zharkova & Siversky 2011; Kontar et al. 2012) that show that the collective Langmuir-wave dynamics of the X-ray generating electrons may be important for interpretations of X-ray spectra from RHESSI spacecraft (Lin et al. 2002).

In the present paper, we have addressed a fundamental plasma physics problem that is related to both the type III-generating electrons and the X-ray-generating non-thermal electrons. We considered the influence of Coulomb collisions and the self-consistent collective effects in the electron beam-plasma interaction problem in 2D velocity space. In the past, the present authors investigated the electron-Langmuir wave collective dynamics, which is relevant to the type III burst electrons, by ignoring the effects of Coulomb collisions (Ziebell et al. 2008). On the other hand, early works on solar X-ray emission ignored the collective dynamics and only considered collisional dynamics. Later works include wave-particle interactions and included Langmuir wave generation, but they only considered the 1D problem, although they included other effects relevant to the solar X-ray problem, such as the inhomogeneity and phenomenological collisional damping. In contrast, we considered the full nonlinear dynamics in the wave kinetic equation without explicit collisional damping (yet), but which included nonlinear wave-particle scattering and three-wave decay interactions in 2D wave number space.

Upon comparing the electron distribution evolution among three situations, namely, one in which only the collisional effects are included, another with only collective dynamics, and the third in which both collisions and waves are incorporated, we found that the early dynamics in the general case follows the collective dynamical pattern, whereas for later times, the dynamics closely matches the collisional case. This transitional behavior has not been demonstrated clearly in the literature (Fig. 1). The comparison between results obtained considering the collisionless weak turbulent dynamics and the collisional weak turbulent dynamics shows that for $\tau \approx 2000$, a normalized time for which the primary Langmuir peak excited by the beam is fully developed and the backward propagating Langmuir peak is already well established, the effect of collisions is already noticeable,

leading to a wider plateau in the distribution function and increased tendency to isotropization, as compared to the collisionless case. For a much longer evolution time, the results show that the distribution function obtained in the collisional case is clearly more isotropic than was obtained in the case without the effect of collisions and also show a noticeable decrease in the energetic tail. Considering the effect of the wave spectra as well, the general comment is that collisions lead to a wider angular spread of both Langmuir waves and electron beam on comparable time scales.

When we compared the wave dynamics between the pure collective case and the general case (for collision only case there is no wave), we found that the late time evolution of the wave spectra also shows a marked difference between the two cases. Specifically, the general case in which both collisions and collective effects were considered shows more symmetric Langmuir wave spectrum at late time periods. The overall conclusion to be drawn from both analyses of the time evolution of the velocity distribution function and of the spectrum of Langmuir waves is that the collisional processes, even if irrelevant on the time scale of the development of quasilinear processes, may lead to effects that are comparable in magnitude to effects of the nonlinear processes on a time scale that is compatible to the time scale of evolution of nonlinear processes in space plasmas.

As noted, the actual application of the present analysis to the solar X-ray problem requires additional effects that are not included here: inhomogeneous density profile, explicit collisional damping terms in the wave kinetic equations, and probably different initial non-thermal electron distribution functions. However, we believe that future applications can be built upon the present formalism.

Acknowledgements. This work was partially supported by the Brazilian agencies CNPq and FAPERGS. P.H.Y. acknowledges support by the BK21 plus program through the National Research Foundation (NRF) funded by the Ministry of Education of Korea, and NSF Grant Nos. AGS1138720 and AGS1242331. E.P.K. was supported by an STFC consolidated grant.

References

- Bian, N. H., Kontar, E. P., & Ratcliffe, H. 2014, *J. Geophys. Res. (Space Phys.)*, **119**, 4239
- Brown, J. C. 1971, *Sol. Phys.*, **18**, 489
- Cairns, I. H. 1987, *J. Plasma Phys.*, **38**, 169
- Dennis, B. R., Benz, A. O., Ranieri, M., & Simnett, G. M. 1984, *Sol. Phys.*, **90**, 383
- Dupree, T. H. 1966, *Phys. Fluids*, **9**, 1773
- Emslie, A. G., & Smith, D. F. 1984, *ApJ*, **279**, 882
- Gaffey, Jr., J. D. 1976, *J. Plasma Phys.*, **16**, 149
- Ganse, U., Kilian, P., Spanier, F., & Vainio, R. 2012a, *ApJ*, **751**, 145
- Ganse, U., Kilian, P., Vainio, R., & Spanier, F. 2012b, *Sol. Phys.*, **280**, 551
- Ganse, U., Kilian, P., Spanier, F., & Vainio, R. 2014, *A&A*, **564**, A15
- Ginzburg, V. L., & Zhelezniakov, V. V. 1958, *Sov. Astron.*, **2**, 653
- Goldman, M. V. 1983, *Sol. Phys.*, **89**, 403
- Goldman, M. V., & Dubois, D. F. 1982, *Phys. Fluids*, **25**, 1062
- Hamilton, R. J., & Petrosian, V. 1987, *ApJ*, **321**, 721
- Hannah, I. G., & Kontar, E. P. 2011, *A&A*, **529**, A109
- Hannah, I. G., Kontar, E. P., & Sirenko, O. K. 2009, *ApJ*, **707**, L45
- Hannah, I. G., Kontar, E. P., & Reid, H. A. S. 2013, *A&A*, **550**, A51
- Holman, G. D., Aschwanden, M. J., Aurass, H., et al. 2011, *Space Sci. Rev.*, **159**, 107
- Ishihara, O., & Hirose, A. 1985, *Phys. Fluids*, **28**, 2159
- Jeffrey, N. L. S., Kontar, E. P., Bian, N. H., & Emslie, A. G. 2014, *ApJ*, **787**, 86
- Kaplan, S. A., & Tsytovich, V. N. 1968, *Sov. Astron.*, **11**, 956
- Karlický, M., & Kontar, E. P. 2012, *A&A*, **544**, A148
- Karlický, M., & Vandam, M. 2007, *Planet. Space Sci.*, **55**, 2336
- Karney, C. F. F. 1986, *Comp. Phys. Rep.*, **4**, 183
- Kasaba, Y., Matsumoto, H., & Omura, Y. 2001, *J. Geophys. Res.*, **106**, 18693

- Kontar, E. P. 2001, *Sol. Phys.*, **202**, 131
- Kontar, E. P., & Pécseli, H. L. 2002, *Phys. Rev. E*, **65**, 066408
- Kontar, E. P., Ratcliffe, H., & Bian, N. H. 2012, *A&A*, **539**, A43
- Ledenev, V. G., Zverev, E. A., & Starygin, A. P. 2004, *Sol. Phys.*, **222**, 299
- Li, B., & Cairns, I. H. 2013, *J. Geophys. Res. (Space Phys.)*, **118**, 4748
- Li, B., Willes, A. J., Robinson, P. A., & Cairns, I. H. 2005, *Phys. Plasmas*, **12**, 012103.1
- Li, B., Robinson, P. A., & Cairns, I. H. 2006a, *Phys. Plasmas*, **13**, 092902
- Li, B., Robinson, P. A., & Cairns, I. H. 2006b, *Phys. Rev. Lett.*, **96**, 145005
- Li, B., Cairns, I. H., & Robinson, P. A. 2008a, *J. Geophys. Res. (Space Phys.)*, **113**, 6104
- Li, B., Cairns, I. H., & Robinson, P. A. 2008b, *J. Geophys. Res. (Space Phys.)*, **113**, 6105
- Lifshitz, E. M., & Pitaevskii, L. P. 1981, Physical kinetics (Oxford: Pergamon Press)
- Lin, R. P., Dennis, B. R., Hurford, G. J., et al. 2002, *Sol. Phys.*, **210**, 3
- MacKinnon, A. L. 1991, *A&A*, **242**, 256
- McClements, K. G. 1987, *A&A*, **175**, 255
- McClements, K. G. 1989, *A&A*, **208**, 279
- Mel'Nik, V. N., Lapshin, V., & Kontar, E. 1999, *Sol. Phys.*, **184**, 353
- Melrose, D. B. 1982, *Sol. Phys.*, **79**, 173
- Pécseli, H. L. 2014, *J. Plasma Phys.*, **80**, 745
- Ratcliffe, H., & Kontar, E. P. 2014, *A&A*, **562**, A57
- Rhee, T., Ryu, C.-M., Woo, M., et al. 2009a, *ApJ*, **694**, 618
- Rhee, T., Woo, M., & Ryu, C.-M. 2009b, *J. Kor. Phys. Soc.*, **54**, 313
- Robinson, P. A., & Cairns, I. H. 1998, *Sol. Phys.*, **181**, 363
- Syrovatskii, S. I., & Shmeleva, O. P. 1972, *Sov. Astron.*, **16**, 273
- Tang, F., & Moore, R. L. 1982, *Sol. Phys.*, **77**, 263
- Tsytovich, V. N. 1967, *Sov. Phys. Uspekhi*, **9**, 805
- Umeda, T. 2010, *J. Geophys. Res. (Space Phys.)*, **115**, 1204
- Wild, J. P. 1950, *Austr. J. Sci. Res. A Phys. Sci.*, **3**, 541
- Wild, J. P., & McCready, L. L. 1950, *Austr. J. Sci. Res. A Phys. Sci.*, **3**, 387
- Yoon, P. H. 2000, *Phys. Plasmas*, **7**, 4858
- Yoon, P. H. 2005, *Phys. Plasmas*, **12**, 052313
- Yoon, P. H. 2006, *Phys. Plasmas*, **13**, 022302
- Zharkova, V. V., & Siversky, T. V. 2011, *ApJ*, **733**, 33
- Zheleznyakov, V. V., & Zaitsev, V. V. 1970, *Sov. Astron.*, **14**, 250
- Ziebell, L. F., Gaelzer, R., Pavan, J., & Yoon, P. H. 2008, *Plasma Phys. Controlled Fusion*, **50**, 085011
- Ziebell, L. F., Yoon, P. H., Gaelzer, R., & Pavan, J. 2014a, *ApJ*, **795**, L32
- Ziebell, L. F., Yoon, P. H., Gaelzer, R., & Pavan, J. 2014b, *Phys. Plasmas*, **21**, 012306
- Ziebell, L. F., Yoon, P. H., Simões, F. J. R., Gaelzer, R., & Pavan, J. 2014c, *Phys. Plasmas*, **21**, 010701
- Ziebell, L. F., Yoon, P. H., Petruzzellis, L. T., Gaelzer, R., & Pavan, J. 2015, *ApJ*, **806**, 237

Appendix A: Fokker-Planck equation coefficients

Here we specifically follow the notations and conventions that can be found in Gaffey (1976), which can be summarized as follows. Starting from the Landau form of the Fokker-Planck collision operator defined in Eq. (3) and absorbing the ambient density into the definition for particle distribution function, $f_a = \hat{n}_a F_a$, we have

$$\begin{aligned} \theta_{ab}(f_a, f_b) &= \frac{2\pi e_a^2 e_b^2 \ln \Lambda}{m_a} \frac{\partial}{\partial \mathbf{v}_a} \cdot \int d^3 v_b \overset{\leftrightarrow}{U} \cdot \left(\frac{1}{m_a} \frac{\partial}{\partial \mathbf{v}_a} - \frac{1}{m_b} \frac{\partial}{\partial \mathbf{v}_b} \right) f_a f_b, \\ \overset{\leftrightarrow}{U} &= \frac{\partial^2 w}{\partial \mathbf{v}_a \partial \mathbf{v}_a} = \frac{1}{w^3} \left(w^2 \overset{\leftrightarrow}{1} - \mathbf{w} \mathbf{w} \right), \\ w &= |\mathbf{w}| = |\mathbf{v}_a - \mathbf{v}_b|. \end{aligned} \quad (\text{A.1})$$

Integrating by parts we obtain

$$\begin{aligned} \theta_{ab}(f_a, f_b) &= \frac{2\pi e_a^2 e_b^2 n_{0b} \ln \Lambda v_{Tb}}{m_a^2} \frac{\partial}{\partial \mathbf{v}_a} \\ &\times \left(\frac{\partial f_a}{\partial \mathbf{v}_a} \cdot \frac{\partial^2 G(x_{ab})}{\partial \mathbf{v}_a \partial \mathbf{v}_a} - \frac{m_a}{m_b} f_a \frac{\partial}{\partial \mathbf{v}_a} \cdot \frac{\partial^2 G(x_{ab})}{\partial \mathbf{v}_a \partial \mathbf{v}_a} \right), \end{aligned} \quad (\text{A.2})$$

where

$$G(x_{ab}) = \frac{1}{n_{0b} v_{Tb}} \int d^3 v_b f_b U_{ab} w_{ab}, \quad (\text{A.3})$$

and $x_{ab} \equiv v_a/v_{Tb}$, with v_{Tb} denoting the thermal velocity for particle species b , $v_{Tb} = (2T_b/m_b)^{1/2}$. Here, n_{0b} is the number density of particles of species b .

At this point we introduce the simplifying argument that in the beam-plasma instability, the most significant evolution occurs in the tail of the particle distribution function, involving particle densities that are much lower than the background density. If so, then it is justified to assume that the most significant collisional effect will be due to collisions between tail particles with particles of the background distribution. Assuming that the background distribution is a Maxwellian distribution, the function G in Eq. (3) may be written as (Gaffey 1976)

$$G(x_{ab}) = \left(x_{ab} + \frac{1}{2x_{ab}} \right) \Phi(x_{ab}) + \frac{1}{2} \Phi'(x_{ab}), \quad (\text{A.4})$$

where $\Phi(x_{ab})$ is the error function, and $\Phi'(x_{ab})$ its derivative,

$$\begin{aligned} \Phi(x_{ab}) &\equiv \frac{2}{\sqrt{\pi}} \int_0^x e^{-t^2} dt, \\ \Phi'(x_{ab}) &= \frac{2}{\sqrt{\pi}} e^{-x^2}. \end{aligned} \quad (\text{A.5})$$

Making use of the auxiliary function Ψ ,

$$\Psi(x) \equiv \Phi(x) - x\Phi'(x), \quad (\text{A.6})$$

and performing some simple algebra, one obtains the following form for the collisional term (Gaffey 1976),

$$\begin{aligned} \theta_{ab}(f_a, f_b) &= \Gamma_{ab} \left[\frac{\partial}{\partial \mathbf{v}_a} \cdot \left(2 \frac{m_a}{m_b} \Psi(x_{ab}) \frac{\mathbf{v}_a}{v_a^3} f_a \right) \right. \\ &\quad \left. + \frac{\partial}{\partial \mathbf{v}_a} \cdot \left\{ \left[\left(\Phi(x_{ab}) - \frac{1}{2x_{ab}^2} \Psi(x_{ab}) \right) \frac{\partial^2 v_a}{\partial \mathbf{v}_a \partial \mathbf{v}_a} \right] \cdot \frac{\partial f_a}{\partial \mathbf{v}_a} \right\} \right. \\ &\quad \left. + \frac{\partial}{\partial \mathbf{v}_a} \cdot \left[\left(\frac{1}{x_{ab}^2} \Psi(x_{ab}) \frac{\mathbf{v}_a \mathbf{v}_a}{v_a^3} \right) \cdot \frac{\partial f_a}{\partial \mathbf{v}_a} \right] \right]. \end{aligned} \quad (\text{A.7})$$

Henceforth, we concentrate on the collision term affecting the electron distribution, so that $f_a = f_e$. Let us write the electron velocity simply as v , use the non-dimensional variables $\tau = \omega_{pe} t$ and $\mathbf{u} = \mathbf{v}/v_{te}$, and write the term describing binary collisions between electrons and particles of species b as

$$\begin{aligned} \theta_{ab}(F_e, F_b) &= (2\pi)gZ_b^2 \ln \Lambda \left[\frac{\partial}{\partial \mathbf{u}} \cdot \left(2 \frac{m_e}{m_b} \Psi \left(u \frac{v_{te}}{v_{tb}} \right) \frac{\mathbf{u}}{u^3} F_e \right) \right. \\ &\quad \left. + \frac{\partial}{\partial \mathbf{u}} \cdot \left\{ \left[\left(\Phi \left(u \frac{v_{te}}{v_{tb}} \right) - \frac{1}{2u^2} \frac{v_{tb}^2}{v_{te}^2} \Psi \left(u \frac{v_{te}}{v_{tb}} \right) \right) \frac{\partial^2 u}{\partial \mathbf{u} \partial \mathbf{u}} \right] \cdot \frac{\partial F_e}{\partial \mathbf{u}} \right\} \right. \\ &\quad \left. + \frac{\partial}{\partial \mathbf{u}} \cdot \left[\left(\frac{1}{u^2} \frac{v_{tb}^2}{v_{te}^2} \Psi \left(u \frac{v_{te}}{v_{tb}} \right) \frac{\mathbf{u} \mathbf{u}}{u^3} \right) \cdot \frac{\partial F_e}{\partial \mathbf{u}} \right] \right], \end{aligned} \quad (\text{A.8})$$

where we have considered $n_e \simeq n_i$, introduced Z_i and Z_e as the ion and electron charge number, respectively, with $Z_i = Z_e = 1$ and used g , as defined in Eq. (6).

In the present application, we consider a 2D system, which serves as a good approximation for the fully 3D case with azimuthal symmetry. In the 2D case, we make use of $(\partial^2/\partial u_x \partial u_x)u = u_z^2/u^3$, $(\partial^2/\partial u_x \partial u_z)u = (\partial^2/\partial u_z \partial u_x)u = -u_x u_z/u^3$, $(\partial^2/\partial u_z \partial u_z)u = u_x^2/u^3$ and write Eq. (7) in the following form,

$$\begin{aligned} \theta_{ab}(F_e, F_b) &= \frac{\partial}{\partial u_x} \left(d_x^b F_e + b_{xx}^b \frac{\partial F_e}{\partial u_x} + b_{xz}^b \frac{\partial F_e}{\partial u_z} \right) \\ &\quad + \frac{\partial}{\partial u_z} \left(d_z^b F_e + b_{zx}^b \frac{\partial F_e}{\partial u_x} + b_{zz}^b \frac{\partial F_e}{\partial u_z} \right), \end{aligned} \quad (\text{A.9})$$

where

$$\begin{aligned} a_i^b &= (2\pi)gZ_b^2 \ln \Lambda \left[2 \frac{m_e}{m_b} \Psi \left(u \frac{v_{te}}{v_{tb}} \right) \frac{u_i}{u^3} \right], \\ \left(b_{xx}^b b_{xz}^b \right) &= \frac{\Gamma_{ej}}{\omega_{pe} v_{te}^3 u^5} \frac{1}{u^5} \left\{ \left[u^2 \Phi \left(u \frac{v_{te}}{v_{tb}} \right) - \frac{1}{2} \frac{v_{tb}^2}{v_{te}^2} \Psi \left(u \frac{v_{te}}{v_{tb}} \right) \right] \right. \\ &\quad \left. \times \left(\frac{u_z u_z - u_x u_z}{-u_x u_z u_x u_x} \right) + \frac{v_{tb}^2}{v_{te}^2} \Psi \left(u \frac{v_{te}}{v_{tb}} \right) \left(\frac{u_x u_x - u_x u_z}{-u_x u_z u_z u_z} \right) \right\}. \end{aligned} \quad (\text{A.10})$$

In addition, it is easy to verify that the equation for the electron distribution function, obtained from (6), can be written for the case 2D in the following form:

$$\begin{aligned} \frac{\partial F_e}{\partial \tau} &= \frac{\partial}{\partial u_x} \left(A_x^{\text{el}} F_e + D_{xx}^{\text{el}} \frac{\partial F_e}{\partial u_x} + D_{xz}^{\text{el}} \frac{\partial F_e}{\partial u_z} \right) \\ &\quad + \frac{\partial}{\partial u_z} \left(A_z^{\text{el}} F_e + D_{zx}^{\text{el}} \frac{\partial F_e}{\partial u_x} + D_{zz}^{\text{el}} \frac{\partial F_e}{\partial u_z} \right) \\ &\quad + \sum_b \theta_{ab}(F_e, F_b), \end{aligned} \quad (\text{A.11})$$

where, as a further and usual approximation, we have neglected the effect of S waves. Making use of $\mu_q^L = 1$, the coefficients A_i^{el} and the D_{ij}^{el} can be written as

$$\begin{aligned} A_i^{\text{el}} &= g \int_{-\infty}^{\infty} dq_x \int_{-\infty}^{\infty} dq_z \frac{q_i}{q_x^2 + q_z^2} \sum_{\sigma=\pm 1} \sigma z_{\mathbf{q}}^L \delta(\sigma z_{\mathbf{q}}^L - q_x u_x - q_z u_z), \\ D_{ij}^{\text{el}} &= \int_{-\infty}^{\infty} dq_x \int_{-\infty}^{\infty} dq_z \frac{q_i q_j}{q_x^2 + q_z^2} \sum_{\sigma=\pm 1} \mathcal{E}_{\mathbf{q}}^{\sigma L} \delta(\sigma z_{\mathbf{q}}^L - q_x u_x - q_z u_z). \end{aligned} \quad (\text{A.12})$$

Bibliography

- [1] A.I. Akhiezer, I.A. Akhiezer, R.V. Polovin, and D. Haar. *Collective oscillations in a plasma*. International series of monographs in natural philosophy. Cambridge MIT Press, 1967. URL: <https://books.google.com.br/books?id=1y1RAAAAMAAJ>.
- [2] YU. L. Klimontovich. *The Statistical Theory of Non-equilibrium Processes in Plasma*. International series of monographs in natural philosophy. M.I.T. Press, 1967. URL: <https://books.google.com.br/books?id=YiVRAAAAMAAJ>.
- [3] J.A. Bittencourt. *Fundamentals of Plasma Physics*. Springer New York, 2013. doi: [10.1007/978-1-4757-4030-1](https://doi.org/10.1007/978-1-4757-4030-1).
- [4] F. F. Chen. *Introduction to Plasma Physics and Controlled Fusion*. Springer, 3rd edition, 2016. doi: [10.1007/978-3-319-22309-4](https://doi.org/10.1007/978-3-319-22309-4).
- [5] Donald A. Gurnett and Amitava Bhattacharjee. *Introduction to Plasma Physics: With Space, Laboratory and Astrophysical Applications*. Cambridge University Press, 2 edition, 2017. doi: [10.1017/9781139226059](https://doi.org/10.1017/9781139226059).
- [6] A.I. Akhiezer. *Plasma Electrodynamics: Non-linear theory and fluctuations*. International series of monographs in natural philosophy. Pergamon Press, 1975. URL: <https://books.google.com.br/books?id=27bvAAAAMAAJ>.
- [7] B. B. Kadomtsev. *Plasma turbulence*. Academic Press, New York, 1965. URL: <http://adsabs.harvard.edu/abs/1965pltu.book.....K>.
- [8] V. N. Tsytovich. Reviews of topical problems: nonlinear effects in a plasma. *Soviet Physics Uspekhi*, 9:805–836, June 1967. URL: <http://adsabs.harvard.edu/abs/1967SvPhU...9..805T>, doi: [10.1070/PU1967v009n06ABEH003226](https://doi.org/10.1070/PU1967v009n06ABEH003226).
- [9] R. Z. Sagdeev and A. A. Galeev. *Nonlinear Plasma Theory*. Frontiers in physics. W. A. Benjamin, 1969. URL: <https://books.google.com.br/books?id=xT3wAAAAIAAJ>.
- [10] V. N. Tsytovich. *Non Linear Effects in Plasmas*. Plenum Press, New York, 1970. URL: <https://books.google.com.br/books?id=0AhRAAAAMAAJ>.

- [11] R. C. Davidson. *Methods in Nonlinear Plasma Theory*. Pure and applied physics. Academic Press, New York, 1972. URL: <https://books.google.com.br/books?id=01FRAAAAMAAJ>.
- [12] V. N. Tsytovich. *An Introduction to the Theory of Plasma Turbulence*. International series of monographs in natural philosophy. Pergamon Press, 1972. URL: <https://books.google.com.br/books?id=JuGZAAAIAAJ>.
- [13] V. N. Tsytovich. *Theory of Turbulent Plasma*. Studies in Soviet science : Physical sciences. Consultants Bureau, New York, 1977. URL: <https://books.google.com.br/books?id=2S9RAAAAMAAJ>.
- [14] D. B. Melrose. *Instabilities in Space and Laboratory Plasmas*. Cambridge University Press, 1986. URL: <https://books.google.com.br/books?id=yVimB3mZv2UC>.
- [15] R. J-M. Grognard. Numerical simulation of the weak turbulence excited by a beam of electrons in the interplanetary plasma. *Solar Physics*, 81(1):173–180, Nov 1982. URL: <https://doi.org/10.1007/BF00151988>, doi:10.1007/BF00151988.
- [16] K. G. McClements. The quasi-linear relaxation and bremsstrahlung of thick target electron beams in solar flares. *Astronomy & Astrophysics*, 175:255–262, March 1987. URL: <http://adsabs.harvard.edu/abs/1987A%26A...175..255M>.
- [17] Alfred Hanssen. Resonance broadening modification of weak plasma turbulence theory. *Journal of Geophysical Research: Space Physics*, 96(A2):1867–1871, 1991. URL: <http://dx.doi.org/10.1029/90JA02307>, doi:10.1029/90JA02307.
- [18] S. D. Edney and P. A. Robinson. Analytic treatment of weak-turbulence Langmuir wave electrostatic decay. *Physics of Plasmas*, 8(2):428–440, 2001. URL: <https://doi.org/10.1063/1.1339839>, doi:10.1063/1.1339839.
- [19] E. P. Kontar. Dynamics of electron beams in the inhomogeneous solar corona plasma. *Solar Physics*, 202:131–149, August 2001. URL: <http://adsabs.harvard.edu/abs/2001SoPh..202..131K>, doi:10.1023/A:1011894830942.
- [20] E. P. Kontar and H. L. Pécseli. Nonlinear development of electron-beam-driven weak turbulence in an inhomogeneous plasma. *Phys. Rev. E*, 65:066408, Jun 2002. URL: <https://link.aps.org/doi/10.1103/PhysRevE.65.066408>, doi:10.1103/PhysRevE.65.066408.
- [21] J. M. TenBarge, G. G. Howes, and W. Dorland. Collisionless damping at electron scales in solar wind turbulence. *The Astrophysical Journal*, 774(2), Sep 10 2013. doi:10.1088/0004-637X/774/2/139.

- [22] P. H. Yoon. Generalized weak turbulence theory. *Phys. Plasmas*, 7:4858–4871, December 2000. URL: <http://adsabs.harvard.edu/abs/2000PhPl....7.4858Y>, doi:10.1063/1.1318358.
- [23] Peter H. Yoon. Effects of spontaneous fluctuations on the generalized weak turbulence theory. *Physics of Plasmas*, 12(4):042306, 2005. doi:10.1063/1.1864073.
- [24] P. H. Yoon. Statistical theory of electromagnetic weak turbulence. *Phys. Plasmas*, 13(2):022302, February 2006. URL: <http://adsabs.harvard.edu/abs/2006PhPl...13b2302Y>, doi:10.1063/1.2167587.
- [25] P. H. Yoon, L. F. Ziebell, R. Gaelzer, and J. Pavan. Electromagnetic weak turbulence theory revisited. *Physics of Plasmas*, 19(10):102303, 2012. URL: <https://doi.org/10.1063/1.4757224>, doi:10.1063/1.4757224.
- [26] L. F. Ziebell, R. Gaelzer, J. Pavan, and P. H. Yoon. Two-dimensional nonlinear dynamics of beam plasma instability. *Plasma Physics and Controlled Fusion*, 50(8):085011, August 2008. URL: <http://adsabs.harvard.edu/abs/2008PPCF...50h5011Z>, doi:10.1088/0741-3335/50/8/085011.
- [27] L. F. Ziebell, P. H. Yoon, R. Gaelzer, and J. Pavan. Langmuir condensation by spontaneous scattering off electrons in two dimensions. *Plasma Physics and Controlled Fusion*, 54(5):055012, 2012. URL: <http://stacks.iop.org/0741-3335/54/i=5/a=055012>.
- [28] P. H. Yoon, L. F. Ziebell, R. Gaelzer, R. P. Lin, and L. Wang. Langmuir turbulence and suprothermal electrons. *Space Science Reviews*, 173(1):459–489, 2012. URL: <http://dx.doi.org/10.1007/s11214-012-9867-3>, doi:10.1007/s11214-012-9867-3.
- [29] L. F. Ziebell, P. H. Yoon, R. Gaelzer, and J. Pavan. Plasma emission by weak turbulence processes. *Astrophysical Journal Letters*, 795:L32, November 2014. doi:10.1088/2041-8205/795/2/L32.
- [30] L. F. Ziebell, P. H. Yoon, R. Gaelzer, and J. Pavan. Transition from thermal to turbulent equilibrium with a resulting electromagnetic spectrum. *Phys. Plasmas*, 21(1):012306, January 2014. doi:10.1063/1.4863453.
- [31] L. F. Ziebell, P. H. Yoon, F. J. R. Simões, R. Gaelzer, and J. Pavan. Spontaneous emission of electromagnetic radiation in turbulent plasmas. *Phys. Plasmas*, 21(1):010701, January 2014. doi:10.1063/1.4861619.
- [32] L. F. Ziebell, P. H. Yoon, L. T. Petruzzellis, R. Gaelzer, and J. Pavan. Plasma emission by nonlinear electromagnetic processes. *The Astrophysical Journal*, 806:237, June 2015. doi:10.1088/0004-637X/806/2/237.

- [33] L. F. Ziebell, L. T. Petruzzellis, P. H. Yoon, R. Gaelzer, and J. Pavan. Plasma emission by counter-streaming electron beams. *The Astrophysical Journal*, 818(1):61, 2016. URL: <http://stacks.iop.org/0004-637X/818/i=1/a=61>.
- [34] L. F. Ziebell, R. Gaelzer, and Peter H. Yoon. Nonlinear development of weak beam-plasma instability. *Phys. Plasmas*, 8(9):3982–3995, Sept. 2001. [doi:10.1063/1.1389863](https://doi.org/10.1063/1.1389863).
- [35] R. Gaelzer, L. F. Ziebell, and Peter H. Yoon. Generation of harmonic Langmuir mode by beam plasma instability. *Phys. Plasmas*, 9(1):96–110, Jan 2002. [doi:10.1063/1.1421371](https://doi.org/10.1063/1.1421371).
- [36] R. Gaelzer, L. F. Ziebell, A. F. Viñas, P. H. Yoon, and C.-M. Ryu. Asymmetric solar wind electron superthermal distributions. *The Astrophysical Journal*, 677(1):676, 2008. URL: <http://stacks.iop.org/0004-637X/677/i=1/a=676>.
- [37] A. G. Emslie and D. F. Smith. Microwave signature of thick-target electron beams in solar flares. *The Astrophysical Journal*, 279:882–895, April 1984. [doi:10.1086/161959](https://doi.org/10.1086/161959).
- [38] I. G. Hannah, E. P. Kontar, and O. K. Sirenko. The effect of wave-particle interactions on low-energy cutoffs in solar flare electron spectra. *Astrophysical Journal Letters*, 707(1):L45–L50, Dec 10 2009. [doi:10.1088/0004-637X/707/1/L45](https://doi.org/10.1088/0004-637X/707/1/L45).
- [39] Valentina V. Zharkova and Taras V. Siversky. The effects of electron-beam-induced electric field on the generation of Langmuir turbulence in flaring atmospheres. *The Astrophysical Journal*, 733(1), May 2011. [doi:10.1088/0004-637X/733/1/33](https://doi.org/10.1088/0004-637X/733/1/33).
- [40] I. G. Hannah and E. P. Kontar. The spectral difference between solar flare HXR coronal and footpoint sources due to wave-particle interactions. *Astronomy & Astrophysics*, 529, May 2011. [doi:10.1051/0004-6361/201015710](https://doi.org/10.1051/0004-6361/201015710).
- [41] M. Karlický and E. P. Kontar. Electron acceleration during three-dimensional relaxation of an electron beam-return current plasma system in a magnetic field. *Astronomy & Astrophysics*, 544, Aug 2012. [doi:10.1051/0004-6361/201219400](https://doi.org/10.1051/0004-6361/201219400).
- [42] Hamish Andrew Sinclair Reid and Heather Ratcliffe. A review of solar type III radio bursts. *Research in Astronomy and Astrophysics*, 14(7):773–804, Jul 2014. URL: <https://doi.org/10.1088%2F1674-4527%2F14%2F7%2F003>, [doi:10.1088/1674-4527/14/7/003](https://doi.org/10.1088/1674-4527/14/7/003).
- [43] Nicolas H. Bian, Eduard P. Kontar, and Heather Ratcliffe. Resonance broadening due to particle scattering and mode coupling in the quasi-linear relaxation of electron beams. *Journal of Geophysical Research - Space Physics*, 119(6):4239–4255, Jun 2014. [doi:10.1002/2013JA019664](https://doi.org/10.1002/2013JA019664).
- [44] Peter H. Yoon, Jinhy Hong, Sunjung Kim, Junggi Lee, Junhyun Lee, Jongsun Park, Kyungsun Park, and Jungjoon Seough. Asymmetric solar wind electron distributions.

- The Astrophysical Journal*, 755(2):112, 2012. URL: <http://stacks.iop.org/0004-637X/755/i=2/a=112>.
- [45] S. F. Tigik, L. F. Ziebell, P. H. Yoon, and E. P. Kontar. Two-dimensional time evolution of beam-plasma instability in the presence of binary collisions. *Astronomy & Astrophysics*, 586:A19, February 2016. [doi:10.1051/0004-6361/201527271](https://doi.org/10.1051/0004-6361/201527271).
 - [46] L. J. Porter and J. A. Klimchuk. Soft X-ray loops and coronal heating. *The Astrophysical Journal*, 454:499, November 1995. URL: <http://adsabs.harvard.edu/abs/1995ApJ...454..499P>, [doi:10.1086/176501](https://doi.org/10.1086/176501).
 - [47] J. L. Kohl, G. Noci, E. Antonucci, G. Tondello, M. C. E. Huber, S. R. Cranmer, L. Strachan, A. V Panasyuk, L. D. Gardner, M. Romoli, S. Fineschi, D. Dobrzycka, J. C. Raymond, P. Nicolosi, O. H. W. Siegmund, D. Spadaro, C. Benna, A. Ciaravella, S. Giordano, S. R. Habbal, M. Karovska, X. Li, R. Martin, J. G. Michels, A. Modigliani, G. Naletto, R. H. O’Neal, C. Pernechele, G. Poletto, P. L. Smith, and R. M. Suleiman. UVCS/SOHO empirical determinations of anisotropic velocity distributions in the solar corona. *Astrophysical Journal Letters*, 501(1):L127, 1998. URL: <http://stacks.iop.org/1538-4357/501/i=1/a=L127>.
 - [48] Astrid M. Veronig, John C. Brown, and Laura Bone. Evidence for a solar coronal thick-target hard X-ray source observed by RHESSI. *Advances in Space Research*, 35(10):1683 – 1689, 2005. URL: <http://www.sciencedirect.com/science/article/pii/S0273117705001353>, [doi:10.1016/j.asr.2005.01.065](https://doi.org/10.1016/j.asr.2005.01.065).
 - [49] John C. Brown, A. Gordon Emslie, Gordon D. Holman, Christopher M. Johns-Krull, Eduard P. Kontar, Robert P. Lin, Anna Maria Massone, and Michele Piana. Evaluation of algorithms for reconstructing electron spectra from their bremsstrahlung hard X-ray spectra. *The Astrophysical Journal*, 643(1):523, 2006. URL: <http://stacks.iop.org/0004-637X/643/i=1/a=523>.
 - [50] E. P. Kontar, J. C. Brown, A. G. Emslie, W. Hajdas, G. D. Holman, G. J. Hurford, J. Kašparová, P. C. V. Mallik, A. M. Massone, M. L. McConnell, M. Piana, M. Prato, E. J. Schmahl, and E. Suarez-Garcia. Deducing electron properties from hard X-ray observations. *Space Science Reviews*, 159(1):301–355, 2011. URL: <http://dx.doi.org/10.1007/s11214-011-9804-x>, [doi:10.1007/s11214-011-9804-x](https://doi.org/10.1007/s11214-011-9804-x).
 - [51] Kulinová, A., Kašparová, J., Dzifčáková, E., Sylwester, J., Sylwester, B., and Karlický, M. Diagnostics of non-thermal distributions in solar flare spectra observed by RESIK and RHESSI. *Astronomy & Astrophysics*, 533:A81, 2011. URL: <https://doi.org/10.1051/0004-6361/201116741>, [doi:10.1051/0004-6361/201116741](https://doi.org/10.1051/0004-6361/201116741).
 - [52] P. H. Yoon, L. F. Ziebell, E. P. Kontar, and R. Schlickeiser. Weak turbulence theory for collisional plasmas. *Physical Review E*, 93:033203, Mar 2016. [doi:10.1103/PhysRevE](https://doi.org/10.1103/PhysRevE).

93.033203.

- [53] A.L. Peratt. *Physics of the Plasma Universe*. Springer New York, 2014. URL: <https://books.google.com.br/books?id=To--jwEACAAJ>.
- [54] S.S.A. Kaplan and V.N. Tsytovich. *Plasma Astrophysics*. International series of monographs in natural philosophy, v. 59. Pergamon Press, 1973. URL: <https://books.google.com.br/books?id=UzasAAAAIAAJ>.
- [55] May-Britt Kallenrode. *Space Physics: an introduction to plasmas and particles in the heliosphere and magnetospheres*. Springer-Verlag Berlin Heidelberg, 3rd edition, 2004.
- [56] H. Alfvén and H. Alfvén. *Cosmical Electrodynamics*. International series of monographs on physics. Clarendon Press, 1950. URL: <https://books.google.com.br/books?id=3tYgAAAAMAAJ>.
- [57] Eugene N. Parker. Modulation of primary cosmic-ray intensity. *Phys. Rev.*, 103:1518–1533, Sep 1956. URL: <https://link.aps.org/doi/10.1103/PhysRev.103.1518>, doi:10.1103/PhysRev.103.1518.
- [58] H. Alfvén. On the origin of cosmic magnetic fields. *The Astrophysical Journal*, 133:1049, May 1961. doi:10.1086/147108.
- [59] A. K. Gailitis and V. N. Tsytovich. Acceleration by radiation and the generation of fast particles under cosmic conditions. III. Time variations in the intensity of radio sources. *Soviet Astronomy*, 8:359, Dec 1964. URL: <http://cdsads.u-strasbg.fr/abs/1964SvA....8..359G>.
- [60] Hannes Alfvén. Plasma physics applied to cosmology. *Physics Today*, 24(2):28–33, 1971. URL: <https://doi.org/10.1063/1.3022564>, doi:10.1063/1.3022564.
- [61] J. Donnert and G. Brunetti. An efficient Fokker–Planck solver and its application to stochastic particle acceleration in galaxy clusters. *Monthly Notices of the Royal Astronomical Society*, 443(4):3564–3577, 08 2014. URL: <https://doi.org/10.1093/mnras/stu1417>, doi:10.1093/mnras/stu1417.
- [62] O. Pezzi, S. Servidio, D. Perrone, F. Valentini, L. Sorriso-Valvo, A. Greco, W. H. Matthaeus, and P. Veltri. Velocity-space cascade in magnetized plasmas: Numerical simulations. *Physics of Plasmas*, 25(6):060704, 2018. URL: <https://doi.org/10.1063/1.5027685>, doi:10.1063/1.5027685.
- [63] Gregory G. Howes. Laboratory space physics: Investigating the physics of space plasmas in the laboratory. *Physics of Plasmas*, 25(5):055501, 2018. URL: <https://doi.org/10.1063/1.5025421>, doi:10.1063/1.5025421.

- [64] Ethan E. Peterson, Douglass A. Endrizzi, Matthew Beidler, Kyle J. Bunkers, Michael Clark, Jan Egedal, Ken Flanagan, Karsten J. McCollam, Jason Milhone, Joseph Olson, Carl R. Sovinec, Roger Waleffe, John Wallace, and Cary B. Forest. A laboratory model for the Parker spiral and magnetized stellar winds. *Nature Physics*, 2019. URL: <https://doi.org/10.1038/s41567-019-0592-7>, doi:10.1038/s41567-019-0592-7.
- [65] National Research Council. *The Sun to the Earth – and Beyond: A Decadal Research Strategy in Solar and Space Physics*. The National Academies Press, Washington, DC, 2003. URL: <https://doi.org/10.17226/10477>, doi:10.17226/10477.
- [66] K. Dialynas, S. M. Krimigis, D. G. Mitchell, R. B. Decker, and E. C. Roelof. The bubble-like shape of the heliosphere observed by Voyager and Cassini. *Nature Astronomy*, 1:0115, Apr 2017. Letter. URL: <https://doi.org/10.1038/s41550-017-0115>.
- [67] National Research Council. *Solar and Space Physics: A Science for a Technological Society*. The National Academies Press, Washington, DC, 2013. URL: <https://doi.org/10.17226/13060>, doi:10.17226/13060.
- [68] S Chapman. Cosmical magnetic phenomena. *Nature*, 124:19–26, 1929.
- [69] Hannu Koskinen. *Physics of Space Storms: From the Solar Surface to the Earth*. Springer Praxis Books. Springer-Verlag Berlin Heidelberg, 1 edition, 2011. URL: <https://doi.org/10.1007/978-3-642-00319-6>, doi:10.1007/978-3-642-00319-6.
- [70] Steven R. Cranmer, Sarah E. Gibson, and Pete Riley. Origins of the ambient solar wind: Implications for space weather. *Space Science Reviews*, 212(3):1345–1384, Nov 2017. URL: <https://doi.org/10.1007/s11214-017-0416-y>, doi:10.1007/s11214-017-0416-y.
- [71] Karl-Ludwig Klein and Silvia Dalla. Acceleration and propagation of solar energetic particles. *Space Science Reviews*, 212(3):1107–1136, Nov 2017. URL: <https://doi.org/10.1007/s11214-017-0382-4>, doi:10.1007/s11214-017-0382-4.
- [72] Benz A. O. *Plasma Astrophysics: Kinetic Processes in Solar and Stellar Coronae*, volume 279 of *Astrophysics And Space Science Library Series*. Springer, 2nd edition, 2002.
- [73] A. Hunter. Origin of the coronium lines. *Nature*, 150(3817):756–759, 1942. URL: <https://doi.org/10.1038/150756a0>, doi:10.1038/150756a0.
- [74] E. N. Parker. Nanoflares and the solar X-ray corona. *The Astrophysical Journal*, 330:474–479, July 1988. URL: <http://adsabs.harvard.edu/abs/1988ApJ...330..474P>, doi:10.1086/166485.
- [75] J. D. Scudder. Why all stars should possess circumstellar temperature inversions. *The Astrophysical Journal*, 398:319–349, October 1992b. doi:10.1086/171859.

- [76] Adolfo F. Viñas, Hung K. Wong, and Alexander J. Klimas. Generation of electron suprathermal tails in the upper solar atmosphere: Implications for coronal heating. *The Astrophysical Journal*, 528(1):509, 2000. URL: <http://stacks.iop.org/0004-637X/528/i=1/a=509>.
- [77] V. Pierrard and M. Pieters. Coronal heating and solar wind acceleration for electrons, protons, and minor ions obtained from kinetic models based on kappa distributions. *Journal of Geophysical Research*, 119(12):9441–9455, 2014. 2014JA020678. URL: <http://dx.doi.org/10.1002/2014JA020678>, doi:10.1002/2014JA020678.
- [78] S. F. Tigik, L. F. Ziebell, and P. H. Yoon. Generation of suprathermal electrons by collective processes in collisional plasma. *The Astrophysical Journal Letters*, 849(2):L30, 2017. URL: <http://stacks.iop.org/2041-8205/849/i=2/a=L30>.
- [79] YU. L. Klimontovich. *Kinetic Theory of Non Ideal Gases and Nonideal Plasmas*. International series in natural philosophy. Pergamon Press, 1982. URL: <https://books.google.com.br/books?id=RdLvAAAAMAAJ>.
- [80] R. C. Davidson. *An introduction to the physics of nonneutral plasmas*. Addison Wesley Publ., Redwood City, CA, 1990. URL: <http://adsabs.harvard.edu/abs/1990ipnp.book.....D>.
- [81] S. F. Tigik. Análise não linear da interação feixe-plasma na presença de colisões binárias. Master's thesis, Universidade Federal do Rio Grande do Sul, Instituto de Física, September 2015. URL: <http://hdl.handle.net/10183/127986>.
- [82] S. F. Tigik, L. F. Ziebell, and P. H. Yoon. Collisional damping rates for plasma waves. *Physics of Plasmas*, 23(6):064504, 2016. doi:10.1063/1.4953802.
- [83] John D. Gaffey. Energetic ion distribution resulting from neutral beam injection in tokamaks. *Journal of Plasma Physics*, 16(2):149–169, Oct 1976. URL: <https://doi.org/10.1017/S0022377800020134>, doi:10.1017/S0022377800020134.
- [84] E. P. Kontar, H. Ratcliffe, and N. H. Bian. Wave-particle interactions in non-uniform plasma and the interpretation of hard X-ray spectra in solar flares. *Astronomy & Astrophysics*, 539:A43, Mar 2012. URL: <http://dx.doi.org/10.1051/0004-6361/201118216>, doi:10.1051/0004-6361/201118216.
- [85] H. Khalilpour and G. Foroutan. Simulation study of collisional effects on the propagation of a hot electron beam and generation of Langmuir turbulence for application in type III radio bursts. *Journal of Plasma Physics*, 79(3):239–248, Jun 2013. doi:10.1017/S0022377812000876.

- [86] Reid, Hamish A. S. and Kontar, Eduard P. Stopping frequency of type III solar radio bursts in expanding magnetic flux tubes. *Astronomy & Astrophysics*, 577:A124, 2015. URL: <https://doi.org/10.1051/0004-6361/201425309>, doi:10.1051/0004-6361/201425309.
- [87] E. N. Parker. Dynamics of the interplanetary gas and magnetic fields. *The Astrophysical Journal*, 128:664, November 1958. URL: <http://adsabs.harvard.edu/abs/1958ApJ...128..664P>, doi:10.1086/146579.
- [88] Vytenis M. Vasyliunas. A survey of low-energy electrons in the evening sector of the magnetosphere with OGO 1 and OGO 3. *Journal of Geophysical Research*, 73(9):2839–2884, 1968. URL: <http://dx.doi.org/10.1029/JA073i009p02839>, doi:10.1029/JA073i009p02839.
- [89] F. V. Coroniti. Energetic electrons in Jupiter’s magnetosphere. *The Astrophysical Journal Supplement*, 27:261, March 1974. URL: <http://adsabs.harvard.edu/abs/1974ApJS...27..261C>, doi:10.1086/190296.
- [90] W. C. Feldman, J. R. Asbridge, S. J. Bame, M. D. Montgomery, and S. P. Gary. Solar wind electrons. *Journal of Geophysical Research*, 80(31):4181–4196, 1975. URL: <http://dx.doi.org/10.1029/JA080i031p04181>, doi:10.1029/JA080i031p04181.
- [91] R. P. Lin. WIND observations of suprathermal electrons in the interplanetary medium. *Space Science Reviews*, 86(1):61–78, 1998. URL: <http://dx.doi.org/10.1023/A:1005048428480>, doi:10.1023/A:1005048428480.
- [92] R. B. Horne, R. M. Thorne, Y. Y. Shprits, N. P. Meredith, S. A. Glauert, A. J. Smith, S. G. Kanekal, D. N. Baker, M. J. Engebretson, J. L. Posch, M. Spasojevic, U. S. Inan, J. S. Pickett, and P. M. E. Decreau. Wave acceleration of electrons in the Van Allen radiation belts. *Nature*, 437:227–230, September 2005. URL: <http://adsabs.harvard.edu/abs/2005Natur.437..227H>, doi:10.1038/nature03939.
- [93] G. Clark, T. W. Broiles, J. L. Burch, G. A. Collinson, T. Cravens, R. A. Frahm, J. Goldstein, R. Goldstein, K. Mandt, P. Mokashi, M. Samara, and C. J. Pollock. Suprathermal electron environment of comet 67P/Churyumov-Gerasimenko: Observations from the Rosetta ion and electron sensor. *Astronomy & Astrophysics*, 583:A24, November 2015. URL: <http://adsabs.harvard.edu/abs/2015A%26A...583A..24C>, doi:10.1051/0004-6361/201526351.
- [94] M. Padovani, P. Hennebelle, A. Marcowith, and K. Ferrière. Cosmic-ray acceleration in young protostars. *Astronomy & Astrophysics*, 582:L13, October 2015. URL: <http://adsabs.harvard.edu/abs/2015A%26A...582L..13P>, arXiv:1509.06416, doi:10.1051/0004-6361/201526874.

- [95] M. de Soria-Santacruz, H. B. Garrett, R. W. Evans, I. Jun, W. Kim, C. Paranicas, and A. Drozdov. An empirical model of the high-energy electron environment at Jupiter. *Journal of Geophysical Research (Space Phys.)*, 121:9732–9743, October 2016. URL: <http://adsabs.harvard.edu/abs/2016JGRA..121.9732D>, doi:10.1002/2016JA023059.
- [96] M. Padovani, A. Marcowith, P. Hennebelle, and K. Ferrière. The plasma physics of cosmic rays in star-forming regions. *Plasma Phys. and Contr. Fus.*, 59(1):014002, January 2017. URL: <http://adsabs.harvard.edu/abs/2017PPCF...59a4002P>, doi:10.1088/0741-3335/59/1/014002.
- [97] J. Deca, A. Divin, P. Henri, A. Eriksson, S. Markidis, V. Olshevsky, and M. Horányi. Electron and ion dynamics of the solar wind interaction with a weakly outgassing comet. *Physical Review Letters*, 118:205101, May 2017. URL: <https://link.aps.org/doi/10.1103/PhysRevLett.118.205101>, doi:10.1103/PhysRevLett.118.205101.
- [98] J. D. Scudder. On the causes of temperature change in inhomogeneous low-density astrophysical plasmas. *The Astrophysical Journal*, 398:299–318, October 1992a. URL: <http://adsabs.harvard.edu/abs/1992ApJ...398..299S>, doi:10.1086/171858.
- [99] S. W. Anderson. Coulomb collisions and coronal heating by velocity filtration. *The Astrophysical Journal*, 437:860–866, December 1994. doi:10.1086/175046.
- [100] J. D. Scudder. Ion and electron suprathermal tail strengths in the transition region: Support for the velocity filtration model of the corona. *The Astrophysical Journal*, 427:446–452, May 1994. doi:10.1086/174155.
- [101] J. D. Scudder. Electron and ion temperature gradients and suprathermal tail strengths at Parker’s solar wind sonic critical point. *Journal of Geophysical Research*, 101(A5):11039–11053, 1996. doi:10.1029/96JA00188.
- [102] John C. Dorelli and Jack D. Scudder. Electron heat flow carried by kappa distributions in the solar corona. *Journal of Geophysical Research*, 26(23):3537–3540, 1999. URL: <http://dx.doi.org/10.1029/1999GL010687>, doi:10.1029/1999GL010687.
- [103] John C. Dorelli and Jack D. Scudder. Electron heat flow in the solar corona: Implications of non-Maxwellian velocity distributions, the solar gravitational field, and Coulomb collisions. *Journal of Geophysical Research*, 108(A7), 2003. 1294. URL: <http://dx.doi.org/10.1029/2002JA009484>, doi:10.1029/2002JA009484.
- [104] Tarcísio N. Teles, Shamik Gupta, Pierfrancesco Di Cintio, and Lapo Casetti. Temperature inversion in long-range interacting systems. *Physical Review E*, 92:020101, Aug 2015. doi:10.1103/PhysRevE.92.020101.

- [105] C. Pollock, T. Moore, A. Jacques, J. Burch, U. Gliese, Y. Saito, T. Omoto, L. Avanov, A. Barrie, V. Coffey, J. Dorelli, D. Gershman, B. Giles, T. Rosnack, C. Salo, S. Yokota, M. Adrian, C. Aoustin, C. Auletta, S. Aung, V. Bigio, N. Cao, M. Chandler, D. Chornay, K. Christian, G. Clark, G. Collinson, T. Corris, A. De Los Santos, R. Devlin, T. Diaz, T. Dickerson, C. Dickson, A. Diekmann, F. Diggs, C. Duncan, A. Figueroa-Vinas, C. Firman, M. Freeman, N. Galassi, K. Garcia, G. Goodhart, D. Guererro, J. Hageman, J. Hanley, E. Hemminger, M. Holland, M. Hutchins, T. James, W. Jones, S. Kreisler, J. Kujawski, V. Lavu, J. Lobell, E. LeCompte, A. Lukemire, E. MacDonald, A. Mariano, T. Mukai, K. Narayanan, Q. Nguyan, M. Onizuka, W. Paterson, S. Persyn, B. Piepgrass, F. Cheney, A. Rager, T. Raghuram, A. Ramil, L. Reichenthal, H. Rodriguez, J. Rouzaud, A. Rucker, Y. Saito, M. Samara, J.-A. Sauvaud, D. Schuster, M. Shapiro, K. Shelton, D. Sher, D. Smith, K. Smith, S. Smith, D. Steinfeld, R. Szymkiewicz, K. Tanimoto, J. Taylor, C. Tucker, K. Tull, A. Uhl, J. Vloet, P. Walpole, S. Weidner, D. White, G. Winkert, P.-S. Yeh, and M. Zeuch. Fast plasma investigation for magnetospheric multiscale. *Space Science Reviews*, 199(1):331–406, Mar 2016. URL: <https://doi.org/10.1007/s11214-016-0245-4>. doi:10.1007/s11214-016-0245-4.
- [106] R. B. Torbert, C. T. Russell, W. Magnes, R. E. Ergun, P.-A. Lindqvist, O. LeContel, H. Vaith, J. Macri, S. Myers, D. Rau, J. Needell, B. King, M. Granoff, M. Chutter, I. Dors, G. Olsson, Y. V. Khotyaintsev, A. Eriksson, C. A. Kletzing, S. Bounds, B. Anderson, W. Baumjohann, M. Steller, K. Bromund, Guan Le, R. Nakamura, R. J. Strangeway, H. K. Leinweber, S. Tucker, J. Westfall, D. Fischer, F. Plaschke, J. Porter, and K. Lappalainen. The FIELDS instrument suite on MMS: Scientific objectives, measurements, and data products. *Space Science Reviews*, 199(1):105–135, Mar 2016. URL: <https://doi.org/10.1007/s11214-014-0109-8>. doi:10.1007/s11214-014-0109-8.
- [107] Daniel J. Gershman, Adolfo F-Viñas, John C. Dorelli, Scott A. Boardsen, Levon A. Avanov, Paul M. Bellan, Steven J. Schwartz, Benoit Lavraud, Victoria N. Coffey, Michael O. Chandler, Yoshifumi Saito, William R. Paterson, Stephen A. Fuselier, Robert E. Ergun, Robert J. Strangeway, Christopher T. Russell, Barbara L. Giles, Craig J. Pollock, Roy B. Torbert, and James L. Burch. Wave-particle energy exchange directly observed in a kinetic alfvén-branch wave. *Nature Communications*, 8:14719 EP –, Mar 2017. Article. URL: <https://doi.org/10.1038/ncomms14719>.
- [108] S. F. Tigik, L. T. Petruzzellis, L. F. Ziebell, P. H. Yoon, and R. Gaelzer. Weakly turbulent plasma processes in the presence of inverse power-law velocity tail population. *Physics of Plasmas*, 24(11):112902, 2017. doi:10.1063/1.5009931.